1-1-2013

Techno-Economic and Fluid Dynamics Analysis for Growing Microalgae with the Intent of Producing Biofuel Using a System Model

Leah R. Raffaeli
University of Denver

Techno-economic and Fluid Dynamics Analysis for Growing Microalgae with the Intent of Producing Biofuel Using a System Model

_____

Presented to

The Faculty of the Daniel Felix Ritchie School of Engineering and Computer Science

University of Denver

_____

In Partial Fulfillment

of the Requirements for the Degree

Doctor of Philosophy

_____

by

Leah R. Raffaeli

November 2013

Advisor: Corinne Lengsfeld

Author: Leah R. Raffaeli
Title: TECHNO-ECONOMIC AND FLUID DYNAMICS ANALYSIS FOR GROWING MICROALGAE WITH THE INTENT OF PRODUCING BIOFUEL USING A SYSTEM MODEL
Advisor: Corinne Lengsfeld
Degree Date: November 2013

Abstract

Techno-economic and systems studies on microalgal growth scenarios to date are abbreviated and missing a number of important variables. By including these variables in a detailed model integrating biology, chemistry, engineering, and financial aspects, a more defined systems analysis is possible. Through optimizing the model productivity based on the resulting net profit, the system analysis results in a more accurate assessment of environmental and economic sustainability of specific algal growth scenarios. Photobioreactor algal growth scenario optimization in the system model has resulted in realistic engineering design requirements based on algal growth requirements and fluid dynamics analysis. Results show feasibility for photobioreactor growth scenarios to be economically sustainable when co-products are included, but definite technological advancements and productivity improvements must be made. The main factors inhibiting a cost effective photobioreactor growth scenario are culture density, temperature, and lighting distribution for solar illuminated photobioreactors, and lighting cost for artificially illuminated photobioreactors. Open pond algal growth scenarios do not show any prospect of economic or environmental sustainability with current technology due to the large amount of surface area required, inefficient water use, and

low culture density. All algal growth scenarios are inferior to petro-diesel regarding energy inputs, carbon emissions, and environmental sustainability. No algal growth scenarios analyzed in this study meet the U.S. requirement of biofuel emitting at least 20% less carbon emissions than diesel from crude oil.

Acknowledgements

I would like to acknowledge the assistance of the PhD committee consisting of Dr. Corinne Lengsfeld, Dr. Yun-Bo Yi, Dr. Matthew Gordon, Dr. Ron McCubbrey, and Dr. Robert M. Dores from the University of Denver, and Larry Clark from Lockheed Martin. Also, my deep appreciation for the assistance of Chad Van Fleet at Mathworks, Colin Beal and Jonathan Trent at NASA OMEGA, Mark Bunger at Lux Research, Inc, Antonietta Quigg at Texas A&M University, Mark Merwin at Lockheed Martin, David Stevens at Xcel Energy, Nick Nagle at NREL, Matthew Posewitz at Colorado School of Mines, and the Senior Design team at University of Denver 2010 & 2011. Finally, I must express my deepest appreciation to my husband, Justin, and my daughter, Beatrix, for supporting me during the last four and three years, respectively.

Table of Contents

List of Tables

List of Figures

Chapter One: Introduction

Global warming can be slowed and perhaps reversed only when society replaces fossil fuels with renewable, carbon-neutral alternatives such as biofuel (Miao & Wu, 2004). Energy self-sufficiency makes geo-political sense in the face of continuing conflicts with oil-generating countries (Putt, 2007). Solar energy is renewable and sustainable, whereas all other fuels including fossil and nuclear are limited in amount and are exhaustible. The photosynthetic process of producing biomass is an efficient use of solar energy, and provides food, fuel and chemicals.

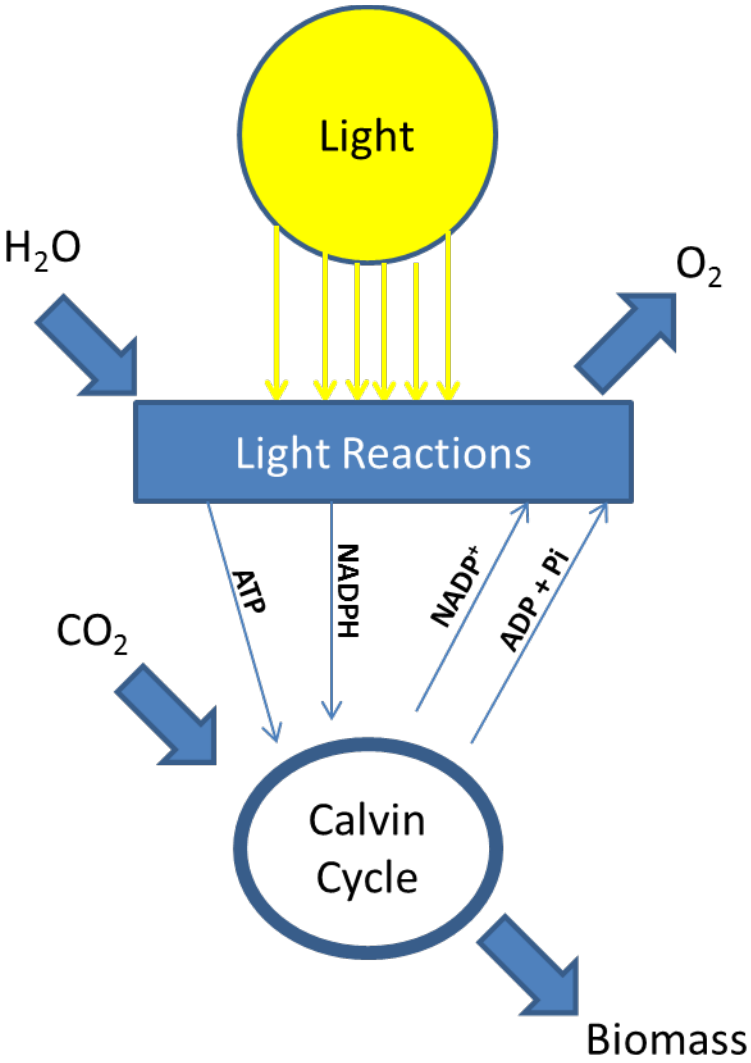

Figure 1: The photosynthetic process.

However, biofuel produced from plants such as palms, corn, sorghum, sugarcane, and soybeans have a number of detrimental effects such as deforestation and food shortages (Richardson, et al., 2010). The CO_2 emissions of these crops are shown to be comparable with that of obtaining oil from tar sands. The U.S. Environmental Protection Agency also suggested that palm oil fails to meet the U.S. requirement of biofuel emitting at least 20% less carbon emissions than diesel from crude oil. Currently, none of the

biodiesel being produced commercially from soybean oil in the U.S. and canola oil in Europe can compete with petroleum-derived diesel economically without tax credits, carbon credits, and other subsidies (Chisti, 2008).

Biodiesel produced from algae could potentially be a 'third generation' biofuel which produces a minimal amount of CO_2, can consume flue gas, clean wastewater, is not a food crop (first generation), and needs no productive land (second generation) (Carrington, 2012). Biodiesel from microalgae may be the only renewable biofuel that has the potential to completely displace petroleum derived fuels without disrupting the food supply and potentially has a negative carbon balance (Richardson, et al., 2010).

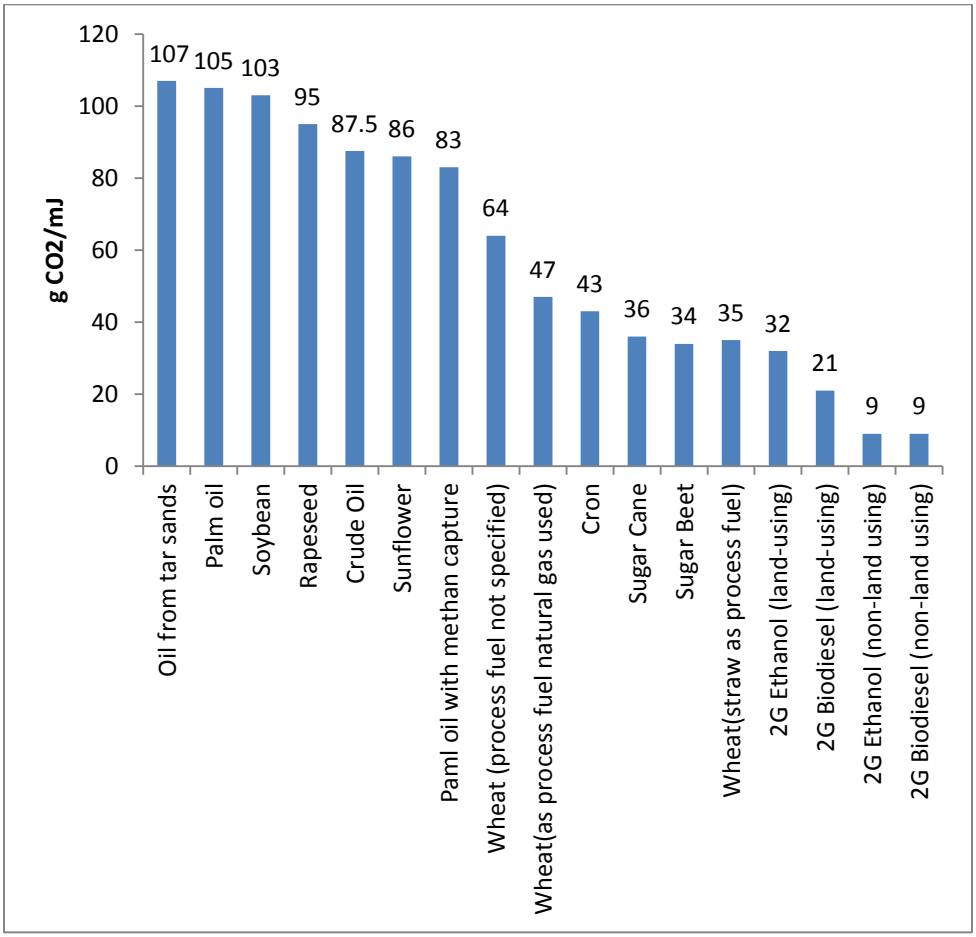

Figure 2: Carbon imprint of Biofuels (Carrington, 2012).

Besides biodiesel, microalgae can be used for the production of various energy carriers, including biomethane, biohydrogen, and bioethanol. Microalgae are unique among biofuel crops in producing lipids which are easily converted to biodiesel with yields per unit area 100 times or more than any other photosynthetic organism. The non-lipid biomass can be used for bioenergy by converting it to methane, hydrogen, and/or electricity. Algal biodiesel fuel is easily stored without pressurization, is high in specific energy and energy density, and is low in sulfur content and other characteristics that allow stringent emission controls (Greene & Plotkin, 2011). Algal oil has been proven to meet fuel standards, and has superior lubricating properties to reduce wear. Fuel efficiency decrease is only about 2% and particulate matter is reduced by about 27% when compared to petroleum diesel (Oilgae, 2013). Biodiesel can be directly used in diesel engines and can play a significant role in diversifying transportation fuels.

Technology for producing and using biodiesel has been known for more than 50 years (Chisti, 2007). For this reason the U.S. federal government and many state governments subsidize diesel fuel and its use has risen exponentially in recent years. The U.S. government has a goal of replacing 20% of transportation fuels with biofuels by the year 2030 (Shen, et al., 2009). This would require 28 billion gallons of biodiesel annually if it were the sole biofuel (Chisti, 2007).

Algae cultivation does not compete with food or feed crops, can be grown with brackish, salt or wastewater, and could benefit the small-scale farmer by generating employment and increasing rural electrification and incomes (Dismukes, et al., 2008)

(Alabi, et al., 2009) (Rittman, 2008). Production of algal biofuels has potential for integration with other environmentally sustainable technologies such as carbon sequestration and clean-up from industrial and agricultural wastes generated from biological wastes and combustion. Algal growth does eliminate NH_4, NO_3, and PO_4 as well as heavy metals from wastewater, and greenhouse gas (GHG) from flue gas (Frac, et al., 2010) (Nagase, et al., 2001) (Olaizola, et al., 2003) (Wang, et al., 2010).

Research conducted to study algae cultivation also benefits ecologists who have need of improving predictions of responses to environmental and climate change in marine ecosystems with phytoplankton at their base. Microalgae contribute approximately half of the planet's annual primary productivity by cycling 111 to 117 Pg carbon molecules annually (Flynn, et al., 2010).

Background and Motivation

Interest in growing algae commercially began nearly 100 years ago. Although microalgal cultivation in laboratories has now been undertaken for over 50 years, our experience is still limited to a few out of the some 50,000 species, and even for these, only 30,000 have been identified with very limited understanding of their biology and ecology (Alabi, et al. 2009) (Frac, et al., 2010) (Chaumont, 1993). The principles of cultivating algae in engineered raceways, open ponds and photobioreactors have been in place since the 1950's. In the ensuing decades the technological development of these principles into methods has been accomplished using the fields of biology, chemistry, mathematics, physics and production engineering. Despite $40 million invested by the U.S. government from 1980 to 1984 and $250 million by Japan in the 1990's, both

programs were abandoned largely because cultivating algae for biofuels alone is not considered economically feasible (Beneman, et al., 2004) (Sheehan, et al., 1998).

Consistently maintaining high yields of healthy algae using a low-energy, reliable, chemical-free system is the biggest challenge to overcome the extra investment cost required in order for algae cultivation to become profitable and fully competitive. However, existing commercial applications remain limited to specialty food and feed ingredients despite repeated and ongoing research and government applications for effluent bioremediation and biofuel production. Numerous photobioreactors have been described in scientific literature and patents, but only a small proportion have been commercialized to date. There exist many conflicting claims pertaining to algal productivity, required growth parameter values, design, and especially techno-economic prospects for growing algae with the intent of biofuel production.

Microalgae systems are currently used worldwide on a limited scale for wastewater treatment where the biomass is usually not harvested, and for some high value end products such as human supplements and aquaculture (Lundquist, et al., 2010) (Benemann & Oswald, 1996). Even in these commercial systems, algae growth is not standardized or optimized, which results in a wide range of quality and quantity of algae produced (Lopez-Elias, et al., 2008) (Degen, et al., 2001). Therefore any improvements are made by empiric observations instead of scientific principles or bioassays. The vast majority of companies trying to commercialize algae cultivation are not worthy of government grants, financial investment, or strategic partnership (Lux Research, 2012).

A rigorous assessment of the economics of production is necessary to establish competitiveness with petroleum-derived fuels (Chisti, 2008). Lack of consistent data can lead to faulty assumptions and makes creating an accurate financial model difficult (R. Lacey, personal communication, May 31, 2011). (Carvalho, et al., 2006) (Chaumont, 1993) (Greenwell, et al., 2010) (Kwangyong & Choul-Gyun, 2002) (Bayless, et al.) (Patil, et al., 2008) (Alabi, et al., 2009) (U.S. DOE, 2010). Many of the scientific and engineering assumptions in past studies require justification, such as the growth rates, productivity and lipid content.

Growth of microalgae is influenced by many factors, such as abiotic factors (e.g., light, temperature, nutrients, dissolved oxygen content, CO_2 concentration, pH, salinity, and toxic chemicals in the growth media), biotic factors (e.g., presence of bacteria, fungi, viruses and other algae), and operational factors (e.g., shear forces generated by mixing, dilution rate, and harvest method and frequency) (Shen, et al., 2009). Less than optimal lighting contributes to lower productivity through either photoinhibition in the intensely illuminated zones or consumption of biomass by respiration in dark zones (Degen, et al., 2001). All of these factors influence each other leading to an infinite number of growth scenarios. Microalgal research is most commonly centered on a single discipline, whether that is biology, chemistry, engineering, or financial. Given the lack of multidisciplinary research and lack of specific productivity and growth parameter data for specific species, a scalable, commercially viable system for producing microalgae has yet to emerge, let alone one which is adaptable for every strategy or environment (Hu, et al., 2008).

> "Successful development of an algae-based biofuels and co-products industry requires the optimum combination of technical innovations in systems and processes, coupled with economic feasibility in the practical implementation and integrated scale-up for commercial production and marketing (U.S. DOE, 2010, p.93)."

Rather than accumulate more data that is largely conjectural, this study intends to synthesize the large amount of data available from hundreds of studies into a reliable simulation for predicting growth rates, productivity, energy balance, cost parameters, and overall economic feasibility. Furthermore, the model is adaptable to the user design, which is necessary given the variety of growth scenarios and environments that are possible. This allows comparisons between various production processes to discover their fundamental limitations and potential for improvements within the scope of a design. While there has been an enormous amount of research devoted to the particulars of algal growth parameters and biology, there is a fundamental need for an integrated systems and financial analysis, which enables use of large amounts of data to design a profitable algal growth scenario.

Hypothesis

Previous economic analyses have been based on a number of site-specific assumptions, lack sufficient design details, and have not adequately addressed interfaces. Review of the decades of microalgal research and data led to the following hypotheses: Modeling an adaptable microalgae growing system enables design optimization to achieve higher productivity and reveals where production costs must be reduced with the goal of achieving economically viable algae biofuel. Variables, analysis and interfaces not included in the previous studies thus far are important and impact results. Factors to

optimize include algal productivity tied to algal species biological characteristics, pond and bioreactor design and operation, harvesting options and investment attractiveness using NPV (net present value) and IRR (internal rate of return).

Commercial production of algae for biofuels has not taken place not only for lack of economic justification but also for lack of detailed systems analysis. The following questions are among many concerning algal growth remaining to be answered: What is the optimal productivity for specific algal species for a profitable algal growth scenario, including required light intensity, oxygen removal, shear stress, and CO_2 availability? How do the geometry, mass flow rate, and culture density interact to affect algae productivity? What are the techno-economic effects when algae are fed flue gas and/or wastewater? What is the optimal approach when cost, CO_2 feed rate, and O_2 removal are integrated? How does the carbon footprint of biofuel produced from microalgae compare to petroleum based fuels? How do the economic feasibility and carbon footprint of open pond and photobioreactor growth scenarios compare?

An integrated approach allows a practical, realistic approach to growing microalgae, which is necessary for commercial applications and for the potential environmental benefits of microalgal growth to be realized.

Research Goals and Approach

The goal is to close the business case for producing biofuel from microalgae by proving it is economically and environmentally sustainable. The approach is to build a tool which enables determination of the economic and environmental feasibility of a certain design before investing time and expense in building it, as well as offer methods

for optimizing the design. Through systems modeling important details may be included and analysis can be accomplished while still in the preliminary stages of the design process through incorporating basic algal biology with cultivation science and engineering.

This study presents an integrated approach to optimize algal growth through photobioreactor (PBR) or open pond design and involves a three-pronged approach: (a) research to gather data on growing specific algae species and expected results, (b) develop a system model for an algae growing operation adaptable to various growth scenarios with various inputs and specific end products, and (c) perform analysis on selected cases using commercial best practices and methods researched in the literature to determine the economic and environmental feasibility of growing microalgae to produce biofuels. Factors to optimize include algal productivity, bioreactor and pond design and operation, harvesting options, and investment attractiveness.

The system model developed and presented in this study is different from past models because it incorporates detail and interfaces not found in other studies. The catch is for the model to simulate reality with sufficient fidelity.

Outline

This dissertation consists of 5 chapters including the background, motivation, hypotheses, and objectives of the research effort in Chapter 1. Chapter 1 also provides a summary of related information and previous research and how it relates to this study. Chapter 2 presents the methodology including model calculations and design, as well as methodology behind the financial analysis. Chapter 3 summarizes results from the model,

optimization and financial analysis. Chapter 4 discusses implications of findings and questions raised from the results. Chapter 5 summarizes this research effort and presents conclusions and recommendations for further research.

Definitions, Acronyms, and Abbreviations

ALR: airlift reactor

ASP: Aquatic Species Program (program run 1978-1996 by the U.S Department of Energy)

ATP: an energy carrier for the reaction that takes place in photosynthesis

BNR: biological nutrient removal

COD: chemical oxygen demand

DOE: U.S. Department of Energy

EROI: energy return on investment ($E_{R(Returned)}/E_{S(System)}$)

FLE: flashing light effect, sometimes called light-dark cycle, intermittent illumination, light intensity fluctuation, or dynamic light condition.

GHG: greenhouse gas

HLTP: horizontal-loop tubular photobioreactor

HHV: higher heating value

LED: light emitting diode

LHV: lower heating value

MWTP: Municipal Wastewater Treatment Plant

NADPH: a co-enzyme carrier molecule to carry ions to a different stage of the photosynthesis reaction

PAR: photosynthetically active radiation (400-700 nm)

Petro-diesel: petroleum-derived diesel

PBR: photobioreactor, includes solar illuminated PBR's and artificially illuminated ALR's in this study

QP: Quadratic Programming

SQP: Sequential Quadratic Programming

TOC : total organic carbon

WWTP: Wastewater Treatment Plant

Literature Review

The difficulty with the data obtained through hundreds of studies performed on microalgae research is there have been widely disparate conclusions drawn about optimal growing conditions and growth rate depending on the study's focus, culture conditions, and species and strain of algae used. The variables influencing algal growth are interdependent. When optimal parameters in one area such as CO_2 feed rate or lighting are reported, other parameters may not be optimal or verifiable, which can lead to faulty conclusions. Also, standards for measuring productivity vary between disciplines.

The following literature review is organized similar to the study along three overlapping focus areas: the biological research, research involving cultivating microalgae in photobioreactors and open ponds, fluid dynamic and biological modeling, and techno-economic studies.

Biological Research

Diatoms are the largest group of biomass producers on Earth. Phytoplankton life forms span a range in size from the smallest uni-cells at a volume of less than 1 μm^3 to large unicellular diatoms which may attain a volume of 10^9 μm^3 (1 mm^3) (Beardall, et al., 2008).

The internal density of diatom cells is an average of 1150 kg m^{-3}, which implies mixing is required to maintain suspension. However, this will change depending on the lipid concentration where a higher lipid concentration will result in a density less than the surrounding media. Thus, in the nutrient deprivation holding tank, the cells should float to the top surface of the media as the lipids increase. The model assumes the algal cell density to be 1150 kg m^{-3} for the purposes of fluid dynamics during the growth period. The cells also maintain suspension through intra-particular force created by a negative charge. The control and understanding of interactions between cells and with surfaces is important, and continues to be a major target of research (Greenwell, et al. 2010).

Determining the extent of nutrient limitation has been a fundamentally important question of aquatic scientists for decades. Nutrient limitation of net primary production can be an important control on phytoplankton growth in aquatic environments and understanding it can help limit eutrophication (Ho, et al., 2003). Metals used by phytoplankton include iron, manganese, zinc, copper, cobalt, cadmium, and molybdenum, in descending importance. A higher metal concentration of one ion can inhibit uptake of other metals and phosphorus (Chisti, 2007). In addition to the metal available in the medium, the quota of trace metal in phytoplankton may depend on the

light regime, the concentrations of major nutrients, and the concentrations of other trace metals. Culture and field studies indicate trace metals can be important in controlling primary production and regulating community structure of marine phytoplankton (Ho, et al., 2003) (Berman-Frank, et al. 2007).

The Redfield ratio for diatoms describes the necessary carbon, nitrogen, and phosphorus ratio: 106:16:1 (Sato, et al., 2010) Diatoms generally require nitrogen, silicon, and phosphorus in a 16N:16Si:1P. Most microalgae also require vitamin B12 (cyanocobalamine), B1 (thiamine), and vitamin H (biotin). EDTA (Ethylenediaminetetraacetic acid disodium salt dehydrate) is added to keep the trace metals in solution, although there are some reports that EDTA can inhibit growth of some species (Sonnekus, 2010).

Chlorella kessleri and *B. braunii* cultures effectively eliminate nitrate and phosphorus in wastewater, reducing it by 88% to 98% in 10 to 14 days. Similar results were obtained using ammonium as the nitrogen source instead of nitrate. Even with concentrations of nitrogen reaching 1400 mg/mL, the culture showed no inhibition as long as pH is maintained within optimal range (Kwangyong & Choul-Gyun, 2002) (Miao, et al., 2008) (Tsukahara & Sawayama, 2005) (Hall, et al., 2010) (Wang, et al., 2010). Five planktonic diatoms showed no preference for organic or inorganic nitrogen sources under high and low light intensities in another study (Fisher & Cowdell, 1982).

If wastewater contains a large amount of total dissolved solids, the resulting algal biomass may be assumed to contain these solids, and effectively limit available end products (Richmond, 2004), but larger particles as well as bacteria can safely and cost-

effectively be removed with filters (Wang, et al., 2010). Chinnasamy, et al. (2010) studied 27 species of green algae, 20 species of cyanobacteria and 8 species of diatoms in both treated and untreated wastewaters. Results showed a consortium of 15 algae produced maximum biomass and lipids and removed 96% of nutrients in 72 hours.

Many algae have the ability to produce 20 - 90% dry cell weight of storage lipids, which has been shown to increase under photo-oxidative stress, nutrient deprivation or other environmental conditions, but this mechanism is poorly understood and depends on the strain of algae (Tsukahara & Sawayama, 2005) (Hu, et al., 2008) (Alabi, et al., 2009) (Food and Agriculture Organization of the United Nations, 1997) (Vega, et al., 2010). Many studies do not report the age of the culture when the lipid content analysis was performed, which may partially account for the wide range of results.

High salinity produced high lipids in only one out of 10 species studied in Sonnekus (2010). Older studies reported that the lipid content of the diatom *Navioua pelliculosa* increased by about 60% during a 14-hour silicon starvation period, but Rijstenbil, et al., (1989) found low salinity leads to inhibition and cell deformation (Food and Agriculture Organization of the United Nations, 1997). Parrish & Wangersky (1987) found nitrogen stress while cultivating *P. tricornutum* does not result in any change in total lipids per cell, but does affect the types of lipids stored. Yongmanitchai & Ward (1991) found increased lipid content and increased growth rates when nitrate and urea concentrations increased, while other studies found increased growth rates but no increase in lipid content (Carden, et al., 2002) (Illman, Scragg, & Shales, 2000). However, more recent studies reveal that nitrogen, silica, and phosphorus deficiency does

produce higher lipid content (Alcain, 2010) (Vega, et al., 2010). Renaud, et al, (1991) found high photon densities significantly reduced the EPA content of *Nannochloropsis oculata*.

It is generally agreed upon the algae must stop dividing before accumulation of lipids occurs, which makes a two stage cultivation process desirable. This is consistent with the view that the greatest accumulation of lipids occurs when algae have been in the same medium for the greatest period of time (Parrish & Wangersky, 1987). Siron, et al. (1989) found that by the end of the stationary phase the fatty acid content in *P. tricornutum* increased to three times of the fatty acid content during the exponential growth phase. This is the same range as that reported for other diatoms, and may be due to the nitrogen deficiency occurring at the end of growth or light limiting due to the high density of the culture. Also, the type of fatty acids changed, with the palmitic lipids increasing and specialized lipids such as EPA and pigments decreasing. This emphasizes the importance of staging tanks to allow harvesting at specific times in the growth cycle depending on the algae species and the desired end products.

Growing Methods

It is possible to grow algae in open ponds, immobilized culture systems, or photobioreactors. Open ponds are seasonal due to light and temperature changes, are easily contaminated, use a relatively large amount of land, yield low productivity, demand higher harvesting costs because of the large volume of water, and lose a large amount of water to evaporation. The algae species which yield a high percentage of lipids also cannot compete with the fast-growing high carbohydrate algal species, so they

must be protected from contamination (Shen, et al., 2009). Up to 25% of the culture is lost at nighttime in open ponds, depending on light level under which the biomass was grown, the growth temperature, and temperature at night (Demirbas & Demirbas, 2010).

Operations parameters for raceways which are candidates for analysis and optimization include temperature, incident radiation, effects of covering raceways with greenhouses, nutrient availability, depth flow characteristics, geometry and channel dimensions and predation (James & Boriah, 2010). The literature in general has found that open raceway ponds have a lower energy use and smaller CO_2 footprint than photobioreactors, but the choice of materials for photobioreactors can make a significant impact on results, and most open pond energy analyses do not consider all the pumping and extra harvesting energy required with a much larger volume of water (Brentner, et al., 2011).

Immobilized culture systems involve immobilizing the algae by growing them in a polymeric matrix or attached communities in shallow streams on rotating biological contactors. Limited research has been done in this area and would be ideal in certain applications for its ease of harvesting, but it is limited to a certain number of algae species, has high material costs, and would be difficult to scale up (Shen, et al., 2009) (Christenson & Sims, 2011). Biofilm reactors are a subject of many companies' pilot demonstrations, but remain to be proven or developed on an industrial scale (Christenson & Sims, 2011).

Internally illuminated photobioreactors are preferable to open ponds for cultivating algae with the intent of biofuel production if they are economically

sustainable and profitable since they are more productive, but have been used in large-scale biomass production only for high-value products (Chisti, 2007). The volumetric productivity of photobioreactors is more than 13 times greater than raceway ponds (Chisti, 2007) (Richmond, 2004**)** (Greenwell, et al. 2010) Numerous photobioreactors have been described in scientific literature and patents, but only a small proportion have been commercialized to date due to high construction and operating costs and complexity (Greenwell, et al. 2010) (Shen, et al., 2009).

A photobioreactor is normally either bubble column or an airlift reactor (ALR), where the latter varies from the former in the type of fluid flow. An ALR directs fluid circulation through the use of channels, with a riser for gas/liquid upflow and a separate channel for downflow (Merchuk & Gluz, 2002). The most suitable algal growth system is situation, species and final purpose dependent (Iancu, et al., 2010).

Gas Exchange

Photobioreactors may be operated in batch, semi-continuous or continuous modes. In a continuous culture, the substrate must be inoculated with a dose of microalgae and then continuously stirred. CO_2 is heavier than water and acidifies water. The gas exchange system which delivers CO_2 and removes photosynthetically generated O_2 is an integral part of the design and through an airlift pump and bubble sparging can provide the physical mixing, as well. Physical mixing is required to ensure nutrients, algae, lighting, metabolites, heat and gases are distributed, and becomes more important as the culture density increases (Qiang & Richmond, 1996) (Carvalho, et al., 2006)(Frac, et al., 2010) (Lee & Palsson, 1994) (Chisti, 2007) (Preston, et al., 2001).

It is important to obtain a reliable prediction of CO_2 transfer rates for accurate design, scale-up and operation, but the range of CO_2 percentages and feed rates in the literature span a wide range. The CO_2 delivery should be regulated through a pH-based monitoring and control system, so that the algae can absorb as much CO_2 as possible while avoiding precipitation into salts and pH imbalance. A balance can be achieved in pH through the acidifying effect of CO_2 and alkalizing effect from nitrogen uptake (Behrens, 2005). Research indicates a pH between 8.2 and 8.6 provides optimal productivity, and is the pH of natural seawater. (Raminathan, et al., 2011) (Alcain, 2010). However, pH for freshwater species will likely be lower at around 7.5 (Kong, et al., 2010).

Some research has used alkalis such as sodium hydroxide and calcium hydroxide to raise the culture pH above 10 to induce lysis, making it easier to harvest lipids (Molina Grima, et al., 2003). The culture pH which induces lysis is species dependent, as more recent research reveals *Chlorella* sp. grows at near optimal productivity in media at a pH of 10 as long as nutrients are available (Wang, et al., 2010).

The relationship between CO_2 and pH, and their effect on phytoplankton requires further investigation, and is an area of increasing interest especially in marine waters due to climate change (A. Quigg, personal communication, May 20, 2011). More studies on long-term exposures to elevated CO_2 and decreased pH are needed to determine the true impacts. There is a need for further experimentation using several strains and a variety of techniques to evaluate the effects on phytoplankton cells in terms of growth and photosynthesis (Beardall, et al., 2008).

Gas inlet CO_2 concentrations in many biological studies are between 0.1 to 2.0%, with some results indicating highest productivity is obtained at 2.0% at 1 - 2 L/min per liter of culture (Hall, et al. 2001) (Ranga & Ravishankar, 2007) (Thomas & Gibson, 1990). Studies more focused on carbon capturing mimic flue gases at up to 12% CO_2 partial pressure (Doshi, 2006). Other studies found 85-85% CO_2 absorption with 6-12% CO_2 content, but determined the efficiency for CO_2 transfer to the medium depends on the flue gas content, culture media alkalinity, water depth, and mixing velocity (Benemann, et al., 2009) Olaizola, et al., (2003) determined microalgae can capture CO_2 under a wide variety of pH and gas concentrations, but the efficiency is directly dependent on the pH of the culture instead of the gas composition differences.

Oxygen removal becomes an issue where the mixing is not optimal and in long, tubular photobioreactors where the oxygen concentration continues to rise along the length of the tube. Within an upright, bubble sparged, artificially illuminated PBR, oxygen escape would be easily facilitated through the top surface of the photobioreactor if considered in the design.

Some studies used fibers instead of a bubble sparger to deliver CO_2 to the culture, which resulted in a physiochemical improvement but not a biotechnological gain (Ferreira, et al., 1998). Research indicates that in cells up to 50 μm in diameter, the boundary layer thickness is equal to the radius of the cell, and whether this boundary layer leads to growth limitation depends on rates of diffusivity and nutrient transport at the cell surface, as well as mixing rate. As mixing rate increases, the laminar boundary layer decreases (Alabi, et al., 2009) (Acien, et al. 2001) (Hondzo & Lyn, 1999). Direct

measurement of boundary layer thickness has only been possible for relatively large colonial planktonic organisms, and evidence for boundary layer effects has been mixed, highlighting the need for further investigation.

The bubble sparger can produce turbulent conditions and high mass transfer, and the turbulence also prevents biofouling on the reactor surfaces. Laminar mixing is to be avoided since it permits cell precipitation and wall growth and does not allow oxygen to be released (Carvalho & Malcata, 2001) (Richmond, 2004) (Beardall, et al., 2008) . It is important to avoid shear stress while mixing, although the amount of shear stress to be avoided depends on the individual species, and intensity of shear stress is difficult to determine in bioreactors (Chisti, 2007) (Peters, et al., 2006). Research has revealed the effective viscosity (and shear rate) increases dramatically if slug flow is allowed to develop (Schumpe & Deckwar, 1987) (Merchuk & Gluz, 2002). Dimensions of fluid microeddies should always exceed those of algal cells. Also, bubble breakup or coalescence can damage algal cells. (Qiang & Richmond, 1996) (Acien, et al., 2001)

Although it is widely recognized that some form of shaking and aeration is necessary for culture health and growth rate, the rates of stirring or aeration are seldom quantified (Savidge, 1981). In none of the studies were degrees of turbulence expressed in terms of variations in strain rate, stress or dissipation rate. Also, there has not been an analysis done on how the culture media, culture density, saltwater, and temperature induced viscosity changes affect the shear stress. The shear stress was quantified indirectly using the flow rate and number and frequency of pump passages or power input. (Michels, et al., 2010) (Thomas & Gibson, 1990) (Contreras, et al., 1998). Most

turbulence related studies induce turbulence on a shaker table, which is not applicable to an industrial scale algal growth facility (Peters, et al., 2006).

In-depth knowledge of hydrodynamics/flow pattern in a photobioreactor design is key for design and scale-up (Al-Dahhan & Luo, 2006). One study reported a velocity lower or higher than 0.055 m s^{-1} inhibited growth, which was found to be related to the specific gas-liquid interfacial area, the length scale of the microeddies and the bubble and viscous shear rate. The geometry in this case was a cylindrical tube 0.09 m in diameter and 2 m high, and used air bubbled though a sparger 0.02 m in diameter with 60 µm pore-size (Contreras, et al., 1998). Laboratory gas inlet velocities with tubes 0.01 - 0.1 m diameter and 1 - 2 m long are normally in the range of 0.04 - 0.09 m s^{-1} (Al-Masry & Chetty, 1996) (Barbosa, 2003) (Al-Dahhan & Luo, 2006). Slightly larger photobioreactors report liquid velocities in the range of 0.5 m/s for a 0.2 m^3 volume. A photobioreactor with a larger volume without any mechanical shaking or stirring will require a higher gas velocity. Doshi (2006) used a velocity of 1 m s^{-1} in a volume of about 6 m^3. This also simulates flue gas conditions while providing the necessary nutrients for a more dense culture and larger volume. Lundquist, et al. (2010) proposed the optimal gas velocity to be 20 to 30 cm s^{-1} for open ponds, counter to a fluid velocity of 20 to 25 cm s^{-1}, resulting in a bubble velocity of 0.05 m s^{-1}. This calculation was primarily based on limiting the power input required for the paddlewheel.

Cleaning

Photobioreactors must be periodically cleaned and sanitized which can be achieved through clean-in-place operations such as use of large slugs of air to

intermittently scour the surface areas, highly turbulent flow, and enzymes which digest the polymer glue that binds algal cells to the walls (Chisti, 2007). Also, if the photobioreactor is large enough, the sides can be cleaned manually immediately following a harvest by wiping the interior surfaces.

Culture Density

Culture density is often not reported, and reported productivities vary widely depending on the study parameters. The U.S. DOE Algal Technology Roadmap (2010) stresses there is an immediate need for standardization of productivity models and establishment of protocols for measuring yields, rates and densities. Recommended optimal growth density in a laboratory is around 1e6 cells mL^{-1} (A. Quigg, personal communication, May 20, 2011), but densities in photobioreactors necessarily exceed that with 2e9 cells mL^{-1} or even 1.2 - 1.4e10 cells mL^{-1} (Chaumont, 1993). Moreover, density reported in cells mL^{-1} does not reflect the size of the cells which can vary significantly depending on the species. Obtaining robust data is difficult, and either commercial reports are grossly exaggerated or research models are grossly incorrect (Richmond, 2004).

The relationship between the biomass concentration and turbidity is described by: $C_b = 0.38 * OD_{625}$ where C_b is the biomass concentration (kg m^{-3}) and OD_{625} is the optical density at 625-nm. (Contreras, et al., 1998)

An equation developed to describe the relationship between the various growth parameters and cell density is $Y = E_m I_o AK(1-e^{-acl}) – GRcV$, where Y = yield (g cells/h), E_m= 0.20(the max attainable photosynthetic conversion on an energy basis), A =

illuminated area (m_2), K=0.156(g cells/h/W)energy equivalent of the algae, I_o = light intensity (W/m^2), a=extinction coefficient (L/cm/g), c = cell concentration (g/L), l = light path (cm), R = respiration rate (g carbon/g cells/h), V = culture volume (L), and G = ratio of g cells to G carbon (2.04) (Radmer, Behrens, & Arnett, 1986) (Janssen, Tramper, Mui, & Wijffels, 2002).

Many studies report that a maximum growth rate was found under certain conditions but don't report what the maximum growth rate was and those that do report a growth rate vary widely, both in how it is computed and the actual amount (Alabi, et al., 2009). Open ponds and raceways report productivity in a range of about 10 - 60 g m^{-2} d^{-1}. However, areal productivity has little meaning when a system is vertical, as is possible when photobioreactors are used (Tredici & Zittelli, 2010). Productivity of algae grown in photobioreactors range from a volumetric productivity of 0.64 g L^{-1} d^{-1} to 173 g L^{-1} d^{-1} (Alabi, et al., 2009) (Kang, et al., 2010) (Lee & Palsson, 1994) (Brune, et al., 2009) (Contreras, et al., 1998) (Raminathan, et al., 2011) (Sheehan, et al., 1998) (Putt, 2007) (Chisti, 2007) (Zou,et al., 2000) (Chaumont, 1993). Also, productivity is often indistinguishable from growth rates in these studies, but in reality they are not synonymous. Productivity includes the resulting cell composition, while growth rate refers only to how quickly the algae reproduce. Achieving maximum growth rate will not always equate to optimal productivity, depending on the desired end products and vice versa (Pittman, et al., 2011).

A culture undergoes an exponential growth phase until the nutrients become limited, self-shading increases, pH rises, and wastes build up. Then the culture may

continue to grow linearally or enters a stationary phase during which density declines and bacteria may proliferate (Creswell, 2010) (Contreras, et al., 1998). Diatoms also secrete autoinhibitors when a culture reaches a certain density. Research indicates the autoinhibitory activity which slows growth at high densities can be reversed when the culture medium is replaced at least every 48 hours, as opposed to simply injecting new nutrients; thereby allowing growth to continue unabated, resulting in an exponential growth phase of up to 12 days (Zou, et al., 2000) It may also be important to consider a lag phase during which the cells become acclimated to a new medium when introduced from an inoculum.

Lighting

The productivity of photobioreactors is largely determined by the light regime inside of the reactors, oxygen removal, nutrient availability, and shear stress (all of which are functions of mixing and gas exchange) (Janssen, et al., 2002). Proper location of the light source and suitable gas-liquid thermodynamics determine growth rate and productivity (Frac, et al., 2010). An efficient PBR should be designed to deliver only the photons required for the microalge to fix CO_2 molecules (Akhilesh, et al., 2011).

Ten patents were issued in two years for lighting inside of culture systems and continue to proliferate (Chaumont, 1993) (McCall, 2011) (Van Walsem, et al., 2011). Horizontal photobioreactors experience strong axial gradients with CO_2, so vertical columns are preferred with CO_2 introduced at the base. However, this introduces less efficient optical density, which is remediated with an internally illuminated vertical

column photobioreactor. Combining efficient illumination at high culture densities with efficient gas transfer is the goal (Richmond, 2004) (Greenwell, et al. 2010).

Irradiance for maximum growth rate varies between studies, from 100-140 µmol photons m^{-2} s^{-1} (Beardall & Quigg, 2003), 150 µmol photons m^{-2} s^{-1} (Quigg, et al., 2006) 280 µmol photons m^{-2} s^{-1}, (this study found higher irradiance inhibited growth) (Hall, et al., 2003), 400 µmol photons m^{-2} s^{-1} (Kang, et al., 2010), 347 to 1584 µmol photons m^{-2} s^{-1} (Lopez-Elias, et al., 2008) 500 µmol photons m^{-2} s^{-1} (Finkel, et al., 2007), to 1200 µmol photons m^{-2} s^{-1} (Contreras, et al., 1998) , and 1712 µmol photons m^{-2} s^{-1} at 5% CO_2. (Chrismadha & Borowitzka, 1994) Zou, et al. (2000) found increased growth rate in *Nannochloropsis sp*. at 3000 µmol photons m^{-2} s^{-1} when the culture medium was replaced every 48 hours, stirring was provided by bubbling 2% CO_2 enriched air, and the light path was kept at 14 mm (not including self-shading).

Augusti & Kalff (1989) found the relationship between cell size and maximum biomass density is independent of lighting and based on a relationship of 0.75 (3/4 rule), as the density varies by the -0.79 power of the cell volume. However, only two light intensities were used (11 and 220 µmol photons m^{-2} s^{-1}), and other physiological factors could have played a role, such as nutrient limitations. Other studies since then have found cultures can be light limited even when irradiated at 220 µmol photons m^{-2} s^{-1}, depending on the culture density and flow conditions (Beardall & Quigg, 2003) (Hall, et al., 2003) (Kang, et al., 2010) (Finkel, et al., 2007)(Contreras, et al., 1998) (Chrismadha & Borowitzka, 1994) (Zou et al., 2000).

The key is for the light and nutrient conditions to be saturating so as to prevent respiration, but not excessive to ensure efficiency and prevent photoinhibition (Sonnekus, 2010). Most algae get light saturated at 20% solar light intensities, which is about 220 μmol photons m^{-2} s^{-1}, and conflicts with reports from studies cited above (Alabi, et al., 2009). Many studies indicate algae productivity increases with higher irradiance, but also depends on other factors such as gas exchange, culture density, mixing rate, and medium replacement (Beardall & Quigg, 2003) (Hall, et al., 2003) (Kang, et al., 2010) (Finkel, et al., 2007) (Contreras, et al., 1998) (Chrismadha & Borowitzka, 1994) (Zou et al., 2000).

Only 48.7% of the incident solar energy reaching the earth's surface is within the photosynthetically active band (400-740 nm) (Zhu, et al., 2008). There are also differing reports on photosynthetic efficiencies depending on lighting source, species, time of day, and methods used. The literature reports photosynthetic efficiencies ranging from 1.3% to 34% (Janssen, et al., 2002) (Ferreira, et al., 1998) (Chaumont, 1993) (Sheehan, et al., 1998) (Miyamoto, 1997) (Behrens, 2005) (Tredici & Zittelli, 2010) (Ragni & D'Alcala, 2007). When considering sunlight as the light source, NREL found an algal photosynthetic average of 1.3% in their research (Sheehan, et al., 1998). Miyamoto (1997) reports photosynthetic efficiency of 3 - 6% of total solar radiation, while Zhu et al (2008) reports 2.4% for C3 and 3.7% for C4 efficiency over a whole growing season. Behrens (2005) reports the photosynthetic efficiency of converting absorbed light into ATP and NADPH is 20% for red light. Janssen, et al. (2003) reports 10 - 20% efficiency of harvesting absorbed light energy in photosynthesis.

Deviations from strictly linear correlations occur under stress conditions such as high photon flux or nutrient limitation. Insufficient caution in lab experiments adds methodical errors, such as changing the medium, and causing different nutrient status. In many cases high light intensities induce limitations in CO_2 fixation. The extent to which changes in energy production and energy quality affect cell function and downstream energy distributions is complex. Some processes in marine primary producers run counter to photosynthetic metabolism and may confuse or complicate the interpretation of measurements. Gas exchange measurements should thus provide estimates of net photosynthesis, if incubation is long enough for respiratory substrates to become labeled (Beardall, et al., 2008) (Suggett, et al., 2009).

The photosynthetic capacity reaches a maximum before the end of the exponential phase of growth and declines thereafter. Higher light intensity causes the photosynthetic capacity to decrease more rapidly, and high irradiance such as experienced in the sun on summer days cause photoinhibition (Tredici & Zittelli, 2010). Cultures exposed to a prolonged period of darkness (up to 16 days at 18°C) maintain a high photosynthetic capacity. (Griffiths, 1973) Research shows that biomass productivity and EPA productivity can be maximized by optimizing cell density, irradiance, addition of CO_2 and mixing. (Chrismadha & Borowitzka, 1994) (Lu, et al., 2001).

P. tricornutum is able to sustain growth even at 10^{-4} of full sunlight, and adjust metabolic activity accordingly. (Beardall, et al., 2003) Dark survival varies between species, may be temperature dependent, and may be prolonged by periodic sub-compensation intensity illumination (Smayda & Mitchell-Innes, 1974). Akhilesh, et al.

(2011) found that no light penetrates deeper than 30 cm irrespective of cell density, but this does not consider turbulence which will move algae in and out of the un-illuminated areas sufficiently to allow exposure to light while avoiding photoinhibition.

At any given instant, most of the cells at optimal cell density are exposed to darkness. The shorter the light path is, the higher the intensity of the light-dark cycles. Combining proper geometry of illumination with medium circulation can ensure cells are circulated at optimal frequency between light and dark zones. The tube diameter is limited by illumination zone, depending on light placement, and the length is limited by maximum velocity without damaging the cells, rate of photosynthesis and removal of oxygen. Research indicates short bursts of intense light followed by longer dark cycles, or ensuring the algae does not remain in either well-lit or dark areas for long periods permit a significant rise in productivity (Chisti, 2007) (Carvalho, et al., 2006) (Richmond, 2004). While there are slight variations on reported optimal light to dark ratio, the general consensus is a light to dark residence time with a ratio of 1:10 will yield optimal productivity (Frac, et al., 2010) (Acien, et al. 2001) (Chisti, 2007) (Lundquist, et al., 2010) (Degen, et al., 2001).

Temperature

Optimal temperature for growing most microalgae is between 20 and 30°C. Photobioreactors with artificial lighting may require cooling at times, but this can be accomodated with cooling the input media as it is fed into the culture, and/or a simple heat exchanger. Tubular PBR's exposed to sunlight will rapidly overheat, unless they are cooled. Cooling can be via heat exchangers or evaporative cooling (Chisti, 2008), but the

latter requires more water, a valuable resource. Open ponds must be protected from both low and high extremes in temperature induced by the environment.

Photosynthetic rate declines most rapidly during growth at higher temperatures, and while growth at lower temperatures does not affect their ability to photosynthesize at lower temperatures, it does reduce their ability to assimilate carbon dioxide at higher temperatures (Doshi, 2006) (Morris & Glover, 1974). Research has been performed at temperatures from 16 - 27°C but most often is performed around 20°C. (Alcain, 2010) (Finkel, et al., 2007)) (Contreras, et al., 1998) 21.5 to 23°C was shown to improve fatty acid production in *P. tricornutum* (Yongmanitchai & Ward, 1991). Other studies suggest a temperature of 24 to 25°C produces better results than room temperature. (Pisutpaisal & Boonyawanich, 2008) *Nannochloropsis oculata* was grown at 27 +/- 1°C in Zou, et al. (2000) (Creswell, 2010).

Harvesting

Harvesting consists of recovery of algae from the media, and recovery of specific products from the algae. Recovery of microalgal biomass requires one or more solid-liquid separation steps which are made difficult due to the small size (3 - 30 µm diameters) of the cells (Molina Grima, et al., 2003). Recovery of biomass from a photobioreactor is much easier than from a raceway pond, due to 30 times the microalgal concentration and much smaller surface area. Filtration and centrifugation can be used for biomass recovery, but is a significant part of the cost model (Chisti, 2007). Using filtration for biomass recovery directly in the media is difficult with the small size of the algae, since the filter would bind almost immediately and would be very slow (Putt,

2007). However, filter presses, which combine filters with mechanical pressing, can effectively be used for denser product following centrifugation. Filter presses are in common use throughout the food processing industry, and can be designed for small particulates such as algae.

A low cost, energy efficient, and simple means of harvesting algae presented by Putt (2007) involves a three step process including flocculation and settling, dewatering, drying, and a mechanical press. Drying the algae in an oven is energy intensive, but methane derived from biomass can be used to power the heater. Supercritical CO_2 is a "green", highly effective solvent, but it requires high pressure equipment that is both expensive and energy intensive. Chemical solvents present safety and health issues, and can be energy intensive. They also lack efficiency when used in saltwater (Bilanovic, et al., 1988). Solvents are often used in combination with mechanical pressing.

Following harvesting of the lipids, they must undergo transesterification (process of adding three molecules of alcohol to one molecule of natural oil) to produce biofuel (Richardson, et al., 2010) (U.S. DOE, 2010) (Verma, et al., 2009). This process is relatively mature and has been commonly used to convert vegetable oils into biodiesel (U.S. DOE, 2010).

Fluid Dynamic and Biological Modeling

Modeling techniques are of potential use to optimize algae growth, bioreactor design and operation, production facility operation, and for coupled operation, financial modeling and risk analysis. Past models have focused on very small scale, and are simplistic, non-dynamic, and non-mechanistic with bioreactor-type applications typically

structured by deterministic ordinary differential equations (Greenwell, et al. 2010). Decades of microalgal research have provided the types of data required to fully develop or parameterize models for commercial exploitation of algae. Coupled fluid dynamics and biological modeling offer additional potential with the main parameters being dilution rates, optical path length, and nutrient and light supply (Richmond, 2004) (U.S. DOE, 2010).

Researchers have sought to explain the complexities of light distribution within photobioreactors using light distribution models which allows productivity to be predicted in some cases. Turbulent flow in a photobioreactor affects culture producivity in part because of the high-frequency flashing light effect (FLE), which has been recognized for decades (Davis, et al., 1953) (Frederickson, et al., 1961). The FLE is sometimes called the light-dark cycle (LDC), intermittent illumination, light intensity fluctuation, or dynamic light condition. Models have also been developed to simulate growth of algae in bioreactors with different lighting schemes, different levels of mixing and reactor design, and one study included various strains of algae (Greenwell, et al. 2010) (Sato, et al., 2010) (Degen, et al., 2001) (Molina Grima, et al., 2000).

Two studies combined the three-state model with a model that predicts the trajectory of cells (Merchuk & Wu, 2003) (Sato, et al., 2009). CFD was used to create a three-state model by Al-Dahhan & Luo (2006) to simulate movement with a radioactive particle to see phase distributions in a photobioreactor, and graph viscosity versus shear stress at different densities. This study found CFD is not ready to be used under dynamic growth of microalgae to predict growth rate, but does have the potential. Sato, et al.

(2010) developed a three-state model as well by incorporating a CFD two-phase turbulent model with a photosynthesis model representing the FLE which calculated the carbon fixation and the growth curve of the microalgae. The results were moderately validated by cultivation experiments using real microalgae, but would benefit from including more parameters such as temperature.

Hall, et al. (2003) proposed to show the influence of superficial gas velocity on gas hold-up, induced liquid velocity, and mass-transfer coefficient. The study only revealed irradiance and gas velocity must be coupled (at 280 µmol photons m^{-2} s^{-1} and gas velocity of 0.41 m s^{-1}) to maximize productivity. In order to model CO_2 mass transfer, hydrodynamic conditions such as gas expansion, bubble rise velocity, culture density, bubble mean diameter and interfacial area must be considered. (Grima, et al., 1993) (Contreras, et al., 1998) CO_2 concentration is affected by two concurrent processes: gas-liquid mass transfer and CO_2 consumption in chemical reaction. At least one study has ignored the chemical reactions and based mass transfer coefficient solely on gas velocity and biomass concentrations (Contreras, et al., 1998). Another more recent study developed a model to simulate physical-chemical parameters with diffusion and physical absorption based on Henry's law and absorption with chemical reactions based on film theory (Iancu, et al., 2010). Chemical reactions may also lead to varied rates of CO_2 absorption, but the influence has not been investigated.

Other fluid dynamic models involved designing arrangement of optical fibers and light distribution in a PBR using Monte-Carlo simulation (Zsuzsa, et al., 2001). Trujillo, et al., (2008) studied enhancement of incident radiation due to bursting of bubbles at the

surface of an externally irradiated bubble tank PBR, experimentally and by CFD simulation. Akhilesh, et al. (2011) attempted to determine light distribution in an open pond and to compare the simulation output to the light distribution obtained by the Cornet model, which was a one-dimensional simulation coupling light transfer and growth kinetics (Cornet, et al., 1992). Data from Akhilesh, et al. (2011) found good correlation with the Cornet model, CFD analysis, and other studies, but examined a limited range of densities, considered solar lighting only, and the initial surface intensity was not explained clearly.

Research has been conducted by mathematically modeling the mass transfer coefficients from titration curves of the carbonic acid, which indicated the liquid flow rate achieved higher efficiencies while the gas flow rate had no effect (Acien, et al. 2001). The volumetric mass transfer coefficient depends on the physical properties of the fluid, the fluid flow and the system and geometry of the gas injector (Iancu, et al., 2010).

Organic substances, solids, phenols, alcohols, acids and electrolytes can appreciably modify density, surface tension, and ionic strength which can reduce coefficient transfer factors. However, this requires further investigation, especially since at least one study revealed the culture density does not significantly affect the viscosity and surface tension of the culture medium (Grima, et al., 1993) (Talbot, et al. 1991) (Lee & Hing, 1989). The highest viscosities and non-Newtonian flow behavior are usually encountered at the end of batch cultivations as the density reaches its maximum (Schumpe & Deckwar, 1987).

Recent studies indicate the algae cells themselves alter the viscosity of the medium, depending on size, density, and whether they are motile or non-motile (Sokolov & Arnason, 2009). A study in France even showed the spherical *Chlamydomonas reinhardtii*, a single-celled green algae with flagella, increase the viscosity of the medium in which they are swimming by a factor of two over the same culture density containing only dead cells (Rafai, et al., 2010). Michels, et al. (2010) found shear-thinning only occured when thickener was added to the culture of *Chaetoceros muelleri* even when the algal concentration was 5 to 10 million cells/mL (5.9 - 11.84 wet g/L).

Studies have been performed to develop computing software to make an energetic evaluation of cultivating marine macro-algae for biomass (Barberio, et al., 2005). A simulation model in another biologically focused study was created consisting of photoadaptation, gross photosynthesis, and respiration under wide irradiance levels (Dismukes, 2008). Yet another study focused on describing growth, CO_2 consumption and H_2 production for *A. variabilis* under different irradiances and CO_2 concentrations. The model predicted growth, CO_2 consumption, and O_2 production within 30% (Berberoglu, et al., 2008).

Techno-economic studies

A few studies have argued that biofuel production from algae is both economical and environmentally sustainable (Chisti, 2008) (Batan, et al., 2010), while most view the long term viability and economics of biofuels from algae skeptically (Lux Research, 2012) (US DOE, 2010) (Frank, et al., 2012) (Sun, et al., 2010). Some techno-economic studies have been conducted which couple wastewater treatment with algal growth, and

these show the most potential of a sustainable and economical algal growth for biofuels scenario (Beal, et al., 2012) (Pittman, et al., 2011) (Christenson & Sims, 2011). One valid criticism of all techno-economic studies is the total cost in fossil fuels for the algal growth facilities, supply of nutrients, and harvesting which result in a net negative energy output are not considered on a realistic scale.

Most financial studies have concluded photobioreactors are not economically feasible except for growing inoculums (U.S. DOE, 2010). The problem with making algae cultivation economical lies with the cost and complexity of the facilities needed to grow algae at an industrial scale (Lux Research, 2012). It is generally agreed the cultivation of algae must be multipurpose to be economically feasible, such as extracting Eicosapentaenoic acid (EPA) from algae lipids prior to using the remaining lipids for biodiesel (Greenwell, et al. 2010) (Pedroni & Benemann, 2003). There is also little published information on the environmental and public health impacts of algae cultivation or effluent compositions (Alabi, et al., 2009).

Economic studies in the literature base capital cost estimates on local experience, assumptions, proprietary data and/or limited research, and are lacking in detailed analysis (U.S. DOE, 2010). The proposed system in the studies is normally based on one or two different designs, and comparisons are impossible since the level of detail is not available while the range of inputs and outputs is extensive when based on experimental research and various species. The U.S. DOE has begun an initiative to obtain consistent quantitative metrics for algal biofuel production in order to establish an “integrated baseline” (ANL;NREL;PNNL, 2012). Richardson, et al., (2010) estimated the

production cost for algae using a Monte Carlo simulation methodology. Critical input variables were determined stochastically, and only two scenarios were included.

James & Boriah (2010) developed an open raceway model to simulate raceway design, algal growth, water quality, hydrodynamic and atmospheric conditions. Several studies have been conducted with life-cycle analysis methods to estimate process energy consumption and greenhouse gas (GHG) emissions. ANL;NREL;PNNL, (2012) harmonized the resource assessment (RA), life-cycle analysis (LCA), and the techno-economic analysis (TEA) to refine the cost estimate. The energy requirements for pumping was estimated as 1.23e-4 kWh per Liter, the pond mixing was estimated as 48 kWh per hectare per day, and the harvesting options only included centrifuge power by gram of biomass and the use of organic solvents.

Life cycle analysis (LCA) is the fundamental tool used to evaluate the sustainability of biofuels. However, published standards are incomplete and not widely adhered to, which makes comparison between studies complicated (Batan, et al., 2010). Clarens, et al (2010) found that when considering nutrient demand, algal biomass can have higher life-cycle analysis than other crops. Batan, et al. (2010) found an energy input of .93 MJ for every 1 MJ of energy produced and avoidance of 75 g of CO_2 emissions per MJ of energy produced. However, as can be seen from comparison in Appendix B, there are many parameters not included in this analysis. A life-cycle analysis (LCA) performed by Brentner, et al. (2011) included 160 pathways or combinations of different technologies for each process stage, but did not include labor, capital machinery, or transport infrastructure. Frank, et al. (2012) found the fossil energy

for algal biofuel production was 2.5 times higher than for petro-diesel due to electricity consumption and nutrient (fertilizer) manufacturing. However, this study also found significant GHG reduction by arbitrarily reducing the paddlewheel mixing power, and including this savings in their results with the higher productivity scenarios.

Bayless, et al, found that assuming power plant lifetime of 30 years, 8.8% auxiliary load for pumping and dewatering at average cost of $0.035 kW-hr, labor cost of $1 per ton for algal production (mostly for hauling biomass), will yield an approximate cost of $8 - 10 per ton of CO_2 removed ($4.50 per ton capital cost, $2-3 operating cost, and $1-2 per ton for operating labor cost). Long-term cost includes only $1.50 per ton for power consumption using self-generated photovoltaic power. This does not include revenue from the sale or use of the biomass. Lundquist (2011) assumed an average design and construction cost of $34,000/hectare per pond, and 2.0 kW/ha for paddlewheel operation.

Lux Research (2012) assumed an algal growth rate based on the amount of sunlight only. This study found the costs to exceed $412 per day, with revenues of only $279 per day assuming multiple end products. Algal oil production costs ranging from $10.87 $gallon^{-1}$ to $13.31 $gallon^{-1}$ were found by Sun, et al., (2010). They also concluded production costs drop dramatically with increased biomass and lipid yields. Cost comparisons were acccomplished using spreadsheets with no simulation to determine operating and material costs. ANL;NREL;PNNL, (2012) found the break even cost of production to be around $9.85 $gallon^{-1}$ of diesel.

Inputs

Nutrients can represent major technical and economic problems at commercial scales. It is largely assumed that tapping into a wastewater source will lower the nutrient costs while making human supplements as a product impossible (U.S. DOE, 2010).

Research began in the 1960's at the University of California Berkeley into the potential of using wastewater as a source of nutrients to grow algae in large open ponds into which flue gas would be injected, harvesting the biomass by settling, digesting it to obtain methane gas which is then burned in the power plant, and recycling the digester effluents and CO_2 back into the ponds (Benemann & Oswald, 1996). This design showed potential of being relatively inexpensive assuming technical problems could be overcome and uncertainties resolved. In fact, a carbon neutral plant has been proposed growing microalgae using flue gas and wastewater, and then burning the biomass to fuel the plant (Olaizola, et al., 2003).

Extensive studies have been performed and microalgae are currently being used to remove nitrogen, phosphorus and heavy metals such as arsenic, cadmium, and chromium from wastewater (Patil, et al., 2008). Algae can remove greater than 96% of nutrients in wastewater (Chinnasamy, et al., 2010). Ammonium sulfate and urea can be used as inexpensive nitrogen sources. *C. vulgaris* was grown very successfully in one study when fed commercial fertilizers (urea, nutri-calcium, ammonium sulfate, phosphorus plus (P+), potash-plus (K+), nitro-20 and di-ammonium phosphate (DAP)) instead of pure nutrient media (Ashraf, et al., 2011). Seawater supplemented with nitrate and phosphate

fertilizers can also be an inexpensive medium for growing marine algae (Molina Grima, et al., 2000) (Frac, et al., 2010).

Chisti (2007) found a biomass production cost of $2.95/kg in a photobioreactor and $3.80/kg in open pond. James & Boriah (2010) quotes a current cost of $8 -1 5/kg for dry biomass, where the cost needs to be $0.25/kg dry biomass to be competitive with petro-diesel. Other studies have found the cost to vary from $0.47/kg (Chisti, 2007, in a forward-looking estimate with one hundred times increased production) to $6.93/kg (Michels, et al., 2010) (Christenson & Sims, 2011).

End Products

Microalgae are cultured for high value products (health supplemental: polyunsaturated fatty acids, vitamins, omega-3, biologically active substances: antiviral, antifungal, pigments, single cell protein), silicon, renewable energy (methane, biodiesel, ethanol, hydrogen), wastewater and animal wastes treatment, and CO_2 fixation (Al-Dahhan & Luo, 2006) (Richmond, 2004). Algae can also be 15-71% protein with well-balanced amino acids, rich mineral content, vitamins, antioxidants, phycobiliprotins, essential fatty acids and polysaccharides. Production cost analysis has been performed for cultivating algae to use in human supplements (Fournadzieva, et al., 2001) (Alabi, et al., 2009) (Frac, et al., 2010).

High oil species of microalgae cultured in growth-optimized conditions of photobioreactors have the potential to yield 19,000 to 57,000 L of microalgal oil per acre per year. (Demirbas & Demirbas, 2010) *P. tricornutum* is typically 25-31% lipid, *Tetraselmis* is 15-32%, while *B. braunii* can contain 29-75% lipids (Fournadzieva,

Bohadgieva, Fytikas, & Popovski, 2001) (Sheehan, et al., 1998). A study in Canada found photobioreactors have a cost of $24.60 per liter of algal oil, with 63% of that cost from capital. The energy balance is -11.5 MJ/L and the CO_2 balance is 4108 g/L with a carbon capture cost of around $793 ton^{-1} (Alabi, et al., 2009). For economic success, productivity of over 100 tons $hectare^{-1}$ $year^{-1}$ is needed according to one report (Pedroni & Benemann, 2003).

Bussell, et al. (2008) conducted a study to determine CO_2 absorption and parasitic load feeding flue gas from two 30kW gas turbines and diesel generators. A 90% plus reduction of CO_2 in exhaust gas was achieved with limited (<2%) parasitic load. Emissions were channelled through absorption columns into man-made algae ponds where CO_2 was metabolized.

Another study developed an economic model involving CO_2 recovery from power plant flue gas and delivery to microalgae ponds. A typical 500 MW power plant was used including CO_2 extraction using compression, dehydration, and transportation to the ponds with a cost of $40 ton^{-1} of CO_2 since directly using the flue gas was found to be more expensive. The lipid profit was estimated at $1.4 $gallon^{-1}$ and CO_2 mitigation at $30 ton^{-1}, so the project overall was shown to be economically attractive (Kaddam, 1997).

Yet another paper presented an initial analysis of potential greenhouse gas avoidance using algal biomass production coupled with recovery of flue gas combined with waste sludge and/or animal manure utilization. The model includes 880 ha of ponds operating at growth rate of 20 g m^{-2} d^{-1} to capture 70% of 30.03 million kg of CO_2 with

20% of biomass used for biodiesel, 50% for animal feed, and 30% digested to produce methane gas, with a greenhouse gas avoidance of 20%, 8.5% and 7.8% respectively, and a total of 36.3% and 26.3% after 10% parasitic energy costs required to deliver CO_2 to algae and to harvest and process biomass and products. Total parasitic energy requirement is estimated at 0.50 kW/kg of biomass. (Brune, et al., 2009) Most studies conclude that recovery of the biomass from the media contributes 20 - 30% of the total cost of producing the biomass (Molina Grima, et al., 2003). Actual production costs of \$15,000 ton^{-1} (James & Boriah, 2008) and \$45,000 ton^{-1} (Tredicci, 2008) were reported for a photobioreactor growth scenario at the 2008 Biomass Summit, but the basis for these calculations remains undisclosed.

Chapter Two: Method

The decades of algal research have produced large amounts of data that can be used to develop a system model incorporating financial analysis with the intent of determining whether algal growth for CO_2 capture, wastewater treatment, and biofuel production is economical and sustainable. Currently, the development process to grow algae with a desired end product in view is highly cost and labor intensive. All preliminary design work, economic and process modeling is done using a complex system of spreadsheets. This approach is not generating sufficient fidelity or sufficient confidence to gain investors due to a wide range of variables and the high potential for human error. System-level analysis can be used to make intelligent trade-offs in a low-risk, cost-effective virtual design environment. Incorporating cost and energy factors enables a financial analysis and reveals whether the design is sustainable environmentally and economically.

Every assumption in a system imposes constraints on innovation, and it is difficult to resolve them incrementally. Up until now, physical experiments growing microalgae have tested at best 3 or 4 variations of designs, with revisions to only one or two parameters. However, through using virtual design one is only limited by the imagination. Algae production with the intent of biofuel production is perfect for system modeling since the design is comprised of many interconnected subsystems that rely on the performance of one another. Physics at multiple scales can be applied to produce a collaborative engineering approach. Software tools have developed to the stage where

system-level simulation is a feasible methodology to rapidly and continually fine-tune the entire product system in a virtual environment well before physical assembly and testing.

Many products fail because multiple physical forces have not been considered, or because individual components fail to perform as expected when brought together. Photobioreactors have literally exploded due to accelerated algae growth unanticipated by researchers. Consumers and partners will not invest in a product until it is proven to be reliable and consistent. Creating such a simulation requires knowledge of the physics as well as data and process management. Iterative analysis is required to test the effects of changing design parameters on the system as a whole.

The model basis assumes biodiesel production from algae lipid content as the principal end product with the option of converting the biomass to methane to be burned for fuel, sold as animal feed, and/or used in human supplements. As a model for a power plant the model uses a coal power plant since coal power plants for electricity generation far outnumber in quantity and emissions other industrial plants (U.S. Environmental Protection Agency, 2006). Another option in the model is a wastewater treatment plant as a nutrient source. The power and wastewater plants both lower costs by alleviating the cost of some nutrients, and increase revenue through CO_2 consumption or wastewater treatment. Integration with wastewater treatment brings cost benefits through nitrogen and phosphorus removal from wastewater.

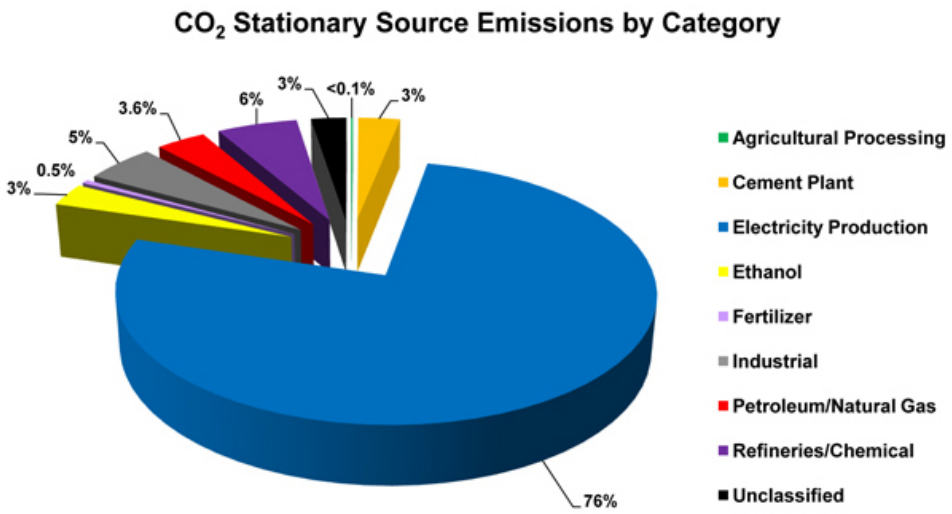

Figure 3: CO2 Stationary Source Emissions by Category (http://www.netl.doe.gov).

The algal plant is modeled as a system that uses open ponds or photobioreactors, and a variety of processing and refining technologies developed and documented in the literature and/or by commercial enterprises.

System Model

The intent of this model is to make it adaptable to optimize for various algae species, inputs, outputs, processes, and designs. A common framework is developed to facilitate comparisons between different algae growth scenarios and to compare results with other transportation fuels. Since many parameters are uncertain, especially productivity, the analysis examined a broad range of these variables. Ultimately the goal is to optimize design parameters to attain the greatest net profit possible. Simulation is a form of hypothesis testing, with each simulation run providing one or more pieces of sample data, which through inferential statistical methods can be used in a formal analysis (Chase, et al., 2006). This analysis will reveal which algal growth scenarios

show the most potential and what innovations and/or improvements must be made to obtain favorable results.

The model incorporates basic algal biology with cultivation science and engineering to suggest improvements in productivity while at the same time lower the cost of production (U.S. DOE, 2010). Variables in this study which were not incorporated in many past techno-economic studies include the specific algal strain, the culture density, the algal strain lipid content and geometry, the growth rate, the lighting source and path length, the effective viscosity, and a fluid dynamics profile (see Appendix A). The first step to model any system is to define the system, which in this study is the result of data collected from previous studies, and commonly results in a range of suitable values. The calculations for productivity are based on purely biological growth rates with the various cellular size of that particular species. The key input variables such as lighting, nutrients, CO_2 were derived from the molecular composition of algae as requirements to support the productivity. Where there is a range of values possible, the probability distribution is obtained using a range with a random number function.

The second and third steps are identifying the system components and defining their properties and physics with equations, which are identified under separate headings within this paper. This involves creating a library of reusable modules, which can then be added to Simulink system models and linked together (Matlab, 2012). Object-oriented design involves identifying the components, analyzing and identifying patterns to determine what components are used repeatedly or share characteristics, and classifying

components on similarities and differences. Use of a library prevents inconsistencies and errors, and enforces a consistent look and feel since changes in the library modules automatically apply to all models using those modules.

Finally the model is built (in this case two models, one representing an open pond growth scenario and one representing a photobioreactor growth scenario), test scripts are written, and the simulation is run and validated. The equations presented in this section are built inside of the specific applicable modules, which are linked to the inputs from other modules while the outputs are fed into other modules. Values for parameters input by the user such as type of lighting, size of the power plant, or algae species are assigned in the module masks or the test scripts. Bringing disparate components together as a system requires integration of hundreds of variables, multi-physics analysis, flexible fidelity, and adaptable outputs. Figure (3) shows the overall algal growth system and input variables, while Figure (4) is similar with a focus on process flow and required equipment. Screen shots of the models, library, and an example of a module are provided in Appendix D.

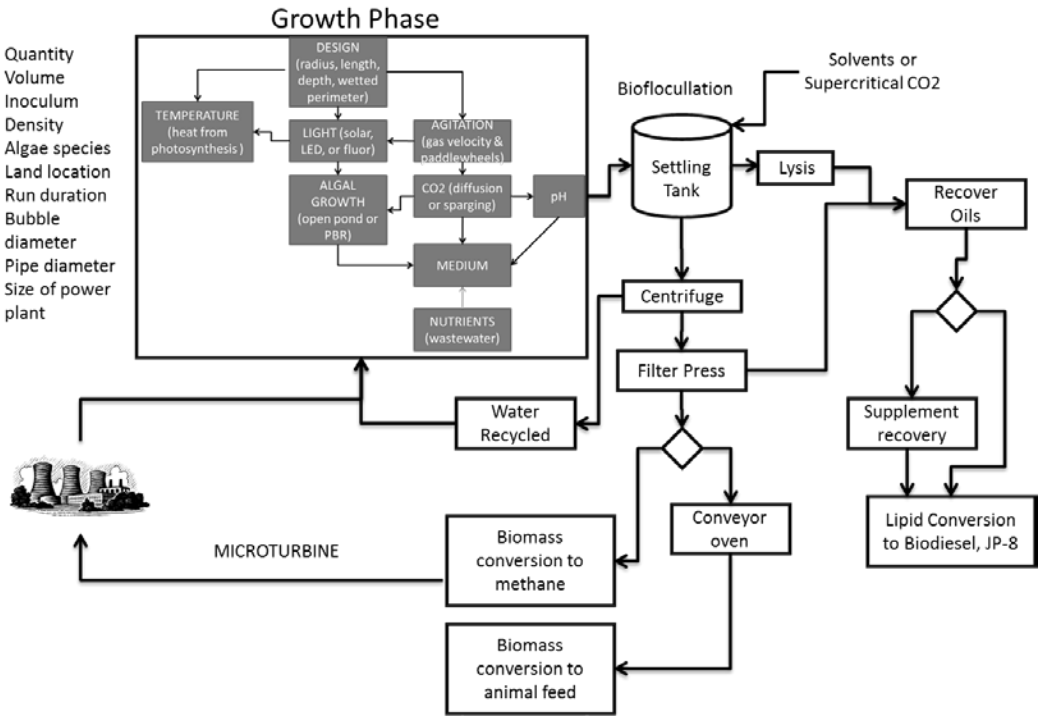

Figure 4: Algal growth flow chart with model inputs.

The level of accuracy of the cost and power estimates depend on the actual project conditions and details. With no input from the design and only choosing between various options available in the model, the model aims to deliver a Class 4 Feasibility or Pre-Design Estimate, which is prepared using cost curves and scaling factors for major processes. Cost accuracy goal is a range from -30% to +50%. A parametric estimate is based upon statistical data and ranges of values collected from vendors.

	Primary Characteristic	**Secondary Characteristics**		
ESTIMATE CLASS	**DEGREE OF PROJECT DEFINITION**	**END USAGE**	**METHODOLOGY**	**EXPECTED ACCURACY RANGE**

Class 5	0% to 2%	Concept screening	Capacity factored, parametric models, judgment or analogy	L: -20% to -50% H: +30% to 100%
Class 4	1% to 15%	Study or feasibility	Equipment factored or parametric models	L: -15% to -30% H: +20% to +50%
Class 3	10% to 40%	Budget authorization or control	Semi-detailed unit costs with assembly level line items	L: -10% to -20% H: +10% to +30%
Class 2	30% to 70%	Control or bid/tender	Detailed unit cost with forced detailed take-off	L: -5% to -15% H: +5% to +20%
Class 1	70% to 100%	Check estimate or bid/tender	Detailed unit cost with detailed take-off	L: -3% to -10% H: +3% to +15%

Table 1: Cost estimate classification for process industries (DOE, 2011).

Data required for a feasibility estimate include the product(s), process description, capacity, a general location, process flow diagram with equipment size and material, equipment list, major land cost, ratioed estimate for engineering, chemical quantities, construction costs (labor and indirect), and overall timing of execution (Kerzner, 2006). Equipment size and quantity will vary depending on the size of the facility which is determined by model inputs. Therefore, this model does have the data necessary for a study or feasibility estimate.

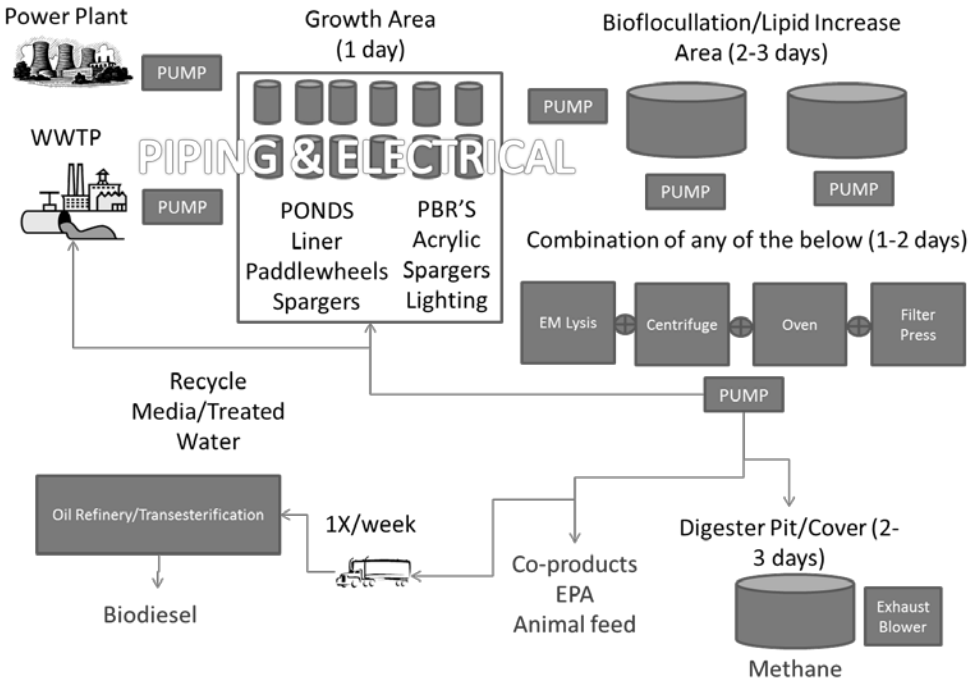

Figure 5: Process flow diagram with equipment.

In order to establish the necessary size of the facility, the investment cost and operational expenses as well as the resulting biomass and oil that a facility will produce must also be calculated. Lack of mature engineering for photobioreactors and systems have made these calculations unreliable, but through more detailed fluids analysis this study attempts to make possible more reliable and efficient designs. Costs include land, design, capital, inoculums (to initiate and restart, depends on species if this is needed and if so where produced), harvesting, oil extraction, wastewater treatment, pumping, fertilizer (nutrients), carbon cost, power cost, labor, cooling, and cleaning. Capital is a significant cost for building photobioreactors.

The engineering design and construction cost estimating of algae production facilities straddle between agricultural, chemical, mechanical and civil engineering. The

goal is to keep costs at an agricultural engineering level while mimicking the technicality of chemical engineering through the use of certain predictable calculations and statistics techniques.

To provide evidence for the sustainability of growing algae for biofuel, the energy outputs must outweigh the energy inputs (Alabi, 2009). In some cases the study attempts a first order EROI, which considers the actual energy production and consumption flows. However, the equipment, processes and methods used vary widely, and the economic and EROI results depend on the technologies used, the inputs, and location. This paper outlines the important parameters to consider, and provides energy consumption and production data for the important processes.

Open Ponds vs. Photobioreactors

Initially, the US Department of Energy became interested in algae due to claims of high productivity growing algae in photobioreactors; however Benemann, et al., (1982) found that open ponds displayed more potential than photobioreactors, which resulted in the ASP devoting most of the government research summarized in Sheehan, et al., (1998) to open pond growth scenarios. The most recent algal technology roadmap released by the U.S. DOE does not consider photobioreactors with artificial lighting, but does acknowledge various benefits of solar illuminated photobioreactors (U.S. DOE, 2010).

Photobioreactors offer the advantages of requiring significantly lower water volume and land area, less CO_2 loss to the atmosphere, better control of culture conditions, higher productivity and density (reducing harvesting costs), reduced

contamination risks, reduced damage from pumping, and yield consistency throughout seasons and weather changes. Photobioreactors can guarantee a sustainable production process essential for industrial applications through providing a homogeneous and stable environment (Tredici & Zittelli, 1998) (U.S. DOE, 2010). Open ponds are severely limited by the need for locations with sunny, temperate climates, sufficiently flat land, supplemental CO_2, and possibly brackish water, seawater, or wastewater. ANL;NREL;PNNL, (2012) found only 5.5% of the land in the conterminous United States to be suitable for large-scale open pond microalgae production.

a) Regions with annual average climate conditions meeting selected criteria: ≥ 2800 hour annual sunshine, annual average temperature ≥ 55° F, and ≥ 200 freeze-free days

b) Fossil-fired power plant sources of CO_2 within 20 miles of municipal wastewater facilities in the preferred climate region

Figure 6: Rough scoping assessment of preferred site locations for outdoor algae production (Source: U.S. DOE, 2010).

Observational data from actual algae facilities show two times to ten times, or more, swings in output between summer peaks and winter months, and between daytime and nighttime, ranging from 7 g/m^2/day to 25 g/m^2/day (Lux Research, 2012). The amount of water lost to evaporation is significant for open ponds even if the source is wastewater, brackish or salt water, and the impacts go further than water cost. If flue gas is used, only 30% of the emissions can be used for open ponds, since the emissions at night or much of the winter could not be used (Benemann & Oswald, 1996). The model

determines the amount of land required for an open pond growth scenario through adding 10% to the surface area required for the ponds. The photobioreactor land area is calculated by Equation (1).

$$L_{PBR} = \pi(D_{PBR} + 1)^2 Q_{PBR} \quad \text{Eq. (1)}$$

where L_{PBR} is the required area of land in m^2,

D_{PBR} is the total PBR diameter in meters,

and Q_{PBR} is the total quantity of PBR's.

The economic advantages of growing phototrophic cultures at very high cell concentrations in terms of reduced production and capital costs are presently curtailed by the necessity to continuously alleviate growth inhibition in such cultures. Efficient growing methods would be characterized by high areal as well as volumetric productivity, which is currently the most possible with artificially illuminated photobioreactors. Also, the issues of oxygen saturation and increasing pH along the length of a culture are easily solved with a vertical, artificially illuminated photobioreactor.

The photobioreactor design requires a concurrent approach to insure that multidisciplinary design goals are achieved, and includes the following parameters: bubble size, gas flow rate, CO_2 content, biomass density, specific growth rate, dissolved oxygen concentration, photosynthetic efficiency, pH, chemical reactions, nutrient sources, algal physiology, geometry, building materials, ease of scale-up, contamination control, and light delivery and distribution.

In order to design a cost and power effective photobioreactor, the following problems must be resolved: 1) design must be universal and permit cultivation of various photosynthesizing organisms, 2) provide for uniform illumination of the culture surface and mass transfer of CO_2 and O_2, 3) prevent or minimize fouling, particularly of light-transmitting surfaces, 4) high rates of mass transfer by means that neither damage cells nor suppress their growth, 5) volume of non- illuminated parts should match optimal light: dark ratio, and 6) energy consumption required for mass transfer and light surface must be optimized (Gabel, et al., 1996).

The suitability for an open pond, photobioreactor, or hybrid system will depend on the upstream and downstream processing, resources available, location, financing, and products of the cultivation system. This requires a techno-economic analysis which incorporates the design of the cultivation system (U.S. DOE, 2010). The various assumed designs included in this study are as follows:

- Open pond design is a user specified number of large surface ponds with a specified number of Liters in each pond with no shade or environmental control, where each pond has one paddlewheel and 20 gas spargers.
- Solar illuminated PBR is a single tube bubble column design to optimize light exposure around the perimeter with a single gas sparger.
- Artificially illuminated PBR is an ALR design with an internal and perimeter fluorescent or LED illuminated area and a single gas sparger.

The total amount of Liters is user specified in both PBR growth scenarios, and the model determines optimal size of each PBR which in turn calculates the quantity of

PBR's needed. All PBR results prior to the optimization section apply to artificially illuminated PBR with ALR design densities of at least 40 g/L unless otherwise noted.

Productivity

The model is designed with options of growing four marine microalgae species: *Phaeodactylum tricornutum* (diatom), *Tetraselmis cordiformis* (flagellated green), *Nannochloropsis salina*, *Chaetoceros muelleri*, and one freshwater species, *Chlorella vulgaris.*

P. tricornutum have a typical cell volume of 120 - 200 μm^3, are typically 20 - 40 µm long and 3.0 - 3.5 µm wide (Olenina, et al., 2006) (Greenwell, et al., 2010). *Nannochloropsis salina* algae are small, nonmotile spheres with a diameter of approximately 2 µm, and can grow in both marine and fresh water environments. They are a rich source of a range of pigments and omega-3 fatty acids such as EPA which are valuable commercially (Hibberd, 1981). *Tetraselmis cordiformis* is elliptical shaped marine algae with a diameter of 16 - 23 µm, and four flagella arising from an anterior depression of the cell body (Eishi & Toshihiko, 2000). *Chlorella vulgaris* is spherical with a volume averaging 78 μm^3. All four species are capable of accumulating lipids, with the highest reported for *Nannochloropsis* at 68%, but reports vary widely (Sheehan, et al., 1998). *Chaetoceros muelleri* is a diatom commonly used as feed for aquaculture, and is cylindrical in shape (Olenina, et al., 2006).

Species	Oil Content % Dry wt.
Ankistrodesmus TR-87	28-40
Botryococcus braunii	29-75

Chlorella sp.	28-32
Cyclotella DI-35	42
Hantzschia DI-160	66
Isochrysis sp.	7-33
Nannochloris	31 (6-63)
Nannochloropsis	46 (31-68)
Chaetocerus m. (Lopez-Elias, et al., 2005)	29
Phaeodactylum tricornutum	31
Scenedesmus TR-84	45
Stichococcus	33 (9-59)
Tetraselmis suecica	24(15-32)

Table 2: Oil content in selected algal species (Sheehan et al., 1998).

Research performed cultivating *Tetraselmis sp*. report a range of lipid values from 8.5 to 23 % of biomass. Robustness and high productivity combined with moderate basal lipid content makes it a good candidate for biodiesel production (Sonnekus, 2010).

Maximum productivity calculations used in the model are based on past research and biological calculations. Since the range of productivity values in the literature is extensive, and depends on many variables, the model begins with a purely biological relationship. Variables can be modified to enable analysis of different designs. Population dynamics may yield nonlinear growth rates. Also, in high volumetric productivity systems, all the parameters related to growth, including oxygen generation, pH, CO_2 absorption, and nutrient depletion change at a high rate (Tredici & Zittelli, 1998). The model assumes productivity can be optimized by applying known fluid dynamic principles to known algal responses (Degen, et al., 2001).

Maximum growth rate for algae ranges between 1.12 and 1.15 per day. Growth rates are determined with $\mu=(\ln c-\ln c_0)/(t-t_0)$ where c is the cell concentration in cells/mL

and t is measured in days. (Quigg, et al., 2006) (Greenwell, et al. 2010) Thus the maximum and minimal growth rate for algae when conditions are optimal can be determined by:

$$c = e^{\mu t + \ln(c_o)} \quad \text{Eq. (2)}$$

The model uses Equation (2) for all growth scenarios growth rate to give open ponds a fair assessment, but conditions in an open pond growth scenario are less than optimal due to photoinhibition and lack of consistent fluid dynamics which affects nutrient availability, temperature changes, and contamination. Therefore, the growth rate as exhibited in past algal growth scenarios and detailed in the literature may differ from Equation (2), especially in open pond growth scenarios. Where 0.08 g/L per day and about 20 g/m^2 per day has been proven realistic, the relationship between pond depth and productivity can be approximated per Equation (3).

$$d = -0.005 * P_d + 0.2 \quad \text{Eq. (3)}$$

where d is cell concentration in g/L per day,

and P_d is pond depth in centimeters.

Production rate	Grams/m^2/day	Notes
Benemann, Goebel, & Weissman (1988)	30	Water was 20 cm deep; strain was Chlorella
Huntley and Redalje (2007)	36	Strain was Haematococcus pluvialis; 35% oil content assumed
Putt (2007)	20	Strain was Chlorella; 100 acre facility w/raceways w/ paddlewheels
Schulz (2006)	30	Strains were Spirulina, Haematococcus, Chlorella, and Dunaliella
Patil, Tran, and Giselrod (2008)	24	Strain was Dunaliella
Schenk et al. (2008)	20	From Seambiotic (Israel)
Schenk et al. (2008)	30-60	
Schenk et al. (2008)	10-25	Operated at depth of 15-20 cm and biomass concentrations of 1 g biomass/dry weight per liter
Schenk et al. (2008)	62	Strain was Tetraselmis suecica w/30% lipid content
Carlsson, van Bellen, Möller, and Clayton (2007)	30	
Neenan et al. (1986)	10-60	Minimum and maximum rates for outdoor raceway productivity from National Renewable Energy Laboratory
Weissman et al. (1989)	3.2-13.1	Small lined ponds in September-December production
Lee (2001)	25	
Benemann (1994)	30-60	Lower estimate was the projected rate for the project and the larger estimate was the theoretical maximum
Chisti (2007)	35	

Figure 7: Productivity in g/m^2 per day in the literature (Richardson, et al., 2010).

Integrating biology in the model involves the cell size as this affects physiological rates, metabolic rate, light absorption, nutrient diffusion, uptake requirements, sinking rate, and grazing rates. Quantitative relationships between phytoplankton cell size and physiological and ecological processes can be used to construct models of primary production (Flynn, et al., 2010).

Volume of *Nanno. s.* was computed as volume of a sphere:

$$\frac{4}{3} * 1 * 10^{-6}\pi = 4.9 * 10^{-18} m^3$$

Volume of *Tetra. c.* is computed as volume of a trapezoid (Olenina, et al., 2006):

$$\frac{1}{2} * 18 * 10^{-6} * 9 * 10^{-6} * (15 * 10^{-6} + 9 * 10^{-6}) = 1.94 * 10^{-15} m^3$$

Volume of *Chaet. m.*is computed as an oval cylinder:

$$\frac{\pi}{4} * (7 * 10^{-6})^2 * 9 * 10^{-6} = 3.26 * 10^{-16} m^3$$

Volume of *Chlorella sp.*is computed as a sphere:

$$(5.23 * 10^{-6})^3 * \pi/6 = 7.49 * 10^{-17} m^3$$

Volume of *Phaedactylum t.* is computed as a half parallelepiped:

$$27 * 10^{-6} * \frac{(3.5 * 10^{-6})^2}{2} = 1.65 * 10^{-16} m^3$$

Species	Volume (m3)	Lipid Content (%)	Marine or Fresh
Phaeodactylum tricornutum	1.65E-16	31	Marine
Chlorella vulgaris	7.49E-17	28-32	Fresh
Nannochloropsis salina	4.19E-18	31-68	Both
Tetraselmis cordiformis	1.94E-15	15-32	Marine
Chaetoceros muelleri	3.26E-16	29	Marine

Table 3: Summary of biological characteristics for algae species used in analysis.

The internal density of diatom cells is an average of 1150 kg m^{-3}, which enables the computation of grams/L from the number and volume of cells and growth rate of 1.12 to 1.15 (Greenwell, et al. 2010). Resulting culture density in g/L for all growth scenarios is calculated using Equation (4).

$$d = 1150 \frac{kg}{m^3} * c * \frac{m^3}{cell} \quad \text{Eq. (4)}$$

Measurement of productivity in the literature is through the optical density of culture using a spectrophotometer or by using gravimetry, essentially drying the volume and weighing it. Dry weight is normally 8.0 to 8.8% of wet weight (Watson, et al., 1963) (Contreras, et al., 1998). The model uses a random number function between 8.0 and 8.8%.

The model uses this growth rate based on various species of algae and their respective cellular sizes for all growth scenarios. The starting density in cells L^{-1} is

varied to result in maximum optimal biomass density depending on the algal size after one day's growth. Normally the exponential growth phase is four days if the medium is not completely replaced (Zou, et al., 2000) (Lee & Palsson, 1994) (Thomas & Gibson, 1990). However, the model assumes the portion of algal growth is harvested every day which will provide for the required density to reach optimal density the following day (detailed in harvesting section of this study). The recommended starting density to result in optimal biomass density after one day's growth is an output from the model. This is an improvement over current commercial methods of beginning cultures by volume of inoculum, which results in different qualities and quantities at the end of the growth period (Lopez-Elias, et al., 2008).

The maximum density for photoautotrophic cultures is a function of light path and intensity, gas-liquid interfacial area, and shear rate. The shorter the light path, the higher the optimal cell density and volumetric productivity (Degen, et al., 2001). Higher densities of 50 – 60 dry cell mass g L^{-1} have been obtainable only with 2000-3000 µmol photons m^{-2} s^{-1}, vigorous stirring, medium replacement every 2 days at high density, and a 20-30 day growing period, which in the majority of scenarios will not be cost-effective or sustainable (Zou,et al., 2000) (Lee & Palsson, 1994).

The model determines optimal density based on the light path length, flow path, and algal cell size versus the power and capital inputs necessary to provide light intensity and path length.

Open pond productivity varies in the literature from 20 - 80 g m^{-3} d^{-1} (depending on the pond depth, where shallower depths result in higher density), which is at the

greatest a resulting density of 0.33 g L^{-1} after four days' growth (.08 g/L d^{-1}) (Beal, et al., 2012). Maximum open pond productivity is obtained with the most shallow pond depth, while lower productivity is associated with greater pond depth. The growth rate for artificially illuminated photobioreactors presented in the previous section is a maximum wet density of 60 g L^{-1}, or 180 times the density of open ponds. Solar illuminated photobioreactors have displayed a growth rate of 1.08 g L^{-1} day^{-1} (Camacho, et al., 1999).

The model incorporates a loss of growth for open ponds from .1 - 10% to account for losses at night, extremely overcast days, and the risk of contamination. Also, there are options for rural land or urban land for both open ponds and PBR's to analyze the impact location has on net profit.

Algae respond to changes in light, temperature, and nutrient availability dynamically through the organization of pigments, end products, and growth rates (MacIntyre & Cullen, 2005). The resulting composition of the algae cell in comparison with the desired end product(s) is what determines the productivity. As mentioned in the literature review, the growth rate may not be optimal in order to achieve maximum productivity. The goal of an algal culturing system is to manipulate the inputs to result in the optimal desired end products with the most efficient cost and use of power. The model uses common patterns across the taxa for nutrient uptake, pigments, photosynthetic response and growth based on the general molecular formula for algae: $CO_{0.48}H_{1.83}N_{0.11}P_{0.01}$ (Demirbas & Demirbas, 2010).

At the core of the simulation are the fluid properties in relation to obtaining optimal algal growth. The fluid dynamic principles in an ALR detailed in the "small

scale turbulence" section are used to optimize growth conditions. An organized mixing pattern is attained through using an ALR resulting in nearly constant light/dark cycle frequency approaching a ratio of 1:10. Combining proper geometry of illumination with medium circulation can ensure cells are circulated at optimal frequency between light and dark zones. The tube diameter is limited by illumination zone, depending on light placement, and the length is limited by the rate of photosynthesis and removal of oxygen.

Lighting

Plants in the wild are evolutionarily invested to ensure survival under extreme stress, at the expense of optimal photosynthetic efficiency. Lighting must support photosynthesis for optimal growth rate while preventing photoinhibition. There is evidence that algae in the wild are light-limited on bright summer days (Tredici & Zittelli, 1998). Spatial light dilution or FLE is a means to overcome the light saturation effect used by plants in nature (Sato, et al., 2010). Studies indicate the light/dark cycle for algae must be constant at different scales (Molina Grima, et al., 2000). Artificial algal cultures have to compromise between maximizing light interception to attain maximum volumetric productivity and avoiding excess light which causes photoinhibition in order to achieve high light conversion efficiency. Verification of photosynthetic efficiency for a specific design is necessary in determining economic feasibility of a plan for growing microalgae. The design should be adaptable to the culture density and provide just enough light needed by the algae for the photosynthetic process.

Solar light intensity varies between about 120 and 1400 µmol photons m^{-2} s^{-1}, but varies depending on day length, season, cloud cover, time of year, and latitude (Torres &

Lopez, 2010). Research indicates *P. tricornutum* is light saturated at 200 µmol photons m^{-2} s^{-1} or about 10% of full-sunlight intensity (Molina, et al., 2000) (Lundquist et al., 2010). Rate of mixing becomes ever more important as algal concentration increases to obtain maximum productivity and photosynthetic efficiency with greater light intensity, so that the higher the intensity of the light sources, the higher the optimal culture density (Qiang & Richmond, 1996). At this point in time with current technology, optimal rate of mixing is only available technologically and from a perspective of energy use in PBR's, while photoinhibition is unavoidable in an open pond growth scenario.

In economic models of algal growth for biofuels the light measurement is a common source of error (Dimitrov, 2007). In order to determine the photosynthetic efficiency one must consider the absorption efficiency and the conversion efficiency.

Conversion Efficiency

Photosynthetic organisms use at least eight photons to convert one molecule of CO_2 into carbohydrate $(CH_2O)_n$; thus the maximum conversion efficiency of turning photosynthetically active radiation (PAR) into carbohydrate (η_{theo}) can be estimated using Equation (5).

$$\eta_{theo} = \frac{HV_{carbohydrate}}{8 * E_{photon}} \qquad \text{Eq. (5) (Dimitrov, 2007)}$$

where $HV_{carbohydrate}$ is the heating value of CH_2O (~468 kJ mol^{-1}) and E_{photon} is the mean energy of a mole of PAR photons (~217.4 kJ). This gives maximum theoretical photosynthetic conversion efficiency (η_{theo}) of 27%. The model assumes the theoretical conversion efficiency (η_{theo}) of 27%.

Absorption Efficiency

Absorption efficiencies are much lower since plants cannot absorb every photon that falls to earth because of photosaturation, photoinhibition, and reflection, plants spend energy on other life-supporting functions, and transmission losses due to self-shading and reflection through the photobioreactor wall or water surface. Dimitrov (2007) estimated only 37% PAR energy is actually used leading to an overall photosynthetic efficiency using solar light of about 10% (27% * 37%). This is still a 30 fold improvement over more normal agricultural yields (Sheehan, et al., 1998) (Miyamoto, 1997) (Zhu, et al., 2008).

The variations in reported photosynthetic efficiencies for microalgal cultures is likely due to differing light sources and the fact that pigment content can vary 20 - 100% diurnally for at least some algae species (Ragni & D'Alcala, 2007). The absorption coefficient is difficult to predict and depends on other factors not completely understood, but it will not be 100% all of the time.

The absorption efficiency can be optimized through light source, light spacing and efficient CO_2 mass transfer. LED (light emitting diodes) provide specific wavelengths, are light, small, have a very long life-expectancy and are so electrically efficient that heat generation is minimized (Lee & Palsson, 1994). LED lighting in only wavelengths used by algae maximizes absorption especially when spacing allows optimal light path length while minimizing self-shading and reflection. Photosynthetic optimal lighting wavelengths are in the blue spectrum at around 450 nm and in the red spectrum around 678 nm. Chlorophyll is excited only by photons with wavelengths of 680 and 700 nm

(red) (Schlagermann, et al., 2012) (Holdsworth, 1985). Spectral ouptut at the photosynthetic absorption spectrum avoids unusable frequencies (converted into thermal energy), and improves overall energy conversion. Although fluorescent lighting is not as an efficient use of energy as LED lighting, it can result in similar algal growth. In fact, the highest reported overall photosynthetic efficiency reported was 34%, and was achieved with fluorescent lighting through improving the gas exchange mass transfer coefficient using microporous hollow fibres (Ferreira, et al., 1998).

Biomass density affects both light intensity and light penetration. According to Akhilesh, et al. (2011), dense cultures' solar light zone is from 12.05 cm for .033 g cell mass per L, to 14.35 cm for .028 g cell mass per L, and up to 16.3 cm for .025 g cell mass per L. The same study concluded that below 30 cm, there is no penetration of required light intensity regardless of the cell concentration. Using the data gathered from Akhilesh, et al., an empirical exponential equation was developed to estimate light penetration in microalgal cultures:

$$PL = 30.0e^{(-0.058d)} \quad \text{Eq. (6)}$$

where PL is the path length in centimeters,

and d is the culture density in g cell mass per L.

This equation is a Beer-Lambert type equation:

$$I = I_0 e^{-kCd}$$

where I_o is the light intensity at the irradiated wall surface,

k is the attenuation constant caused by algal concentration, (C)

and d is the distance from the irradiated surface.

This equation underestimates penetration since it does not include the scattering phase function from the Radiative Transport Equation (RTE). Light penetration will also be a condition of turbulence in the culture, which is discussed in the following section. In addition, other studies indicate algal growth continues at greater depths and at less than the required 200 µmol photons m^{-2} s-1 (Quigg, et al., 2006). Air bubbles reportedly increase light penetration depth (Lee & Palsson, 1994). Carvalho (2008) states a light path length of 2 - 5 cm for dense cultures. Additionally, most laboratory conditions for simple flasks with no or minimal induced fluid dynamics and diameters up to 8 cm easily obtain culture densities of 1e9 cells/L or at least 0.086 g/L (A. Quigg, personal communication, May 20, 2011) (Al-Dahhan & Luo, 2006). Wu and Merchuk (2003) demonstrated that algal growth up to 5.0e10 cells/L or about 4.3 g/L with very minimal air sparging and less than 200 µmol photons m^{-2} s^{-1} light intensities is possible. As shown in the literature review, much higher densities up to 200 g/L (1e10 cells/mL) have been obtained in photobioreactors with LED lighting and optimal fluid dynamics. Richmond (2004) asserted ultra-high density cultures are obtainable in photobioreactors with light path lengths of 0.5 – 1.0 cm.

Summarizing the range of possibilities available, Equation (7) was chosen to calculate light path length based on culture density in the model.

$$PL = 35.0e^{(-0.035d)} \qquad \text{Eq. (7)}$$

where PL is the path length in centimeters,

and d is the culture density in g cell mass per L.

Furthermore, the model has a range of absorption efficiencies (Q_{abs}) depending on the lighting and gas exchange design. LED lighting, assumed in PAR wavelengths of blue and red, with light path of <6 cm and optimal CO_2 mass transfer results in the highest efficiency of 90%, while sunlight and bubbled CO_2 is assumed at the lowest absorption efficiency of 40% . The development of absorption factors in Table (2) are based on the above absorption efficiency analysis. The factors which apply to the design for light source, light path, and gas exchange are totalled and divided by 10 to arrive at the photosynthetic absorption efficiency (Q_{abs}).

Light source	Absorption Factor
LED in red and blue	4
Flourescent	3
solar	2
Light Path (cm) at Optimal Density	
>10	3
6-10	2
<6	1
Gas Exchange	
diffusion	2
sparging	1

Table 4: Photosynthetic absorption factors.

Overall Photosynthetic Efficiency

By summing the absorption factors from Table 4 which are applicable to the design, dividing by 10, and then multiplying by the conversion efficiency (η_{theo} = 27%), one arrives at the total photosynthetic efficiency (Q_T) of the design. The light path will

vary as the optical density increases and decreases, which means the efficiency may decrease as the culture grows, unless the design accomodates increasing density with the light spacing or fluid dynamics.

Another factor for determining photosynthetic efficiency involves the breakdown of carbohydrates by a photosynthetic organism when ATP energy (derived from PAR energy) is not available. However, this should not be a significant factor in an artificially illuminated photobioreactor since the dark period will be a period of seconds rather than 12 hours. Algal culture systems using solar light only will experience a reduction in photosynthetic efficiency reflected by $Q_{dark} = 0.72$ (Dimitrov, 2007). The resulting total photosynthetic efficiency for algal cultures relying on only solar light is calculated with the following equation:

$$Q_T = Q_{dark} * \eta_{theo} * Q_{abs} \qquad \text{Eq.(6) (Dimitrov, 2007)}$$

The resulting total photosynthetic efficiency for algal cultures relying on artificial light is calculated with the following equation:

$$Q_T = \eta_{theo} * Q_{abs} \qquad \text{Eq.(7) (Dimitrov, 2007)}$$

However, there are other lighting factors to consider including the transmission coefficient (Q_{tr}) and cleanliness of the reactor wall (Q_{clean}) (Dimitrov, 2007). The likely material for any photobioreactor is polycarbonate with a transmission factor of 0.9, and cleanliness should be maintainable at 0.95. The reduction in efficiency due to self-shading is considered in the next section with path length, and light reflection should not be a significant factor for an internally illuminated photobioreactor. One other consideration which is highly likely when using flue gas is the nitrogen source will be

NO_x instead of ammonia, which requires energy from algal cells to process. The assimilation of nitrate involves two transport and two reduction steps to produce ammonium in the chloroplast (Wang, et al., 2010). This factor is labeled as Q_{life}, and is roughly equivalent to 0.9. This factor is omitted only if the design is supplying nitrogen in the form of ammonia, which is likely if municipal wastewater is used.

Thus for an internally illuminated photobioreactor:

$$Q_T = \eta_{theo} * Q_{abs} * Q_{tr} * Q_{clean} * Q_{life} \quad \text{Eq.(8)}$$

For solar illuminated photobioreactors:

$$Q_T = Q_{dark} * \eta_{theo} * Q_{abs} * Q_{tr} * Q_{clean} * Q_{life} \quad \text{Eq.(9)}$$

And for open ponds:

$$Q_T = Q_{dark} * \eta_{theo} * Q_{abs} * Q_{life} \quad \text{Eq.(10)}$$

Thus, best case scenario (internally illuminated photobioreactor with ammonia as the nitrogen source) would be a resulting overall photosynthetic efficiency of:

$Q_T = .9 * .27 * .9 * .95 = .21 = 21\%$

And worst case would be the solar illuminated photobioreactor with an overall photosynthetic efficiency of:

$Q_T = .72 * .4 * .27 * .9 * .95 * .9 = .06 = 6\%$

This value concurs with Tredici & Zittelli (1998) with photosynthetic efficiency values for solar illuminated photobioreactors between 4.8 - 6.6%.

Open ponds are a slight improvement over a solar illuminated photobioreactor with an overall photosynthetic efficiency of:

$Q_T = .72 * .4 * .27 * .9 = .07 = 7\%$

When solar is the light source, however, another factor should be considered when the light is in excess and photoinhibition or light saturation occurs. The resulting photosynthetic efficiency can decrease by up to 75%, resulting in the 1-3% efficiency reported in the literature for open ponds and solar illuminated photobioreactors (Sheehan, et al., 1998) (Lundquist, et al., 2010) (Tredici & Zittelli, 1998). However, this can be minimized through turbulent mixing and spatial light dilution. Also, photoinhibition can be avoided for the most part in artificially illuminated photobioreactors through optimal light intensity and placement, which is discussed in the gas exchange section of this paper.

Light Irradiance

Required light intensity or irradiance can be determined from Equation (11).

$$Q_{avg} = \frac{BY[E_c(1-L)+ E_tL]}{TQ_T} \qquad \text{Eq.(11) (Chisti, 2007)}$$

where Q_{avg} is the annual average required PAR energy (W L^{-1}),

BY is the wet algal biomass yield in g L^{-1},

T is time (86400 s d^{-1}),

Q_T is the theoretical total photosynethic efficiency,

E_c is the energy necessary for building 1 g of carbohydrate (17 KJ g^{-1}),

E_t is the energy necessary for synthesizing 1 g of lipid (38 KJ g^{-1}) (Shen, et al., 2009) (Chisti, 2007),

and L is lipid content.

Q_{avg} thus incorporates the total photosynthetic efficiency (Q_T) determined in the previous section which will depend on the design. This analysis reveals partly why there

exists a wide range in reported photosynthetic efficiencies, irradiance levels, and productivities. The required Watts per Liter can vary by a factor of three depending on the lighting and gas exchange design.

The model determines required watts per Liter and sizes the fluorescent or LED lighting accordingly so that negligible photoinhibition will result. Of course, this is not possible with solar lighting, so one could expect some photoinhibition and loss in productivity in a solar illuminated photobioreactor or open pond growth scenario.

Gas Exchange

Carbon dioxide in atmospheric air is far too dilute to support algal maximum growth rate. One solution to providing increased concentration of CO_2 to algal cultures is pumping exhaust gas from a stationary source straight into the algal culture. There are some 5,000 stationary CO_2 sources available in the United States and Canada. Natural gas power plants emit flue gas with the lowest percentage of CO_2 at 3 - 5% while coal plants emit 9 - 14%, which all are within the range acceptable for algal growth (Lundquist, et al., 2010).

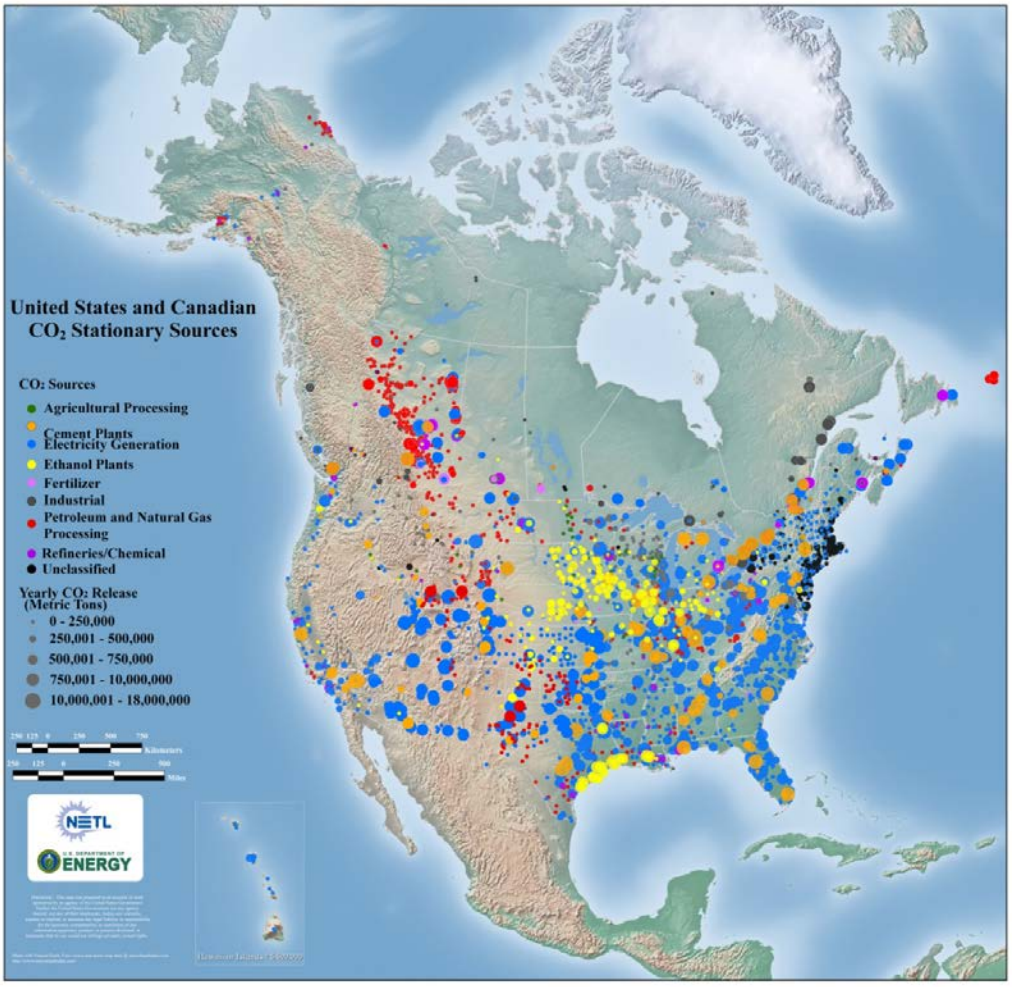

Figure 8: United States and Canadian CO_2 Stationary Sources (Source: http://www.netl.doe.gov).

Power plants also have up and down cycles, so there must be storage available or a design which accomodates pumping atmospheric air to the culture when flue gas is not available which averages between 11 - 35% of available hours in the year depending on the station and the year for an electricity generating coal plant (xcelenergy.com, 2011). The PBR growth scenario model includes cost for pumping and storing the flue gas to

maintain in storage at least one day's requirement for the algal culture size and growth rate.

Composition of flue gas depends on the source as shown in Table (5).

Fuel type	A. Bituminous coal	B. Sub-bituminous coal	C. Natural gas	D. Natural gas	E. Fuel oil
Gas (wt)	Utility boilers			Gas Turb Comb	Diesel
CO_2 (%)	18.1	24.0	13.1	5.7	6.2
O_2 (%)	6.6	7.0	7.6	15.9	17.0
N_2 (%)	71.9	68.1	79.3	78.4	76.7
SO_2 (ppm)	3504.0	929.7	0.0	0.0	113.1
NO (ppm)	328.5	174.3	95.1	22.1	169.7
NO_2 (ppm)	125.9	66.8	36.5	8.5	65.0

Table 5: Composition of gas mixtures according to combusted material (Olaizola, et al., 2003).

The potential exists that particulate matter and heavy metals from flue gas could inhibit growth or will produce inconsistent results in biomass and lipid productivity, but this has not been thoroughly investigated. An existing power plant likely has methods in place for removing particulates and heavy metals from the flue gas to meet EPA regulations. Therefore, the model assumes no additional cost for treatment of the flue gas then would likely already be present.

Nitrogen is between 4 and 8 percent of dry weight of algae (80g per kilogram of algae), and phosphorus is 0.1 percent. If wastewater or flue gas is not used, these nutrients, as well as iron and salt, if a marine diatom is being cultivated, must be purchased.

A significant part of the energy equation and CO_2 balance is based on securing a nitrogen source. Nitrogen is more expensive than oil by a factor greater than three:

nitrogen costs $1.4/kg, while oil costs $0.4/kg. A nitrogen source or nitrogen recovery and recycling is critical for large scale microalgae production to be cost effective and environmentally sustainable. Combustion systems such as incinerator or power stations can provide nitrogen in gaseous forms, NO_x. Securing flue gas as a nitrogen source also has the added benefit of reducing NO_x emission, which is needed to reduce ground level ozone (smog) (Richmond, 2004) (Nagase, et al., 2001) (Cantrell, et al., 2008). Unless an ammonia source (wastewater or fertilizer) is available, the model uses the growth factor (Q_{life} = 0.9 detailed in previous section) to reflect the lost algal productivity due to the need to fixate nitrogen.

Minimal nutrition and CO_2 requirements can be estimated using the general microalgal biomass stoichiometry: $CO_{0.48}H_{1.83}N_{0.11}P_{0.01}$ (Demirbas & Demirbas, 2010). Where the ratio between carbon in a molecule of CO_2 to an algal cell is 1:1, the ratio of oxygen is about 4:1. Therefore, carbon is limiting the algal growth, and it takes one molecule of CO_2 (with a mass of 44 g) to produce an algal biomass of 23.36 g (12+0.48*16+1.83*1+.11*14+.01*31). Thus the relationship in Equation (12) can be found for the total amount of CO_2 needed for a given mass of algae.

$$x = \frac{23.36y}{44} \qquad \text{Eq. (12)}$$

where x is the mass of CO_2 in grams,

and y is the mass of dry algal biomass.

Adding in the molecular weights of the elements yields:

$C(1.0*12)H(1.83*1)O(0.48*16)N(0.11*14)P(0.01*31)=C_{12}H_{1.83}O_{7.68}N_{1.54}P_{.31}$

Thus, the model determines the quantity of carbon, hydrogen, oxygen, nitrogen, and phosphorus consumed and contained in the resulting algal biomass where:

C = 51%, H = 8%, O = 33%, N = 7%, and P = 1% of dry weight biomass yield. Data from a typical coal plant operating during 2010 is used to estimate approximate grams of nitrogen, phosphorus, and carbon available from the flue gas per MW of the power plant. Since the N: O_x molecular mass will be in different ratios due to molecules of NO, NO_2, NO_3, and NO_4, the estimate assumes the N will be 0.3 the mass of the NO_x. The Redfield ratio for diatoms describes the necessary carbon, nitrogen, and phosphorus: 106:16:1 (Sato, et al., 2010), which implies the required nitrogen may be greater in proportion to carbon and phosphorus than the molecular formula indicates. The model assumes the necessary carbon is 53% of the biomass, necessary nitrogen is 8% of the biomass, necessary phosphorus is 5% of biomass, and silicon in the case of marine diatoms is equivalent to the nitrogen at 8% of biomass.

A factor to consider from a carbon sequestration standpoint is that marine phytoplankton generally excrete 5% to 20% of the carbon they fix, but more may be released under stress. Concentrations of dissolved organic carbon (DOC) in shallow and deep seas range from 0.4 to 7 g m^{-3}, being highest and most variable in the photic layer (Jenkinson, 1986). Therefore, some carbon fed to a culture will be released to the atmosphere. The model considers only the amount of carbon contained in resulting biomass when calculating cost benefits of carbon sequestration from flue gas.

Determining gas exchange is more complicated than the molecular formula for algae. The fluid dynamics play a crucial role in gas exchange, but has been rarely

quantified in the literature. Understanding of the productivity data in the literature is greatly increased if the gas recirculation is known, but measurements are uncommon. Theoretical methods for predicting the gas circulation do exist at least for one type of photobioreactor (Merchuk & Berzin, 1995).

Fluid Dynamics

Fluid dynamics is an important physical factor affecting the spatial distribution, nutrient uptake, and waste removal of microalgal cells within cultures; all of which affect the productivity (Preston, et al., 2001) (Degen, et al., 2001). Over the size scales relevant to low Reynolds' number organisms (10 - 100 μm), the motion is isotropic and homogeneous regardless of the manner in which it is generated (Preston, et al., 2001). It is likely that fluid motion determines the rate of a physiochemical process which is associated with the cell surface absorption or active absorption unique to each ionic species. Also, research indicates that the stimulus from fluid motion is transient (Savidge, 1981). It is important for a design to consider not only the amount of turbulence desired, but also the method of inducing the turbulence.

Inputs required for fluid motion analysis include: geometry of the growth volume, gas input geometry and flow volume, algae size, media viscosity, mechanical stirring geometry and rate, and light source geometry and intensity. Outputs needed which affect algal growth rates include: eddy size (L_K), dissipation rate (ε_D), local shear rate (τ_i), interfacial area (a), mass transfer coefficients (K_L), gas holdup (φ), shear rate (γ), heat generation (degrees Celsius), and light/dark cycle time (FLE). These variables determine

what cost and energy input are required to result in optimal algal growth and productivity.

Large Scale Turbulence

Large-scale turbulence is important to intermittently mix cells into lighted zones, distribute nutrients, prevent cell aggregates, and prevent temperature gradients for maximum photosynthesis and growth (Thomas & Gibson, 1990) (Merchuk & Gluz) (Degen, et al., 2001). Mixing the cells into lighted zones was previously discussed in this paper, and in the literature as flashing light effect (FLE). A typical light harvesting antenna in green algae consisting of 200 - 300 chlorophyll molecules can capture about one photon every 0.5 ms. Ideally, each algae cell would be exposed to high light for only the 0.5 ms required to capture one photon. However, this length of time is also dependent on the pigment content of each algae cell, which varies diurnally and by species. The reaction centers in the cell can only process one exciton about every 5 ms, so the cell should then be kept in the dark for at least that period of time or the length of time required to achieve a light to dark residence time of 1:10 (Lundquist, et al., 2010) (Degen, et al., 2001).

Open ponds experience a dark cycle every night, and while this is not optimal FLE, it does provide for a light: dark cycle seen in nature. It has been demonstrated that algae often experience photoinhibition in full sunlight, and there will not be a large amount of self-shading due to a lower culture density. However, the turbulence in an open pond will not be sufficient to provide sufficient culture mixing to induce a light:

dark cycle, so the model generates pond depth is equal to the light path length determined by Equation (7), except where noted.

Mixing the culture through gas exchange is an ideal method of avoiding photoinhibition if designed correctly, especially in photobioreactors. The gas must be supplied to provide nutrients anyway so there would be no or minimal added cost to use the gas supply as a source of agitation in the culture medium. Mixing the culture with the gas supply also provides the necessary turbidity to avoid algal conglomeration in certain spaces and adhesion to surfaces for the most part, while allowing the CO_2 and nitrogen to reach the cells and the oxygen to escape. All of these interactions require modeling to achieve the optimal mixing rate with the lighting and density of the culture.

For open ponds the gas exchange has normally been designed to be counter to the liquid flow, which in most cases results in a very slow bubble rise velocity and laminar flow. As mentioned in the literature review, laminar flow is to be avoided in order to prevent algal conglomeration and temperature gradients, to better provide nutrients, and allow oxygen to be released (Carvalho & Malcata, 2001) (Richmond, 2004) (Beardall, et al., 2008) (Merchuk & Gluz, 2004). Higher velocities must be avoided as well since they consume excessive energy and can create enough shear stress to damage the algae.

In open ponds and perhaps large photobioreactors mechanical mixing is required in addition to the mixing provided by gas exchange. Paddlewheels used in open ponds result in turbulence at the paddles and laminar flow elsewhere. However, there is evidence there is a helical flow pattern at the 180 degree turn in an open pond raceway, which would provide for some improvement from a laminar flow (James & Boriah,

2010). Also, temperature gradients, while yielding less than optimal algal growth, could assist in creating laminar flow in an open pond scenario.

A type of bioreactor which has been shown to provide optimal flow dynamics is an airlift reactor (ALR) (Merchuk & Berzin, 1995). The design of an ALR can be modified to result in variations in fluid dynamics, bubble disengagement, and flow rates of the various phases (Merchuk & Gluz, 2002). It also may be successfully used to control the mixing pattern to enable a regular light versus dark residence time of 1:10, with the objective of coming as close as possible to .5 ms to 5 ms (Degen, et al., 2001). Camacho, et al. (1999) found a solar illuminated vertical ALR to have higher photosynthetic efficiency than a horizontal-loop tubular photobioreactor (HLTP) despite higher light availability in the HLTP due to superior light-dark cycling. The fluid

dynamics of an ALR will be further discussed in the following section.

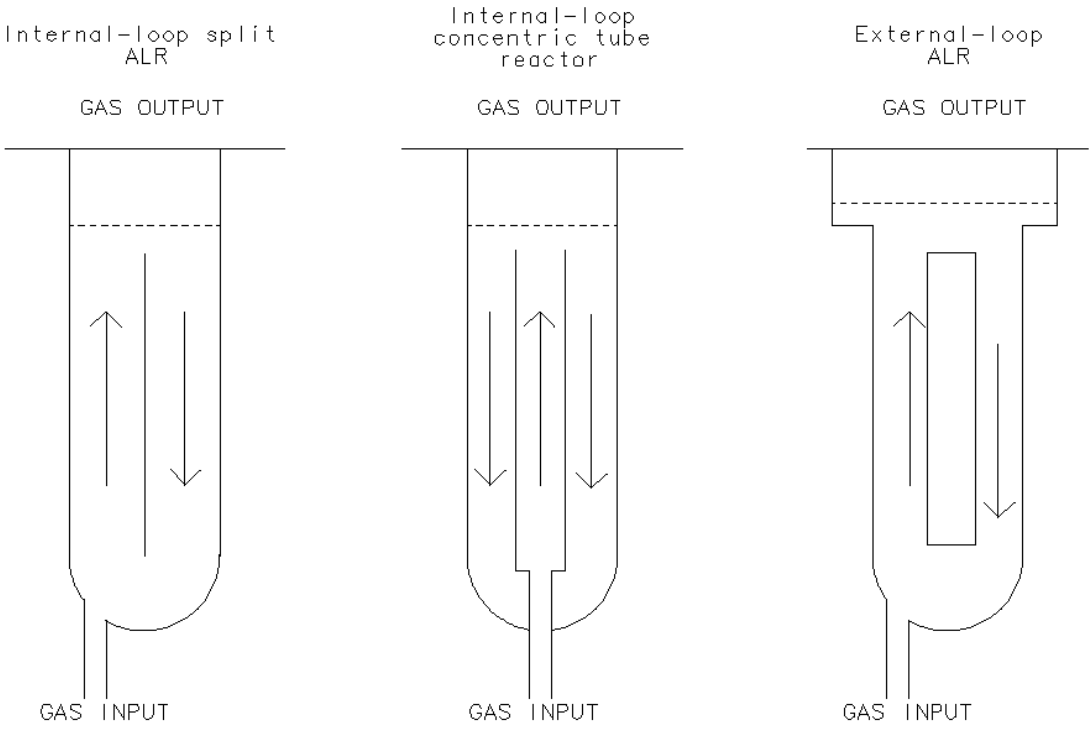

Figure 9: Different types of ALR's (adapted from Merchuk & Gluz, 2002).

Thus, the light path length determined in the previous section can be multiplied by ten when optimal turbulence is present in a PBR to determine a diameter. The model assumes an ALR design where the total diameter is a summation of light path length around the perimeter, light path length in the inner diameter, and ten times the light path length between the illuminated portions.

Figure 10: ALR design showing light: dark ratio (not to scale).

Paddlewheels

Power use increases by the cube of the flow velocity for open pond paddlewheels. The mixing energy required is calculated using Manning's equation:

$$H_b = \frac{Kv^2}{2g} \qquad \text{Eq.(13)}$$

where H_b = headloss in the bend (m),

v = velocity (m s^{-1}),

g = acceleration due to gravity (9.81 m s^{-2}),

and K = kinetic loss coefficient for 180° bends (theoretically = 2).

This will apply to sump pumps also since the flow will be directed around a baffle with 4x 90° bends.

Head loss due to friction along the length of the raceway and through PVC pipe is calculated as:

$$H_c = v^2 n^2 \left(\frac{L}{R}\right)^{\frac{4}{3}} \quad \text{Eq.(14)}$$

where n=roughness factor (0.018 for clay beds, 0.013 for concrete, 0.01 for PVC pipe),

L = length (m),

and R = hydraulic radius (A/P = D/4).

The model considers head loss due to friction, bends, gas sumps, paddlewheels, and raceway depth. The power savings are significant for concrete beds over clay beds, so the concrete roughness factor is used for all results.

The power required to overcome the total head loss is given by Equation (15):

$$W = 9.80\left(\frac{Qwh}{e}\right) \quad \text{Eq.(15)}$$

where W = power required (W),

Q = channel flow ($m^3 s^{-1}$),

w = unit mass of water, 998 kg m^{-3},

h = total head loss (m),

e = paddle wheel and drive system efficiency (40% assumed),

and 9.80 = conversion factor in $\frac{W*s}{kg*m}$.

Finally the total energy consumption is represented by:

$$E = \frac{t_{op}*W*3600}{1000} \quad \text{Eq. (16)}$$

where t_{op} = average time in hours pumps and paddlewheels are operating in a day,

1000 = watts/kilowatt,

3600 = seconds/hour,

and E = kwh day^{-1}.

Average time for pump and paddlewheel operation is assumed to be eight hours per day for open ponds, and two hours per day for photobioreactor pumps. Open ponds must pump additional water into the ponds to compensate for evaporation and have greater distance to pump the water and culture. Paddlewheels are assumed to operate during for 8 hours during daylight, which is a conservative estimate since daylight would likely be more than eight hours.

Pumps

The head loss for pumping water and media into photobioreactors and open ponds is the sum of length traveled and change in elevation through pipes, valves, bends and tees to reach each photobioreactor or pond.

$$h_T = h_B + h_f + h_E \qquad \text{Eq.(17)}$$

The head loss for pumping in open ponds would be predominantly due to greater length and volume, while head loss from pumping to photobioreactors would be mostly due to elevation gain, which would be regained when the culture is harvested. Assuming the desired velocity is low enough for the flow to remain laminar, and also assuming the medium viscosity and density are equal to water, the power required to pump water and media can be calculated with the Hagen-Poiseuille equation:

$$h_f = \frac{32\mu LV}{\rho g D^2} \qquad \text{Eq.(18)}$$

where h_f = head loss (m),

μ = dynamic viscosity (1.08×10^{-3} Pa s for seawater, or 1.003×10^{-3} Pa s for fresh water, $1.983*10^{-5}$ Pa s for air),

L = length of pipe (m),

V = velocity,

D = hydraulic diameter (m),

ρ = fluid density (kg/m^3),

and g = acceleration of gravity ($9.81\ m/s^2$).

Equation (15) is also used to determine the pump power required to pump media into and out of the cultures for both open ponds and photobioreactors, except the assumed efficiency for the pump is 70%.

The model uses dynamic viscosity calculated due to culture density, wastewater or media, salt, and temperature.

Small-Scale Turbulence

The amount of shear stress which is healthy for an algal culture depends on the size and species of the algae, the culture density, and the viscosity of the medium. A certain amount of turbulence is desired since it is necessary for gas exchange and nutrient availability, as well as preventing algae from adhering to surfaces. Experiments reveal a hyperbolic relationship between shear forces and nutrient uptake rate, as well as algal culture growth rate (Peters, et al., 2006).

Damage induced by shear stress has been demonstrated both in bubble columns due to gas sparging and in pumps due to the pumping action, where shear stress was quantified indirectly through liquid flow rate or the number and frequency of pump

passages (Michels, et al., 2010). Cell damage in sparged reactors and open ponds can be classified into five possible mechanisms, one involving purely hydrodynamic forces acting on the cell (shear stress), and the other four involving interactions with bubbles. The cell-bubble damage mechanisms are: (1) cell interactions with bubble generation at the sparger (2) cell interactions with rising bubbles (3) cell interactions with bubbles coalescing and breaking up in the region of the bubble rise; and (4) cell interactions with bubbles at the air-medium interface (Contreras, et al., 1998). For this reason, turbulence created through the gas delivery system requires further scrutiny in regards to cell interactions with bubbles and microeddies created by bubbles breaking up, but otherwise fluid motion is isotropic and homogeneous regardless of the manner in which it is generated over algal cell size scales (Preston, et al., 2001).

Small-scale effects of turbulence may include mechanical interference with cell functions, cell damage, or disruption of low-nutrient microzones around cells that facilitate nutrient uptake and waste removal (Thomas & Gibson, 1990). Higher flow velocity has been shown to reduce microzone magnitude and overcome diffusive transport limitations which aid in algal nutrient uptake (Savidge, 1981) (Thomas & Gibson, 1990). Also, research indicates nutrient uptake differs depending on which nutrient is being taken up for the same algae species, which means there are benefits to variations in turbulence (Thomas & Gibson, 1990) (Savidge, 1981) (Peters, et al., 2006).

Shear stress in the correct quantity stimulates microalgae. There is evidence that some dinoflagellate microalgae species respond to shear stress through population growth inhibition and escape behavior such as bioluminescence. Although it is not yet known

whether algae are responding to the fluid force, shear-stress dependence has been reported in other cell types, where the physical deformation of the cell by fluid forces acting on it elucidate a response from the cell (Maldonado & Latz, 2007). Diatoms also have sensing systems for detecting and responding to shear stress within seconds, and make intracellular adjustments to changes in the cell boundary layer on the order of minutes (Falciatore, et al., 2000). Studies reveal the dinoflagellates are the most sensitive to small-scale effects of turbulence, with diatoms, blue-green algae, and green algae being progressively less sensitive, in that order (Thomas & Gibson,1990).

Fluid motion continues to have greater influence on rate-limited processes even when algae are capable of swimming (Preston, et al., 2001). While research has produced evidence that turbulence affects several microalgal physiological processes, these effects have not been often quantified in terms of dissipation rate (ε), strain rate (γ), or shear stress (τ). Thomas & Gibson (1990) found values of $\varepsilon > 1.8 \times 10^{-5}$ $m^2 s^{-3}$, $\tau >$ 0.04 dynes cm^{-2} (0.002 N m^{-2} or Pa), and $\gamma > 4.4$ rad s^{-1} ($L_K > .4$ mm), resulted in culture degradation for flagellates, and Garcia Camacho, et al. (2007) found a strain rate above 0.12 s^{-1} resulted in damage to *Protoceratium reticulatum*. Flagellates are the most sensitive, so most algae species should be well within suitable growth conditions with values greater than those above.

Indeed, for non-motile algal species it is especially important to provide sufficient turbulence in order to avoid sedimentation. Flow intensities of up to 30-40 oscillations/minute were necessary to avoid sedimentation for *N. oculata* in 12 mL volume of 2.0e6 cells/mL suspension. 40 oscillations/minute produced peak productivity

at $\varepsilon = 6.9 \times 10^{-4}\ m^2 s^{-3}$, $\gamma = 6.77\ s^{-1}$, and $L_K = 0.2$ mm (Preston, et al., 2001). Contreras, et al. (1998) found *P. tricornutum* demonstrated peak productivity at a shear rate of $\gamma = 7{,}000\ s^{-1}$. Maximum shear rate while maintaining laminar flow is about $150\ s^{-1}$, and shear rates up to $14{,}000\ s^{-1}$ ($\tau \approx 20$ Pa) can occur inside of a photobioreactor (Michels, et al., 2010) (Contreras, et al., 1998). In the sea, strain rate (γ) varies from $0.0003\ s^{-1}$ to ~35-$250\ s^{-1}$, assuming that $\eta \approx 1$ mPa s, calculated from values of viscous dissipation of energy per unit volume, ε, for tumbled waves (Jenkinson, 1986). Freshwater ponds and lakes exhibit strain rate (γ) values of $.1\ s^{-1}$ to $10\ s^{-1}$ ($\varepsilon \approx 10^{-8}$ to $10^{-4}\ m^2\ s^{-3}$) under intense conditions (Preston, et al., 2001). The model uses strain rate also as an indicator of microeddy length scale compared to the algae size to maintain the microeddy length approximately 10μm longer than the cell length. Although shear rate aids in estimating whether specified turbulence is advantageous to culture health, damage to algal cells depends on shear stress not on shear rate, except where the shear rate is indicative of microeddy length scale.

Maximum shear stress prior to 52% to 66% loss in cell viability for the diatom *Chaetoceros muelleri* was found to be between 1 and 1.3 Pa when it is artificially induced through increasing viscosity of the medium using a thickener, and shear stress of 1.8 Pa could be applied to a culture with no thickener in the medium without losing viability indicating that flow instabilities could have influenced results (Michels, et al., 2010). Loss began in the first minute and continued only for 8 minutes, and further increases in shear stress did not result in further loss of viable cells, indicating only a certain percentage of cells are sensitive to shear stress. Michels, et al. (2010) and other studies

induced stress mechanically rather than through turbulence created by inlet gas velocity (Maldonado & Latz, 2007) (Kong, et al., 2009) (Wang, et al., 2009). Studies have speculated that shear stress disrupts cell division, so it is the cells in the process of dividing which lose viability. No external damage is observed at shear stress up to 19.4 Pa, indicating the damage is internal. Complete destruction of cells only occurs at much higher shear of 50 - 100 Pa (Michels, et al., 2010). While establishing a rough boundary of limits, the studies have been inconclusive on determining maximum shear stress.

Maximum shear stress accommodated by the algae is a function of the algal cell size, species, viscosity, and the design of the photobioreactor. General assumptions must be made and ranges decided on depending on the algae species and the required design. While shear stress is likely to negatively affect algae in a photobioreactor, reducing fluid velocity can lead to other complications, such as mass transfer which also negatively affects growth rate. Studies indicate optimal mass transfer rates occur when the flow is heterogeneous or churn turbulent flow (Schumpe & Deckwar, 1987) (Merchuk & Gluz, 2002). Shear stress results depend on the culture density, gas velocity, viscosity, and temperature. Model scenarios are chosen in which the shear stress is within 4 – 15 Pa, but the optimal shear stress will depend also on interfacial area and heterogeneous flow, which is covered in the following section.

The shear stress (τ, Pa) is related to the fluid shear rate (γ, s^{-1}) and dynamic viscosity (η, Pa*s) by:

$$\tau = \eta\gamma \qquad \text{Eq. (19)}$$

Viscosity is the measure of the ease with which a fluid moves in reponse to an applied force. If the medium viscosity changes, the shear stress will be affected, even if the shear rate remains the same. For a fluid sheared at a constant rate, the resulting shear stress will proportionally increase with gains in viscosity. Thus, shear stress increases linearly with viscosity increase, resulting in a lower threshold for cultures in which the viscosity is raised by nutrients, algal cells, and/or wastewater.

The viscous dissipation rate, ε (m^2/s^3), is related to the kinematic viscosity (m^2/s) and shear rate by:

$$\varepsilon = \gamma^2 \upsilon \qquad \text{Eq.(20)}$$

The kinematic and dynamic viscosity are related by:

$$\upsilon = \eta/\rho \qquad \text{Eq.(21)}$$

where ρ is the fluid density (kg/m^3) .

However, in a bioreactor there are additional factors to consider that contribute to dissipation rate which include wall friction and dissipation associated with bubbles with the latter being by far the greatest factor (Merchuk & Berzin, 1995).

Microeddies resulting from turbulence must remain larger than the algae size, or damage to the algal cell and culture devastation will result. The size of the smallest eddies is approximated using the Kolgomorov length scale:

$$L_K = \left(\frac{\upsilon^3}{\varepsilon}\right)^{\frac{1}{4}} \qquad \text{Eq.(22)}$$

Past results indicate in the vast majority of cases the Kolgomorov length scale will be greater (0.3 mm – 1.78 mm) than the algae length (10 - 100 μm) (Preston, et al., 2001). The microeddy length is extremely sensitive to simulated strain-dependent effective

viscosity (Jenkinson, 1986). The boundary between turbulent and laminar flow is estimated by the Kolmogorov turbulence microscale, defined as the size at which turbulent eddies are dampened by molecular viscosity to laminar fluid shear. Thus, microalgae experience fluid motion as laminar shear and velocity gradients within the fluid can cause mechanical shear stress on plankton (Preston, et al., 2001) (Hondzo & Lyn, 1999).

Fluid dynamics research indicates cell damage occurs when microeddy length is less than the length of the cell experiencing the eddy, and studies reveal the maximum growth rate for algae is obtained when turbulence is maintained such that microeddy length scale is approximately equal to or slightly greater than the algal cell length. The growth rate not only decreases when the microeddies are smaller than the cellular dimension, but it also decreases when the microeddy length increases approximately 10 μm beyond the length of the cell (Preston, et al., 2001) (Contreras, et al., 1998).

The model incorporates calculation of Kolgomorov length from viscous dissipation and bubble dissipation as a check to verify the resulting Kolgomorov length is no less than, but as close as possible to the cell length. Strain rate is chosen within range of 250 - 15,000 s^{-1} to compare with shear stress and interfacial area.

Rheology Most studies assume the viscosity of the medium is equal to fresh water, but in fact there are many variables to consider before assuming the viscosity. When marine algae are being grown and sea water is used, different properties than fresh water must be assumed. Based on the relationship $\eta = \rho\upsilon$, seawater has a dynamic viscosity (η) of 1.076 x 10^{-3} Pa s, density (ρ) of 1028 kg m^{-3}, and kinematic viscosity (υ)

of 1.047 x 10^{-6} m^2 s^{-1} at 20ºC compared to 1.0027 x 10^{-3} Pa s, 998 kg m^{-3}, and 1.0047 x 10^{-6} m^2 s^{-1}, respectively, for fresh water at 20ºC (Kaye & Laby, 2005).

However, there are other factors affecting the viscosity including temperature, nutrients added which may be in excess if wastewater is used, and the algae itself as the culture density increases.

Temperature

A change in termperature has a higher impact on the kinematic viscosity (ν) of water than on the dynamic viscosity or density (Herbing & Keating, 2003). Temperature of a culture can vary between 20ºC and 30ºC, with average assumed to be 25ºC. The dynamic viscosity of water decreases with increasing temperature so that the viscosity of fresh water at 25ºC is 8.90e-4 Pa s. Seawater change in kinematic viscosity (ν, x 10^{-6} m^2 s^{-1}) can be determine with Equation (23).

$$\nu = 0.0005T^2 + 0.0496T + 1.8355 \quad \text{Eq.(23)}$$

where T is measured in degrees Celsius (Rawson & Tupper, 1968).

Freshwater dynamic viscosity variation with temperature (within 253.15K ≤T≤383.15) at 0.1 MPa is described by Equation (24) (Huber, et al., 2009).

$$\eta = \int_{i=1}^{4} a_i (T)^{b_i} \quad \text{Eq. (24)}$$

where T=T/(300K) and a_i and b_i are coefficients given in Table (6).

i	a_i	b_i
1	280.68	-1.9
2	511.45	-7.7

3	61.131	-19.6
4	0.45903	-40

Table 6: Coefficients a_i and b_i for the viscosity of water at 0.1 MPa.

The temperature dependent density is determined using Equation (25).

$$\rho = \beta_0 + \beta_1 T + \beta_2 T^2 + \beta_3 T^3 + \beta_4 T^4 + \beta_5 T^5 + \beta_6 T^6 \quad \text{Eq.(25)}$$

where ρ is the density of water in kg/m^3 (Perry & Green, 2008).

T is the water temperature in degrees Celsius,

and β is defined as:

$\beta_0 = 998.845916$
$\beta_1 = 6.5700985E\text{-}02$
$\beta_2 = -8.7817835E\text{-}3$
$\beta_3 = 8.3996043E\text{-}5$
$\beta_4 = -7.8432029E\text{-}7$
$\beta_5 = 4.6724264E\text{-}9$
$\beta_6 = -1.2487522E\text{-}11$

Suspension

Solid particles suspended in a conventional Newtonian liquid form a suspension. The f/2 medium with necessary nutrients used to grow marine cultures increases liquid density by 0.118 - 0.127 kg/m^3, and the Bristol medium used for growing freshwater species adds 0.625 kg/m^3. Wastewater density can vary, but typically has a density of 0.525 kg/m^3 more than water alone, with unknown viscosity. While the nutrients contained in growth mediums will be dissolved, Einstein's intrinsic viscosity factor can be used to determine the effective viscosity from the particles in the wastewater (Einstein, 1906) (Einstein, 1911).

The viscosity increases as the density of the culture increases for non-motile algae and at a certain density for motile algae when the density affects their motility. In passive suspensions, the viscosity increases with the volume fraction of particles. The volume fraction is defined as the volume of the set of particles divided by the total volume of the suspension.

$$\varphi = \frac{\frac{4}{3}N\pi R^3}{V} \quad \text{Eq.(26)}$$

where N is the number of particles,

V is the volume of the suspension,

and φ is the volume packing fraction.

The effective viscosity (η_{eff}) of a suspension of passive spherical particles in a solvent of viscosity η_o depends on its volume packing fraction (φ). Krieger & Dougherty's (1959) semiemperical law provides a relationship:

$$\eta_{eff} = \eta_o\left(1 - \frac{\varphi}{\varphi_m}\right)^{-\alpha\varphi_m} \quad \text{Eq. (27)}$$

where φ_m is the maximal packing volume fraction, which is set at 0.62. For a dilute regime, where $\varphi << 1$, Equation (27) reduces to $\eta_{eff} \approx \eta_o(1 + \alpha\varphi)$. Where α is known as Einstein's intrinsic viscosity, and $\alpha = 2.5 \pm 0.1$ for passive and spherical particles in a strong dilution. Rafai, et al., (2010) showed that the swimming motion of *Chlamydomonas reinhardtii* results in $\alpha = 4.5 \pm 0.2$. Also, Brenner (1969) found a relationship for intrinsic viscosity of particles with gravity hindered rotation to be about 4. These relationships only apply to dilute solutions, but even at the optimal harvest density of 60 g/L, the solution is still strongly dilute (packing volume fraction (φ) of

~.06). At such a strong dilution in a turbulent flow, rotation will be more influenced by fluid motion than gravity so that the rotation is not considered gravity hindered.

Therefore, $\alpha = 2.5 \pm 0.1$ is assumed for the algal culture in open pond and photobioreactor growth scenarios. The change in viscosity resulting from the algal culture itself at expected maximum density from the literature (60 g/L) is determined to be 1.6e-4 Pa s for seawater or 1.5e-4 Pa s for fresh water if the algae is non-motile. (Motile live algae could increase the dynamic viscosity even more by a factor of 127% to 1.36e-3 Pa s, but are not included in the analysis to follow.)

The particles (TOC and COD) in wastewater can be calculated similarly, where TOC total 0.140 g/L and COD total 0.258 g/L after initial treatment, or a total of 398 g/m^3. The size of these particles have been found to range from 0.4 - 200 μm, while the particles 100 - 200 μm will settle more easily, which means the majority of the particles remaining would be 0.4 – 5.0 μm in size, making the volume average 8 - 9e-18 m^3 (Tiehm, et al.) (Wu & He, 2009). The average density for these small particles are assumed to be roughly equivalent to water, so that 0.398 g/L = 0.398e-6 m^3/L or 0.398e-3 m^3/m^3.

Adding all the viscosity factors together results in Equation (28).

$$\eta_T = \eta_{eff} + \eta_{nut} + \eta_{salt} + \eta_{ww} + \eta_{temp} \qquad \text{Eq.(28)}$$

All the factors influencing the viscosity including the nutrients, culture density, salt or fresh water, wastewater and temperature effects are included in the model.

Newtonian vs. Non-Newtonian Flow

Oceanographers consider the sea to be newtonian, which is to say the viscosity depends only on temperature and pressure, and the stress (τ) versus strain rate (γ), or viscosity, is linear. However, research suggests microalgae cultures produce non-Newtonian properties in growth media such as time-dependent shear thinning (Jenkinson, 1986) (Rafai, et al., 2010). Studies indicate assuming Newtonian behavior of cell cultures could cause substantial error in shear stress estimates (Michels, et al., 2010).

Non-Newtonian properties have been predicted for algal cultures since Newtonian fluid is valid only when particles rotate with the local vorticity of the fluid motion. Free motion is only possible when the individual particles are not acted on by any external forces. However, the center of mass of each inhomogeneous algal cell is not always at the geometric center, hence the gravitational field could be one of those external forces (Brenner, 1969).

When the externally applied torqe is anti-parallel to the vorticity, the torque slows down particle rotation, more mechanical energy is dissipated, and the effective viscosity is increased. However, when the particle rotation is enhanced by the external torque, it is easier to shear the suspension and effective viscosity decreases (Brenner, 1969). The design must consider the orientation of external gravitational, magnetic, and electrical fields in order to accurately determine the fluid behavior, a type of configurational anisotropy.

Non-Newtonian flow may also result from cells producing polysaccharides and/or clustering, but are not necessary to obtain a strong modification of the effective viscosity (Merchuk & Gluz, 2004) (Jenkinson, 1986). Clustering occurs when particles group

together in elongated aggregates due to dipole-dipole interaction of mechanical or electrical origin (Jibuti, et al., 2012). Both external fields acting on the rotation of particles and the fields surrounding each particle have the possibility of changing the mechanical properties and thus the rheology of the medium (Jibuti, et al., 2012). The model assumes the required turbulence will prevent any clustering, and will prevent any strong modification of viscosity from the external field, since the culture density is very low. This is proven analytically below.

A non-Newtonian fluid is one whose flow curve (shear stress versus shear rate) is non-linear or does not pass through the origin. In other words, the apparent viscosity is not a constant at a given temperature and pressure, but also is dependent on flow conditions such as flow geometry, shear rate, and sometimes even on the kinematic history of the fluid element under consideration. Shear-thinning or pseudoplastic fluids are the most common type of time-independent non-Newtonian fluid behaviour observed, and are characterized by an apparent viscosity which decreases with increasing shear rate (Chhabra & Richardson, 2008). However, generally speaking the fluid will become Newtonian again at very high ($>10^5$ s^{-1}) and very low ($<10^{-2}$ s^{-1}) shear rates, although the exact values will depend on the material (Chhabra & Richardson, 2008).

The following analysis assumes microalgal suspensions are dilute sheared suspensions of non-colloidal approximately spherical particles in an external field. Nishikawa, et al. (1977) found a direct proportionality between the superficial gas velocity and the global shear rate in Equation (29).

$$\gamma = 5000 * V_G \quad (V_G > 0.04 \text{ m/s})$$ Eq.(29)

Equation (29) has been used exclusiviely for bubble columns with gas-liquid and gas-liquid-solid viscous systems (Al-Masry & Chetty, 1996). Schumpe & Deckwar (1987) found the shear rate to be smaller than predicted by Equation (29) (Merchuk & Gluz, 2004). The correct solution for determining viscous shear rate is still to be found, and can vary up to three orders of magnitude depending on the equations used (Merchuk & Gluz, 2002). Since the literature reveals a range of maximum shear stress levels, and Equation (29) has been widely accepted despite criticism, the model uses the above equation with a maximum shear stress predicted in the literature (~15-16 Pa) along with other factors to be detailed in the following sections.

$$\eta = \eta_o \left(1 + \frac{5}{2}\varphi\right)$$ Eq.(30) (Einstein, 1906)

Equation (30) is the viscosity of the suspension in the absence of an external field, or when the vorticity of the fluid motion is dominant over the external field.

The hydrodynamic couple exerted by the fluid on the *i*th particle can be calculated using Faxen's law:

$$L_i = 8\pi\eta_o a^3(\omega_o - \omega)$$ Eq. (31)

where a is the sphere's radius, ω the angular velocity of the sphere,

and ω_o is the vorticity vector associated with the undisturbed flow:

$$\omega_o = \tfrac{1}{2}\ \mathbf{rot}\ \mathbf{V_o}$$ Eq. (32) (Brenner, 1969)

where $\mathbf{V_o}$ is the velocity field in absence of particles.

However, Brenner (1969) showed balancing the hydrodynamic and external couples on each particle is implicitly equivalent to satisfying the angular momentum in Equation (33).

$$\mathbf{T_x} + \mathbf{G} = 0 \qquad \text{Eq. (33)}$$

where $\mathbf{T_x}$ is the deviatoric stress tensor or the vector invariant of the deviatoric stress in Cartesian tensor notation defined in Equation (34).

$$(\mathbf{T_x})_i = -\varepsilon_{ijk} T_{kj} \qquad \text{Eq. (34)}$$

where ε is the alternating isotropic triadic,

and **G** is the external body couple per unit volume of suspension defined in Equation (35).

$$\mathbf{G} = -6\eta_o \varphi(\omega_o - \mathbf{\Omega}) \qquad \text{Eq.(35) (Brenner, 1969)}$$

Gravity gives structure to the suspension. However Brenner (1969) showed that when the shear rate effectively destroys the structure given by gravity, the Einstein Equation (30) applies. The determining factor is a dimensionless constant defining the ratio betweeen the strengths of the dipolar and hydrodynamic couples, λ.

$$\lambda = \frac{\rho g d}{6\eta_o \omega_o} \qquad \text{Eq. (36) (Brenner, 1969)}$$

where ω_o is the angular rotation of the particles,

and $d = |d_i|$, where d_i is the vector drawn from the geometric center of sphere *i* to its center of mass.

As $\lambda \to \infty$, gravitational forces dominate, and where $\lambda \to 0$, the shear rate dominates. Hence, when $\lambda \leq 1$, the Einstein Equation (30) applies to derive the effective viscosity.

Analysis reveals in most cases, the cell radius (maximum d) is small enough to maintain $\lambda \leq 1$ where $\rho \approx 1100$ kg/m^3, g = 9.81 m/s^2, $d \leq 0.0003$ m, $\eta_o = 1.076 \times 10^{-3}$ Pa s, and $\omega_o > 500$. Where $-\gamma/2 \leq \omega_o \leq \gamma/2$, shear rate must be at least 1000 s^{-1} in order to apply the Einstein equation ($V_G \geq 0.2$ m/s). Jibuti, et al. (2012) also showed that when $\varphi << 1$, $\Delta\eta_{eff}$ tends to $5/2\varphi$. When $\varphi < 28\%$, $\Delta\eta_{eff}$ is linear, and it is fitting to follow the empirical law in Equation (37).

$$\Delta\eta_{eff}(\varphi, \theta) = \Delta\eta^{o}_{eff}(\varphi)(1 + \frac{3}{5}\theta) \qquad \text{Eq. (37) (Jibuti, et al., 2012)}$$

where $\theta = (\frac{\gamma}{2} + \omega_o) / (\frac{\gamma}{2})$ represents the relative angular velocity of the particles divided by the vorticity of the shear flow (Jibuti, et al., 2012).

Also for a dilute regime ($\varphi << 1$), Faxen's law can be applied to derive the shear stress exerted on each particle in Equation (38).

$$\sigma_{xy} = \frac{N}{2V} 8\pi R^3 \omega_o \eta \qquad \text{Eq. (38) (Jibuti, et al., 2012)}$$

where N is the number of algal cells,

V is the volume of the liquid (m^3),

R is the radius of the algal cells (m),

and ω_o is the vorticity = $\gamma/2$ (s^{-1}).

ALR Analysis Through including these factors in the calculation of the viscosity for dilute suspensions in the model, the shear stress profile can be derived or verified for a given design, so that photobioreactor size, culture density, gas inlet velocity, gas inlet size and spacing, and light spacing can all be optimized. CO_2 transfer also may be optimized using fluid dynamics analysis to achieve heterogeneous flow, while avoiding

bubble breakup and small microeddies which may damage the algae (Contreras, et al., 1998). Open ponds will experience turbulence and resulting shear stress at the paddlewheels, with laminar flow downstream throughout the majority of the flow regardless of design. The fluid dynamics for open ponds will not be optimal, which is reflected in the decreased culture density.

The model calculates dissipation due to viscosity and bubbles. While the dissipation due to wall friction is very small, the energy dissipation due to the presence of bubbles should be considered. Total energy dissipated from bubbles can be calculated using Equation (39).

$$\varepsilon_D = Q_{in} P_4 \ln \frac{P_4}{P_1} \qquad \text{Eq. (39) (Merchuk \& Berzin, 1995)}$$

where Q_{in} is the incoming flow rate of gas (m^3/s),

and P_4 and P_1 are the pressures in the designated areas of the ALR shown in Figure (11).

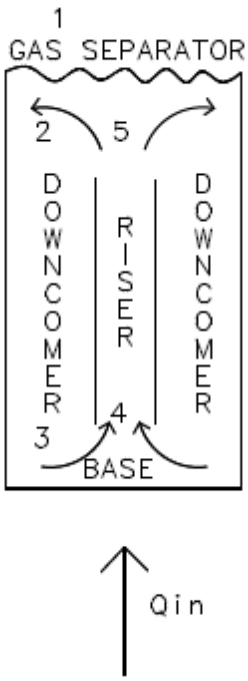

Figure 11: Schematic representation of ALR pressure regions (adapted from Merchuk & Berzin, 1995).

In conventional stirred tanks, ponds or bubble column photobioreactors, the energy required for movement of the fluids is introduced focally. Consequently, energy dissipation is very high in the immediate surroundings of the stirrer or sparger, and decreases away from it towards the walls. This means the shear stress also will be greatest near the stirrer or sparger, and the culture will experience a large shear gradient, while a large portion of the culture experiences less than optimal turbulence (Merchuk & Gluz, 2004).

The ALR avoids these complications by using the pressure differential between the riser and downcomer to create fluid motion as defined in Equation (40).

$$\Delta P = \rho_L g(\varphi_r - \varphi_d)$$ Eq.(40) (Merchuk & Berzin, 1995)

where ΔP is the pressure difference between riser and downcomer,

ρ_L is the liquid density,

g is the gravitational constant (9.81 m/s^2),

and φ_r and φ_d are the fractional gas holdup of the riser and downcomer, respectively.

Energy input for an ALR is superior to that of agitated systems and bubble sparging for a given mass transfer rate, since the pressure differential produces much of the flow (Merchuk & Gluz, 2004). Maximum shear in an ALR should be located at the 180° turn at the bottom of the reactor, but otherwise heterogeneous turbulence should be distributed in both the riser and the downcomer (Merchuk & Gluz, 2004). There are four distinct sections with different flow characteristics in an ALR: the riser, the downcomer, the base, and the gas separator.

The gas holdup is the volumetric fraction of the gas in the total volume of a gas-liquid-solid dispersion as defined in Equation (41).

$$\Phi_i = \frac{V_G}{V_G + V_L + V_S}$$ Eq.(41) (Merchuk & Berzin, 1995)

where the subindexes L, G, and S indicate liquid, gas, and solid, and i indicates the region in which the holdup is located (Merchuk & Gluz, 2004).

Holdup both gives an indication of mass transfer and flow circulation, although mass transfer also depends on the bubble size and distribution. Where the flow is non-slip, and the gas velocity equals the liquid velocity, the gas holdup (Φ) is equal to the flowing volumetric concentration ($\beta = \frac{J_G}{J} = \frac{Q_G}{Q_G + Q_L}$) (Merchuk & Berzin, 1995). An example of

such a case is when there are very small bubbles moving in a relatively fast liquid, and there is no influence of one phase of motion on the other. Where the gas holdup is less than the flowing volumetric concentration, $\Phi < \beta$, the liquid is driven by the gas (condition in the riser), and in the opposite case where the gas holdup is greater than the flowing volumetric concentration, $\Phi > \beta$, the gas is driven by the liquid (condition in the downcomer). The gas recirculation rate and downcomer gas holdup are calculated with Equation (42).

$$J_{Gd} = 3.508\varphi_d^2 + 0.22\varphi_d + 0.00011 \qquad \text{Eq. (42)(Merchuk \& Berzin, 1995)}$$

Thus, the true gas superficial velocity can be calculated by adding the recirculating gas rate to the gas inlet rate.

The drift velocity of a swarm of bubbles is given by Equation (43).

$$V_d = 1.53\left[\left(\frac{\sigma g \Delta\rho}{\rho L^2}\right)\right]^{0.25}(1-\Phi)^{1.5} \qquad \text{Eq. (43) (Merchuk \& Berzin, 1995)}$$

where σ = surface tension (N/m),

g= gravitational acceleration (9.81 m/s),

$\Delta\rho$ = difference in density between gas and liquid (kg/m^3),

and ρ = density of liquid (kg/m^3).

Surface tension is determined by Equation (44) (Vargaftik, et al., 1983):

$$\sigma = 0.2358\left[\frac{647.15 - T_K}{647.15}\right]^{1.256}\left[1 + -0.625\frac{647.15 - T_K}{647.15}\right] \qquad \text{Eq. (44)}$$

where T_K is the temperature in Kelvin.

Equation (43) is valid for bubbles of diameters on the order of 0.1 to 2 cm, which covers those commonly observed in algae bioreactors. Lower gas velocities produce finer

bubbles, so laboratory conditions with lower gas velocities may result in gas bubble diameters for which Equation (43) does not apply. Generally, the bubble drift velocity should be representative of the two-phase flow in the riser of an ALR. The distribution parameter (C_o) has a narrow range, and one can make a judicious guess of its value in an unknown system (1.00 - 1.11). The gas inlet velocity can be added to the drift velocity to determine the superficial gas velocity.

The liquid velocity in the riser can be obtained using Equation (45).

$$V_{Lr} = \frac{J_{Gr}\left(\frac{1}{\Phi_r} - C_o\right) - (V_G - J)}{C_o(1 - \Phi_r)}$$ Eq. (45) (Merchuk & Berzin, 1995)

Geometric design of the bioreactor has a significant impact on gas holdup. It is interesting to analyze variations in hydrodynamics created by changes in geometry of the ALR. The bottom clearance can be used as a tool to increase the shear to control aggregation and produce turbulence needed by the algae to varying degrees.

Gas holdup is also an important factor involved with removal of waste oxygen from the culture media. Oxygen removal is crucial in order to avoid damage to the culture, and must be kept below 35 mg/L according to one study (Carvalho, et al., 2006), and below 20 mg/L according to another (Acien, et al., 2001). To prevent inhibition and damage, the maximum tolerable dissolved oxygen level should not generally exceed about 400% of air saturation value (or about 1 g/L) according to Chisti (2007). Under high irradiance an algal culture can produce oxygen at a rate of 10 g m^{-3} min^{-1} (Chisti, 2007), but this would depend on the culture density. The equation for photosynthesis reveals that for every molecule of CO_2 used in photosynthesis, one molecule of H_2O is

used, and one molecule of O_2 is released as waste. Calculations indicate 1.932 g/L of O_2 will be produced to reach optimum culture density of approximately 60 g/L.

$$CO_2 + H_2O \xrightarrow{\text{Sunlight}} [CH_2O] + O_2 \qquad \text{Eq. (46) (Schlagermann, et al., 2012)}$$

The model determines the quantity of oxygen produced by the specific culture density and the maximum length for the volume of algae so that the amount of dissolved oxygen doesn't exceed .028 g/L, assuming turbulence is sufficient and the top of the photobioreactor allows escape into the atmosphere. The volume of algae per length is dependent on both the algal density and the optimal photobioreactor diameter(s). The depth of open ponds is verified by calculating quantity of g/L oxygen generated, and making some assumptions about how long it would take that oxygen to escape to the atmosphere. The assumption is once the dissolved oxygen makes contact with air, the majority would escape as long as below 400% of air saturation or approximately below 1 g/L.

Mass Transfer

Information needed to characterize flow in a bioreactor include gas holdup, bubble size, liquid velocity, and mass transfer rates, all being a function of the gas input rate and geometry of the system (Merchuk & Berzin, 1995). In order to design a bioreactor with optimal CO_2 mass transfer rates, the mean circulation time for the gas to complete one loop must be calculated and then used in Equation (47) to determine the residence time in any section of the reactor:

$$(t_r)_n = t_c \frac{V_n(1-\varepsilon_n)}{V_D(1-\varepsilon)} \qquad \text{Eq. (47) (Contreras, et al., 1998)}$$

where t_c is the mean circulation time,

V_n is the volume of the section,

V_D is the volume of the reactor,

and ε_n is the dissipation rate in that section.

Characteristic mass transfer time for CO_2 (t_t) was evaluated by Doran (1993) in Equation (48).

$$t_t = \frac{1}{K_L a_L(CO_2)} \quad \text{Eq. (48)}$$

Where $K_L a_L(CO_2)$ is the volumetric mass transfer coefficient for CO_2, which is linearly related to culture density and independent of gas velocity conditional upon the flow remaining heterogeneous. During growth, the characteristic consumption time for CO_2 was expressed by Doran (1993) in Equation (49).

$$t_r = \frac{C^*_{CO_2}}{\left[\frac{1}{Y_{CO_2}\mu C_b}\right]} \quad \text{Eq. (49)}$$

where $C^*_{CO_2}$ is the equilibrium constant of CO_2 (0.45e-3 kg/m^3),

μ is the growth rate,

C_b is the biomass concentration (kg/m^3),

and Y_{CO2} is the CO_2 yield coefficient, assumed to be 0.55 (Contreras, et al., 1998).

Mass transfer is a function of interfacial area (a_L) calculated with the mean bubble diameter in Equation (50).

$$a_L = \frac{6\varepsilon}{d_B(1-\varepsilon)} \quad \text{Eq. (50) (Contreras, et al., 1998)}$$

where d_B is the mean bubble diameter,

and ε is the dissipation rate which depends on shear rate, viscosity, and bubble associated dissipation. The available transfer time can be calculated using Equation (51).

$$t_{t-available} = \frac{a_L}{V_d + V_i}$$ Eq. (51) (Contreras, et al., 1998)

where V_d is the drift velocity,

and V_i the gas inlet velocity.

The shear rate in any zone can be estimated using Equation (52).

$$\gamma_n = \frac{\varepsilon_n (t_r)_n}{H_n V_n (a_L)_n \eta_L}$$ Eq. (52) (Contreras, et al. 1998)

where n subscript indicate property of the particular zone,

H is the height,

V is the volume,

and η is the growth rate.

Thus, we have a relationship between mass transfer rate and shear rate for growth in a photobioreactor. This approach offers a possibility of developing general correlations for mass transfer rate, applicable to any liquid of known rheological behavior (Merchuk & Berzin, 1995). The areas of highest shear are near the bubble surface due to the velocity gradient experienced near the bubble walls. Also, the wake behind bubbles is perfectly mixed and is the main factor of energy dissipation in a reactor.

Nutrients

The cost of supplementing nutrients can be complicated, especially if suitable seawater, flue gas, and/or wastewater is not available. As presented in a previous section one arrives at the following nutrients needed derived from algal stoichiometry: C = 51%, H = 8%, O = 33%, N = 7% and P = 1% of dry weight biomass yield. Additional nutrients/supplements include iron, salt, vitamin B12, biotin, thiamine, pH buffer, and antibiotics. Vitamin B12, biotin, and thiamine are cost prohibitive, so for the purposes of

this study the assumption is that they will be supplied by wastewater or otherwise not needed as supplements.

The literature proposes growth media are generally inexpensive if supplemented with commercial nitrate and phosphate fertilizers and a few other micronutrients (Chisti, 2007) (Molina Grima, et al., 2000). The three most common forms of nitrogen are ammonia, nitrate and urea (U.S. DOE, 2010). Nitrate is a poor form of nitrogen both because it is expensive and because it requires energy from cells to break it down, which is true for any form of nitrogen other than ammonia, and is included in the photosynthetic efficiency calculation. However, if flue gas is being used the cost is alleviated and the loss in photosynthetic efficiency is not significant enough to offset the additional cost of supplying nitrogen as ammonia unless wastewater is available.

Phosphorus, trace amounts of iron, and silicon or salt for marine algae must be supplemented in addition to the flue gas and/or wastewater depending on the composition of the wastewater in particular. Phosphorus must be supplied in abundance since it tends to complex with metal ions so that not all of it is bioavailable (Chisti, 2007). Phosphate fertilizers are known to be environmentally damaging and unsustainable. There have been calculations which indicate the world's supply of phosphate is in danger of running out (U.S. DOE, 2010).

Strong evidence implicates dissolved iron as being a limiting resource for phytoplankton growth in the open ocean, particularly in high nutrient, low-chlorophyll regions. The relationship between bioavailable iron and cellular response is not linear but depends on the history and physiology of the cells where cells regulate iron assimilation

at very low concentrations unless the cell is extremely iron-starved. Research reveals the iron must be supplied at approximately 50 to 60 pM (Falciatore, et al., 2000). However, the use of pH buffers also affects the availability of trace metals (Shi, et al., 2009), so an excess of iron must be supplied. Ferric supplement can be used in the harvesting process as a flocullant, as well.

Nutrients may also be recovered from the biomass after lipid extraction and recycled into the media. Anaerobic digestion can be used to obtain an effluent of concentrated nutrients, but this has not been demonstrated in practice, would need a method of screening contaminants and digesters, and removes the possibility of using the biomass for other end products. Therefore, the only nutrient which is assumed to be recycled in the model is salt at a rate of 80% assumed recycled.

Assuming all nutrients must be supplied to the culture, energy requirements for CO_2, nitrogen, phosphorus and antibiotics have been calculated to be 7MJ/kg, 59 MJ/kg, 44 MJ/kg, and 50 MJ/kg, respectively (Beal, et al., 2012). The energy inputs for the above nutrients are included in the carbon footprint and MJ_{in}/MJ_{out} calculations.

pH buffer is another significant cost factor, which is often not included in techno-economic analyses. Using bubbled CO_2 for pH control is unreliable. Excess CO_2 generally results in a more acidic culture, but it can also cause a more alkaline culture to become more alkaline (Kong, et al., 2010) (Shi, et al., 2009) (Oaizola, et al., 2003) (Iancu, et al., 2010). The pH of the culture determines what occurs when the CO_2 dissolves in water. If the water is the natural pH of seawater more than 95% becomes bicarbonate (HCO_3^-), the preferred carbon source for marine algae. However in very

alkaline water with a pH of over 10.4 the predominant form is carbonate (CO_3^{2-}), and in water where the pH dips below 6.5, carbonic acid (H_2CO_3) becomes dominant (Greenwood & Earnshaw, 1997). Thus, a low pH rapidly leads to more acidity while a high pH rapidly leads to more alkalinity.

Both scenarios are likely due to excess CO_2 from flue gas and the alkalizing effect of algal growth (Lopez-Elias, et al., 2008). Key chemical parameters are interdependent and are affected by the growth of the culture. Therefore, two pH buffers (an acid and a base) are likely needed. The amount will vary, but should be generally small.

Sodium hydroxide (NaOH) can be used as an alkaline buffer, and reports even suggests it can be used to induce lysis (Wolf, 2012) (Molina Grima, et al., 2003). At $230 - 290/ton, the price averages $.000276/gram. Hydrochloric acid can be used as an acidic buffer. Potassium hydrogen phthalate is used with sodium bicarbonate and hydrochloric acid to create the buffer, but is expensive at around $.0395/gram. Hydrochloric acid costs 0.000135 - $0.00027/gram. The model assumes 2 - 200 grams of sodium hydroxide and/or hydrochloric acid (without the buffer) will be used per Liter per day to adjust the pH when the culture becomes too acidic or alkaline, respectively.

The costs for supplying carbon, phosphorus, nitrogen, pH buffer, iron, antibiotics and salt to produce a given amount of biomass are included in the model (see Appendix C). When wastewater and/or flue gas are supplied, the amount of carbon, phosphorus, and nitrogen decrease correspondingly.

Temperature

Temperature must be maintained between 20 and 35º C in general and in a more specific range depending on the species. An internally illuminated photobioreactor design must include a consistent building temperature to house the photobioreactors and a method of cooling the cultures such as a heat exchanger or cooling media input.

Temperature is a major limiting factor for open ponds and solar illuminated photobioreactors. Even in deserts where algae growth in open ponds should be possible, cold night-time temperatures can significantly impact growth during the day. Since the normal depth for an open pond is 10 - 35 cm, the water body does not moderate the temperature and is subject to atmospheric fluctuations to a large extent (James & Boriah, 2010). One solution used in practice is to transfer algae to deeper settling ponds at night-time and then back to shallow growth ponds during the day. Another option is to cover the ponds with greenhouses or regulating the temperature, both of which will increase costs.

Solar illuminated photobioreactors must be cooled with water sprays which may result in water losses as large as that of open ponds to evaporation. However, the further complications to the media and disposal of brine common to open pond evaporation could be avoided. The model does not include the cost of extra cooling needed when using solar illuminated photobioreactors, but is suggested as an additional area of research.

Photosynthetic organisms use at least eight photons to convert one molecule of CO_2 into carbohydrate $(CH_2O)_n$; thus the heat generated during photosynthesis (Q_{theo}) can be estimated using Equation (53).

$$Q_{theo} = HV_{carbohydrate} - (8*E_{photon}) \quad \text{Eq. (53) (Dimitrov, 2007)}$$

where $HV_{carbohydrate}$ is the heating value of CH_2O (~468 kJ mol^{-1}),

E_{photon} is the mean energy of a mole of PAR photons (~217.4 kJ),

and Q_{theo} = -1271.2 kJ per mol of CO_2 converted to carbohydrate (Dimitrov, 2007) (Zhu, et al., 2008). The change in culture media temperature can be calculated using Equation (54).

$$\Delta T = \frac{Q_{theo}}{c_p m} \quad \text{Eq. (54) (Dimitrov, 2007)}$$

where m is the mass of media in kilograms,

and the specific heat (c_p) of water is 4.19 kJ/kg*°C.

The model uses Equations (53) and (54) to calculate increase in temperature as a function of culture density, as well as the necessary temperature of input water to replace the volume used by the photosynthetic process.

The cooling due to the latent heat of evaporation (2257 kJ/kg) is used in determining the resulting temperature of open ponds. However, since radiation from the Sun falls on the Earth at about 1368 W/m^2, there should also be a heating affect in open ponds. Where the albedo of open bodies of water is approximately 10 - 60%, depending on the sun's altitude, an average of 30% is used in the model, so the radiation is equal to 957.6 W/m^2. Also, the photosynthetic process will use approximately 3% of the sunlight, leaving, 928.87 W/m^2.

$$T^4 = \frac{928.87\ W/m^2(1-albedo)}{4\sigma}$$ Eq. (55)

where σ is the Stefan –Boltzmann constant at 5.7 x 10^{-8} W/ (m^2 * K^4).

Using Equation (55), the resulting temperature is 252.6 K, or -20.55 °C, so the remaining thermodynamics of evaporation, weather, cooling at nighttime, heat absorbed by the clay or concrete bed are assumed to balance each other. The model does not include cost of cooling or heating the open pond, but does calculate what the temperature of water to replace that used by photosynthesis should be to counteract additional heat generated from photosynthesis for all the growth scenarios. More detailed analyses of the thermal dynamics of open ponds and solar PBR's have been attempted and are recommended for further research.

Contamination

Algal predators are pervasive and little understood. Whether the biotic environment can be controlled sufficiently to prevent culture contamination with zooplankton such as rotifers, bacteria, viruses, and/or fungi is an unanswered question in algal biofuels production (Lundquist, et al., 2010) (U.S. DOE, 2010). Zooplankton grazing is one of the major algae production problems that must be overcome for open ponds. The photobioreactor growth scenario has much more potential in this regard.

The model incorporates a contamination risk of losing 0.1 - 10% of harvest for open ponds (this also incorporates loss of growth at nighttime). This is a very conservative estimate since Chisti (2007) estimated 25% of the culture would be lost at nighttime alone.

Wastewater, Brackish and Seawater

Many studies promoting algal growth for biofuel production include wastewater, brackish or seawater as sustainable and cost saving alternatives. This requires further scrutiny.

Wastewater treatment is a complex process which involves significant cost. Contributing to the cost is the removal of the nutrients nitrogen and phosphorus. Emphasis in wastewater treatment has changed to removing nutrients, chiefly nitrogen and phosphorus, which are the root causes of eutrophication of inland waterways and coastal dead zones (Lundquist, et al., 2010) (Kong, et al., 2010). Capital costs of $0.41 to $2.41 per gallon of design flow to reduce nitrogen content to 5 mg/L have been cited (Hartman & Cleland, 2007). As long as the essential nutrients are bioavailable in sufficient quantities so that no nutrients are limiting algal growth, research has indicated the growth rates remain close to optimal using wastewater as a growth medium (Wang, et al., 2010).

When wastewater is used to sustain algal growth, the nutrients are removed from the wastewater, and the algal growth sustained results in additional products, benefitting both industries (Pittman, et al., 2011) (Beal, et al., 2012). In order for algal growth with biofuel production to be truly sustainable, it cannot compete with agriculture, which means fresh water must not be used or must be limited to small amounts. There are many sources of wastewater with different compositions including municipal, runoff from feedlots, energy power plants, and almost every other type of industrial plant. Over 8,000 municipal wastewater ponds exist in the U.S. (Lundquist, et al., 2010).

Coal power plant wastewater varies widely from plant to plant, but is generally acidic and supersaturated with gypsum (hydrated calcium sulfate), high concentrations of dissolved and suspended solids consisting of minerals, salts or metals, heavy metals, chlorides and occasionally organic compounds. Studies indicate algae can thrive in media with high amounts of calcium and phosphorus, and even foster the precipitation of calcium phosphates, which allows easier removal when wastewater treatment is desired as an end product. Although sulfur is not used by algae generally, research indicates that the precipitation and removal of the calcium sulfate and calcium phosphate can be facilitated by feeding the wastewater to the algal culture (Wang, et al., 2010). However, power plant cooling water is normally recycled and used over and over, so the option to use it to feed an algal plant is not optimal or likely from the power plant's perspective.

Studies in this field predict using wastewater will produce inconsistent results in biomass and lipid productivity similar to the claims concerning using flue gas in algal cultures. There are indications the lipid content drops when algae is grown in wastewater (Wang, et al., 2010) (Pittman, et al., 2011) (Chinnasamy, et al., 2010). Phosphates are common in septic tanks, runoff from feedlots, runoff from agriculture and wastewater treatment plants, but with the exception of the latter, all these sources are likely contaminated with organic compounds and bacteria, which can be undesirable for controlled growth in algae cultures. The inconsistent results will likely occur if the algae culture is fed untreated industrial, municipal, and feedlot waste streams, but this option is not included in the model since to benefit from wastewater treatment profits, a wastewater treatment plant must be present, which would enable primary wastewater

treatment prior to feeding to the algae (Clarens, et al., 2010). Also, the large particles and bacteria can be removed from wastewater prior to use in the culture using glass microfiber filters, but the cost of filters for this application are not included in the model (Wang, et al., 2010).

Municipal wastewater is attractive since it is high in nitrogen and phosphorus that must be removed in the wastewater treatment process anyway (Siemens, 2011). A municipal wastewater treatment plant (MWTP) has different points in the treatment process, and studies conflict as to the best point at which to insert an algal growth scenario.

Some studies promote the centrate stage, which is the waste generated in the sludge centrifuge and results in the highest concentration of nutrients for the algae. Traditional wastewater treatment at the centrate stage involves introducing activated sludge, which is a biological flocullant to degrade organic carbonaceous matter to CO_2, but algae has been shown to assimilate the organic pollutants in a more environmentally friendly way without producing CO_2. When organic material is available to use as the carbon source, this also reduces the amount of CO_2 needed by the algal culture, although the CO_2 will still be necessary as a carbon source. Centrate has an N/P ratio of 0.36 (Wang, et al., 2010), when the molecular formula and Redfield ratio shows a ratio of 11 - 16:1 is optimal, and a pH of around 10 when 8.2 to 8.6 is optimal. The N/P ratio may be acceptable as long as the culture is not nitrogen limited. As previously shown, a high pH can not necessarily be lowered (and growth rate increased to the optimal 1.12 – 1.15 day^{-1}) through increasing feed rate of flue gas (with increased CO_2). Despite these

challenges, Chlorella grown in wastewater centrate has been shown to have a growth rate of 0.948 day^{-1}, and is capable of removing 83.0% of oxygen consuming organics over a 3 day period in centrate material (Wang, et al., 2010).

Other studies have indicated the ammonia to be too high in centrate to facilitate optimal algal growth, but the centrate can supplement ammonia in the final plant effluent which has been chlorinated and dechlorinated, and still requires biological nutrient removal (BNR) (Beal, et al., 2012). BNR is a relatively new requirement for WWT and is not always required. Research indicates the energy return on investment values for wastewater treatment plant and algal biofuels production facility independently are 0.37 and 0.42 respectively, but when combined the EROI is 1.44 (Beal, et al., 2012).

Typical municipal wastewater characteristics per Liter are: 140 mg total organic carbon (TOC), 75 mg HCO_3, 5 mg CO_3, 40 mg total N, 7 mg total P, and 430 mg chemical oxygen demand (COD) (Tchobanoglous, et al., 2003). 40% of the COD is removed after primary clarification, leaving 258 mg COD/L. Roughly 66% of nitrogen and 75% of phosphorus are bioavailable in secondary effluent, leaving 26.4 mg/L and 5.3 mg/L, respectively (Sturm & Lamer, 2011). 18.75 mg/L of carbon is available from bicarbonate, assuming the pH of the culture remains at the optimal 8.2 to 8.6. Assuming all of the TOC is bioavailable, and adding in 1 mg L^{-1} carbon from the CO_3, the total carbon available for algal growth is 159.3 mg/L.

Wastewater treatment plants also generate 2.04 tCO_2/day through methane conversion to electricity, which could be fed to the algae (Beal, et al., 2012). If no flue gas is available to supplement carbon supply, the limiting nutrient will be carbon,

however, if flue gas is provided, nitrogen is limiting. Also, the low N/P ratio for the wastewater at about 5:1 (when 11-16:1 is optimal) may be corrected through using flue gas as a source of nitrogen, also.

Wang, et al., (2010) found heavy metals (Al, Ca, Fe, Mg, Mn, and Zn) were removed from wastewater at a rate of 56.5 to 100%. Metals used by phytoplankton include iron, manganese, zinc, copper, cobalt, cadmium, and molybdenum, in descending importance. Thus, cobalt and molybdenum needed by the algae would be lacking in the wastewater, while aluminum and magnesium are not needed for algal growth. However, since they were removed from the wastewater in the above study, they are absorbed by the algal cells. Aluminum would be undesirable if the biomass were used for human supplement or animal feed. As long as the desired end products do not involve human supplement or animal feed, algae are very adaptable to available nutrients, and the option of using wastewater not only provides wastewater treatment, it also allows an inexpensive source of nutrients for the algal culture.

Heavy metals present in the gases or wastewater may be assimilated into the biomass which significantly limits the available end products. If heavy metals are not removed from the wastewater prior to injection into a culture, they will either become part of the biomass or remain in the culture medium. If the end product is animal feed or human supplements the culture should be kept free of bacteria, suspended solids, dissolved metals and pesticides (Creswell, 2010) (Richmond, 2004). The acceptability, digestibility, and nutritive value of the resulting algae biomass would need to be evaluated in each case. Therefore, the model details costs and profits for human

supplements, aquaculture and animal feed separately as options for end products when flue gas and/or wastewater are used as inputs.

Diatoms generally require nitrogen, silicon, and phosphorus in a 16N:16Si:1P ratio (although *Dunaliella salina* is grown in hypersaline medium >3 times seawater to discourage competing algae and grazers, while inducing high content of carotenoids within the algal cell) (Lundquist, et al., 2010)) (Sato, et al., 2010). Depending on location when growing diatoms seawater can be an inexpensive option for growth media with basic fertilizer added for nutrients (Molina Grima, et al., 2000). This is likely the most cost effective option if the culture is located close to the ocean or in areas of New Mexico where there is an underground salt aquifer, but it is uncommon for the power plant to be located adjacent to the beach. Additionally, the salt water must be supplemented with large amounts of fresh water or the culture will become too saline (Patil, et al., 2008), and contaminants must be removed via filtration or treatment, similar to wastewater. This also applies to brackish water.

While it is desirable to use brackish or seawater since it removes the necessity for fresh water to some extent, fresh water will continue to be a necessity to dilute the salinity, especially in an open pond growth scenario where large quantities of water are lost to evaporation. The amount of water lost to evaporation is significant for open ponds even if the source is wastewater, brackish or salt water, and the impacts go further than just more water consumption. The evaporation rate in the sunny warm regions suitable for algae growth such as Tucson, Arizona are 100 inches $year^{-1}$ (nsdl.org), which means an algae farm sized to consume flue gas from a 1,000 MW power plant (15,000 acre

(Benemann & Oswald, 1996)) would lose 5.4e9 ft^3 (1.5e11 liters) of water $year^{-1}$ to evaporation. Equation (56) is used in the model to calculate water loss in m^3 per day.

$$W_L = 0.0069596 * A \quad \text{Eq. (56)}$$

where A is area in m^2.

This is also a consideration for density changes of the medium since in an average pond depth of 25 to 35 cm over a four day period, evaporation would result in a density change of up to 14%, depending on the pond depth. The "blow-down" ratio (BNR) has been defined as the volume of water discharged divided by the volume of water supplied to the pond.

$$BNR = \frac{V_{ev}}{V_{supply}} \quad \text{Eq. (57)}$$

Assuming no additional water is supplied for four days the resulting BNR of 14% would result in salinity nearly 10 times that of the influent water. Also, the excess salts or brine must be recycled or disposed of either through injection underground or drying the salts and having them buried (Lundquist, et al., 2010). Not only will this add cost to the process, but permits will also need to be acquired, not to mention this is not a sustainable or environmentally friendly practice.

Thus, the approach used in the model still applies whether fresh water, brackish or seawater is used, which is to assume the cost of replacing water lost to evaporation. The cost of supplementing salt as a nutrient would be negated by using brackish or seawater, but this would be more than offset by the need to dispose of excess salts or brine.

In order for wastewater from any source to be considered a cost effective and desirable water and nutrient source for the algae culture resulting in optimal productivity,

the culture must have access to or include in the design some level of wastewater treatment plant, which is included in the model as an option. It is important to have control over media inputs in order to mitigate risk of a culture crash or contamination which will damage the end product. The potential cost benefit to a wastewater treatment plant was chosen conservatively to offset $0.06/gallon for WWTP operating costs and $0.41/gallon for WWTP capital costs (Hartman & Cleland, 2007). This cost benefit is calculated in the model per the size of the algal farm in Liters.

The model assumes 90% of the culture water not lost to evaporation is recycled. The water cost is a summation of water to replace that lost to evaporation (for open ponds only), to replace that lost to photosynthesis, and to replace the 10% lost to the process. Therefore, there is no cost benefit assumed to be gained from using brackish or seawater.

Harvesting

The harvesting process consists of many different steps which may include some or all of the following: flocculation, settling, centrifuging, lysis, membranes, solvents, filtration, and drying. Combinations of methods can be classified as dry extraction (include filter press with solvents) or wet extraction (lysis induced through ultrasonication or raising the pH above 10), where dry extraction is the more proven technology. While both electromagnetically and pH induced lyses are included in the model for cost comparisons, metabolically induced secretion is not included due to major hurdles that must be overcome.

Optimizing the harvesting methods will depend on the algal strain, the growth scenario and resulting density, the location, and the planned end products. Despite rough

estimates in some studies, energy requirements of harvesting options are largely unknown, and depend heavily upon the final algae concentration (U.S. DOE, 2010). The model compares various harvesting options, none of which have been practiced on a large commercial scale for algal production, but all of which have been proven in the laboratory and/or for comparable commercial systems.

Open ponds offer low construction and maintenance costs and are easy to scale up if the land space is available, but the loss in productivity does not allow them to be long term solutions and in the majority of cases, the land is not available. Capital expenditure for photobioreactors is commonly assumed to be many times more than that of open ponds (Benemann, et al., 1982) (Sheehan, et al., 1998) (U.S. DOE, 2010). Harvesting costs are generally assumed to contribute 20-30% of total cost of oil production through algal biomass (Verma, et al., 2009) (Hall, et al., 2003).

Settling and Flocullants

Research detailed in the literature review indicates a portion of the algal growth should be moved from the growth tank to a settling tank or clarifier every day (Lundquist, et al., 2010) (Zou, et al., 2000) (Lee & Palsson, 1994). The medium can be drained from the growth tank with sufficient algae remaining to reach optimal density again after one day's growth. It is especially important to drain the medium if the species used is a diatom since the growth inhibitors secreted by the algal cells when the culture reaches high density will be present in the "old" medium. Further investigation is required to determine what level of treatment or duration of rest the medium should undergo prior to

recycling back into the growing algae culture. Therefore, the goal is to prevent the culture from reaching high densities, especially in a PBR growth scenario.

The algal culture removed from the culture can be fed into settling tanks where cellulose and/or flocullants are mixed with the culture. Given the right nutrient and light deprivation the algal lipid content should increase while in the settling tanks (Vega, et al., 2010) (Lu, et al., 2001). Clarifiers are relatively inexpensive to create, increase lipid productivity and significantly decrease harvesting costs. The culture density can increase by 30 to 50 times when allowed to settle, depending on the algae species (Lundquist, et al., 2010).

However, the resulting density for open pond culture will still be 60 times less than that of cultures grown in photobioreactors prior to settling. Open pond productivity varies in the literature from 20 - 80 g m^{-3} d^{-1} (depending on the pond depth, while shallower depths result in higher density), which is at the greatest a resulting density of 0.33 g L^{-1} (0.03%) after four days' growth (Beal, et al., 2012). However, the growth rate for photobioreactors presented in a previous section of this paper should result in a wet density of approximately 60 g L^{-1} (6%), or 180 times the density of open ponds. Where the required density of slurry to begin harvesting is at least 1%, culture from photobioreactors can begin the harvesting process immediately, while the open pond culture must first be dewatered. The literature assumes this required densification for open pond cultures to be through the use of clarifiers, settling or bioflocullation; thus, requiring no energy input (U.S. DOE, 2010) (Vasudevan, et al., 2012).

Multivalent cations and cationic polymers which neutralize the algal cells' negative charge are useful as flocculants which include ferric nitrate, polyferric sulfate, chitosan, polyacrylamide, ferric chloride, aluminum sulfate, and ferric sulfate (Molina Grima, et al., 2003) (Kong, et al., 2010). Metal salts may be unacceptable if biomass is to be used for aquaculture or other applications. Polyacrylamide and chitosan are the only cationic polymers (non-metal), but they are not as effective for salt water flocculation (Molina Grima, et al., 2003). Also, chemical flocculants make it more difficult to use biomass for anaerobic digestion to produce methane gas (Lundquist, et al., 2010)

Flocculant effectivity increases with culture density, but research indicates there is no consistent correlation between the algae species and the quantity needed for optimal flocculation. If a flocullant is used, the amount of flocculant required ranges between 40 and 150 mg L^{-1}, with costs estimated at $126/Mg (Benemann & Oswald, 1996). Since ferric chloride costs only $4.4e-5/gram, the costs for flocullants are less than a dollar/day for a ~100,000 kg/year biomass facility. Since the costs are minimal and the use of flocullants is not desirable or necessary, the model does not include a cost for flocculation material.

Bioflocullation involves gravity settling that results in a 40- to 60-fold concentration factor and has been adopted by nearly all commercial algae producers, but has yet to be proven at a full-scale process (Benemann & Oswald, 1996) (Lundquist, et al., 2010). This process may require a six-hour retention time to remove 95% of the algae biomass (Lundquist, et al., 2010). The cost for bioflocullation is included in the

model through the cost of settling tanks sufficient to hold one third the total algal volume at a time.

Lysing

Another option to aid in or avoid flocculation and many of the harvesting steps all together is using alkalis such as sodium hydroxide and calcium hydroxide to raise the culture pH above 10, which is reported to induce lysis (Molina Grima, et al., 2003) (Wolf, 2012). The lysis occurs because of a cation/anion differential causing the algae lipid vacuole to attach to the cell membrane and then excrete the lipids through the cell wall. This affect can also be achieved through voltaic impulsion, and is being used as a proprietary process by Origin Oil and independent researchers (Origin Oil, 2012) (Wolf, 2012) (Lundquist, et al., 2010).

Thus, the cation/anion differential can be used to release the lipid content from the cells, where it will rise to the top of the media, while the biomass will sink to the bottom. Then harvesting consists of skimming the lipids from the top of the media and the biomass can be retrieved more easily once it has settled to the bottom. This also alleviates the cost of hauling the entire biomass to a central oil extraction plant. Another advantage of this method is preventing the algae from using carbohydrate energy stores by killing the algae quickly (Dimitrov, 2007). The option of lysis through voltaic impulsion as a harvesting method is included in the model since equipment is available to purchase through Origin Oil (Origin Oil, 2012). The use of pH to induce lysis is included as a cost comparison, but the process is yet to be proven and costs would be minimal.

Centrifuge, Filter Press and Conveyor Oven

A centrifuge can be used with efficiencies of >95% at removing water content depending on the algal species and method of centrifugation (Molina Grima, et al., 2003). Most studies claim at the current time the high capital investment and operating costs make centrifuge economically and sustainably impractical (U.S. DOE, 2010). Evodos (2011) has developed a centrifuge especially for microalgae, which, while being pricier than other types of centrifuge, is much more efficient and claims to produce a paste suitable for transport from a farm to a biomass processing facility. The model compares both options of centrifuge: traditional and Evodos.

Filters can also be used to remove water, but microfiltration was not used in the model since this is more cost-effective for small volumes, while centrifugation is more suited to larger volumes (Molina Grima, et al., 2003). Filtration in large quantities would require almost constant cleaning of the filters which does not allow them to be cost-effective. Also, membranes were not included as an option since the technology is not developed sufficiently to be cost-effective and suitable for large volumes (Origin Oil, 2012).

However, a filter press could remove even more water following use of the centrifuge, and is commonly used for other products in the food processing industry. An industrial filter press is included in the model for capital and operating cost comparisons. The biomass slurry must be processed rapidly or it can spoil within a few hours (Molina Grima, et al., 2003). A conveyor oven can further dry the algae biomass to prevent spoiling for shipment and is included in the model for capital and operating cost

comparisons. Algae can be spray dried, freeze dried, drum dried, sun dried, or oven dried and could be wound paper-like onto rolls for storage and shipment, if cellulose flocculent was used (Putt, 2007).

Both filter press and conveyor oven cost values were derived from industrial products that were available in the market at the time of performing this research.

Solvents

There are significant energy benefits through avoiding conventional algal mass dehydration prior to lipid extraction (Soh & Zimmerman, 2011). Additionally, protein extraction requires biomass that has not been dried previously (Molina Grima, et al., 2003). Solvents can be used prior to the dehydration step to increase the efficiency of extracting lipids and specific metabolites such as EPA, astaxanthin, and DHA from algal biomass, but many of these solvents such as hexane are toxic to the environment and render the remaining biomass unusable for animal feed or aquaculture (Molina Grima, et al., 2003) (Bligh & Dyer, 1959). Also cell pre-treatments that disrupt the cells; sonication, microwave, bead beating and lyophilization, have shown to enhance extraction yield by facilitating solvent contact with the cell contents (Soh & Zimmerman, 2011).

Organic solvents such as hexane, chloroform, and methanol are expensive, require several rinsing steps, and generate significant waste and environmental and health risks (Soh & Zimmerman, 2011). Lundquist, et al. (2010) found the operational and capital cost for a solvent extraction facility to be $2,390,000 and $12,200,000, respectively, to process 105 MT d^{-1}. Free fatty acids have been extracted successfully by direct

saponification of wet biomass with KOH-ethanol mixture, but this process is not suitable for sensitive end products such as proteins (Molina Grima, et al., 2003).

One green solvent proven to work that is not proprietary is supercritical carbon dioxide. Extraction using supercritical CO_2 at 100ºC and 30 MPa would take 1840 kWh of electricity while conventional press and hexane extraction would take 69 kWh of electricity and 17360 MJ of heat energy for drying to make 10^4 MJ of biodiesel (Soh & Zimmerman, 2011). Converting to energy, conventional harvesting requires 17600 MJ (4.752e-7 kWh/Joule biodiesel) while super critical CO_2 only requires 6850 MJ (1e-7 kWh/Joule biodiesel). Also, CO_2 may be fed back to the cultures to facilitate increased production.

The model uses both the costs of methanol and hexane themselves as well as the operating costs compared to the operating costs involved with bringing the required portion of CO_2 fed to the culture to supercritical state.

End Products

Products are partitioned into fuel products and co-products. The nature of the end products will be determined by the location and economics of the system.

Potentially viable fuels produced from algae range from hydrogen and methane to alcohols, oil, biodiesel and coke. The model targets transportation fuels and methane as desired fuel products. Transportation fuels are the primary products from crude oil, are more compatible with existing fuel-distribution infrastructure in the U.S., and adequate specifications for these fuels already exist. Also, it has been proven that biofuel derived from algae meets or exceeds the performance specifications for jet fuel, gasoline and

diesel (U.S. DOE, 2010). Methane is included since the energy derived from methane can be fed back to the power plant supplying flue gas or applied to algal plant energy use.

Biomass for Methane Production

Power derived from biomass processing to methane can be used as the primary source of energy for most of the production and processing of the algal biomass or fed back to the power or wastewater plant. Using the methane as close as possible to the source also reduces the amount of leakage from pipelines which is a large contributor to greenhouse gases at 1.4% of natural gas transported (Lelieveld, et al., 2005).

Biogas yield in Joules, energy produced by microturbines using the methane, and profit per kW is calculated in the model simulation. The amount of methane gas obtained from anaerobic digestion of algae biomass averages 5.0 cubic feet for every pound of biomass (Golueke, et al., 1956). Analysis indicates that algal biomass cultivated in photobioreactors will yield 7,300 gallons and open ponds up to 6,000 gallons of methane fuel per acre per year. In comparison, corn yields about 50 gallons of methane fuel per acre per year (Chisti, 2007).

Content of algal biomass prior to lipid harvesting is represented by: $CO_{0.48}H_{1.83}N_{0.11}P_{0.01}$ (Demirbas & Demirbas, 2010) (Chisti, 2007). Oil content is normally 70-75% carbon and 15-17% hydrogen (Food and Agriculture Organization of the United Nations, 1997) (Soh & Zimmerman, 2011), so the content after lipid removal should be:

$C(1-(1*0.73)\ H(1.83-(1.83*.16) = C_{0.27}H_{1.53}O_{0.48}N_{0.11}P_{0.01}$

Adding in the molecular weights of the elements yields:

$C(0.27*12)H(1.53*1)O(0.48*16)N(0.11*14)P(0.01*31)=C_{3.24}H_{1.53}O_{7.68}N_{1.54}P_{.31}$

Therefore hydrogen is 1.53/13.46 = 11.4% of the algal biomass following lipid extraction, which is above the average 6 - 7% of most feedstocks where higher hydrogen content indicates higher quality of feedstock. Energy contents of fuels are normally reported as Lower Heating Value (LHV) and Higher Heating Value (HHV). HHV is greater by 10% than LHV for natural gas, but HHV is more difficult to achieve. The appropriateness of using LHV or HHV depends on both the application where HHV is more appropriate for stationary combustion since the exhaust gases are cooled prior to discharging and the composition of the feedstock where higher hydrogen content leads to higher heating value. With this background in mind, the energy derived from methane is set in the model at 48 MJ/kg (LHV of natural gas is 47.141 MJ/kg and HHV of natural gas is 52.22 MJ/kg) (GREET, 2010). However, this energy still must be converted to electricity to be used by the algal or power plant. (A green crude can be obtained from the entire biomass including lipids, but this option is not included in the model since profit from biodiesel and methane are relatively similar.)

Microturbines are available to generate electricity from methane with efficiencies of 22 - 30% (EPA, 2004) (Columbia Boulevard Wastewater Treatment Plant, 2006). The assumed composition of the biogas is 35% CO_2 and 65% CH_4 (Lundquist, et al., 2010).

Another consideration of methane production is the generation of methane and N_2O emissions, which can be 14% and 23%, respectively, of total pathway GHG emissions (Frank, et al., 2012). While recovery is possible, this requires more energy

input. Methane itself has a higher global warming potential than CO_2; hence, any methane production scenario must handle the GHG accounting carefully.

Biomass Recycling as Nutrient Source

Efficiency of 90% can be assumed for recycling biomass to use as a nutrient source for the growing culture. An anaerobic digester must be available and a method for screening or filtering the digester effluent prior to re-injection into the culture. Nitrogen in the form of ammonia can be recovered from the methane liquid effluent and recycled to the culture (U.S. DOE, 2010). It is more sustainable and environmentally responsible to recycle nitrogen for use in growing more algae or other crops. This option is not included in the model, but results are compared if the nutrient cost is alleviated. Similar to a wastewater treatment scenario, pH, salt and antibiotics still must be supplied, which are the majority of the nutrient cost. (Salt is already assumed recycled at 80%).

Biodiesel

Algal oil can be used to produce green diesel with higher energy density, better cold flow performance, and compatibility with existing petroleum based infrastructure (James & Boriah, 2010). Biofuel production in terms of gallons $acre^{-1}$ $year^{-1}$ are commonly given in the literature, but this is done only for open pond growth scenarios based on photosynthetic effectivity (1.8% - 4.7%) and average solar insolation (22MJ m^{-2} day^{-1}) (Vasudevan, et al., 2012) (U.S. DOE, 2010). Fuel percentage has been calculated in the past as general lipid content with no consideration for conversion to biofuel. Biodiesel yield in the model is calculated as 80% of the lipid content with an energy content of 37,800 MJ ton^{-1} (Chisti, 2008).

The model captures the inputs/outputs to the transesterification process without the conversion to jet fuel, gasoline and diesel, since these are common to crude oil. There are various methods to carry out transesterification, but the model uses the operating costs of the most common; chemical transesterification through which 3 molecules of an alcohol and a catalyst, such as sodium methoxide are added to the fatty acid (Verma, et al., 2009). The model estimates transesterification costs using 20% energy content of biodiesel produced plus the cost of the methanol (Prueksakorn & Gheewala, 2006).

It is difficult to predict the value of algae oil as a biodiesel feedstock since the exact composition of the algal oil depends on the species used and the process parameters, but this is similar to other alternative oils (Alabi, et al., 2009). Additional, difficult-to-value incentives such as carbon credits and self-sufficiency with respect to oil would also accrue.

Co-Products

In order for an algal growth scenario to be economical, co-products must be considered in the analysis. Deriving value from post-extraction algal residues is essential to the overall economic sustainability of algal fuel production (General Atomics, 2009). Of those shown below, EPA, animal feed, wastewater treatment, and animal feed are considered in the model. Profit from CO_2 mitigation is volatile and not a reality in many areas yet, but is included, as well. Carotenoids, beta-carotene and astaxanthin are similar in profit to EPA, and algae for human supplements are already being grown commercially on a large scale. Any human supplements gleaned as co-products increase

the need for a sanitary and consistent growth system. Chemicals as an end product requires further research not included in this study.

Chemicals

Other products include high value chemicals to be used in plastics and pharmaceuticals.

EPA

EPA retails at $2154 per kg, and requires 56.3 kg of *P. tricornutum* and 9400 L of solvent for every kilogram of the fatty acid. The value of the residual algae oil after extraction of EPA is that of biodiesel feedstock at $0.50 per L. The content of EPA averages between 2.57 and 3.47% content of dry cell mass for *Nanno. sp.* (Zou, et al., 2000).

Animal Feed

After removal of lipids, algae cake can be sold as high quality animal feed at $246 ton^{-1} (Alabi, et al., 2009) (Creswell, 2010). The challenge will be to certify the algal protein for animal use, to market it to farmers, and to transport it to customers (Dimitrov, 2007). Protein-based animal feed is a medium value product, offers low production costs, no carbon credit potential, and there is danger of market saturation.

Human Food Supplement

Spirulina sells plant gate for about $10,000 ton^{-1} and higher, depending on quality and origin (Lundquist, et al., 2010). All commercial *Spirulina* production currently uses raceway ponds.

Carotenoids, beta-carotene and astaxanthin

Biomass sells plant gate for >$100,000 MT^{-1} with a 2% astaxanthin content (Lundquist, et al., 2010). Production is limited to 100 MT per year worldwide and mostly with algae species *Haematococcus* in photobioreactors.

Carbon Credits

CO_2 capture technologies range from $40 - $150 per ton. The CO_2 price forecast is detailed as starting at $15 per ton throughout the present decade, and increasing to $30 - $50 per ton by the year 2030 (Johnston, et al., 2011). The model uses a potential profit of $20 per ton for CO_2 consumption from an industrial flue gas, assuming the period of implementation will be later on in this decade.

Wastewater Treatment

As covered in the previous section the potential cost benefit to a wastewater treatment plant was chosen conservatively to offset $0.06 per gallon for WWTP operating costs and $0.41 per gallon for WWTP capital costs (Hartman & Cleland, 2007). This cost benefit is calculated in the model per the size of the algal farm in Liters.

Sensitivity Analysis

The sensitivity analysis is a result of running the model simulation which has been built based on published algal growth parameters, fluid dynamics, known commercial practices, and laboratory findings which have been detailed in this paper. Because of the large number of input variables, a sensitivity analysis is performed for the two models (open pond and photobioreactor growth scenarios) in order to determine the sensitivity of net profit to input variables. Sensitivity is determined by evaluating the

change in the average net profit, normalized, to the change in the input variable, normalized. The sensitivity is determined by Equation (58):

$$S = \frac{\frac{Y_i - Y_{i-1}}{Y_i}}{\frac{X_i - X_{i-1}}{X_i}} \qquad \text{Eq. (58)}$$

where S is the sensitivity,

Y is the performance parameter (average net profit),

and X is the input variable.

The larger the sensitivity value, the more sensitive the performance parameter is to the input variable. Only input variables with $S \geq 0.10$ in one or both growth scenarios are included in the optimization.

Each input variable included in Table (7) is assigned a value, X_i, the model is run and the average net profit is recorded. Then the value for the input variable is changed to a new value, X_{i-1}, the model is run a second time, and the change in average net profit is recorded. It is recommended to vary the initial starting value and the amount of change in X, in order to determine if the resulting sensitivity is a result from the normalization or selection location. This is performed for each input variable specific to each growth scenario. Each growth scenario has 18 input variables, but there is a quantity of two specific to PBR/ALR growth scenario: lighting and gas delivery through diffusion or sparging, and quantity of two specific to the Open Pond growth scenario: pond depth and paddlewheel velocity.

PBR/ALR	Open Pond
culture density	culture density
number of pbrs/ponds	number of pbrs/ponds
lipid content	lipid content
volume of pbr/pond	volume of pbr/pond
bubble diameter	bubble diameter
run duration	run duration
gas velocity	gas velocity
filter press	filter press
traditional centrifuge	traditional centrifuge
evodos centrifuge	evodos centrifuge
lysis	lysis
organic solvents or sc co2	organic solvents or sc co2
conveyor oven	conveyor oven
wastewater	wastewater
pipe diameter	pipe diameter
cost of land (rural or urban)	cost of land (rural or urban)
lighting (fluor or led)	pond depth
diffusion or sparging	paddlewheel velocity

Table 7: Input variables manipulated for Sensitivity Analysis.

Optimization

Optimization of algal growth is an iterative effort involving many factors. When only considering the algal growth factors, the parameters detailed in Figure (12) are involved. The model analysis detailed in the fluid dynamics section determines how to optimize circulation time, hydrodynamic stress, lighting, mass transfer, and oxygen accumulation. However, the goal of the optimization is maximum net profit, so growth factors are optimized in relation to the resulting net profit. This means the optimized solution will not necessarily be the most productive solution, and the system optimum will not always be the unit optimum. Also, when exhibiting an average net profit, the

solution will optimize to a larger facility, while the opposite is true when a net loss is exhibited.

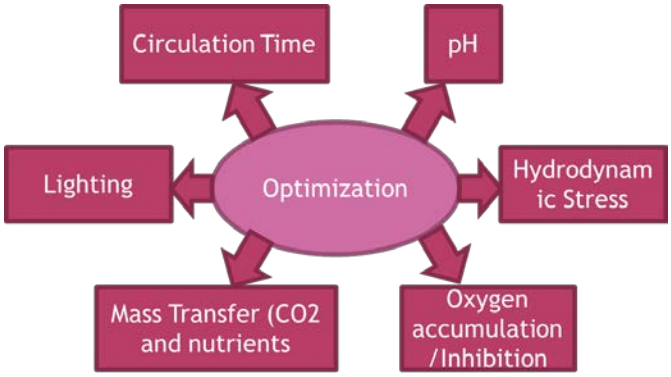

Figure 12: Parameters affecting algal growth rate.

The parameters to optimize for net profit in the PBR/ALR growth scenario include the culture density, geometry, and facility size. The amount of oxygen/L produced is an important factor to consider in the design of the growth scenario geometry. The turbulence analysis results make it possible to include fluid dynamics optimization in the model calculations outside of the optimization test scripts. The model is also modified to calculate photobioreactor diameters and length, as well as pond depth based on the culture density, so that through optimizing the net profit based on the culture density the other parameters are optimized, as well. With an artificially illuminated ALR design the internal lighted diameter and total diameter are outputs from the model. Solar illuminated is a PBR tubular design with only an outer diameter (no internal lighting) and length as outputs.

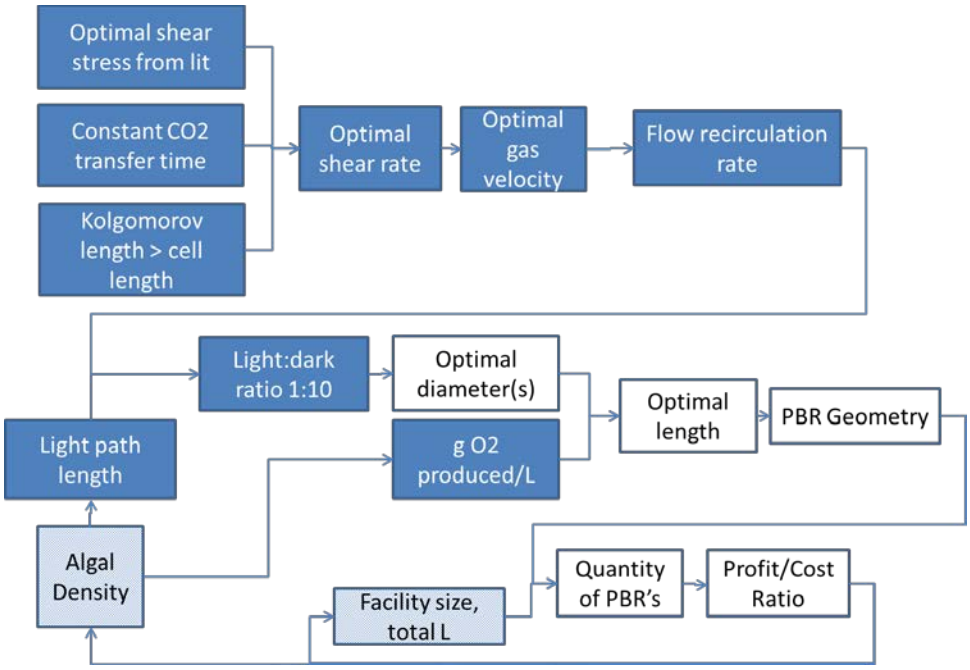

Figure 13: PBR/ALR optimization flow.

Light path length is calculated using the culture density, which is then used in the mass transfer module to determine the ALR diameters based on the 1:10 light path length and assuming constant flow velocity (detailed in the small scale turbulence section). The resulting diameter is then used with the grams of oxygen produced to determine the maximum length so as not to exceed oxygen content of 0.028 g/L.

Open pond growth scenario factors to optimize for net profit are facility size, inoculum density, and pond depth. The open pond depth is simply a matter of determining the light path length based on the culture density, and using this value as the pond depth. The oxygen saturation is found to not play a factor in pond depth since the culture density is low enough that the light path length is dominant.

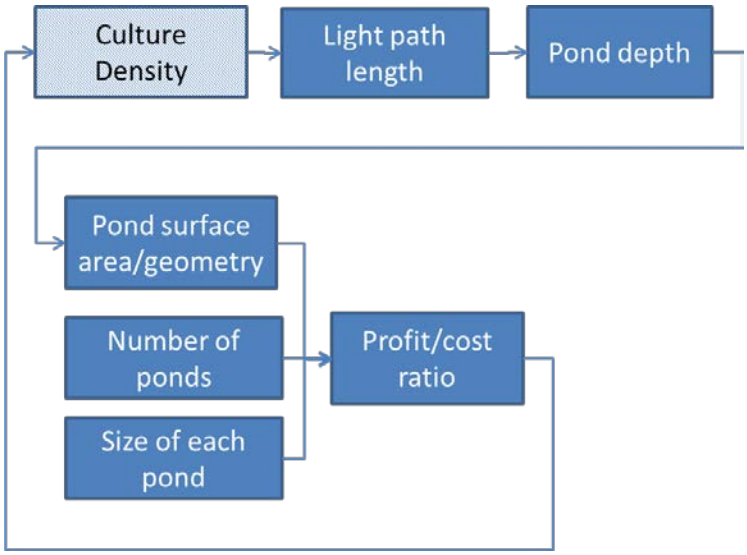

Figure 14: Open Pond optimization flow.

Facility size is straight forward since a net profit causes facility size to go to a maximum while a net loss causes facility size to go to a minimum. Therefore, for the initial optimization, which did not include the financial analysis, the only parameter to optimize is the inoculum density for both growth scenarios. The optimization which includes financial analysis does reveal some exceptions with the facility size, but generally the same rule applies, and even then only increases the parameters to optimize to two.

In constrained optimization, the general aim is to transform the problem into an easier sub-problem that can then be solved and used as the basis of an iterative process. Three different constrained optimization methods were used to verify results. A large-scale algorithm was used first (interior point method), followed by a medium-scale algorithm (sequential quadratic programming). A direct search was used as the third method.

The large-scale algorithm calculates the Hessian by a dense quasi-Newton approximation and by a limited-memory, large-scale quasi-Newton approximation (Biggs, 1975). The Newton step is a linear approximation using a direct step, which is tried first. If the algorithm cannot take a direct step then a conjugate gradient step is tried using a trust region. If an attempted step does not decrease the merit function, returns a complex value, NaN, infinite or an error, the algorithm rejects the step and attempts a new, shorter step. Equation (59) defines the direct step. The Hessian can handle a matrix of variables to optimize, but the sensitivity analysis and modifications of the model simplify the optimization, which both speeds up the process and reduces chance for error.

$$\nabla^2_{xx}L(x,\lambda) = \nabla^2 f(x) + \boldsymbol{\Sigma}\lambda_i\nabla^2 c_i(x) + \boldsymbol{\Sigma}\lambda_j\nabla^2 ceq_j(x) \qquad \text{Eq. (59) (Byrd, et al., 2000)}$$

Equation (59) solves the approximate problem through a sequence of equality constrained problems, which are easier to solve then the original inequality constrained problem (Equation 60).

$$minf_{net\ profit}\ , subject\ to\ min \leq ID_{net\ profit} \leq max \qquad \text{Eq. (60)}$$

where ID is the inoculum density.

Equation (61) defines the conjugate gradient step where the algorithm tries to minimize a norm of the linearized constraints inside the trust region of radius R (Byrd, et al., 2000).

$$\nabla_x L(x,\lambda) = \nabla_x f(x) + \boldsymbol{\Sigma}\lambda_i\nabla c_i(x) + \boldsymbol{\Sigma}\lambda_j\nabla ceq_j(x) = 0 \qquad \text{Eq. (61)}$$

The medium-scale algorithm uses Kuhn-Tucker equations, also known as a Sequential Quadratic Programming (SQP) method since a QP sub-problem is solved at

each major iteration (Biggs, 1975) (Byrd, et al., 2000) (Han, 1977). The second method uses more memory, but also increases functionality for better performance. A step-size procedure is added to maintain the decrease of the merit function which enables global convergence, and makes it an extension to the Newton method (Han, 1977) (Matlab, 2012). A quadratic approximation of the Lagrangian function shown in Equation (62) is used.

$$L(x, \lambda) = f(x) + \sum_{i-1}^{m} \lambda_i g_i(x) \qquad \text{Eq. (62)}$$

Similar to the large-scale algorithm, if an attempted step does not decrease the merit function, returns a complex value, NaN, Inf or an error, the algorithm rejects the step and attempts a new, shorter step. At each major iteration a positive definite quasi-Newton approximation of the Hessian of the Lagrangian function (Equation 62) is calculated. Then the SQP method is solved using the form shown in Equation (63) for each matrix element.

$$minq(d) = \frac{1}{2} d^T H d + c^T d \qquad \text{Eq. (63)}$$

The algorithm first calculates a feasible point if one exists, and then generates an iterative sequence of feasible points to converge to the solution. The solution to the QP sub-problem produces a vector which is used to form a new iteration. By providing a feasible point for the initialization, the minimum solution will be found more quickly through decreasing the merit function.

The direct search does not require any information about the gradient of the objective function, but instead searches for a set of points around the current point, looking for a value lower than the value at the current point. The set of points is called a

mesh, which is formed by adding the current point to a scalar multiple of a set of vectors called a pattern. Various poll and search methods to improve efficiency may be used depending on the type of problem. This method is desirable for finding global solutions involving more than one variable.

The optimization is run using a set of two test scripts for each growth scenario (see Appendix E) (Matlab, 2012). The objective function assigns initial values to the parameters which optimize the net profit, the algorithm, tolerances, maximum iterations, maximum and minimum limits, and the function to minimize. The variables to optimize are included in the X0 matrix consisting of total Liters, inoculum density in cells/mL, and the lipid content for the PBR/ALR growth scenario. The variables to optimize in the open pond growth scenario are only the inoculum density in cells/mL and the lipid content. The objective function labels the results from the constraint function as 'InitialCost'. The screen prints the initial values for the X0 matrix. The constraint function assigns the values to X, calls the appropriate model for simulation, and runs the optimization to minimize the mean of the costs per day. Finally, the objective function displays the final values for the X0 matrix, as well as the minimized costs per day as 'FinalCost'.

The constraint function represents the function to minimize, and runs the model while assigning the values from the first test script for parameters and returning the results as the mean of the costs per day minus the profits per day, which is the variable to minimize. The objective and constraint functions are combined into a merit function. In order to locate local and global minimums, the initial values, tolerance on the constraints, the tolerance on the function to minimize, maximum evaluations, step length, quantity of

past iterations to remember, and the solver can all be modified to achieve improved results. It is possible to watch the values in the model as displays while the iterations accumulate as well as produce a graph of the function results as a function of the iteration in order to verify if the results are converging or settling in a local minimum.

Business Model

In order to prove algal growth for CO_2 capture and biofuel generation is economically feasible, the parameters must be narrowed down and years of research data must be compiled and integrated. Flue gas and wastewater have proven to be efficient CO_2 and nutrient culture sources. The studies in the literature have shown flue gas is a biological solution to providing CO_2 enriched air to the culture, and wastewater is similarly biologically feasible for providing necessary nutrients.

The process model allows system integration with the necessary outputs, as well as the monetary values attached to the end products and inputs. The business model details the necessary infrastructure, government incentives, laws, regulations and potential customers. Key components of a successful agricultural based bioenergy industry are securing an economical and environmentally sustainable supply of biomass, creating value, added co-product streams, and improving delivery logistics. By shifting the modeling approach and fidelity level in a customized manner, the model can be used to maximize speed and cost effectiveness while still ensuring the appropriate degree of accuracy for each stage of product design. Simulations enable businesses to start with a systems model and then flow down requirements. Trading off design features with performance criteria to optimize results is enabled before production even begins.

The model optimizes the cost/profit parameters with the algal growth and physics factors to determine the most profitable growth scenario considering cost of production. Further analysis is then completed which determines the financial feasibility of the project which is key to obtain investors. The financial feasibility for investors contained in this paper is a one point in time analysis, so potential investors are advised to consider further analysis as well as additional factors to the two parameters defined herein. A decision for investment is a complex process involving many factors which are specific to each scenario, environment, timing and the investor him/herself.

The model assumes daily product and the cost of transporting to a refinery is not included. The literature has found the key cost and price variables likely to have the biggest impact on the economic performance of the algal cultivation are those for petroleum crude, algal oil, carbon credits from carbon dioxide capture, and commercial fertilizer (Putt, 2007).

Funding/Investment

Commercial-scale production of biodiesel from microalgae requires massive investments in production facilities. Evaluating the financial feasibility of a project can be done through calculating return on investment (payback), internal rate of return (IRR), and net present value (NPV) (Kerzner, 2006). The payback period is the exact length of time needed for a firm to recover its initial investment from cash inflows. It must be used as a supplemental tool to accompany other methods.

NPV is calculated with equation (64).

$$NPV = \sum \left[\frac{FV_t}{(1+k)^t}\right] - \Pi \qquad \text{Eq. (64)}$$

where FV is the future value of the cash inflows ($FV_i = PV\ (1 + k)^n$, where FV_i is the initial value of the investment.),

k is the discount rate equal to the firm's capital (8% APR used in model),

t is the time in number of years,

and Π represents the initial investment.

The NPV rule states that if the NPV is greater than or equal to zero dollars, accept the project. If the NPV is less than zero dollars, reject the project (Kerzner, 2006).

The IRR determines the minimum future growth rate where the present rate of cash inflows exactly equals the initial investment. It is an indicator of the efficiency, quality, or yield of an investment, where the NPV is an indicator of the magnitude of an investment. When the IRR is above bench mark it is attractive; otherwise the company is relatively unattractive.

IRR is calculated with equation (65).

$$IRR = \sum \left[\frac{FV_t}{(1+IRR)^t}\right] - \Pi \qquad \text{Eq. (65)}$$

where IRR is the discount rate when NPV = 0.

The timing of the cash flows is also important, where earlier cash flows are more advantageous. The algal growth model does enable cash flows every week for the financial analysis, regardless of the farm size. While cycle time can improve the IRR, reducing costs and increasing revenue have a much larger impact. Reducing investment capital costs has the biggest impact on IRR, especially since in this case all capital investment is at the beginning of the project. The IRR rule states that if the IRR on a project is greater than the minimum required rate of return – cost of capital (in this case

8%, or 8.32% since cash flow is weekly) – then the decision would generally be to go ahead with it. Otherwise the best course of action would be to reject the investment.

It is important to consider the fact that a higher interest rate then 8% may be charged for financing since this is an unproven and relatively risky venture. To determine the cost of financing the site in terms of annualized capital cost (p) and daily capital cost, Equation (66) was used.

$$p = \frac{t(1+r)^n r}{(1+r)^n} - 1 \qquad \text{Eq.(66)}$$

where t is the total amount financed,

r is the rate of return (8%),

and n is the lifetime of the project in years (15).

The cost of financing and operating is deducted from the total profit from products to determine the daily cash inflow.

Also, insurance is not included, but must be considered a significant cost factor, possibly on the order of six figures.

Risk Analysis

Risk is high with algal growth on an industrial scale in general since algal growth on a large scale is uncommon and doesn't exist with the goal of biofuel production. Most studies to date have analyzed algal biomass and lipid production under laboratory conditions over short durations. Although harvesting options have been proven in the laboratory, and for small scale commercial systems and/or comparable food systems, no harvesting options have been practiced on a large commercial scale for algal production.

In an open pond scenario a culture crash would most likely mean at least one entire pond's growth lost, and likely several ponds. A photobioreactor growth scenario would contain the contamination to one photobioreactor at a time, and contamination would be more unlikely than in an open pond scenario.

Another risk unique to open ponds is poorer than average weather. While the weather will affect solar illuminated photobioreactors to some extent, the effect on an open pond growth scenario would be much greater, and could mean little to no growth for an entire week or season at a time.

Incentives

The current tax credit for agriculturally-derived biodiesel is $1 per gallon. (Dimitrov, 2007) Starting in 2012, biofuel produced from algae is included in a $1.01 per gallon production tax credit. In the US, the Energy Dept. has granted a total of $348 million in loans, grants, and tax exemptions since 2004 for research centers, fuel producers, and refiners. The U.S. Department of Defense has awarded multi-year grants in millions of dollars to develop scalable processes for the cost-effective large-scale production of algae oil and jet fuel. None of this subsidizing is included in the model but are potential aids to minimize the risks detailed in the previous section.

The EPA employs the Clean Air Interstate Rule (CAIR) and Acid Rain Program to reduce sulfur dioxide (SO_2) and nitrogen oxides (NO_x) emissions by 70% in 28 eastern states and the District of Columbia using a cap and trade system (Environmental Protection Agency, 2012). However, since the cap and trade systems are revised and/or

dissolved often, and are different in each state, any potential profit from the cap and trade emission reduction from feeding flue gas to algae is not included in the model.

Environmental Impact

The environmental performance of algal biofuel production can vary considerably and is influenced by design and location considerations. Life-cycle assessments of fuel production systems differ significantly in their assumptions and scope. Vasudevan, et al. (2012) found wet extraction to be environmentally more favorable than petro-diesel, but the study only considered energy involved with the harvesting options and assumed a high yield per acre. Many studies assume the use of brackish water as opposed to fresh water will automatically make an algal growth system environmentally sustainable. However, they do not consider the energy involved with supporting growth and harvesting. In order for algal growth to qualify as a green clean technology, each scenario must be examined to determine the actual carbon footprint.

Algae Control & Regulation

Successful implementation of algal growth on an industrial scale will predicate more control and regulation. While the specifics of such control and regulation are yet to be seen, any investor must keep the potential of such in mind. Assuming no biological altering of the microalgae and recycling most of the media helps alleviate some of this concern. Also, microalgal growth with the intent of biofuel production is many years away from successful implementation on an industrial scale.

Customers

The U.S. Navy is on an aggressive national security timetable to convert to 50% alternative fuels by 2020, which would require 8 million barrels per year in jet and marine fuels. They put out a request for the first 500,000 gallons of biofuels within a year of May 23, 2011 (Gardner, 2011). The U.S. Government invoked the Defense Production Act of 1950 which authorizes the President and Congress to directly invest in the commercialization of vital defense technologies that would not otherwise reach commercial-scale production at affordable prices. The DOE, USDA, and the U.S. Navy is each making $170 million available towards the commercialization of advanced biofuels, and that figure is expected to be matched at least 1:1 by the private sector. Starting in 2012 airline carriers with European routes have had to participate in the EU's cap-and-trade system for CO_2 and have to buy additional permits if they exceed limits. (Bloomberg Businessweek, 2011)

On July 1, 2011, ASTM International gave approval for commercial airlines to mix fuel made from organic waste and nonfood plants with kerosene. Airbus estimates that by 2030 plant-derived formulas could make up as much as 30 percent of the market for aviation ($140 billion). (Bloomberg Businessweek, 2011) The climate change impacts of biofuels depend not only on the lifecycle emissions and indirect land use effects, but also on the effects of high-altitude emissions when used as aviation fuel where the lowest amount of sulfur and contaminants are desired (Greene & Plotkin, 2011). Algal based jet fuel contains no sulfur and is low in contaminants. Also, the Air Force has strict safety and quality standards for aviation fuel, which algal oil satisfies

(Gardner, 2011). Through funding from airlines and the government, the start-up and demonstration of the facility can be completed, and subsequently the project can be refinanced at commercially viable rates (Lane, 2012).

Partners

Research collaborations exist between the military, federal agencies, universities, and industrial partners. These partnerships enable a pooling of resources in pursuit of a shared R&D objective with benefits to both private and public entities. The R&D focus should be on eliminating or minimizing the high risk barriers confronting the algal growth for biofuels industry. Industry benefits through technological innovation, which in turn increases capital efficiency. The partnerships should be based on common interest and benefits to all involved parties while not conflicting with the interest of other groups.

Utilities and the Public Utility Commissions (PUC), whose statutes and rules the utilities must abide by, are conservative entities and need firm forecasts to allow algae entrepreneurs to form alliances and allow sharing of land and resources. Carbon caps will aid in this if and when they are instituted in the U.S., but even then and until then, algal companies must be capable of demonstrating technical and economic feasibility.

CO_2 mitigation is considered a valuable end product as many industries seek to reduce their carbon footprint and carbon credits are becoming a commodity. Producing 1 kg of algal biomass fixes 1.6 - 1.8 kg of CO_2, and biomass doubling time can be as short as 3.5 hours. (Patil, et al., 2008). One mole of CO_2 is required for the growth of one mole of microalgae, so one kg of CO_2 can produce 25/44 kg of microalgae and 32/44 kg of oxygen.

Processing CO_2 close to power plants eliminates the capital and operating costs for transportation, and eliminates opposition from localities opposed to pipelines. More efficient plants may even exceed the requirement and sell their allowances. Power plants will have powerful incentives to consider long-range strategic partnerships to bring algae to scale. Studies have found the use of biofuels does recycle all or most carbon (less for open pond growth scenarios), which substantially reduces the net release of CO_2 to the atmosphere (Wyman, 1994) (Bussell, et al., 2008). The literature claims that for each liter of biodiesel consumed in place of fossil diesel, 3.3 kg of CO_2 emissions are avoided (Alabi, et al., 2009).

Electrical power plants are responsible for over one-third of the US emissions, or about 1.7 Gt CO_2 per year. Industrial processes most contributing to CO_2 atmospheric concentrations consist of electric plants, hydrogen and ammonia production plants, cement factories and fermentative and chemical oxidation processes (Alabi, et al., 2009) Power-plant flue gas can serve as a source of CO_2 for microalgae cultivation, and the algae can be co-fired with coal. There are potentially significant benefits to recycling CO_2 toward microalgae production, and there are a number of companies involved in algae-based CO_2 sequestration worldwide (Kadam, 2002).

The DOE's goal is to reduce the cost of carbon sequestration below $10 per ton of avoided net cost. Presently it ranges from $35 to $264 per ton of CO_2 by desulfurizing flue gas (Olaizola, et al., 2003). Gas scrubbing could be simplified since NO_x and SO_x can also be effectively used by nutrients by the algae. Scrubbing heavy metals from the flue gas, which is in most cases already an EPA requirement, prior to pumping into the

microalgal culture will enable the microalgae to be used for high value end products such as feed supplements and is in place already for power plant emissions.

Chapter Three: Results

The only true test of a simulation is how well the real system performs with implementation of the model results. Simulation results are also commonly evaluated using statistical procedures such as variance, regression analysis, and *t* tests (Chase, et al., 2006). There are three realistic alternatives to validate accuracy of the model: (1) print out all calculations used in the simulation and verify the calculations by separate computation, (2) verify model results with those reported in the literature, and (3) simulate present conditions and compare simulation results with the existing system (Chase, et al., 2006).

This model has been validated through presenting the methodology and equations used to create the model, and now the results can be validated by comparing them with those reported in the literature. In some cases the results differ with the literature, and when this occurs, the methodology is examined again to determine factors which cause the differences. (Key outputs from the model are detailed in Appendix A, as well as a comparison with other studies as to the level of detail contained within Appendix B.)

Results in the following sections up to the optimization section are results considering culture densities and corresponding light path length, which have been proven in real algal growth scenarios, except where noted to illustrate model results. The maximum culture densities used are 40 - 50 g/L for artificially illuminated ALR's, around

1 g/L for solar illuminated PBR's, and 0.33 g/L for open ponds. The light path length is calculated with Equation (7) unless otherwise mentioned.

Algal Size and Density

As mentioned previously, very few if any studies consider the algal density in terms of g/L based on the algal cell size. Phytoplankton size ranges over nine orders of magnitude in cell volume from <2 μm to 2000 μm. The resulting density affects the desired inoculum density, the desired growth duration, light path length (and in turn photobioreactor geometry and pond depth), the pH, required CO_2, and the amount of oxygen produced.

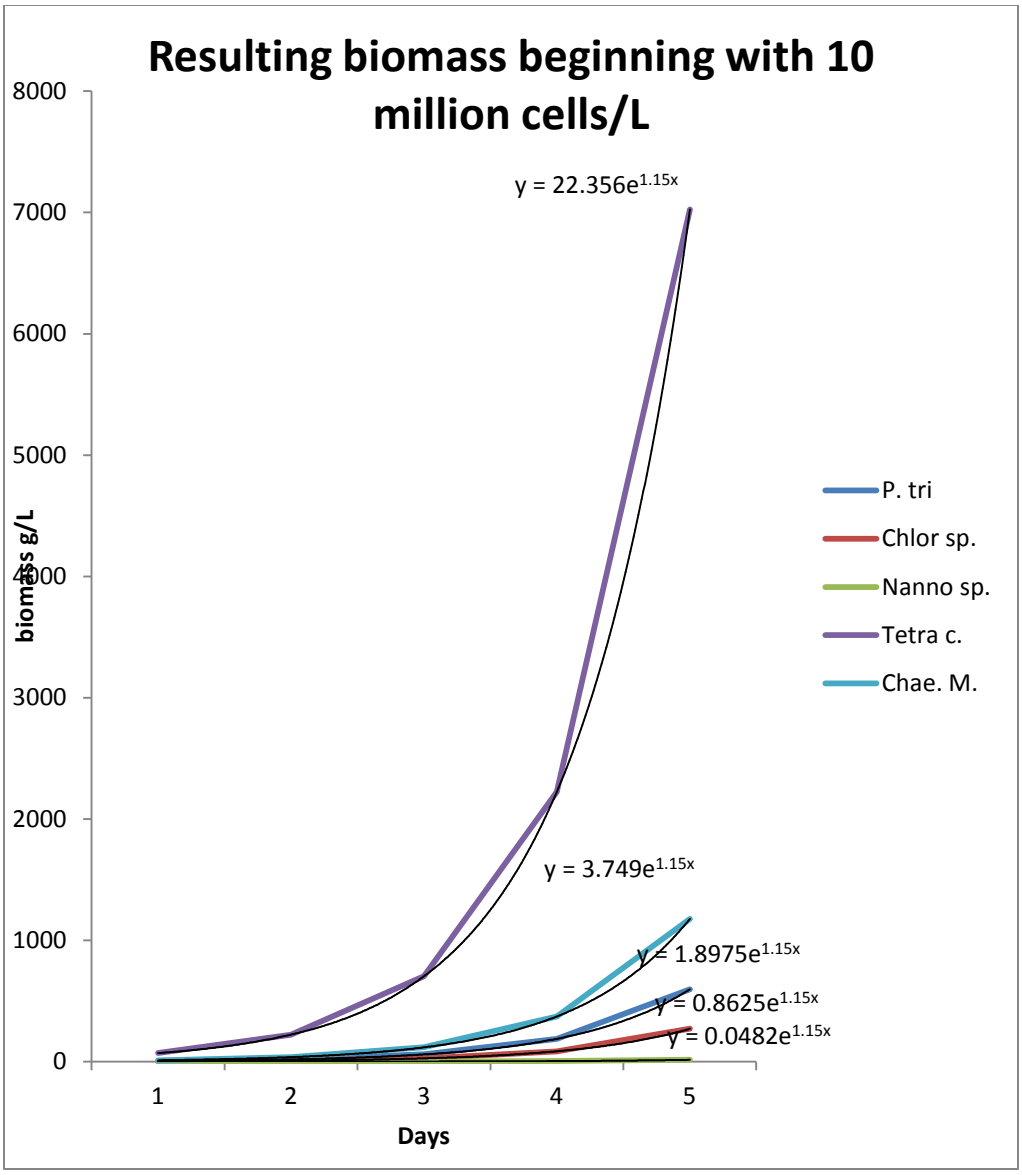

Figure 15: Comparison between 5 algal species and resulting culture density after growth duration in days.

The model allows the selection of one of the five algal species (detailed in methodology/system model/productivity section of this paper), which selection affects the algal cell size and the lipid content. The inoculum density is adjusted in cells/mL, and the model calculates the equivalent in g/L per species with and without the growth

rate. The density in g/L is then used for viscosity, geometry and lighting calculations. As is evident from Figure (15), the g/L is vastly different depending on the algae species chosen.

Lighting & Productivity

The model is designed to determine the light path length based on the culture density. Analyzing the light path length alone provides invaluable insight into maximum culture density depending on the growth scenario considered. The basic algal growth rate (Equation 2) yields maximum open pond density of 16.99 g/L at a depth of approximately 20 cm when Equation (7) is used to determine light path length. However, this high density in an open pond growth scenario has never been proven in the literature.

When the light path length and g/L of algal growth supported is combined with the pond depth to derive the productivity in g/m^2 per day, the maximum areal productivity becomes apparent at a depth of slightly greater than 20 cm. Also, shallower depths should be avoided for open ponds since they would encounter other issues such as greater photoinhibition and difficult to manage temperature increases.

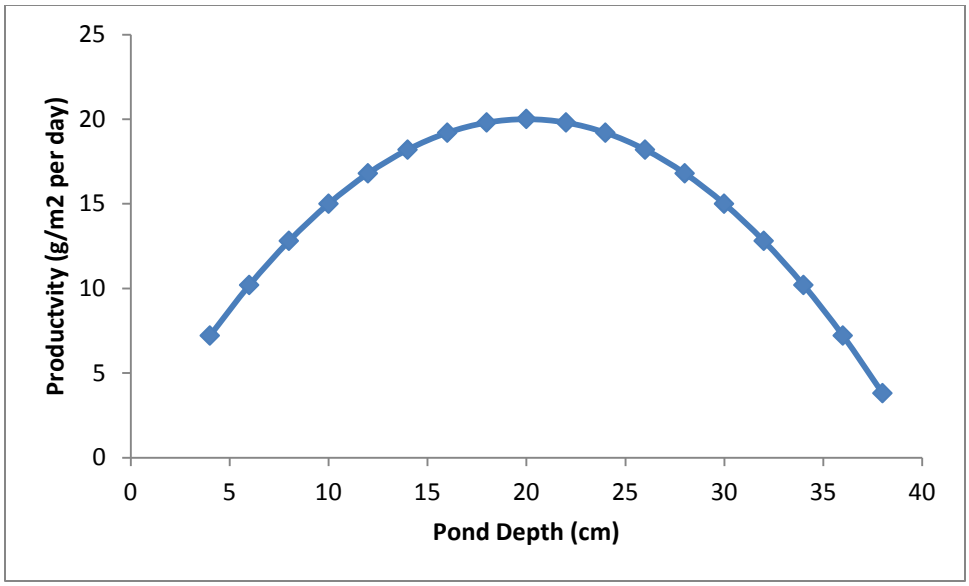

Figure 16: Open pond areal productivity.

However, where costs associated with greater surface area are much higher than profits associated with algal end products, the highest areal productivity does not result in the most cost efficient growth scenario. Additionally bear in mind the possibility of lower productivity due to risks not included in the model calculations such as nighttime losses, contamination causing culture crash, and poor weather.

Results from calculations contained in method/system model/lighting section of this paper reveal a wide range in Watts per Liter required depending on the design, light source, light path length, culture density, and gas delivery. The most effective system requiring the least Watts per Liter is LED lighting, a light path length > 10 cm, and using a diffused gas delivery system.

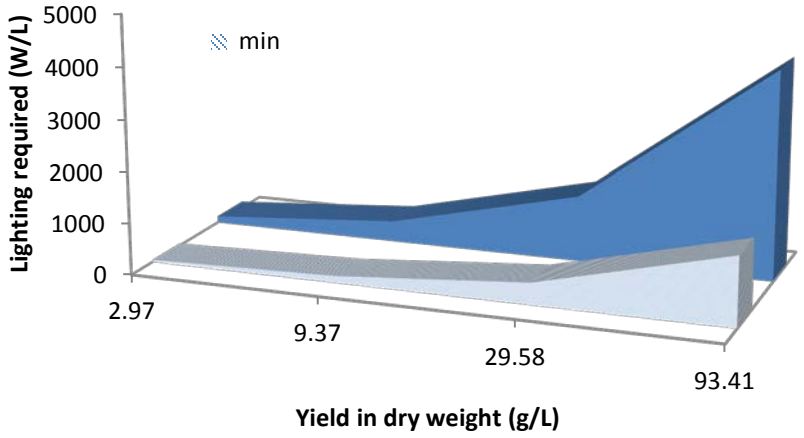

Figure 17: Lighting required vs. algal biomass yield.

Results for the net profit as a function of the culture density and lipid content are as expected. The culture density is a very strong influencer on the algal facility net profit. Due to high losses in the open pond growth scenario, however, the higher culture density doesn't surmount the costs so the culture density is inversely related to the net profit.

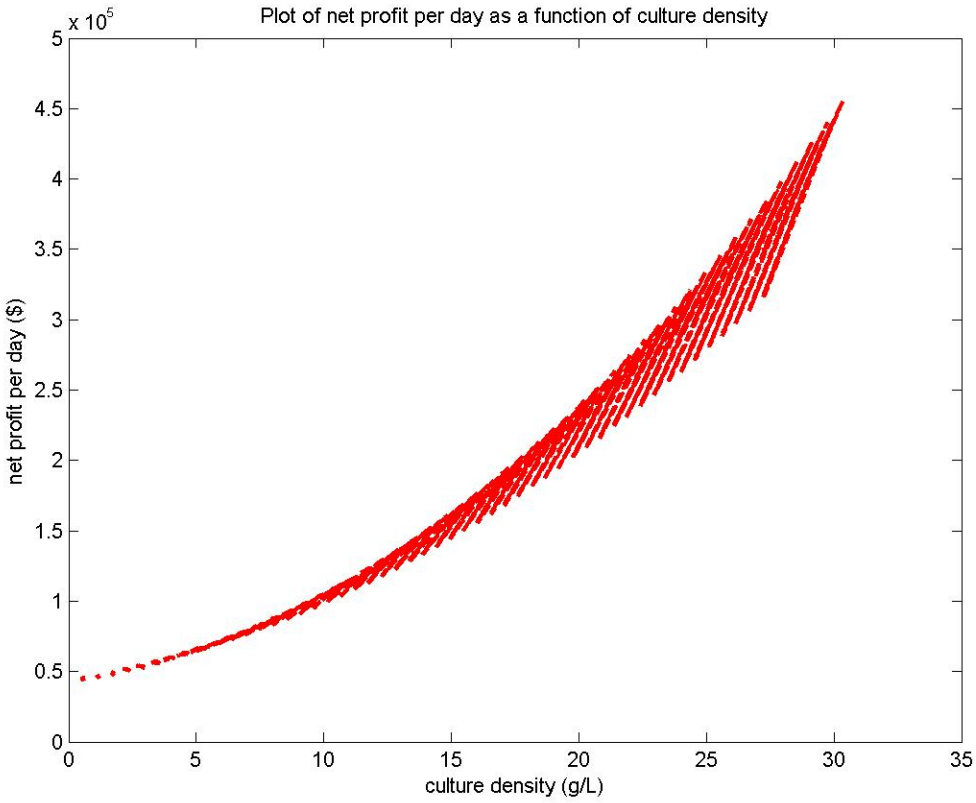

Figure 18: Net profit as a function of culture density for PBR growth scenario.

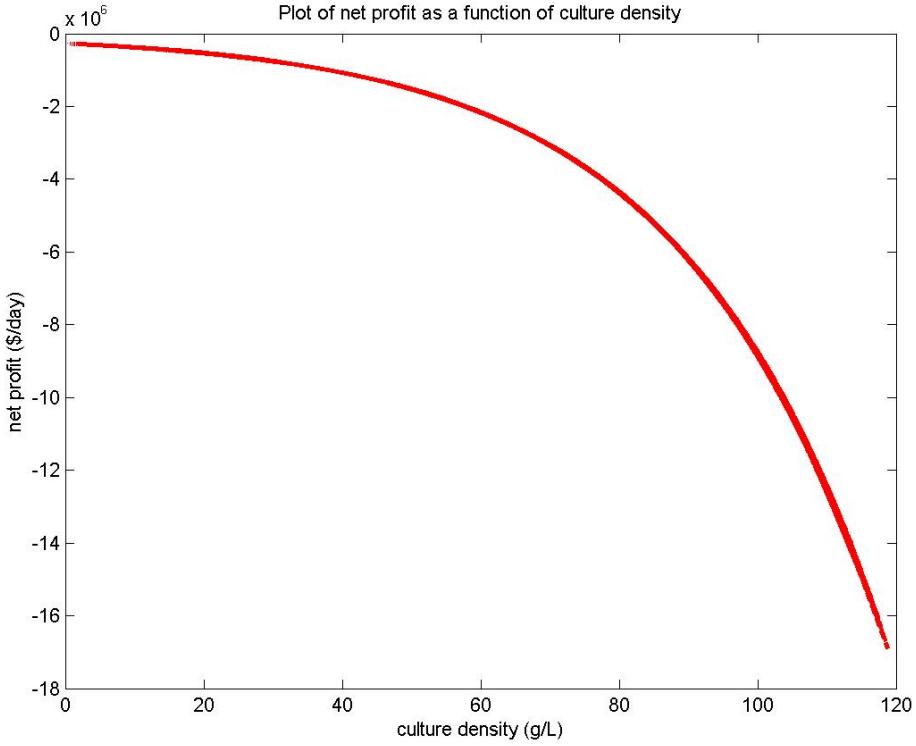

Figure 19: Net profit as a function of culture density for open pond growth scenario.

Lipid content increases net profits for all growth scenarios but not as strongly as culture density. Also, losses in the open pond growth scenario are so great that the lipid content barely has an effect on the net profit.

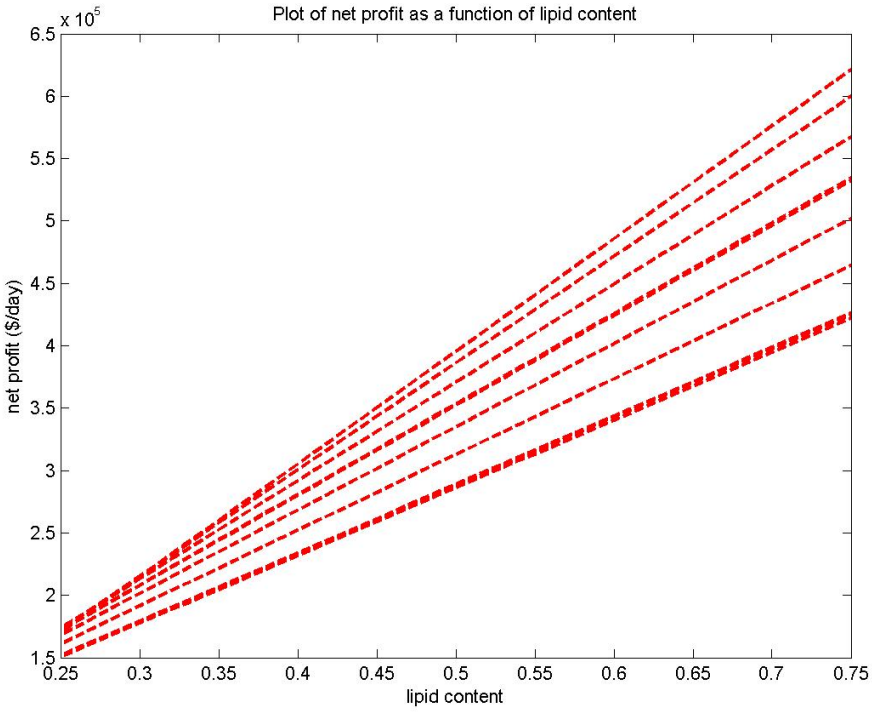

Figure 20: Net profit as a function of lipid content for PBR growth scenario.

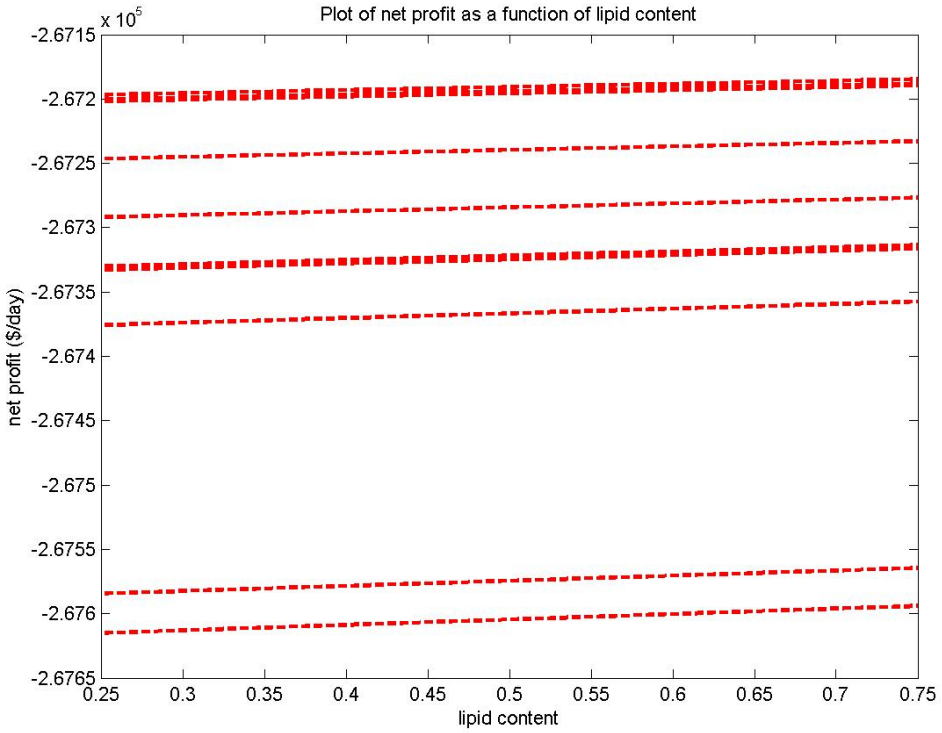

Figure 21: Net profit as a function of lipid content for open pond growth scenario.

Large Scale Turbulence

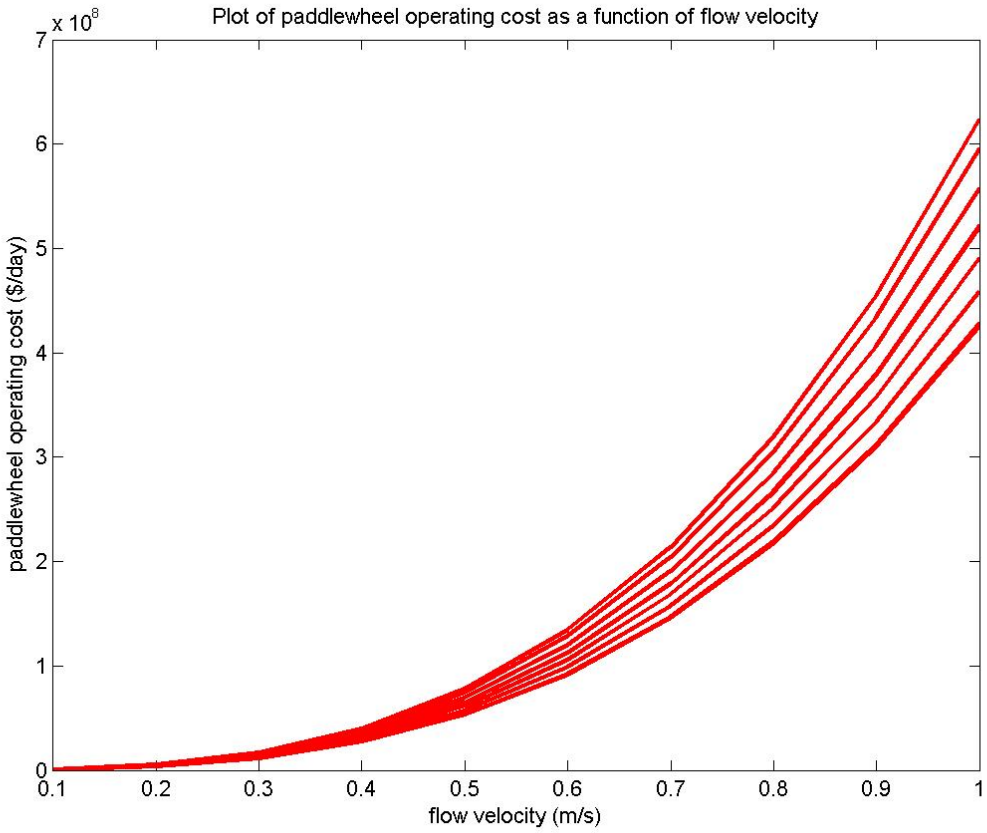

Figure 22: Paddlewheel operating cost as a function of flow velocity in a 100,000 kg biomass/year facility.

Flow velocity in an open pond growth scenario is a result of the paddlewheel velocity minus the head loss. Assuming a paddlewheel velocity of 1 - 2 m/s, the resulting flow velocity in a pond of 20,000 Liters with head loss due to friction, bends and gas sumps considered is 0.03 m/s. To maintain a flow velocity of 1 m/s in all areas despite head loss due to friction, gas sumps, and bends is cost prohibitive (see Figure 22).

Results reveal the power consumption for raceway paddlewheels lowers by 40% when the surface is concrete instead of clay, which at a rate of $0.11 per kWh would

result in a savings of $2.087e11 per year over a clay surface assuming a constant 8 hours/day flow velocity of 1 m/s and an algae farm of 25 ponds, each holding 20,000 Liters. The model uses a roughness factor for concrete for all remaining open pond growth scenario calculations.

Results for ALR geometry including the light path length, light: dark ratio of 1:10, and maximum oxygen saturation at expected culture densities of 40 - 50 g/L are shown in Figure (23).

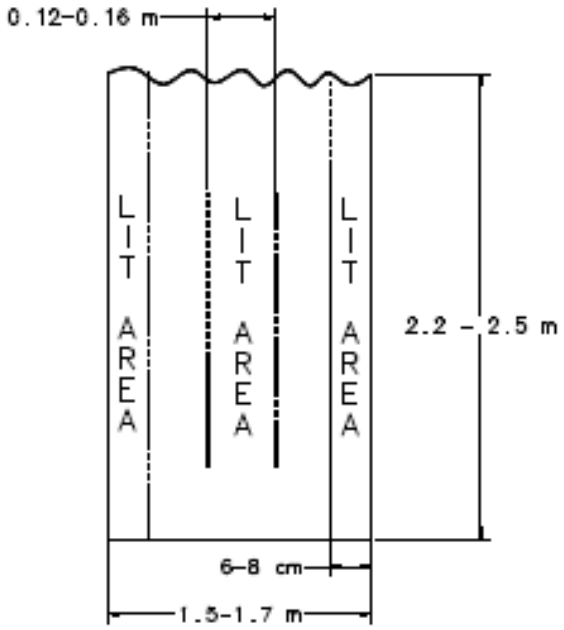

Figure 23: ALR design geometry results for culture density 40 - 50 g/L (not to scale).

Small Scale Turbulence

The model calculates Kolgomorov length from both viscous and bubble dissipation.

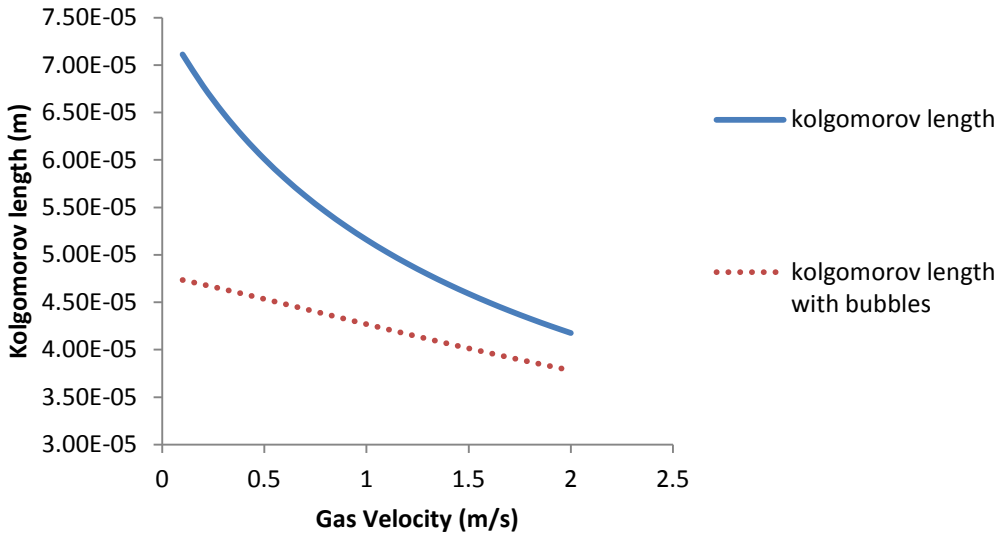

Figure 24: Kolgomorov length and with bubbles as a function of gas velocity.

Even when including bubble dissipation, the Kolgomorov length is longer than the cell by 5.4e-6 meters before maximum shear stress is reached at around a gas velocity of 2.5 m/s (see Figure 30). Since the optimal flow dynamics are experienced approximately between 0 - 10 µm greater than the length of the algal cell, the hyperbolic effect on productivity will be evident as the length extends over 10 µm producing less than optimal results (Contreras, et al., 1998) (Preston, et al., 2001) (Peters, et al., 2006). Figure (25) reveals that in the 0.04 – 0.09 m/s gas velocity range used in laboratory studies, the Kolgomorov length is approximately 140 µm greater than the cell length.

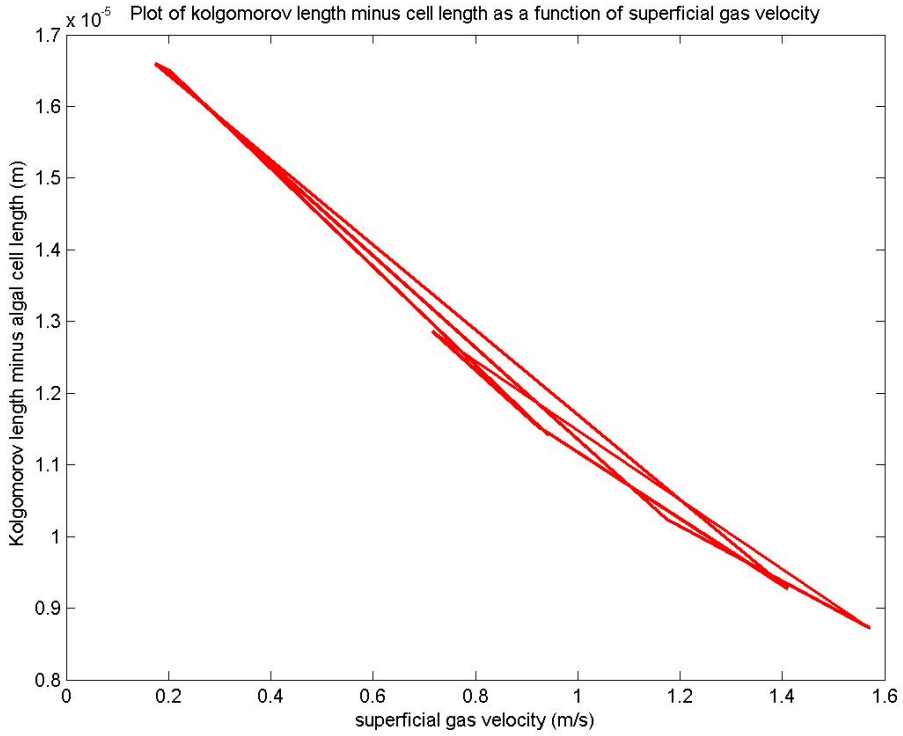

Figure 25: Kolgomorov length minus *Nanno s.* cell length vs. superficial gas velocity.

Rheology and effects on the culture viscosity reveal the flow is Newtonian at expected culture densities even when considering temperature increases and using wastewater as the culture medium. Figure (26) compares expected packing fraction for microalgal cultures to results from Jibuti, et al. (2012). In the range of expected densities, the model results concur with previous results and do not show any evidence of

non-Newtonian flow.

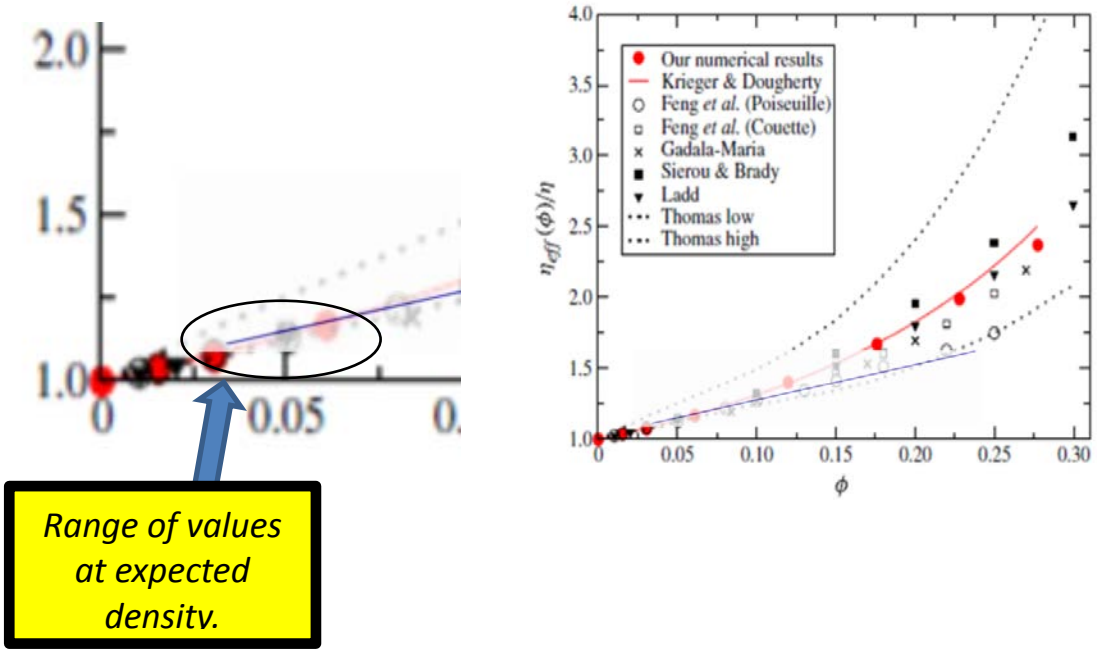

Figure 26: Effective viscosity as a function of volume packing fraction - Blue line indicates model results, other results from Jibuti, et al., 2012.

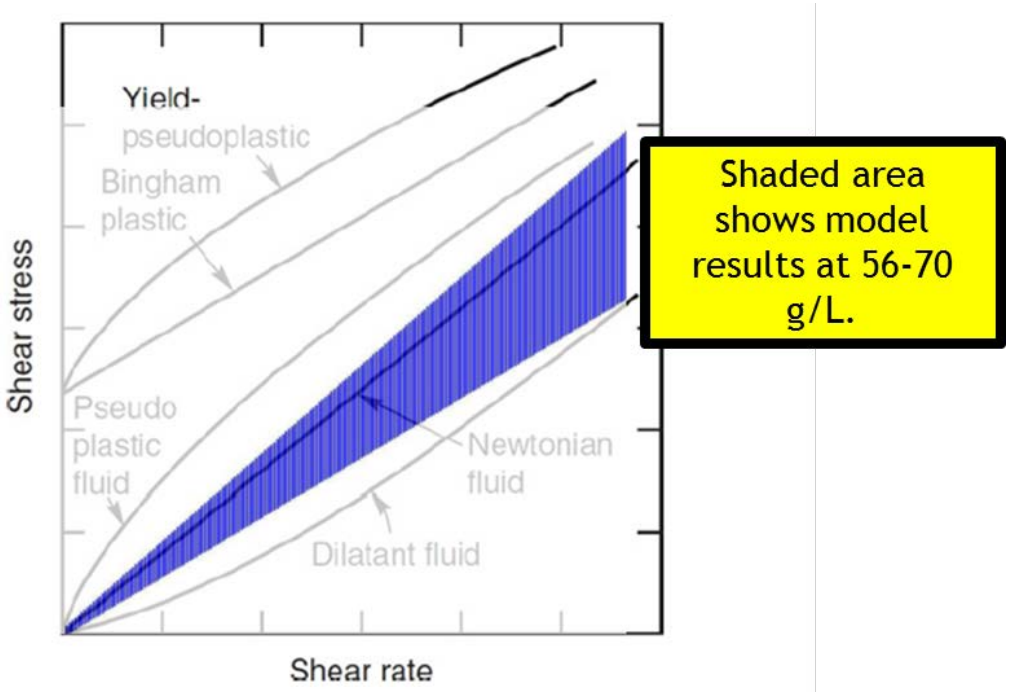

Figure 27: Newtonian flow characteristics -- Blue shaded area indicates model results, other results from Chabra & Richardson, 2008.

Results in Figure (27) indicate Newtonian flow in a range of expected photobioreactor culture densities. When the culture density is increased beyond maximum, one does start to see the characteristics of a non-Newtonian flow. Figure (28) shows the results at densities up to 270 g/L, and it is evident shear-thinning, or decreasing viscosity with increasing shear rate is taking place. In this case, the model confirms data in the literature, but in normal operating conditions the culture density will never reach such a high density due to temperature, nutrient, light path length, and gas exchange restraints.

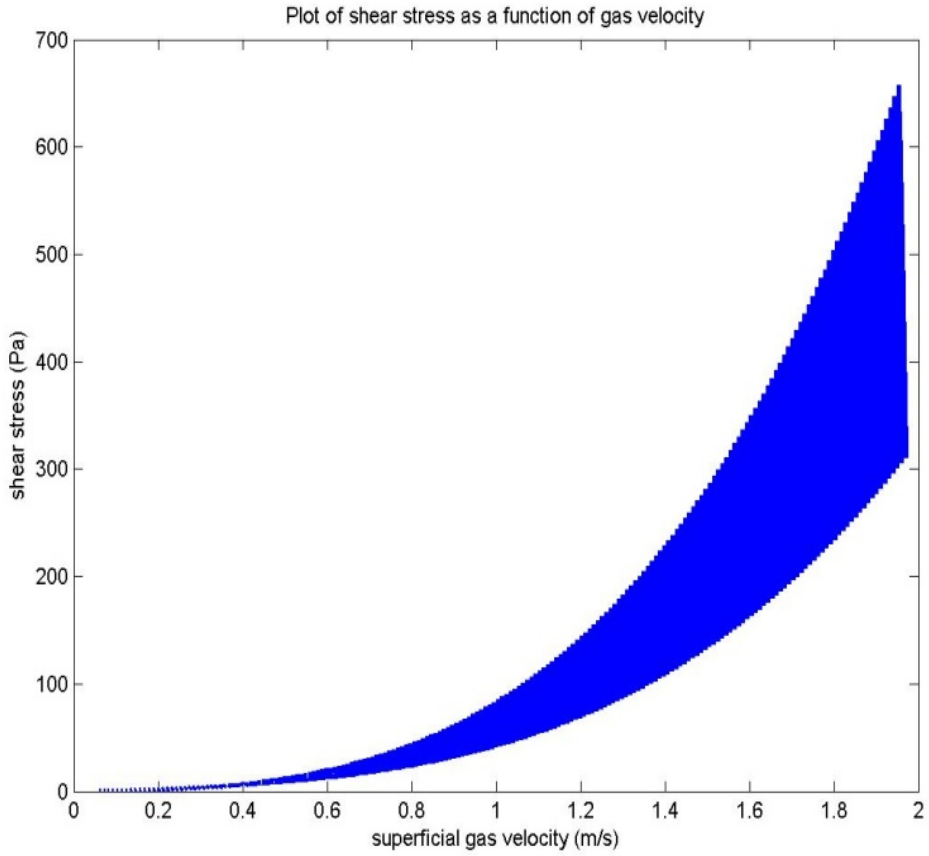

Figure 28: Shear stress vs. superficial gas velocity at 42 - 270 g/L culture density where non-Newtonian flow is evident.

Gas velocity ranges from around 0.3 m/s to 2.5 m/s result in a range of shear stress values which are as expected and may be acceptable for algal growth. Further analysis reveals there is room to optimize the gas velocity based on shear stress per cell, interfacial area, geometry, and heterogeneous flow. First, liquid velocity in the riser is analyzed for conditions when the liquid is driven by the gas (gas velocity > liquid velocity), which is evident zooming in at gas velocities in a range from 1.4 – 1.6 m/s (see Figure 30).

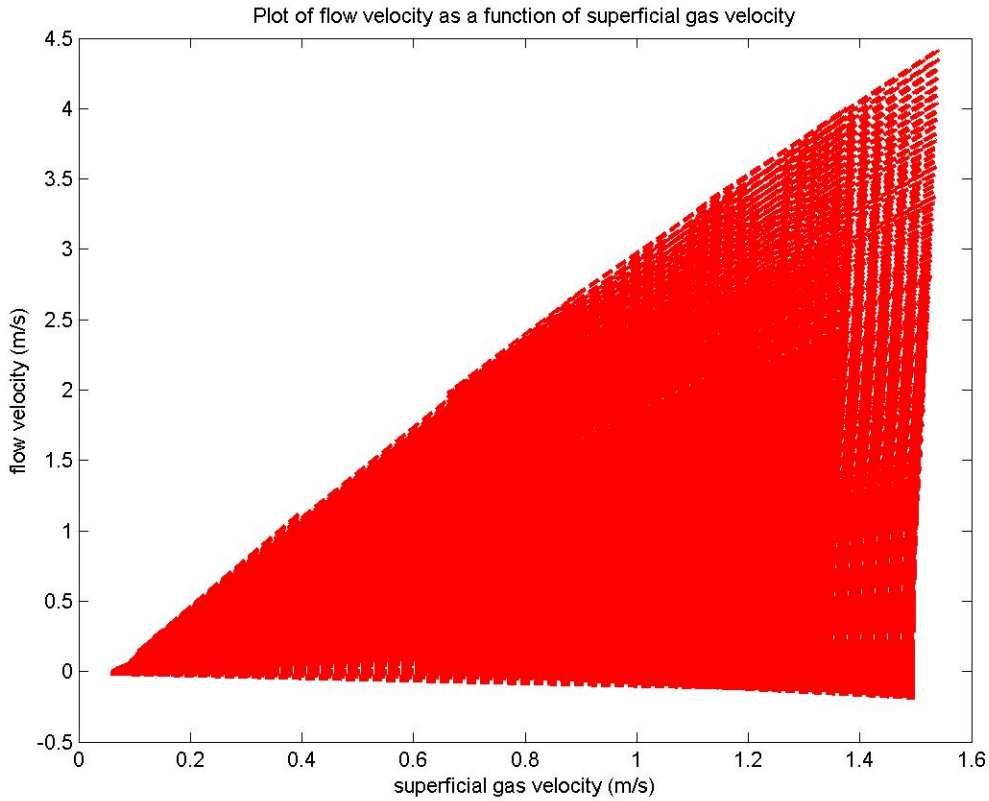

Figure 29: Liquid velocity in the riser as a function of superficial gas velocity (0 - 1.6 m/s).

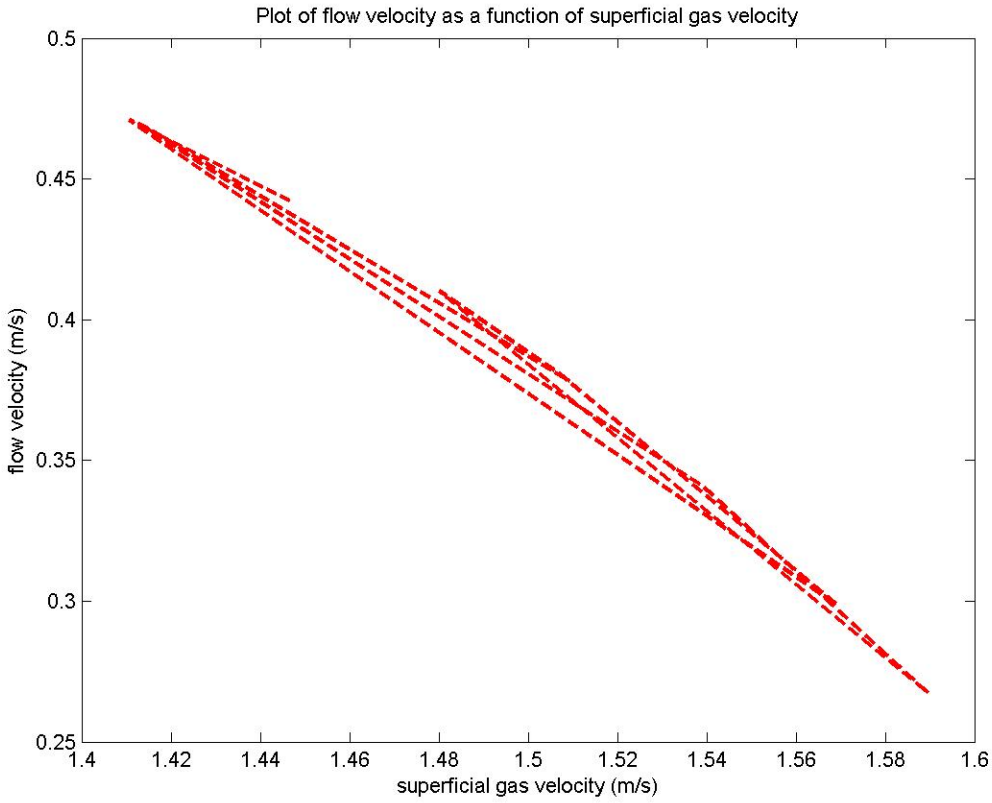

Figure 30: Liquid velocity in the riser as a function of superficial gas velocity (1.4 - 1.6 m/s).

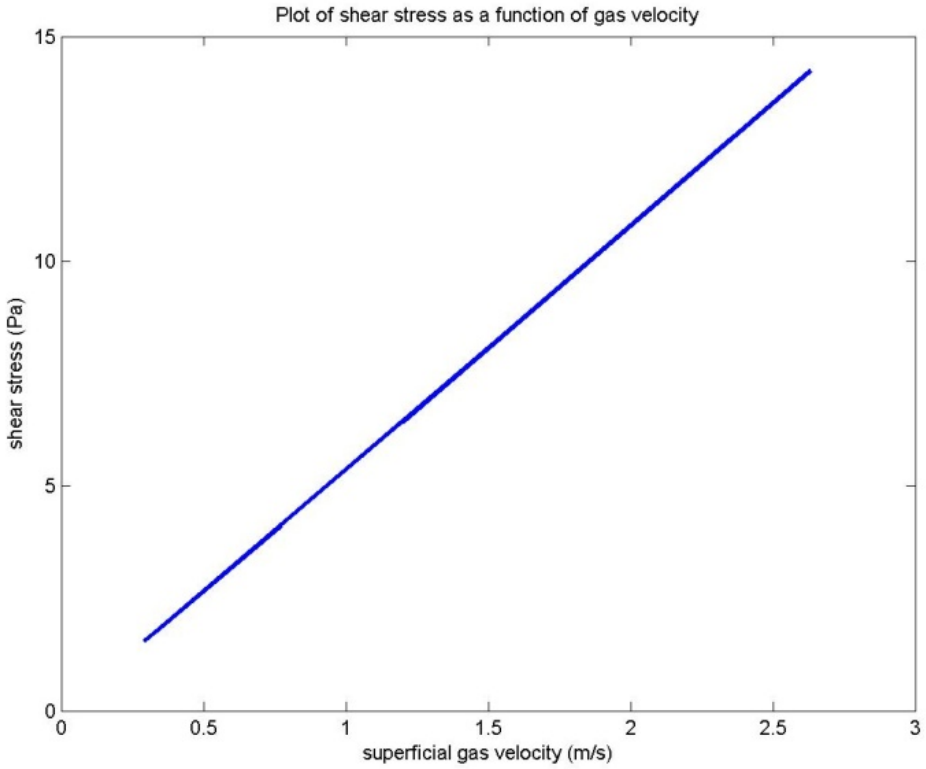

Figure 31: Model results for viscous shear stress as a function of superficial gas velocity.

Model results for viscous shear stress reveal maximum shear stress is reached at a gas velocity between 2.5 and 3 m/s. Using Equation (40), the shear stress per cell can be calculated as a function of culture density and vorticity, and reveals extra margin at relatively low algal densities. At a maximum of 4.5e-7 Pa shear stress per cell when culture density reaches 70 g/L, the viscous shear stress is dominant, and it seems reasonable to establish a maximum viscous shear stress at ~15-16 Pa.

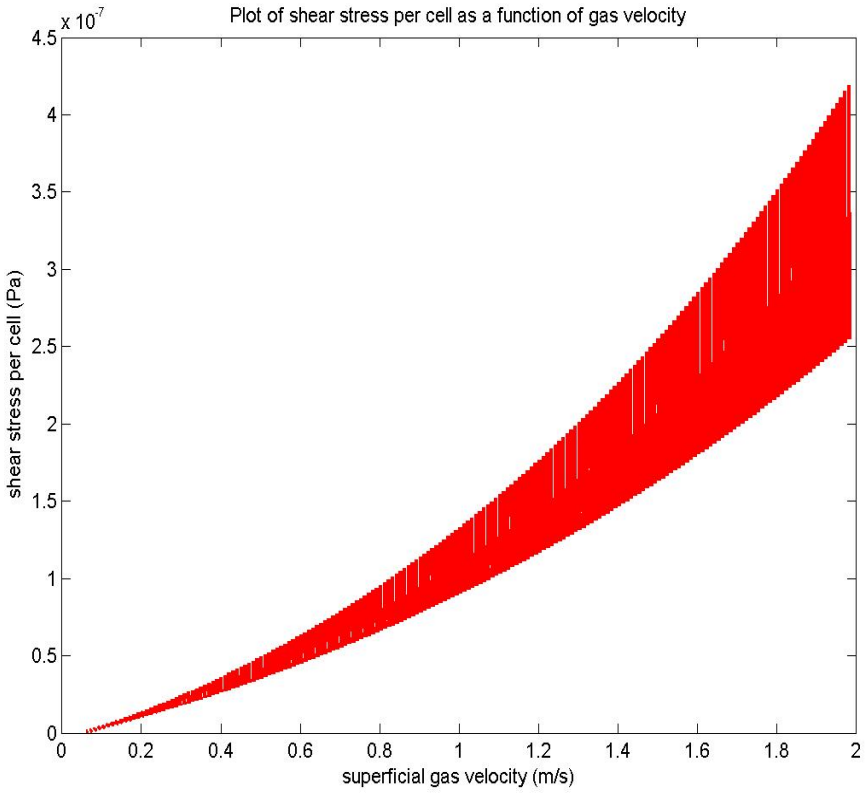

Figure 32: Shear stress per cell vs. superficial gas velocity (culture density of 42 - 70 g/L).

Figure (33) validates the CO_2 transfer rates at low culture densities calculated by equations detailed in the small-scale turbulence section of this paper. The culture density was intentionally set at 0 - 2 g/L to compare the CO_2 transfer rates from the literature to the model. This low culture density is within the range of culture density expected for open ponds, but these equations only apply to ALR's, where the expected culture density is much higher.

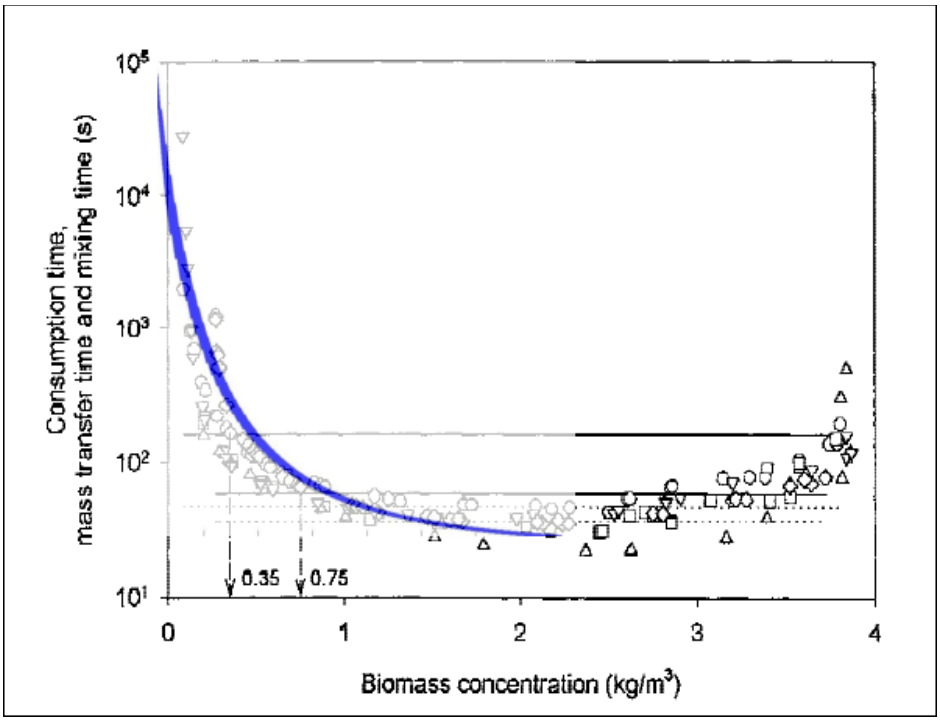

(J_{Gr}): (○) 0.0169 m/s, (□) 0.0450 m/s, (△) 0.0551 m/s, (▽) 0.0652 m/s, (◇) 0.0855 m/s.

Figure 33: CO_2 transfer time vs. superficial gas velocity of .01 - .085 m/s at 0 - 2 g/L culture density -Blue line is model data, other results from Contreras, et al., 1998.

Since it has been determined it is important to achieve and maintain heterogeneous flow, model results were analyzed for indication of transition from bubbly flow to heterogeneous flow. Transition to heterogeneous flow is very evident at low culture densities in Figure (36), and slightly evident at expected optimal culture densities in Figure (35).

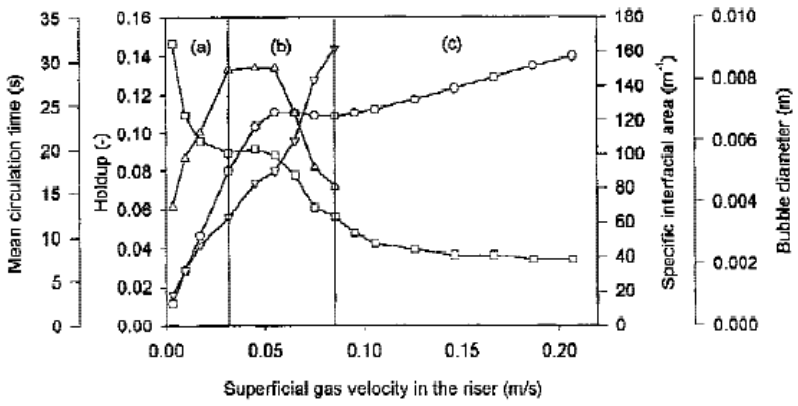

Figure 2. Overall holdup (○), mean circulation time (□), specific interfacial area (△) and bubble diameter (▽) as functions of superficial gas velocity: (a) bubble flow regime, (b) transition regime, (c) heterogeneous regime.

Figure 34: Mean circulation time, holdup, bubble diameter, and interfacial area as a function of superficial gas velocity (Contreras, et al., 1998).

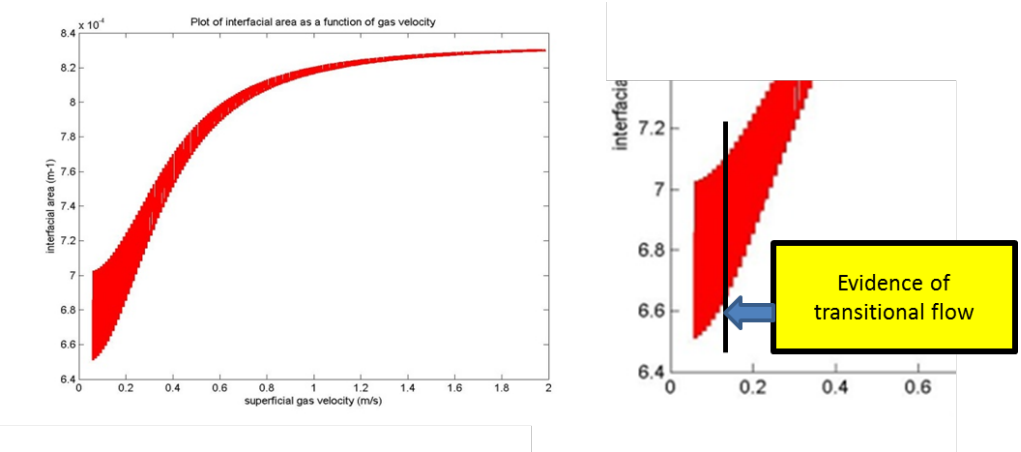

Figure 35: Interfacial area as a function of superficial gas velocity (culture density 42-70 g/L).

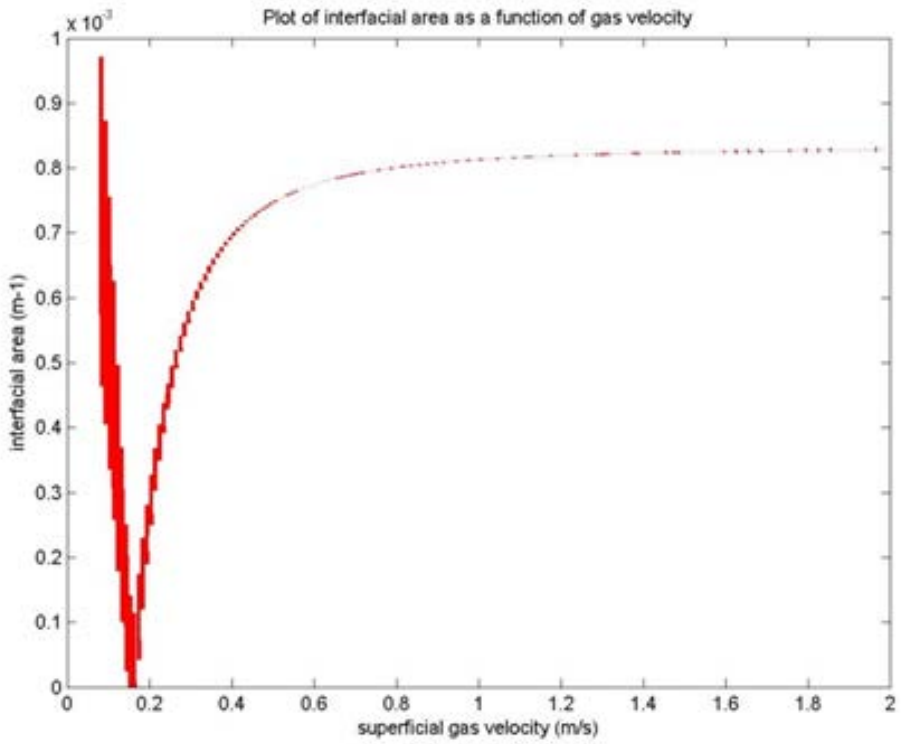

Figure 36: Interfacial area as a function of superficial gas velocity (culture density 4-27 g/L).

The bubble shear rate also shows a spike between .15 and .20 m/s especially evident with lower culture densities as shown in Figure (37). It is possible optimal flow conditions have not been obtained in some studies because this initial hurdle to heterogeneous flow has been avoided, since the bubble shear rate sustained at this velocity will damage the microalgae. Since the assumptions regarding Newtonian flow and the flow dynamics having more influence than gravity are reliant upon $\lambda \leq 1$ (shear rate > 1000 s^{-1}, gas velocity > 0.2 m/s), there is additional reason to aim for heterogeneous flow. Also, in laboratory test set-ups the photobioreactor diameter will be smaller which makes damaging slug flow more likely at lower gas velocities (Merchuk & Gluz, 2002).

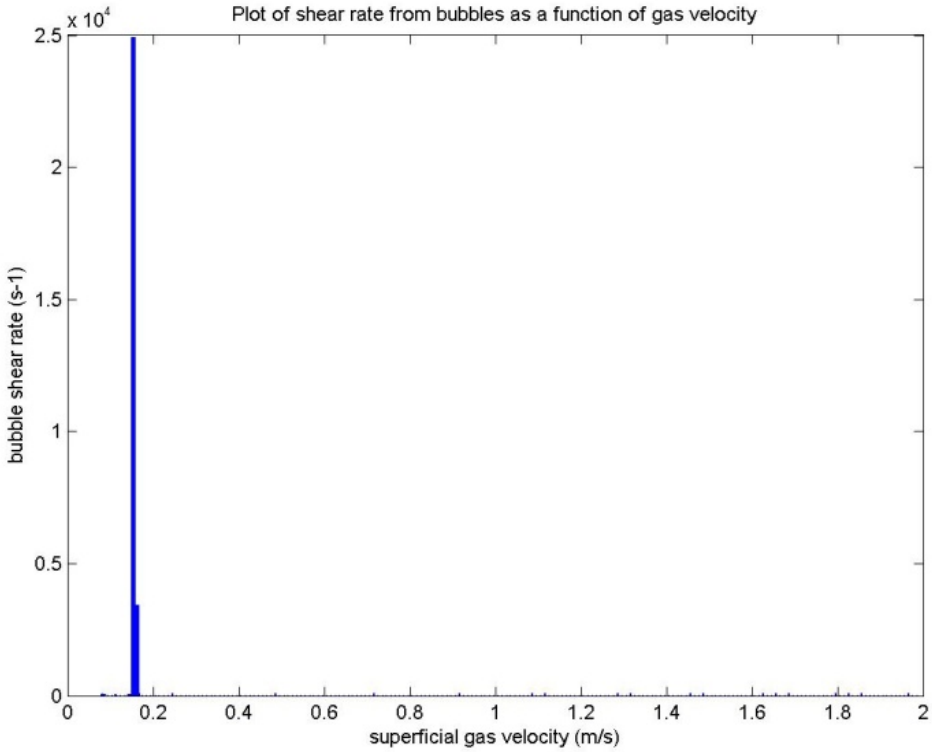

Figure 37: Bubble shear rate as a function of superficial gas velocity (culture density 4-27 g/L).

Optimal conditions are attained when the flow is heterogeneous and circulation time is independent of gas velocity. The model is analyzed for gas velocity when the interfacial area reaches a near constant, which value is dependent on the geometry. The results in Figure (39) with a smaller volume reveal more precisely than Figure (38) with a larger volume the gas velocities which produce a nearly constant interfacial area.

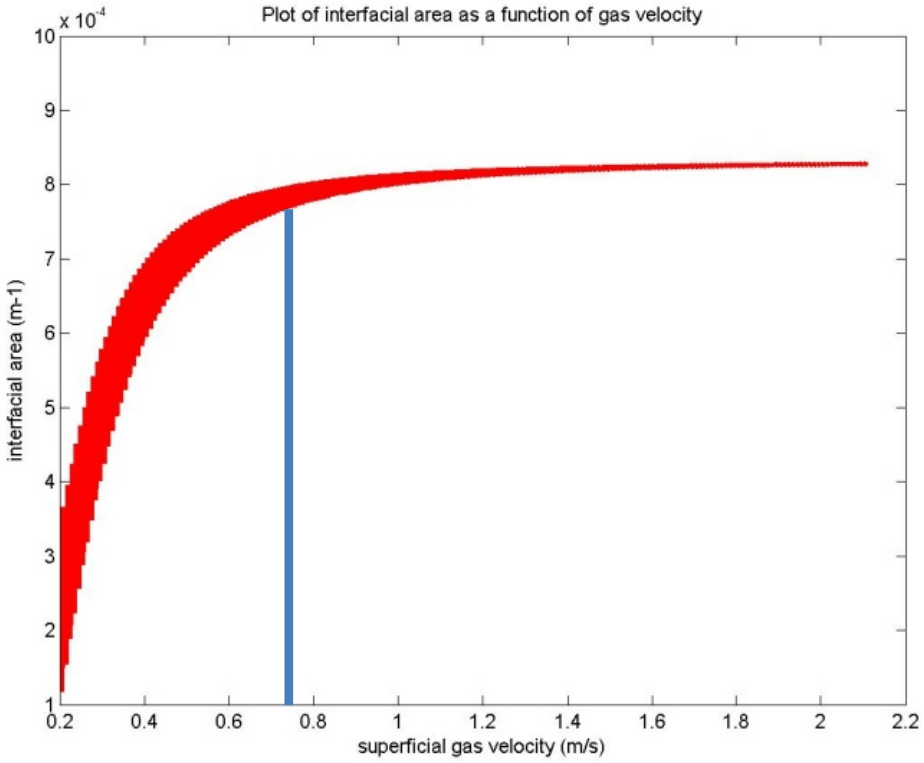

Figure 38: Interfacial area as a function of superficial gas velocity in 785 L volume.

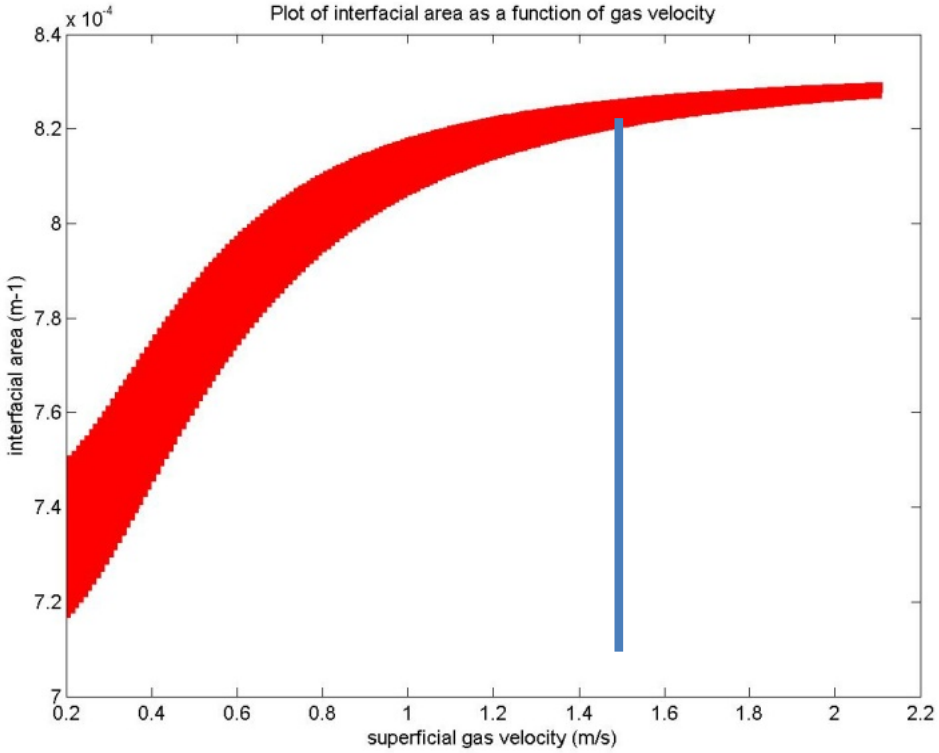

Figure 39: Interfacial area as a function of superficial gas velocity in 100 L volume.

Through combining shear stress, heterogeneous flow, and interfacial area, optimal growth conditions become apparent. The model is modified to set to maintain shear rate between 7,000 and 8,000 s^{-1} (shear stress of 7 - 9 Pa) for the following results and optimizations.

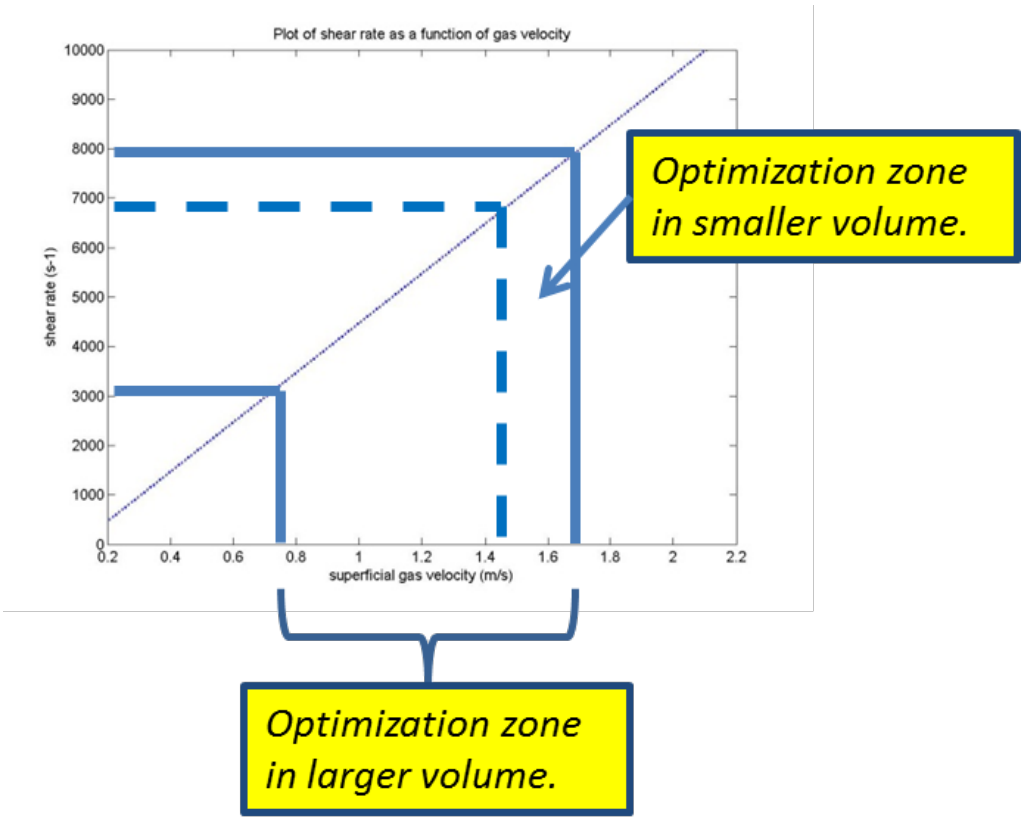

Figure 40: Optimization zone for fluid properties based on shear rate, shear stress, heterogeneous flow, and interfacial area.

Results concur with studies which state that the heterogeneous flow regime where circulation time is independent of velocity contains optimal characteristics for culture growth (Schumpe & Deckwar, 1987) (Doran, 1993). The results also reveal it is possible to model the ALR flow dynamics using known equations in order to determine input parameter values which result in optimal flow conditions for algal growth.

ALR Geometry and Pond Depth

As presented previously, the model determines the maximum length for the volume of algae so the amount of dissolved oxygen does not exceed 0.028 g/L. The pond depth and culture density are based on the light path length, since density is low enough

in open ponds that the light path length will limit algal growth long before oxygen saturation occurs. Even at maximum density in the model for ponds of 16.99 g/L at minimum depth of 19.62 cm, there will be 0.002 g/L oxygen generated for every minute of growth. Therefore the light path length is dominant for determining pond depth which means calculation of oxygen generated is for information only, and does not affect the design.

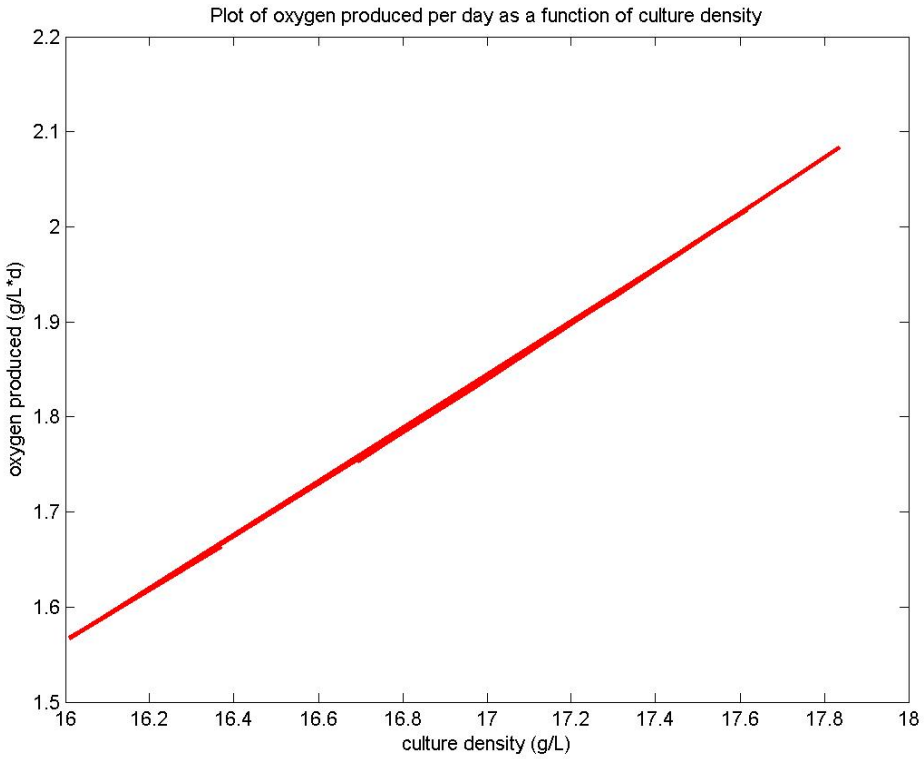

Figure 41: Amount of oxygen produced per day as a function of open pond culture density.

The volume of algae per length of ALR is dependent on both the algal density and the optimal ALR diameters, which are based on light path length.

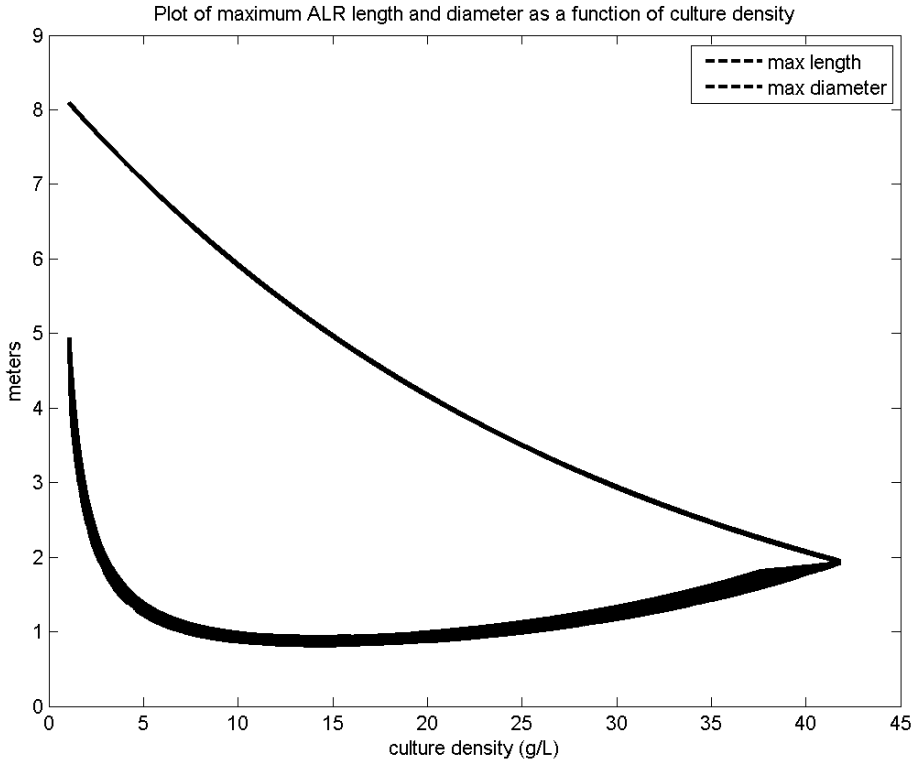

Figure 42: ALR geometry as function of culture density (bottom line is length and top line is diameter).

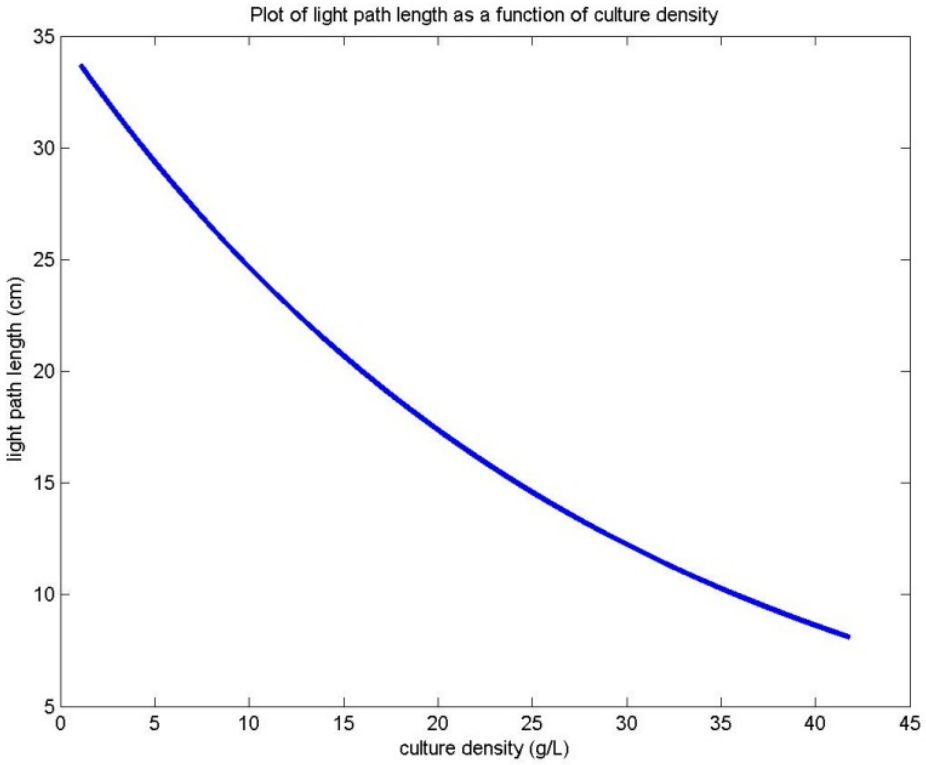

Figure 43: Light path length as a function of culture density.

As the culture density increases the diameter goes to 0 based on light path length, which causes the length to become unrealistic, but these high algal densities are not expected. Also, this length is not realistic since growth will be limited by temperature, acidic pH effects, and higher pressure and viscosity changes at depth. It is interesting that right about what will be found as optimal algal density (40 - 60 g/L) the length and diameter converge.

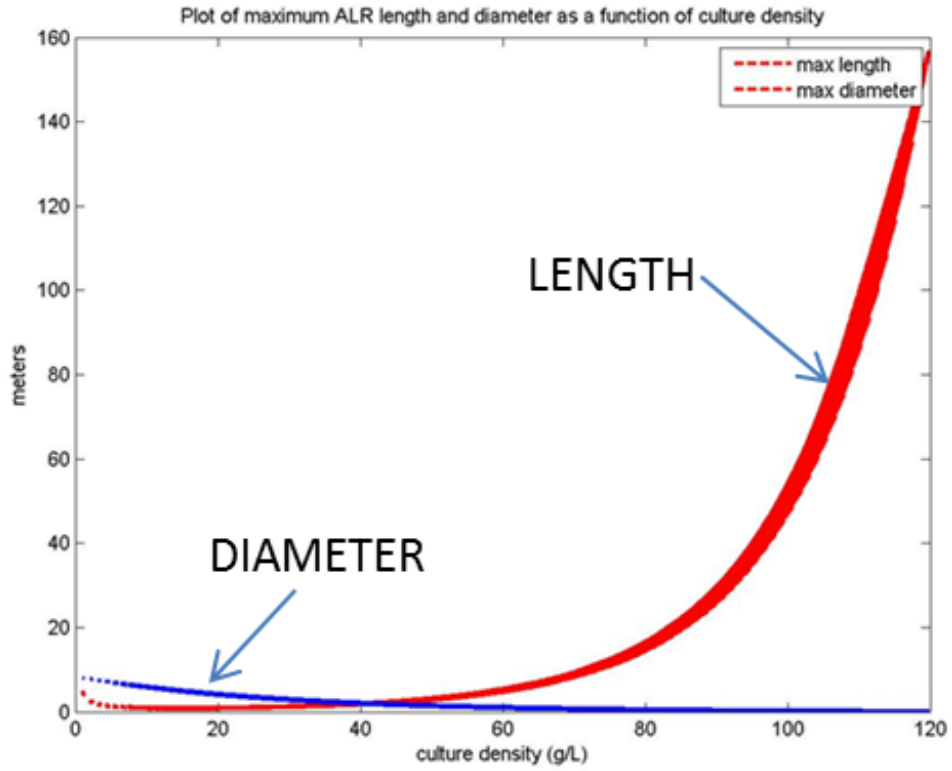

Figure 44: ALR geometry as function of culture density.

Nutrients

The results indicate there will be a wide range of nitrogen and CO_2 available depending on the power plant, but most certainly the nitrogen will be the limiting factor when no wastewater is available as an additional nitrogen source. A large algal facility would be necessary to consume the maximum amount of flue gas, and even then there will be a large amount of CO_2 which will not be consumed. The scenario represented in Figure (45) is representative of the PBR growth scenario required to consume all of the nitrogen from the flue gas of a 1000 MW power plant. The facility will cover 17 acres

and produce nearly 1,900 barrels of biodiesel per day. An open pond growth scenario with similar production and nitrogen consumed would require a facility of 9.4e9 acres.

Flue Gas Components/Algal Biomass Supported per MW			
CO2 kg/day	kg dry biomass/day	N kg/day	kg dry biomass/day
4121-5297	8080.4-10386	1.55-4.55	22.14-65

Table 8: Estimates of nitrogen and CO_2 available from coal power plant flue gas and algal biomass supported (Comanche station emissions, 2010, Xcel Energy).

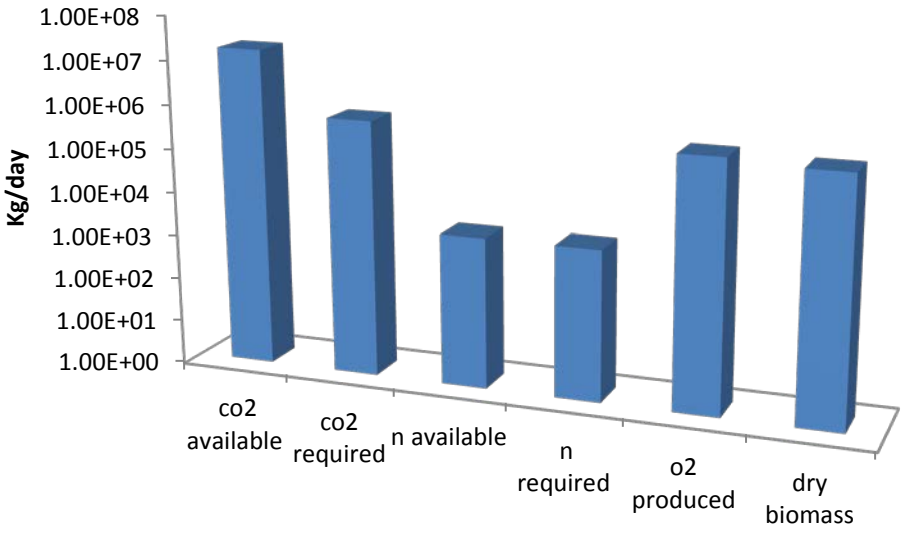

Figure 45: 1000 MW coal power plant/PBR (7.5e7 L, 3.38e5 kg dry biomass/day) growth scenario.

Nutrients which must be administered by the Liter of culture include salt, pH buffer and antibiotics. Open pond growth scenario nutrient costs for these items are very high due to the large volume and low culture density. Even with 80% of the salt recycled and the relatively cheap price of salt, it still remains the highest cost of all the nutrients. Also, even with the use of flue gas and wastewater or recycling biomass, all three of these

costs remain. The cost of salt could be alleviated through the use of brackish or seawater, or through growing a fresh water species.

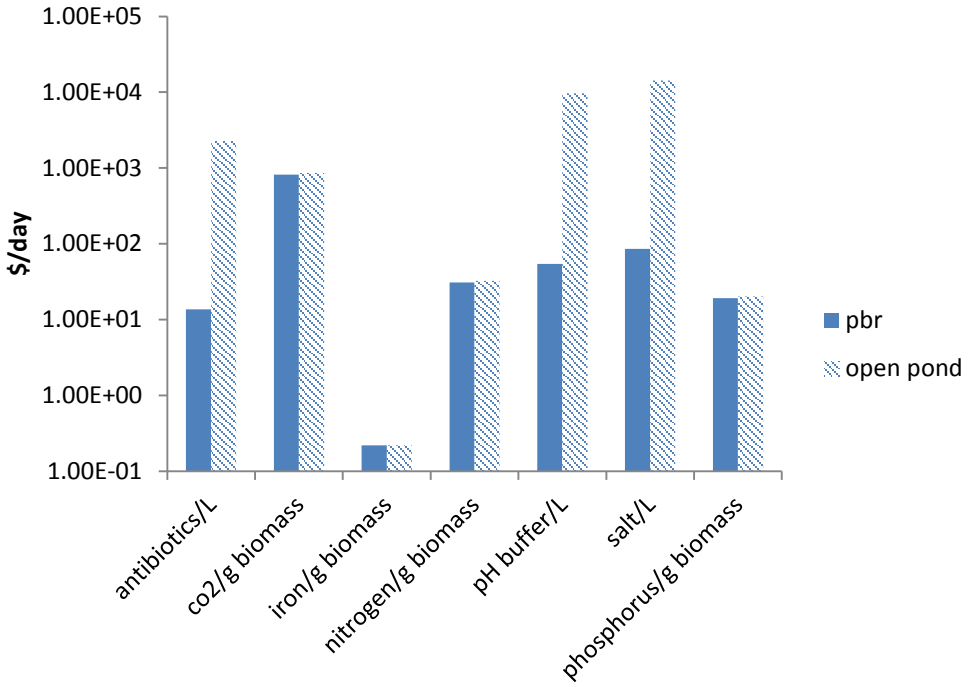

Figure 46: Nutrient costs per day for PBR and open pond growth scenarios sized to produce ~100,000 kg dry biomass per year.

Temperature

Results partially reveal why culture density is limited at 60 - 70 g/L, since temperature would be unmanageable, although the light limitation would slow the photosynthetic process, effectively limiting temperature increase. Through artificially increasing the culture density in the model it is verified the model is working correctly both with the increasing culture temperature and the decreasing cooling water temperature.

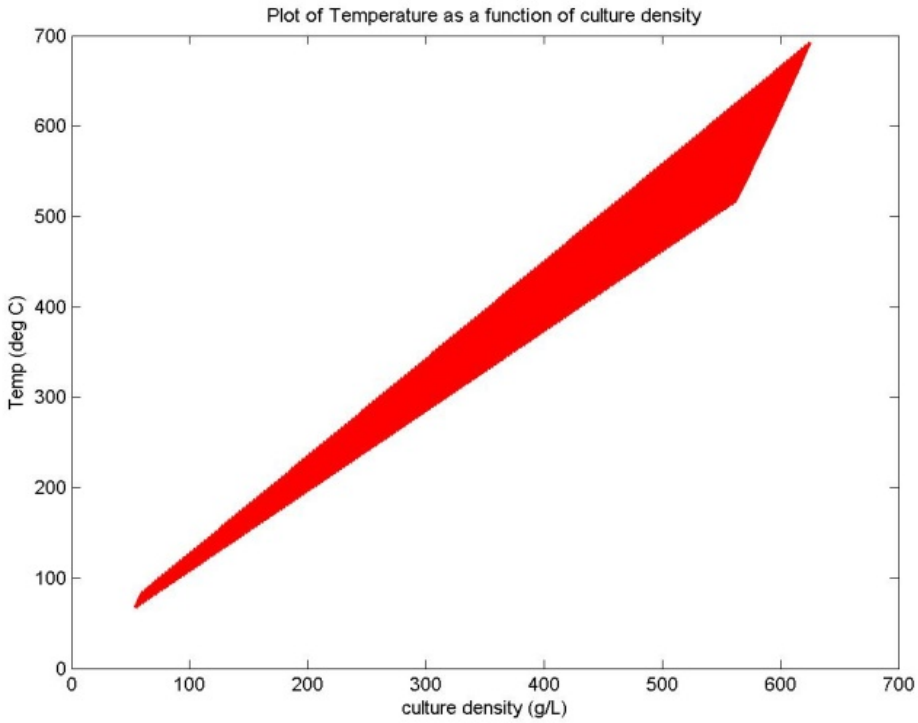

Figure 47: Temperature increase (from photosynthetic process only) vs. culture density at ultra-high culture densities.

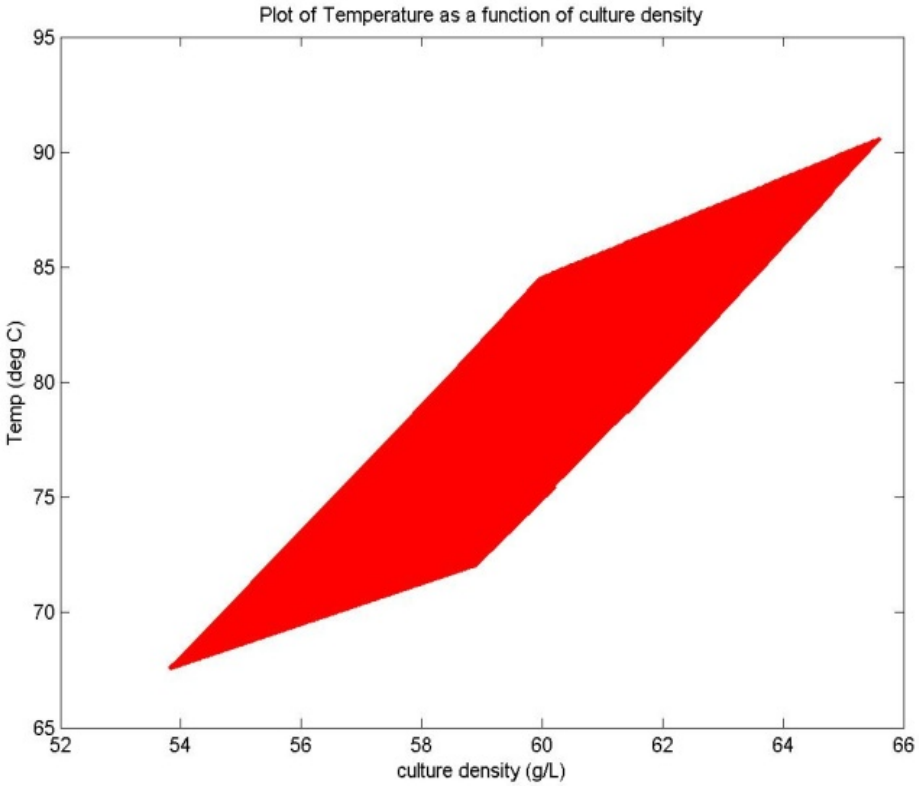

Figure 48: Temperature increase (from photosynthetic process only) vs. culture density at expected maximum culture densities.

Figure (47) shows the temperature increase when the culture density is increased beyond expected maximum, while Figure (48) displays the expected temperature increase at more realistic photobioreactor culture densities. Figure (49) below proves the required temperature of water to keep the culture density at 20ºC is manageable. The volume of water is calculated as the quantity required to replace the amount used in the photosynthetic process.

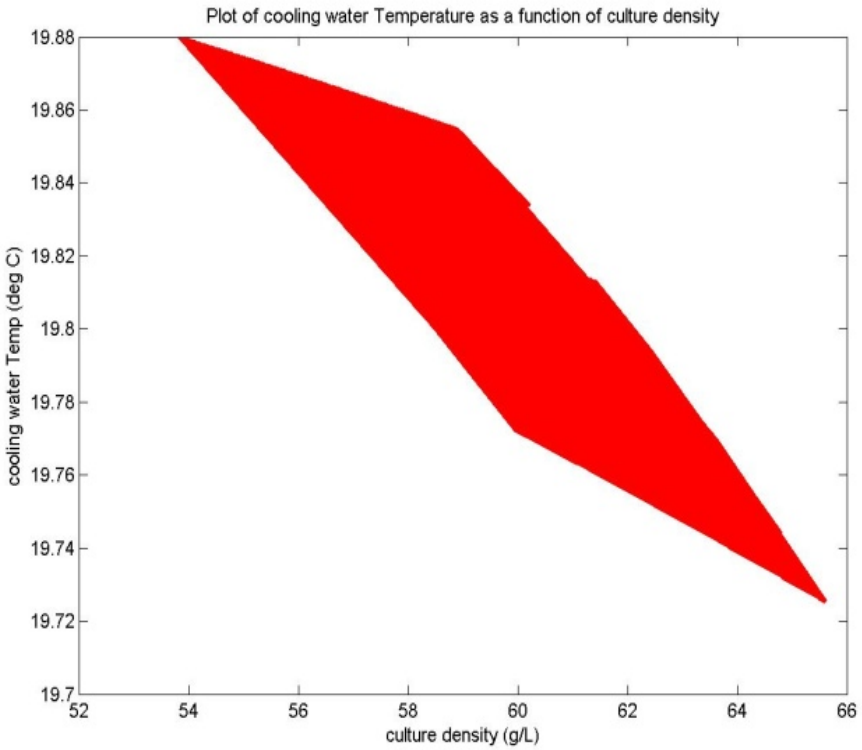

Figure 49: Cooling water temperature vs. culture density (water replaced for what is used in photosynthesis, to keep the culture at 20ºC).

Capital Costs

Despite claims that capital expenditure for photobioreactors is many times more than that of open ponds (Benemann, et al., 1982) (Sheehan, et al., 1998) (U.S. DOE, 2010), the results show otherwise. Model results for ~100,000 kg of biomass/year show capital costs for open pond growth scenario to be 19.23 times more than for a photobioreactor growth scenario. This is due to a much larger surface area and Liters of culture (with much lower culture density) required for an open pond scenario. Capital costs which are unique to ponds are the pond liner and paddlewheels. Cost items

common to both growth scenarios tend to be much more expensive for open ponds because of the large surface area and greater dilution of the culture.

In order for algal growth with biofuel production to be truly sustainable, it cannot compete with agriculture. Results show the required land for an open pond growth scenario is not environmentally or financially sustainable. If the U.S. government's goal of replacing 20% of transportation fuels with biofuels by the year 2030 were to be fulfilled through open pond algal growth alone, about 25% of the total U.S. land area would be covered in algae ponds (~6.25e8 acres). Land cost is the most significant contributor to open pond capital costs in an urban setting ($1.27e9), with installation costs ($9.40e7) being a close second and the primary cost in a rural scenario. Financing cost for a 100,000 kg of biomass per year open pond urban scenario is $150,000 per day and $14,500 per day for a rural scenario.

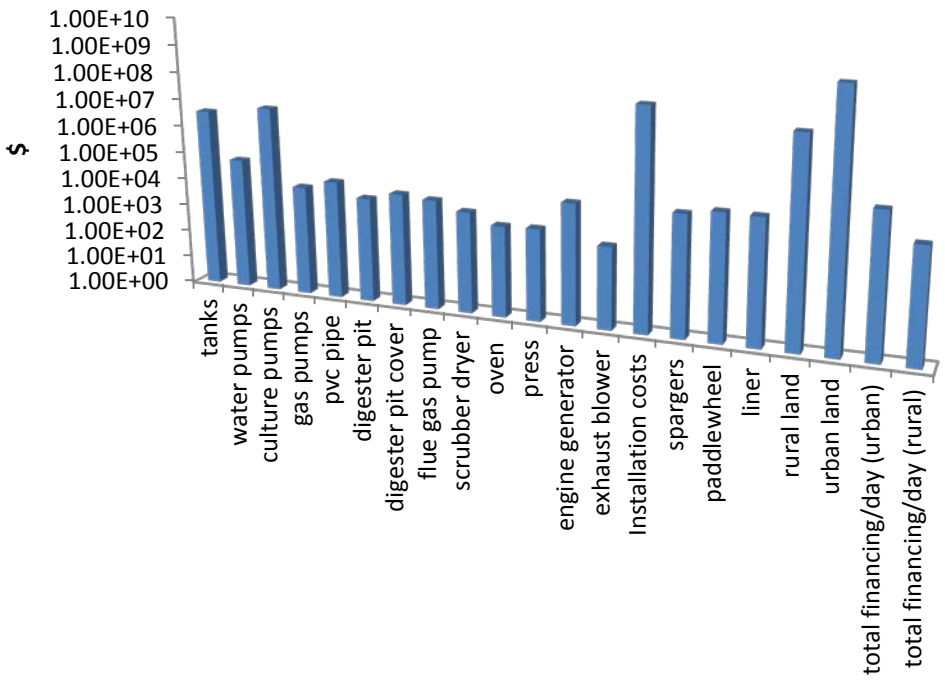

Figure 50: Capital costs for 100,000 kg biomass/year open pond growth scenario.

Capital costs unique to photobioreactors include acrylic or glass and the lighting. At expected size for the tanks (over 200 gallons), the cost of glass and acrylic are about the same. Glass is more likely to break or leak, but acrylic is easier to scratch and yellows under UV lighting. Acrylic is also easier to mold into usable shapes and is much lighter for shipping. The material cost is set high enough ($7.50/L) to provide for 2 - 3 replacements over the 15 year financing for capital costs set in the model. At a facility sized to produce 100,000 kg of biomass per year, the LED lighting capital cost is $6.51e7, while the capital cost for fluorescent lighting is $7.49e6. Financing cost for a 100,000 kg of biomass per year LED lighting urban scenario is $7,150 per day and $870 per day for a rural scenario.

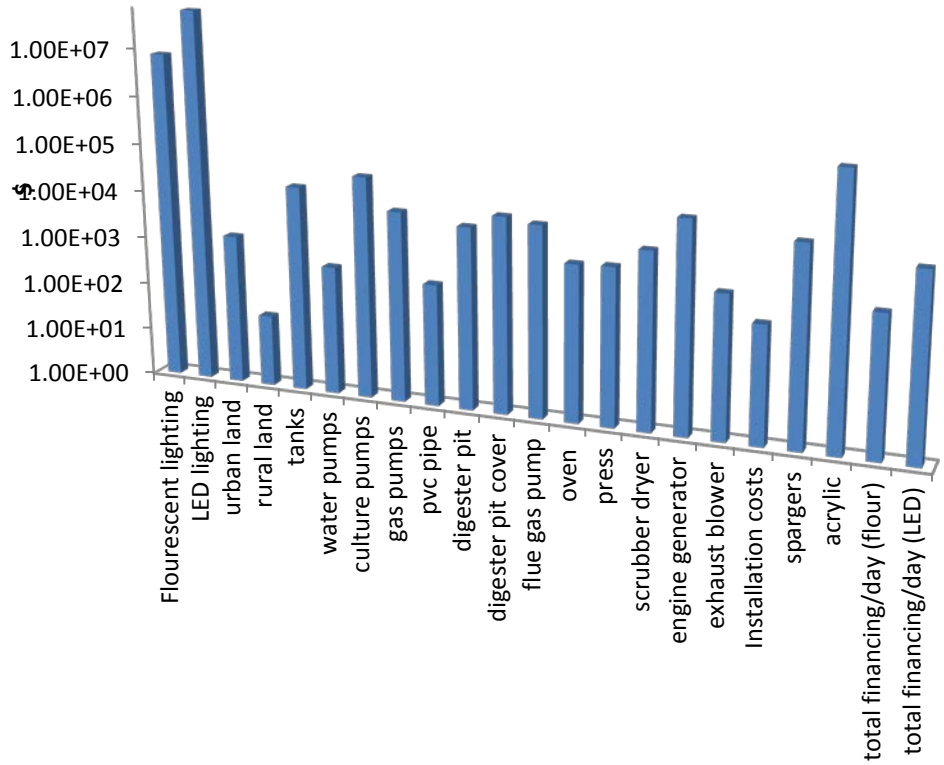

Figure 51: Capital costs for 100,000 kg biomass/year PBR growth scenario.

Table (9) shows a comparison of investment per acre between model results and that found in the literature. It becomes apparent why there is such a wide range of values when one considers how various growth scenarios differ in results and how variables not included in other techno-economic studies affect results (the studies used for comparison below are also included in Appendix B with variables included). Also, despite higher costs per acre, the PBR growth scenarios are more cost effective when considering the profit: cost ratio rather than the areal productivity.

Investment $/acre						
Model (ALR)	*Model (Solar PBR)*	*Model (Pond)*	*Richardson, et al (2010)*	*Lux Research (2012)*	*Putt (2007)*	*Shen (2008)*
7.30E+09	5.55E+09	196,272	42,774-77,095	81,704	13,897	266,640

Table 9: Investment per acre for different growth scenarios and comparison with the literature.

Harvesting Options

Costs for photobioreactors are commonly reported to be many times more than that of open ponds, but higher volume due to greater dilution in an open pond growth scenario reveal otherwise. The capital expenditure and operating expenses of photobioreactors can be designed to compete with and be less than open ponds from economical and energy perspectives. Production and cost data for various harvesting options in open ponds and PBR growth scenarios are shown in Figure (52).

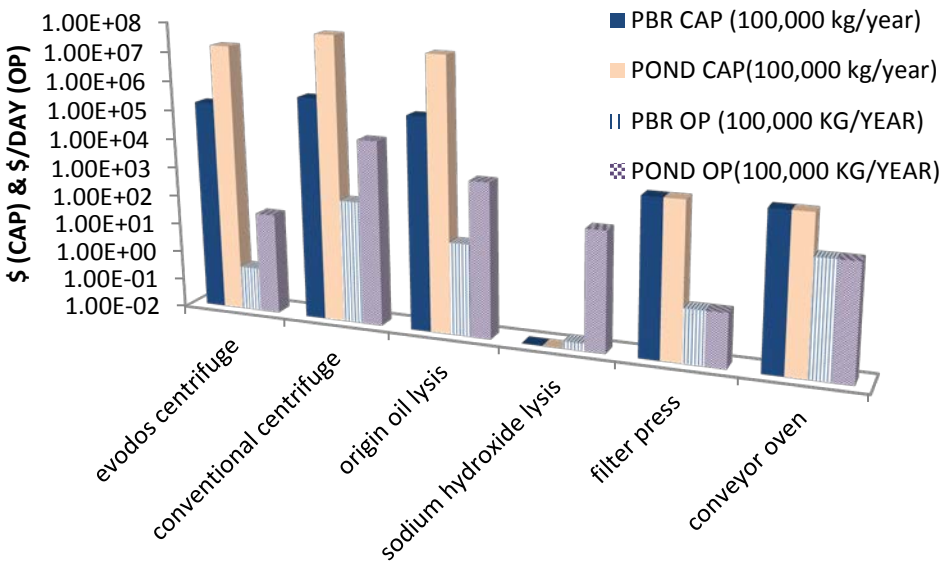

Figure 52: Cost comparison of various harvesting options.

Sodium hydroxide lysis is included for a cost comparison, and costs are minimal, but this method of lysing algal cells is unproven outside of the laboratory. Filter press and oven costs are minimal and similar for both growth scenarios since most of the culture medium is assumed to be recycled at this point in the process resulting in a similar culture concentration. While the Evodos centrifuge costs more per unit, it has higher capacity and lower operating costs than a traditional centrifuge. Despite claims in the literature, use of a centrifuge for ALR culture density is affordable, especially for an Evodos centrifuge. Origin Oil lysis uses electromagnetic impulse, but is 25% more expensive than an Evodos centrifuge and cost is dependent on the culture density similar to centrifuges (Origin Oil, 2012). The model results indicate financing harvest capital and operating costs contribute 1 - 5% toward the total cost (not including distribution pumping) (see Table 10), which is much lower than the 20 - 30% of total cost assumed in the literature (Verma, et al., 2009) (Hall, et al., 2003).

Operating Costs

The only costs for an open pond growth scenario which are manageable are replacing water other than that lost by evaporation and the cost of using supercritical CO_2 as a solvent. Each of the individual remaining costs surpasses daily profits without even considering their summation. The only PBR operating cost which surpasses daily profits on its own is the use of organic solvents, which can be avoided by using supercritical CO_2 as a solvent.

Replacing water lost to evaporation ($4.36e7 per day for a 100,000 kg biomass per year facility) is by far the most significant operating cost for an open pond growth

scenario. The cost of replacing water not including evaporation is minimal since the model assumes 90% of the media is recycled, which addresses health and safety concerns regarding disposal and reduces costs significantly. The cost of replacing water not including evaporation is calculated as 10% loss plus that used for photosynthesis for an open pond growth scenario ($341 per day for open pond 100,000 kg of biomass per year facility). The highest operating cost for the PBR growth scenario are organic solvents, if used ($24,100 per day for a 100,000 kg of biomass per year facility) followed by the gas pump power ($2,210 per day for a 100,000 kg of biomass per year facility).

Employees are a significant cost for open ponds because of the large surface area required. The model calculates 0.08 employees are required per hectare. Lighting is not a significant operating cost factor for a PBR growth scenario despite the high capital costs. Nutrients are a high cost factor for open ponds because of the items required per Liter, including the pH buffer, salt, and antibiotics. Water and gas pump and paddlewheel power are also significant cost factors for open ponds because of the increased distance involved with the large surface area and larger volume compared to the PBR growth scenario.

One key finding is the amount saved by using supercritical CO_2 as a solvent instead of traditional organic solvents (saves ~$25,000/day for 100,000 kg of biomass per year facility). The cost of the supercritical CO_2 includes only the energy cost of bringing the CO_2 to supercritical state since the CO_2 cost itself is minimal and may be fed back to the growing algae culture. The total cost of the organic solvents calculated by the model

includes the cost for the materials and energy costs calculated by Soh & Zimmerman (2011).

Water pump operating costs are calculated as 2 hours per day each for water and media for PBR's, and 8 hours/day each for open pond growth scenarios. Gas pump operating costs are calculated assuming they must be operating 24 hours per day since gas circulation is needed whenever light is present for algal growth, but also to maintain fluid dynamics necessary to distribute nutrients and to keep algae from settling and/or flocullating. The gas pump operating costs are higher for PBR's than open ponds ($1411 > $119) because the gas is being pumped into the culture at a greater depth requiring more power.

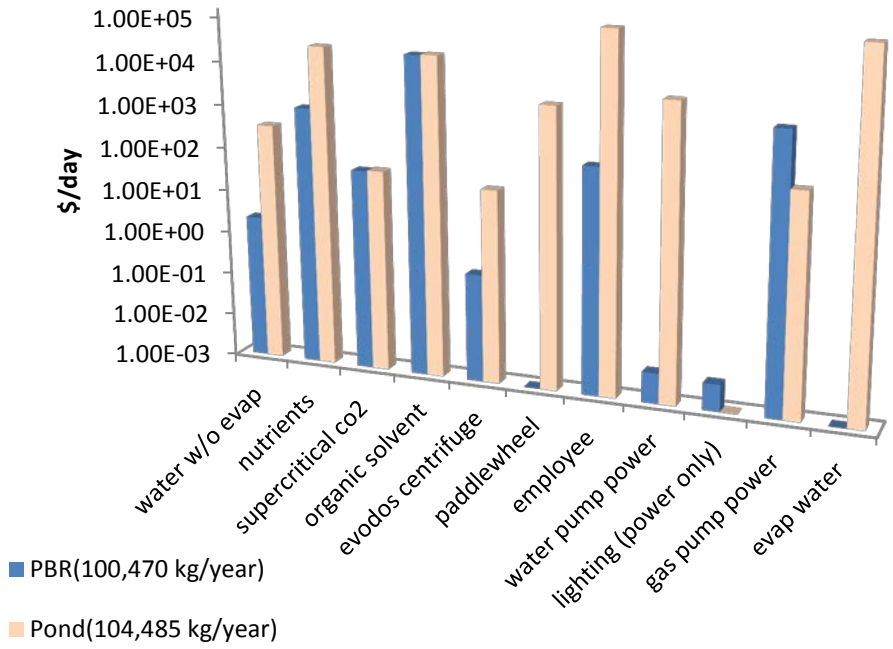

Figure 53: Operating costs per day for open pond and PBR growth scenarios producing approximately 100,000 kg dry biomass per year.

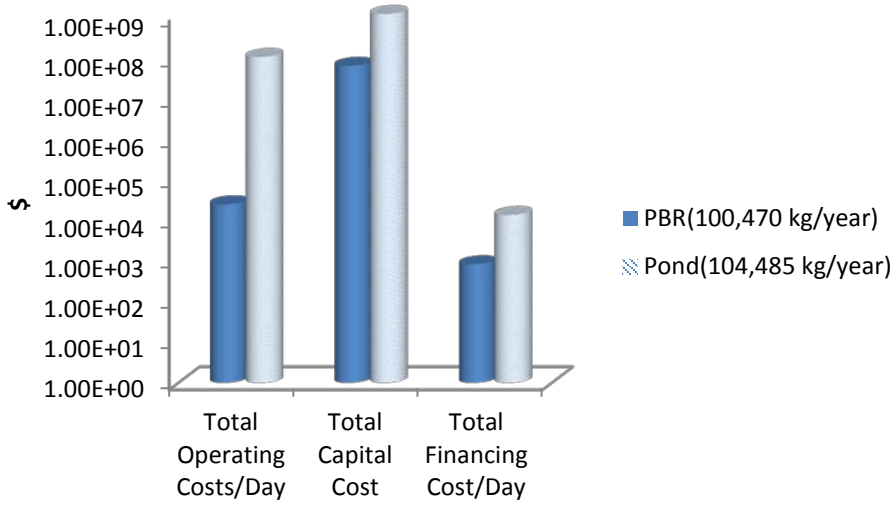

Figure 54: Comparison between capital and operating costs per day for open pond and PBR growth scenarios producing approximately 100,000 kg dry biomass per year.

End Products

Price for a barrel of biodiesel would need to be at least $10,313 to break even with the cost of production assuming no co-products in the most favorable algal growth scenario simulated with proven culture densities. EPA profit is significant enough to get close to a profitable scenario, but the only product which yields sufficient profit to counter the costs of the algal growth facility and cost required to harvest and produce end items for a PBR growth scenario is wastewater treatment.

Alibi, et al. (2009), found photobioreactors have a cost of $24.60 per liter of algal oil, with 63% of that cost from capital. Model results reveal the cost per Liter of oil is much higher for all growth scenarios, while capital cost is a smaller portion of total cost,

especially for an open pond growth scenario. For economic success, productivity of over 100 tons per hectare per year is needed according to one report (Pedroni & Benemann, 2003). However, assuming this study is referring to dry weight biomass, even at approximately 16,000 tons of biomass/hectare per year, the scenario closest to showing a net profit (the artificially illuminated PBR) remains economically unsustainable. Results are more positive for the solar illuminated PBR's when wastewater is included since the culture density allows for greater volume and more Liters of wastewater to be treated per algal biomass yield.

Variable	Artificially lit ALR	Solar lit PBR	Raceway ponds
Profit per day	$8,613.37	$8,698.77	$8,406.42
Costs per day	$10313 (FLUOR)$11092(LED)	$18,376.50	$7,184,000.00
% of cost from financing capital	39%(FLUOR)43%(LED)	21%	8%
Acres	0.02	0.23	6,601.30
kg biomass/year per acre	5,882,352.94	434,782.61	15.15
Cost per hectare	$39,686.00	$197,766.90	$2,693.74
Cost per Liter of oil	$91.04(FLUOR)$96.89(LED)	$160.53	$64,783.05
Cost per kg of biomass	$37.64(FLUOR)$40.49(LED)	$67.07	$26,221.60
Nutrient cost per day	$1,057.00	$4,562.25	$25,618.00
Nutrient cost per kg biomass	$3.86	$16.65	$93.51
Harvesting cost per day	$65.70	$658.28	$1,872.57
Harvesting % of total costs/day	1%	3.58%	0.03%
Biodiesel barrels per day	0.95	0.96	0.93
Biodiesel barrels/acre per year	20,397.06	1,523.48	0.05
Biodiesel profit per day	$130.51	$131.23	$127.08
Animal feed profit per day	$40.31	$41.15	$39.70
CO2 credit profit per day	$11.94	$11.94	$11.94
EPA profit per day	$8,442.55	$8,514.45	$8,227.70
Net profit per day	-$1687.6(FLUOR)-$2466(LED)	-$9,677.73	-$7,175,593.58
Net profit per day w/WWTP	$7618(FLUOR)$6840(LED)	$42,460.23	-$5,977,974.08

Table 10: Cost and profit comparisons for three different growth scenarios.

Table (10) contains the mean of the model results where each algal growth scenario is sized to produce approximately 100,000 kg of dry biomass per year, which explains why the products have similar profits and yields. Assumed algal densities are 40 - 50 g/L for artificially illuminated ALR's, around 1 g/L for solar illuminated PBR's, and

0.33 g/L for open ponds. Lipid content is an optimistic average of 46% of algal biomass for all three growth scenarios. The nutrient cost for salt, pH buffer and antibiotics are per Liter of culture, which explains the rise in costs for solar illuminated PBR's and open pond growth scenarios. The harvesting scenario is the same for all three growth scenarios and includes the Evodos centrifuge, filter press, supercritical CO_2, and a rural location. Harvesting costs increase as the culture density decreases and volume of media increases.

Wastewater Treatment

The profit from wastewater treatment increases as the volume of water increases from artificially illuminated to solar illuminated PBR's since the nitrogen and phosphorus removal is accomplished by a minimum culture density of 0.53 g/L. Nonetheless, integration with water treatment facilities shows the most potential of any of the available co-products.

Municipal Wastewater Nutrients/Algal Biomass Supported					
N mg/L	mg bm	P mg/L	mg bm	C mg/L	mg bm
26.4	377.1	5.3	530	159.3	312.4

Table 11: Algal biomass supported by municipal wastewater nutrients (mg of biomass).

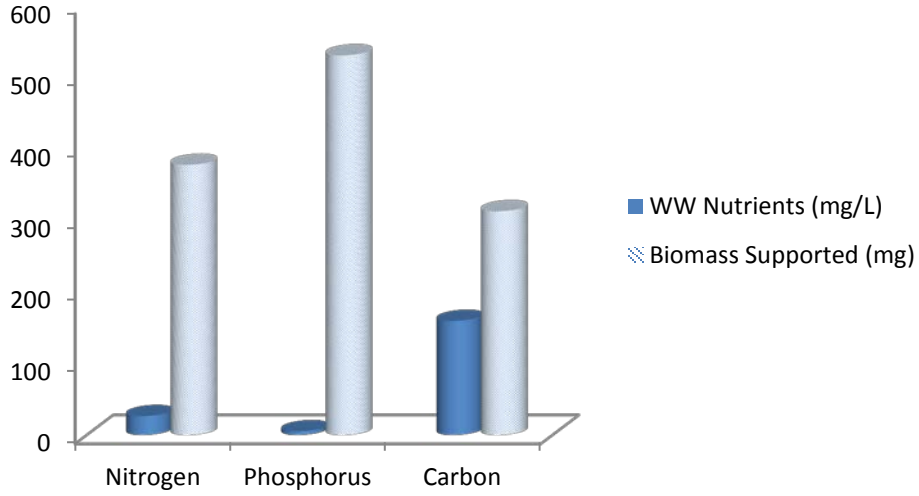

Figure 55: Algal biomass supported by municipal wastewater nutrients.

All bioavailable nitrogen and phosphorus would be removed in a PBR scenario, both solar and artificially illuminated, while it is likely at least 10 mg/L nitrogen and 160 mg/L phosphorus would be remaining in an open pond scenario due to lower culture density (at assumed density of 0.33 g/L). Photobioreactors are also advantageous over open ponds for wastewater treatment since water would not be lost to evaporation, and more control of the effluent is enabled. However, the time required for the algal culture to achieve the same treatment efficiencies of the traditional activated sludge process is 3 - 4 days compared to 4 - 6 hours for the traditional process (Wang, et al., 2010). It is important to bear in mind that additional BNR (biological nutrient removal) may be necessary if nutrients are in excess of what is used by the algae. Effluent from the algal culture will require treatment, but incorporating microalgal growth may remove the need for additional BNR.

Methane

Methane yield in Joules as a function of dry weight biomass yield without considering conversion to electricity using microturbines is shown in Figure (56).

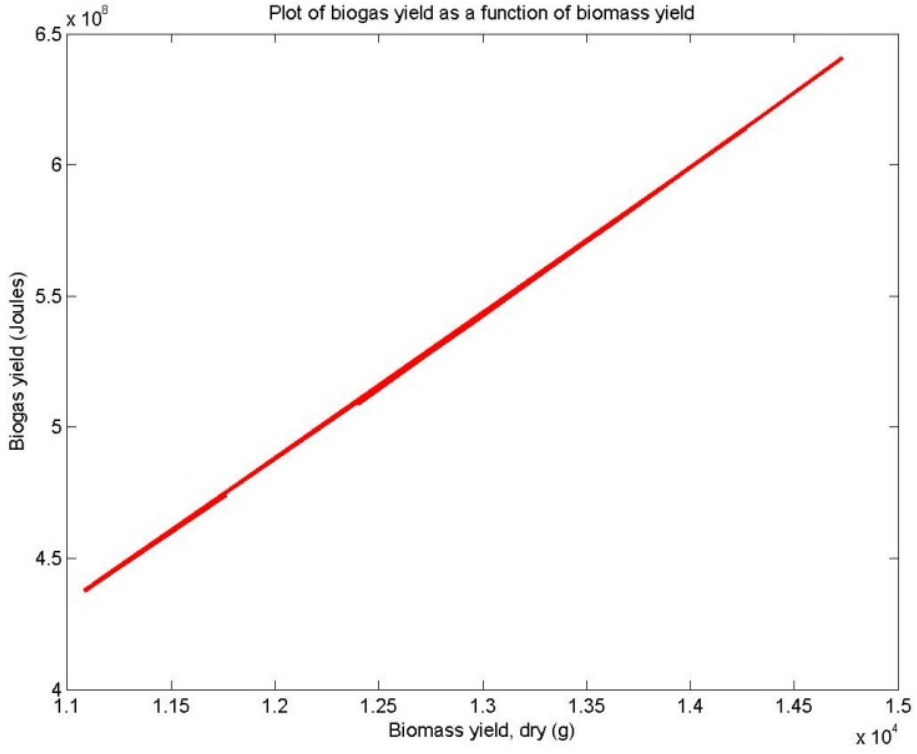

Figure 56: Biogas yield as a function of biomass yield.

Approximately 39,000 – 45,000 Joules of biogas can be produced from each gram of dry weight biomass after lipids are removed. When the dry weight biomass yield is 10 – 15 kg per day, the profit from biogas is approximately $13 - $19 per day when considering no loss in converting Joules to Watts. However, when adding the conversion to electricity the results are somewhat disappointing. The cost of financing the micro-turbines (approximately $30,000/day for a 100,000 kg/year facility) is greater than the profit from the electricity produced (nearly $100/day for a 100,000 kg/year facility).

Biodiesel

Tables (12) and (13) show there is wide disparity in fuel yields per acre depending on the study and growth scenario chosen, which is why areal productivity results can be misleading. The results for gallons per acre per year differ widely with Chisti (2007) claiming yields of 1000 - 6500 gallons per acre per year and Vasudevan et al. (2012) claiming 950 - 8100 gallons per acre per year. ANL;NREL;PNNL (2012) adjusted the expected gallons per acre per year to between 1000 and 1500.

Production gallons of fuel/acre/year					
Model (ALR)	*Model (Solar PBR)*	*Model (Pond)*	*Richardson, et al (2010)*	*Lux Research (2012)*	*Putt (2007)*
1080765	421.45	0.0365	834390-1663305	17549	1.78

Table 12: Gallons of fuel/acre/year from model and various algal studies.

CROP	OIL YIELD (GALLONS/ACRE/YR)
Soybean	48
Camelina	62
Sunflower	102
Jatropha	202
Oil palm	635
Algae	1,000-6,500[b]

[a] *Adapted from Chisti (2007)*
[b] *Estimated yields, this report*

(*DOE National Algal Biofuels Technology Roadmap, 2010)*

Table 13: Biofuel gallons of fuel/acre/year for various crops.

Model results reveal profit from biodiesel to be only $0.40 - $0.50/kg of dry weight biomass yield at the current rate of $120 - $150 per barrel of oil. The algal facility cannot compete with the price for petro-diesel, even at maximum productivity.

The most optimistic cost of producing biodiesel from microalgae is $10,313 per barrel ($245.55 gallon^{-1}).

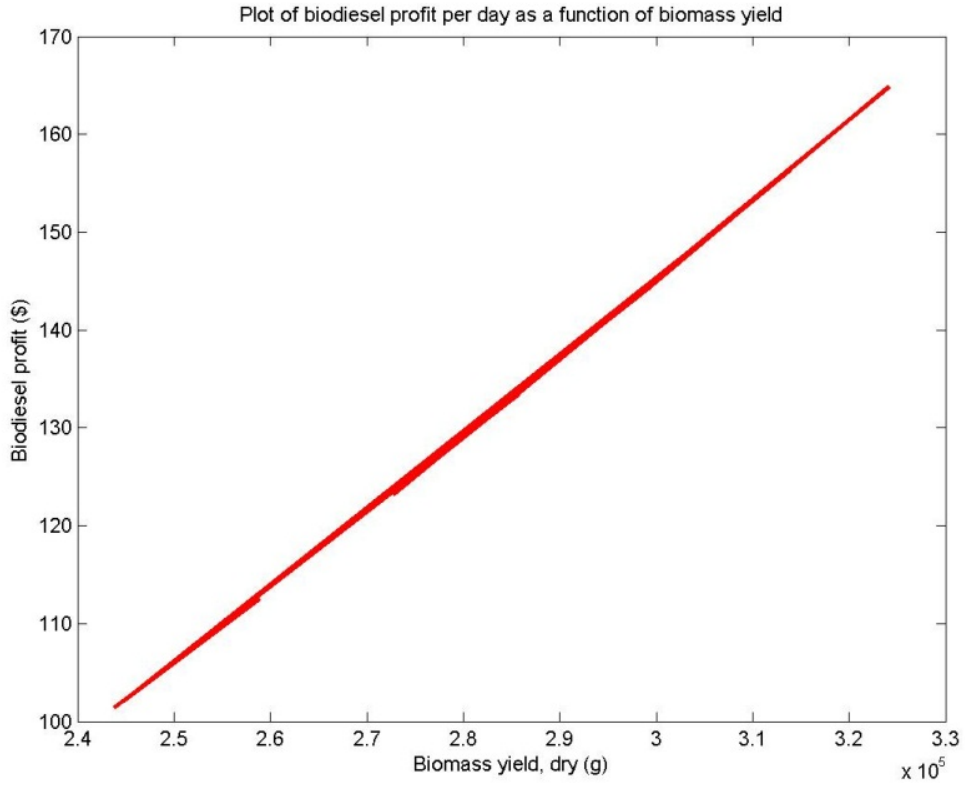

Figure 57: Biodiesel profit per day as a function of dry biomass yield per day.

The cost of transesterification is approximately $25 per barrel of oil, so it represents 16 - 25% of biodiesel profit, but it contributes at most 0.2% to the algal facility overall costs.

Human supplements

The co-products which show the most potential of enabling a profitable biofuel production from algal growth facility are wastewater treatment and human supplements

(EPA, Carotenoids, beta-carotene and astaxanthin). However, as shown in Table (14), the worldwide market for human supplements is quickly saturated with minimal biodiesel production. Even when meeting all the market demand for human supplements, the biodiesel yield remains a small percentage (at best 0.05%) of what is consumed in the U.S. every day.

Supplement	Worldwide Market/year	% of total market*	Biodiesel yield **	Acres(pond)***	Acres(PBR)***
EPA/DHA omega 3	$34,700,000,000.00	0.01	10000	3.033 billion	135.80
Beta-carotene	$285,000,000.00	.016-6.5	15.38-6250	4.6 - 188 million	.2-84.87
Astaxanthin	$255,000,000.00	3	33.3	10 million	0.45

*~100,000 kg/year algal facility
**barrels/day at supplement market saturation, 18.96 million barrels consumed in US per day
***US total land area is 2.3 billion acres

Table 14: Worldwide market for human supplements vs. algae biodiesel yield and acres required. (Worldwide Market for Human Supplements Source: BCC Research, Inc, 2012).

Carbon Credits

Carbon credits only contribute approximately $12 per day in profits for a 100,000 kg dry biomass per year facility. Even at $50 per ton predicted by 2030, the profits remain minimal at approximately $30 per day.

Animal Feed

Animal feed profit is minimal at approximately $40 per day for a 100,000 kg dry biomass/year facility, but offers more potential than methane with no required conversion or processing. No transportation costs are included in the model and the market could be quickly saturated, so this value may be more optimistic than is warranted.

Life-Cycle Costs

Life-cycle costs are the total cost to the organization for the ownership and acquisition of the product over its full life. They include the cost of research and development, production, operation, support, and in some cases, disposal. The analysis contained in this paper is a steady-state estimate, assumes all research and development is complete at the time of production, and does not include all overhead costs such as executive salaries or holiday/vacation pay. Fabrication and assembly cost is calculated by acre, has few spare parts, assumes no training is required for the employees, and does not calculate disposal costs for used materials. As such, the costs for a real world scenario would likely be higher than what is computed here by as much as 15%.

Carbon Emissions & Energy Balance

Even if algal growth utilizes waste streams and under-utilized resources, it still presents an environmental profile far inferior to fossil fuels. Operating costs for the growth scenarios are calculated as 140.525 kilograms of CO_2 produced per year for every kWh operating cost. No carbon emissions resulting from materials have been included except for nutrients. Carbon emission results from the model reveal algal growth facilities produce at least thirteen times more carbon emissions than petro-diesel per MJ even when energy contributions from methane and carbon consumption from flue gas are included. Table (15) is presented as a conventional harvesting scenario using filter, oven and supercritical CO_2 as a solvent. PBR column applies to artificially and solar illuminated photobioreactors. Carbon emissions per year resulting from using the

lighting is less than one gram for LED lighting and some 60,000 grams for fluorescent lighting.

The energy put into the process is at least ten times more than the energy harvested from biodiesel and methane combined (MJ_{in}/MJ_{out}). Also, the open pond growth scenario produces nearly two times more carbon emissions than photobioreactors. The cost per ton of CO_2 captured far exceeds the DOE's goal of carbon sequestration costs below $10 per ton, or even the current costs for carbon sequestration of $35 to $264 per ton of CO_2.

Carbon emissions & energy balance at a ~100,000 kg biomass/year facility		
VARIABLE	PBR	POND
MJ in/Mj out	1.09E+01	5.49E+01
g of co2 produced by algal facility	6.78E+09	1.19E+10
g of co2 consumed/year from power plant	2.40E+08	2.09E+08
tons of co2 consumed/year from power plant	2.64E+02	2.30E+02
cost/ton of co2 "captured"	1.43E+04	1.54E+08
Total CO2 Emissions in grams	6.54E+09	1.17E+10
Barrels Biodiesel produced/year	3.43E+02	3.40E+02
MJ biodiesel produced/year	1.55E+06	1.51E+06
g of CO2/MJ biodiesel	4.22E+03	7.76E+03
MJ methane produced/year	4.25E+06	4.25E+06
g of CO2/MJ methane	1.54E+03	2.76E+03
g of CO2/MJ biodiesel + methane	1.13E+03	2.03E+03
g of CO2/MJ petro-diesel	8.60E+01	

Table 15: Overall carbon emission results compared to petro-diesel.

Additionally, the energy contained in methane must be converted to electricity or burned directly to fuel the algal or neighboring power plant, and micro-turbines have an

efficiency of only 27%, which will affect the MJ_{out} value from the methane not included in the calculation in Table (15).

The carbon capture cost of around $14,258.00 per ton for a PBR growth scenario and $154,222,422.79 per ton for an open pond growth scenario far exceeds that predicted by Alabi, et al. (2009), of $793 per ton. Additionally, the capture process is incomplete since when the fuel is used the same carbon will be released into the atmosphere. Table (16) contains more detail on contributing processes to the carbon emission operating cost total contained in Table (15), as well as the carbon emission operating costs for the centrifuge, organic solvents and lysis.

g of CO2 produced per year at a ~100,000 kg biomass/year facility		
VARIABLE	PBR	POND
Organic solvents	2.85E+08	2.89E+08
Supercritical CO2	6.00E+07	6.08E+07
Lysis power	1.92E+07	2.45E+09
Nutrients	2.30E+08	1.16E+09
Transesterification	3.37E+06	3.51E+06
Lighting power (FLUOR)	6.46E+04	N/A
Gas pump power	6.43E+09	1.53E+08
Water/Media pump power	2.80E+03	6.65E+09
Oven power	1.10E+08	1.10E+08
Centrifuge power	4.00E+05	3.89E+07
Paddlewheel power	N/A	3.80E+09

Table 16: Comparison of operating carbon emissions involved in algal growth processes.

Sensitivity Analysis

Each of the input variables shown in Tables (17) and (18) was manipulated to verify changes resulting from selection of initial and final values resulting from the delta

between X_i and X_{i-1}. However, there are input variables which have only two choices, so the values for X were either 0 or 1 with the exception of diffusion or sparging which is either 1 or 2 (reasons for this are detailed in Lighting/Absorption Efficiency section). These input variables include choice in lighting and gas delivery for PBR/ALR growth scenarios; and whether wastewater treatment is included or not, and the harvesting options of filter press, centrifuge, lysis, organic solvents or supercritical CO_2, and conveyor oven for all growth scenarios. Those variables use the value 0 for not incorporating the variable in the run and 1 for adding the variable into the run (or 1 for sparging and 2 for diffusion). When the results were as expected and either a yes or no, the test runs were limited to one or two.

Results for the remaining input variables were compared over several runs with different selections for a single variable, especially when sensitivity was found to be > 0.10 or the results seemed surprising. Results in Tables (17) and (18) show one sample of values used for X_i and X_{i-1}, but the resulting sensitivity was equivalent for any of the input values. Sensitivity values did not show any results tied to selection location or the selection of input variable value. Using the average, maximum or minimum net profit for Y also showed no impact on the resulting sensitivity, as long as the same selection of average, maximum or minimum was used for both Y_i and Y_{i-1}. The variable row represents the X values, and the net profit row represents the Y values.

Sensitivity results indicate the economic viability of an algal growth scenario is most strongly tied to the parameters shown in Figure (51), where only factors with $S \geq$ +/- 0.10 in one or both growth scenarios are included (input variables for which $S <$ +/-

0.10 include gas bubble diameter, gas velocity, filter press, traditional or Evodos centrifuge, lysis, conveyor oven, gas delivery through diffusion or sparging, flow velocity in pipes, and pipe diameter). One variable had sensitivity value of zero for both growth scenarios, which was the gas bubble diameter. This is expected since it does not have an influence on sparger costs, nor increase the growth rate in the model.

PBR/ALR	Runs	X_i and Y_i	X_{i-1} and Y_{i-1}	Normalization	S (PBR)
culture density	5	35	60	0.416666667	-1.55829
net profit		10250	6214.8	-0.649288794	
number of pbrs/ponds	4	70	71	0.014084507	1.021365
net profit		8077.9	8195.8	0.014385417	
lipid content	2	0.46	0.24	-0.916666667	0.747717
net profit		8195.8	4862.8	-0.685407584	
volume of pbr/pond	3	785	800	0.01875	1.036726
net profit		4862.8	4959.2	0.019438619	
bubble diameter	2	0.005	0.006	0.166666667	0
net profit		4960.7	4960.7	0	
run duration (days)	10	1	10	0.9	0.169996
net profit		1020300	1204600	0.152996845	
gas velocity	3	0.01	1.01	0.99009901	0.014735
net profit		2026.3	2056.3	0.014589311	
pipe diameter	3	0.1	0.5	0.8	-0.05584
net profit		1020300	976670	-0.044672202	
filter press	1	0	1	1	8.34E-05
net profit		3957.87	3958.2	8.33712E-05	
evodos (0) or traditional (1) centrifuge	2	0	1	1	-0.05029
net profit		1020300	9.71E+05	-0.050285655	
lysis	1	0	1	1	0.011915
net profit		3911.04	3958.2	0.011914507	
organic solvents (0) or sc co2 (1)	2	0	1	1	7.344247
net profit		-25111.8	3958.2	7.344247385	
conveyor oven	1	0	1	1	0.026585
net profit		3852.97	3958.2	0.026585317	
fluorescent lighting (0) or LED (1)	2	0	1	1	-0.46451
net profit		1135.2	775.14	-0.464509637	
Integration with wastewater	3	0	1	1	0.158082
net profit		4638.8	5509.8	0.158081963	
sparging (1) or diffusion (2)	2	1	2	0.5	0.081012
net profit		3958.2	4125.3	0.040506145	
cost of land (rural or urban)	2	2300	103000	0.977669903	-0.00031
net profit		4960.7	4959.2	-0.000302468	

Table 17: PBR/ALR sensitivity analysis results.

Open Pond	Runs	X_i and Y_i	X_{i-1} and Y_{i-1}	Normalization	S (pond)
culture density (w/o link to surface area)	5	3.00E-01	4.00E-01	0.25	-0.00472
net profit		-5001400	-4995500	-0.001181063	
culture density (with link to surface area)	2	0.3398	1.133	0.700088261	-0.03488
net profit		-1.40E+11	-1.43E+11	-2.44E-02	
number of pbrs/ponds	2	13	14	0.071428571	-0.97978
net profit		-99056	-106510	-0.069984039	
lipid content	2	0.46	0.24	-0.916666667	0.941436
net profit		-106510	-777350	-0.862983212	
volume of pbr/pond	3	700000	710000	0.014084507	-0.97954
net profit		-106510	-108000	-0.013796296	
bubble diameter	1	0.005	0.006	0.166666667	0
net profit		-1.40E+11	-1.40E+11	0	
run duration (days)	7	1	10	0.9	-0.00024
net profit		-1.40E+11	-1.40E+11	-0.000214577	
gas velocity	2	0.1	2	0.95	-0.04716
net profit		-142250	-136150	-0.044803526	
pipe diameter	2	0.1	0.5	0.8	0.00817
net profit		-1.40E+11	-1.41E+11	0.006535948	
pond depth (w/o link to surface area)	4	35	25	-0.4	0.496005
net profit		-108000	-90120	-0.19840213	
pond depth (with link to surface area)	2	34.59	33.64	-0.02824019	-0.8647
net profit		-1.40E+11	-1.43E+11	0.024419173	
flow velocity	10	0.1	1	0.9	-1.11041
net profit		-395034	-623403540	-0.999366327	
filter press	1	0	1	1	7.15E-05
net profit		-1.40E+11	-1.40E+11	7.15154E-05	
evodos (0) or traditional (1) centrifuge	2	0	1	1	7.15E-05
net profit		-1.40E+11	-1.40E+11	7.15103E-05	
conveyor oven	1	0	1	1	7.15E-05
net profit		-1.40E+11	-1.40E+11	7.15154E-05	
organic solvents (0) or sc co2 (1)	5	0	1	1	1.834355
net profit		-136150	163180	1.8343547	
lysis	1	0	1	1	-0.00071
net profit		-136247	-136150.3	-0.000710244	
Integration with wastewater	4	0	1	1	1.784634
net profit		-2721500	3468498	1.784633579	
cost of land (rural or urban)	3	2300	103000	0.977669903	0.59175
net profit		-108000	-256250	0.578536585	

Table 18: Open Pond sensitivity analysis results.

The results for run duration were difficult to interpret due to the fact that the run duration did increase net profits as the duration increased up to ten days, but any further increase after ten days had no influence on the net profit. The sensitivity of run duration for PBR/ALR growth scenarios is > 0.10 (0.17), so run duration is analyzed for impact in the PBR/ALR optimization. The resulting sensitivity for the first ten days is < 0.10 (and zero over ten days) for the open pond growth scenario, but it was still considered in the optimization. The open pond depth which was calculated prior to connecting the pond depth to the resulting surface area was only related to the light path length and the resulting culture density. The results indicate the shallower depth of 25 cm yields less loss than a depth of 35 cm since greater culture density results in higher profits. However, after connecting the culture density, light path length, pond depth, and surface area so that a change in one affects all the others, thus, reflecting reality, results show the greater depth results in higher profits because the cost of the land is a bigger factor than any profit derived from the algae itself. Also, it is interesting to note that after connecting the culture density and pond depth, the results from the same run indicate the sensitivity for pond depth is higher than for culture density (0.86 > 0.03), since the culture density must increase more for a corresponding increase in pond depth.

There are not any harvesting options which have a significant sensitivity except for using supercritical CO_2 as a solvent as opposed to traditional organic solvents, especially for PBR/ALR growth scenario since the harvesting options represent a higher percentage of overall costs in this growth scenario. Integration with wastewater has a higher sensitivity in an open pond growth scenario because a higher volume of water may

be treated resulting in higher profits than for a PBR/ALR growth scenario. (This fact is ignoring the open pond culture density will likely not accomplish complete BNR.) The PBR/ALR culture density shows a loss in average net profit when increased from 35 g/L to 60 g/L, which concurs with the optimization results. The pipe diameter shows a higher net loss as it increases because of the increasing cost of the pipe material in both growth scenarios.

It's also interesting to note the results for increasing the number of PBR's/ponds and increasing the corresponding volume of each has opposite effects on each growth scenario. Increasing facility size increases net profits for the PBR/ALR growth scenario while it decreases net profits for the open pond growth scenario. Also, in both growth scenarios the net profits are slightly improved by increasing the PBR/pond size rather than increasing the number of PBR's/ponds (only in relation to each other).

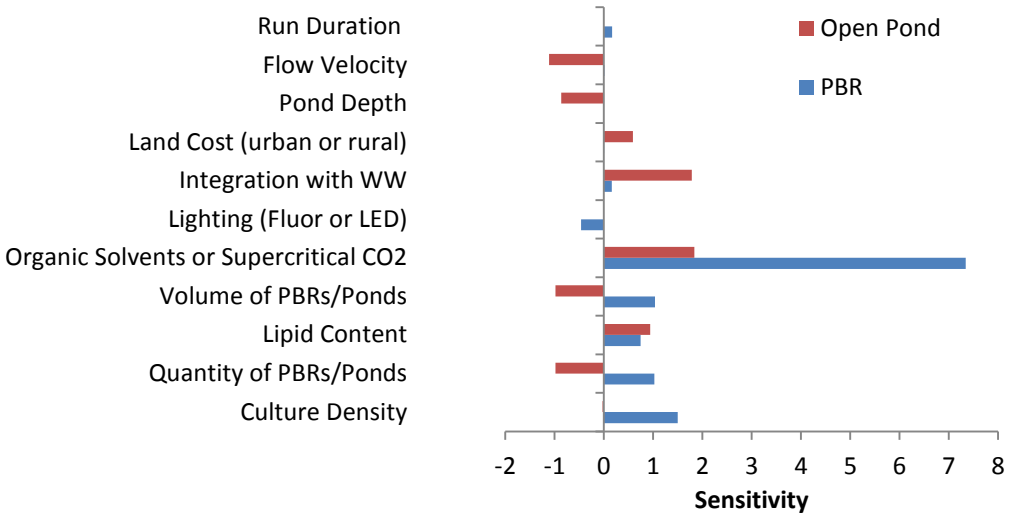

Figure 58: Sensitivity Analysis results summary for variables with sensitivity > +/- 0.10.

Integration with wastewater treatment, land cost, lighting choices for photobioreactors, and organic solvents or supercritical CO_2 used in harvesting operation all affect the outcome significantly but since they are on/off, it is not necessary to use an optimization tool to determine which choice is more cost effective. For example, it is more cost effective to integrate wastewater treatment, locate the facility in a rural area, choose fluorescent lighting for artificially illuminated ALR's, and use supercritical CO_2 as a solvent rather than organic solvents. The results of the optimization are analyzed for affects from including or not including wastewater treatment and choice in lighting. All optimization scenarios assume a rural location and supercritical CO_2 as a solvent rather than organic solvents.

Lipid content, pond/PBR quantity and volume, culture density for a PBR growth scenario, and PBR volume/pond depth are the variables which affect the profit margin to a significant extent and which may be optimized. Lipid content for all growth scenarios is optimized through choosing the algal species with the highest lipid content (*Nanno. s.* at 46%). *Botryococcus braunii* has the potential for the highest lipid content in the literature (see Table 2) at 75%. Comparisons are run in the optimization with 75% lipid content in an effort to improve the net profits.

Flow velocity is optimized by the model by maintaining flow conditions within results detailed in the results/small scale turbulence section for the artificially illuminated ALR growth scenario. The flow velocity for open ponds is set at 0.03 m/s since this is the maximum attainable velocity considering head loss as detailed in the results/large scale turbulence section.

Thus, the culture density as it relates to PBR geometry and pond depth (which are both related to culture density), and facility size and run duration when including financial analysis are the only variables necessary to optimize for a photobioreactor growth scenario. Since pond depth is dependent on light path length which is dependent on culture density, the only variable to optimize is inoculum density resulting in culture density for the open pond growth scenario. Similarly, since PBR volume is a function of light path length which is dependent on culture density, the optimal culture density will also result in the optimal PBR volume/geometry.

Optimization

This analysis met the requirements for a Class 4 Feasibility or Pre-Design Estimate, which means the cost accuracy goal is a range from -30% to +50%. Therefore, results could be 30% improved or 50% worse than predicted by the average net profit. Also, specific values for net profit in the text are averages of the results, where the figures demonstrate there is a larger potential for higher losses/lower profits than vice versa.

All of the optimizations include rural land cost and supercritical CO_2, oven, and filter press for harvesting options; as well as multiple end products including methane, biodiesel, human supplements such as EPA, and carbon credits. The effects of including wastewater treatment and different lighting choices for photobioreactors are included in the results. The tolerance on constraints for all scenarios is 1e-12, and the tolerance on convergence is 1e-14. Table (19) is a sample of optimization runs selected to demonstrate the range of values used and where the optimization found local or global minimum net costs or was constrained. The 'Final Cost' is the objective function, where

a negative value indicates a net profit. All three optimization methods were used with similar results.

The global minimum for open ponds is around an inoculum density of 5,000 cells/mL, which is a culture density of 5.7e-4 g/L for algae species *Nanno. s.* As the algal species is modified, the matching global minimum exists at the inoculum density which results in the equivalent culture density. (Results for *Tetraselmis* are around 12 cells/mL or 6.5e-4 g/L.). The PBR and ALR growth scenarios have a global net cost minimum at the maximum culture density allowed by the model, but the artificially illuminated ALR's also show a local minimum detailed in the sections to follow.

Growth Scen.	Global/Local	Run No.	Variable	X0 initial	X0 final	InitialCost	FinalCost	Minimum	Maximum
Fluorescent ALR - w/o wastewater	constraint max	1	L_total	7500	7500	203.9	-679.14	7500	7500
			inoculum_density	20000	6.50E+08			2000	6.50E+08
			lipid_content	0.75	0.75			0.75	0.75
	local	2	L_total	7500	7500	203.9	-469.64	7500	7500
			inoculum_density	20000	4.29E+08			2000	4.30E+08
			lipid_content	0.75	0.75			0.75	0.75
	constraint max	3	L_total	7500	1.00E+06	203.9	-88467	1	1.00E+06
			inoculum_density	5.00E+08	5.00E+08			2000	5.00E+08
			lipid_content	0.75	0.75			0.75	0.75
	constraint max	4	L_total	7500	7.50E+03	883.36	-488.58	7500	7.50E+03
			inoculum_density	5.00E+08	5.00E+08			5.00E+08	5.00E+08
			lipid_content	0.1	0.75			0.1	0.75
Fluorescent ALR - w/ wastewater	constraint max	1	L_total	7500	7500	85.056	-496.876	7500	7500
			inoculum_density	2000	4.20E+08			2000	4.20E+08
			lipid_content	0.75	0.75			0.75	0.75
	constraint max	2	L_total	7500	10000	85.056	-722.452	1	10000
			inoculum_density	2000	4.20E+08			2000	4.20E+08
			lipid_content	0.75	0.75			0.75	0.75
	global	3	L_total	7500	10000	85.056	-1.62E+07	1	10000
			inoculum_density	2000	8.50E+10			2000	Inf
			lipid_content	0.75	0.75			0.75	0.75
LED-w/o wastewater	local	1	L_total	7500	7.50E+03	203.9	-393.53	7500	7.50E+03
			inoculum_density	2.00E+04	4.29E+08			2.00E+04	4.30E+08
			lipid_content	0.75	0.75			0.75	0.75
	constraint max	2	L_total	200	7.50E+05	180.02	-55859	200	7.50E+05
			inoculum_density	2000000	4.30E+08			2.00E+04	4.30E+08
			lipid_content	0.1	7.50E-01			0.1	0.75
	global	3	L_total	200	7.50E+05	180.02	-1.49E+07	200	7.50E+05
			inoculum_density	2000000	8.48E+10			2.00E+04	Inf
			lipid_content	0.1	7.50E-01			0.1	0.75
LED ALR-w/ wastewater	constraint max	1	L_total	200	7.50E+05	176.85	-68826	200	7.50E+05
			inoculum_density	2000000	5.00E+08			2.00E+04	5.00E+08
			lipid_content	0.1	7.50E-01			0.1	0.75
	local	2	L_total	200	7.50E+05	177.85	-67748	200	7.50E+05
			inoculum_density	2000000	4.29E+08			2.00E+04	4.30E+08
			lipid_content	0.1	7.50E-01			0.1	0.75
	global	3	L_total	200	7.50E+05	178.85	-1.49E+07	200	7.50E+05
			inoculum_density	2000000	8.48E+10			2.00E+04	Inf
			lipid_content	0.1	7.50E-01			0.1	0.75
solar lit PBR-w/o wastewater	constraint max	1	L_total	200	7.50E+05	179.96	-92341	200	7.50E+05
			inoculum_density	5.00E+06	4.00E+08			2.00E+04	4.00E+08
			lipid_content	0.75	7.50E-01			0.75	0.75
	constraint max	2	L_total	200	7.50E+05	179.62	-150790	200	7.50E+05
			inoculum_density	5.00E+06	6.00E+08			2.00E+04	6.00E+08
			lipid_content	0.75	7.50E-01			0.75	0.75
	constraint max	3	L_total	200	7.50E+06	176.87	-1497900	200	7.50E+06
			inoculum_density	5.00E+07	6.00E+08			2.00E+04	6.00E+08
			lipid_content	0.75	7.50E-01			0.75	0.75

Growth Scen.	Global/Local	Run No.	Variable	X0 initial	X0 final	InitialCost	FinalCost	Minimum	Maximum
solar lit PBR-w/ wastewater	constraint max	1	L_total	200	7.50E+06	176.7	-1616700	200	7.50E+06
			inoculum_density	5.00E+07	6.00E+08			2.00E+04	6.00E+08
			lipid_content	0.75	7.50E-01			0.75	0.75
	constraint max	2	L_total	200	7.50E+06	176.45	-230290	200	7.50E+06
			inoculum_density	5.00E+06	6.00E+07			2.00E+04	6.00E+07
			lipid_content	0.75	7.50E-01			0.75	0.75
	constraint max	3	L_total	200	7.50E+06	177.81	-230290	200	7.50E+06
			inoculum_density	5.00E+06	6.00E+07			2.00E+04	6.00E+07
			lipid_content	0.1	7.50E-01			0.1	0.75
Open Pond-w/o wastewater	global	1	inoculum_density	1	5307	1.38E+11	1.36E+11	1500	Inf
			lipid_content	0.46	0.75			0.46	0.75
	global	2	inoculum_density	5000	5074.4	1.36E+11	1.36E+11	1500	Inf
			lipid_content	0.1	0.75			0.1	0.75
	global	3	inoculum_density	10000	5103.5	1.36E+11	1.36E+11	1500	Inf
			lipid_content	0.1	0.75			0.1	0.75
Open Pond-w/ wastewater	constraint min	1	inoculum_density	1.50E+07	1.50E+03	2.44E+11	1.39E+11	1500	Inf
			lipid_content	0.75	7.50E-01			0.46	0.75
	global	2	inoculum_density	1	5375.2	1.38E+11	1.36E+11	1500	Inf
			lipid_content	0.75	0.75			0.46	0.75
	global	3	inoculum_density	1	5000	1.38E+11	1.36E+11	1500	Inf
			lipid_content	0.46	0.75			0.46	0.75

Table 19: Summary of optimization parameters and results for all growth scenarios included in this study.

Open Pond

Surprisingly, the optimal culture density is not a significant profit factor for an open pond growth scenario due to the growth rate/pond depth/cost relationships. Despite lower growth rate and productivity with increasing depth, the solution goes to the greatest depth and nearly the lowest density possible in order to minimize the surface area. Even when the costs of land and water evaporation are not included, the other costs dominate the optimization so that the growth scenario optimizes to the minimal size farm, regardless of loss in algal growth and productivity. The dominate parameter is the size of the farm, with the optimization leading to the smallest farm possible. The inoculum density goes nearly to the minimum to allow the greatest depth and smallest land area for the set quantity of Liters. The minimum loss is seen at a culture density around 5e-4 to

6e-4 g/L for the light path length determined by Equation (5), even when including wastewater treatment.

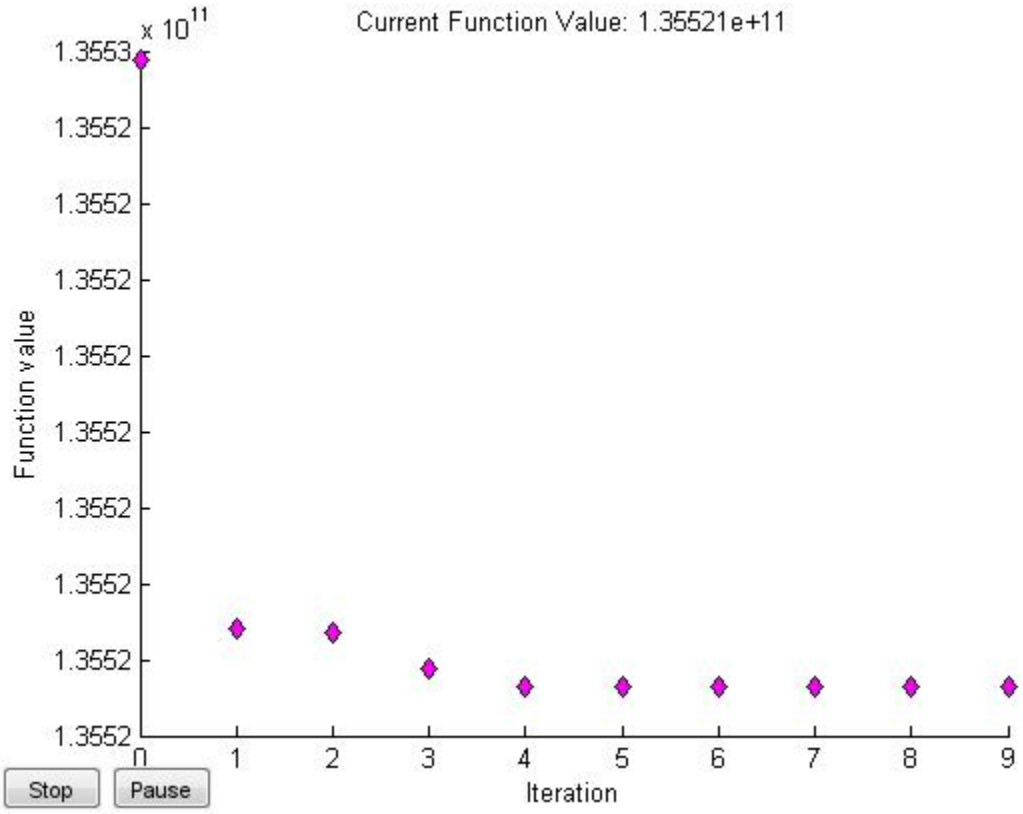

Figure 59: Final Cost as a function of run iterations for open pond optimization.

Even with an optimal depth for productivity of 19.31 cm (the minimum), a culture density of 16.99 g/L (0.33 g/L is expected), and a lipid content of 75%, the model still shows an average net loss of $491,820.00 per day in a rural open pond growth scenario with one pond of 20,000 Liters and filter press, oven, and supercritical CO_2 as solvent harvesting options.

The losses begin to increase at the expected density of 0.3398 g/L if calculation of light path length is modified to Equation (63). At this density and light path length

calculation, losses remain at $1e8 per day or $4e7 per day if paddlewheel, pump and evaporating water cost are not included. Open pond growth scenario shows a net profit only if Equation (63) is used for light path length, financing for harvest and land capital, pump power, paddlewheel power, evaporated water cost, and employee cost are not included. The net profit is seen beginning at a culture density of 226 g/L and depth of 35.88 cm, maximizing at 2265 g/L at a depth of 4.671 cm. However, this high culture density is impractical and unrealistic for open ponds due to temperature, nutrient, light path length, and gas exchange restraints.

$$PL = 45.0e^{(-0.001d)} \qquad \text{Eq. (63)}$$

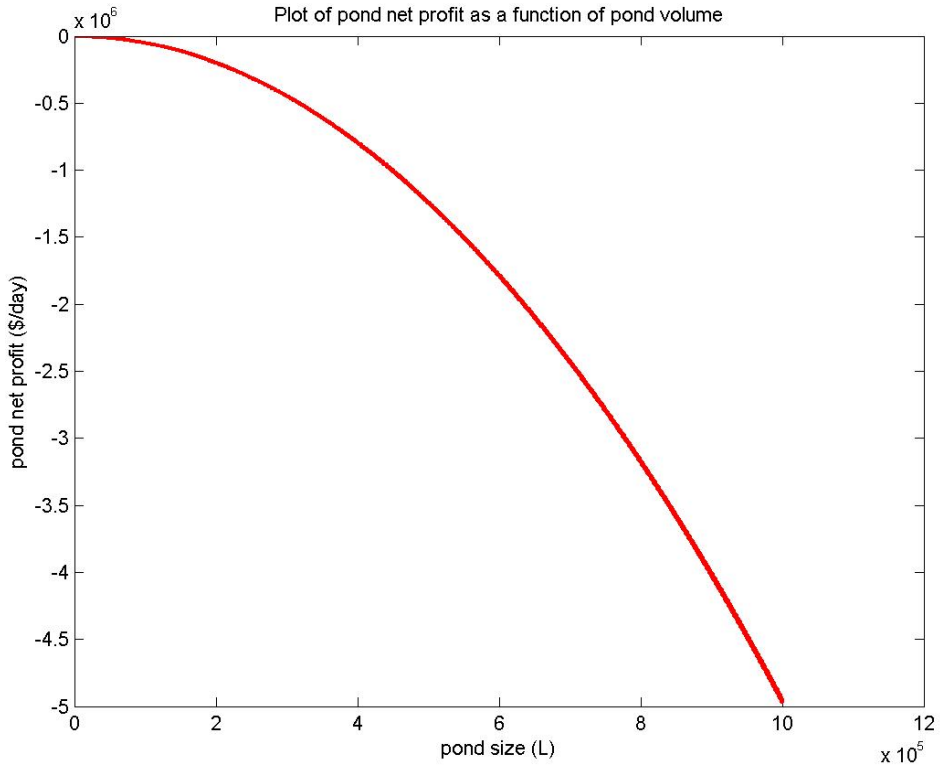

Figure 60: Open pond net profit as a function of pond size.

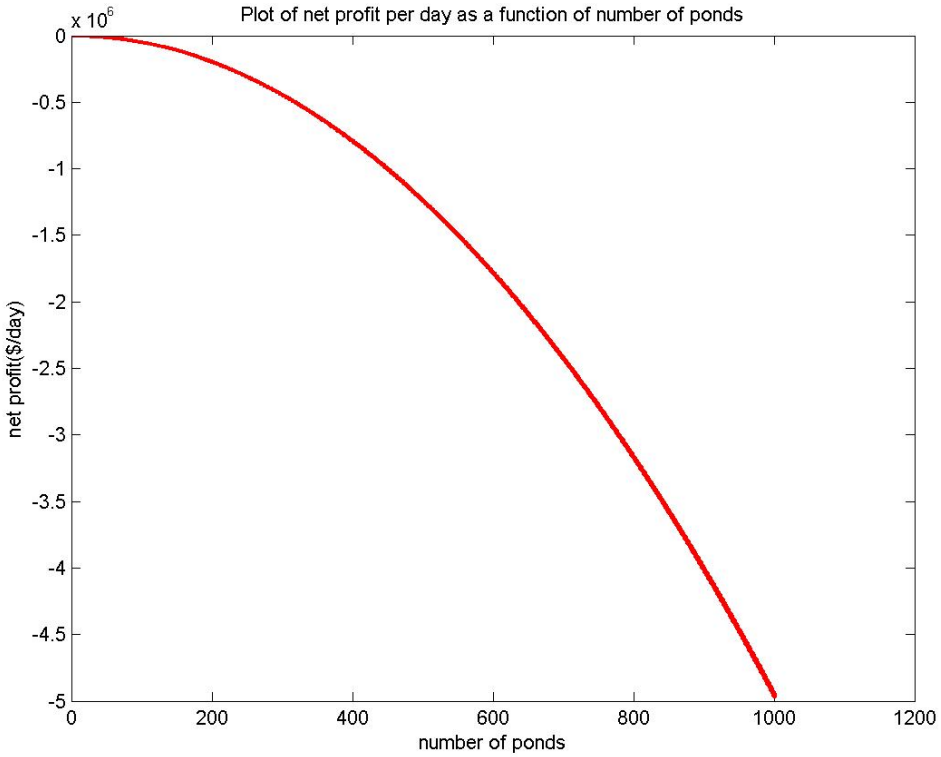

Figure 61: Open pond net profit as a function of quantity of ponds.

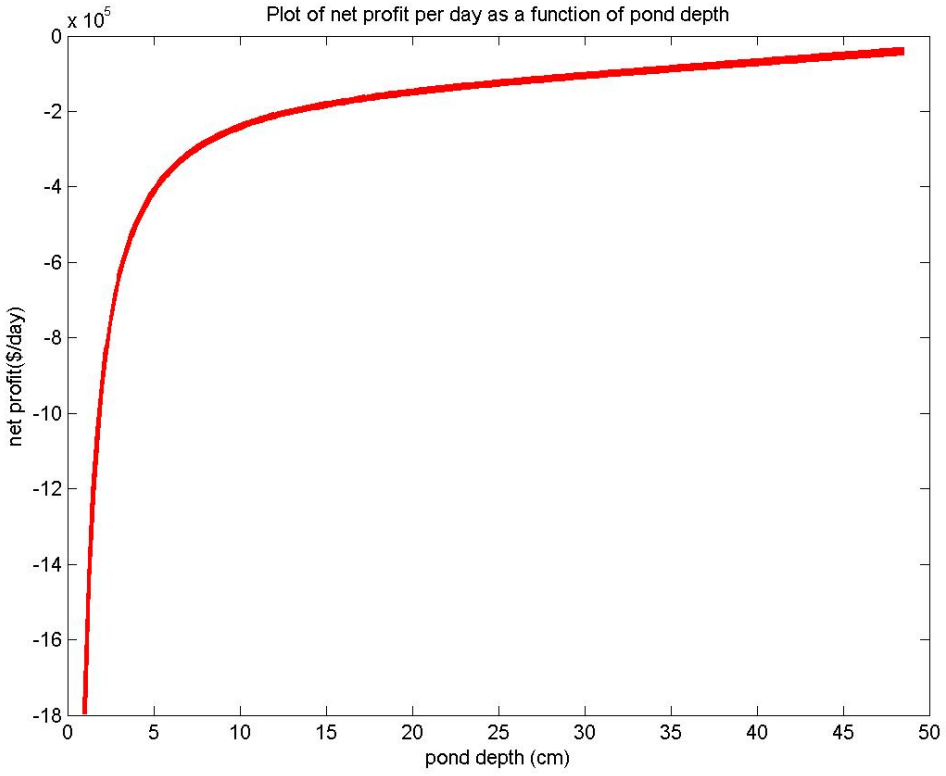

Figure 62: Open pond net profit as a function of pond depth.

Net losses increase as the farm size is increased, regardless of whether pond size or quantity of ponds is increased. Wastewater treatment does decrease the net loss but is not sufficient to create a profitable scenario, and losses continue to increase as density and size increase. Run duration only increases the cumulative net loss, so increasing the run duration is negative as indicated in the sensitivity analysis (see Table 18).

Solar Illuminated PBR

Solar illuminated PBR's will optimize at the highest density and largest facility possible, including when wastewater treatment is included. However, as stated previously, around 1 g/L is proven density for this growth scenario, and a density above

about 50 g/L is impractical due to temperature, nutrient, light path length, and gas exchange restraints. An average net profit can be seen starting at a culture density of 2.5 g/L, and diameter of 0.34 m when not incorporating wastewater treatment. It is important to remember the model does not include additional cooling required for solar illuminated PBR's during the heat of the day.

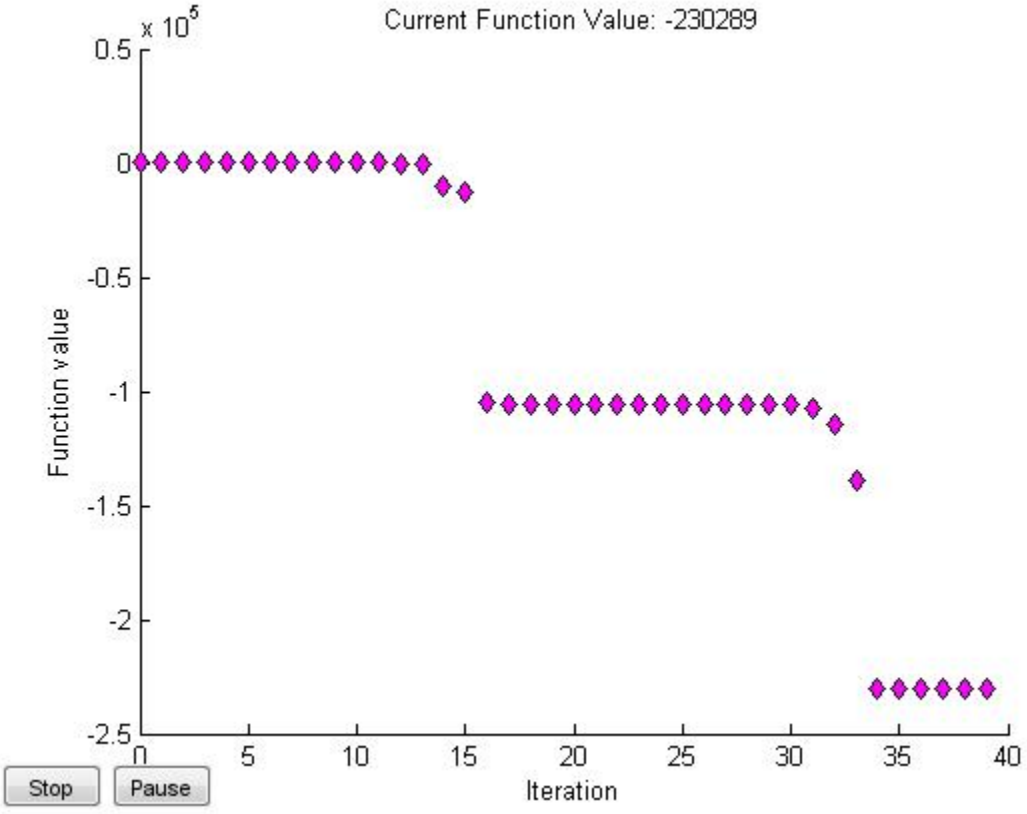

Figure 63: Final Cost as a function of run iterations for solar illuminated PBR optimization.

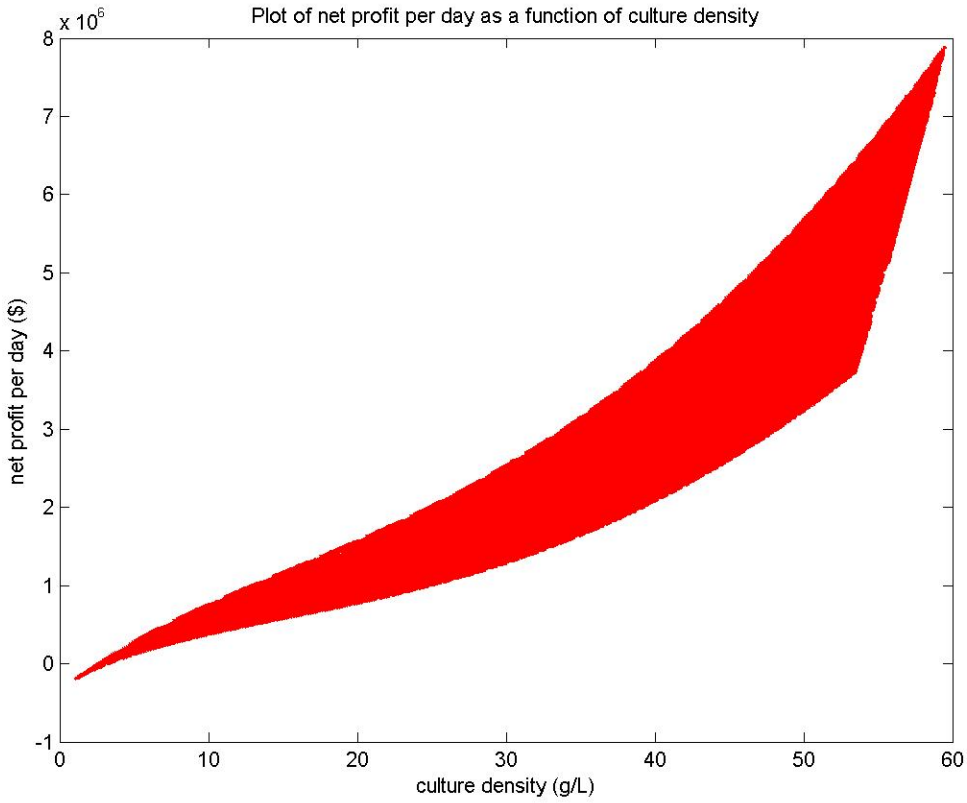

Figure 64: Net profit as a function of culture density for solar illuminated PBR's without wastewater treatment and lipid content of 75% (0-60 g/L).

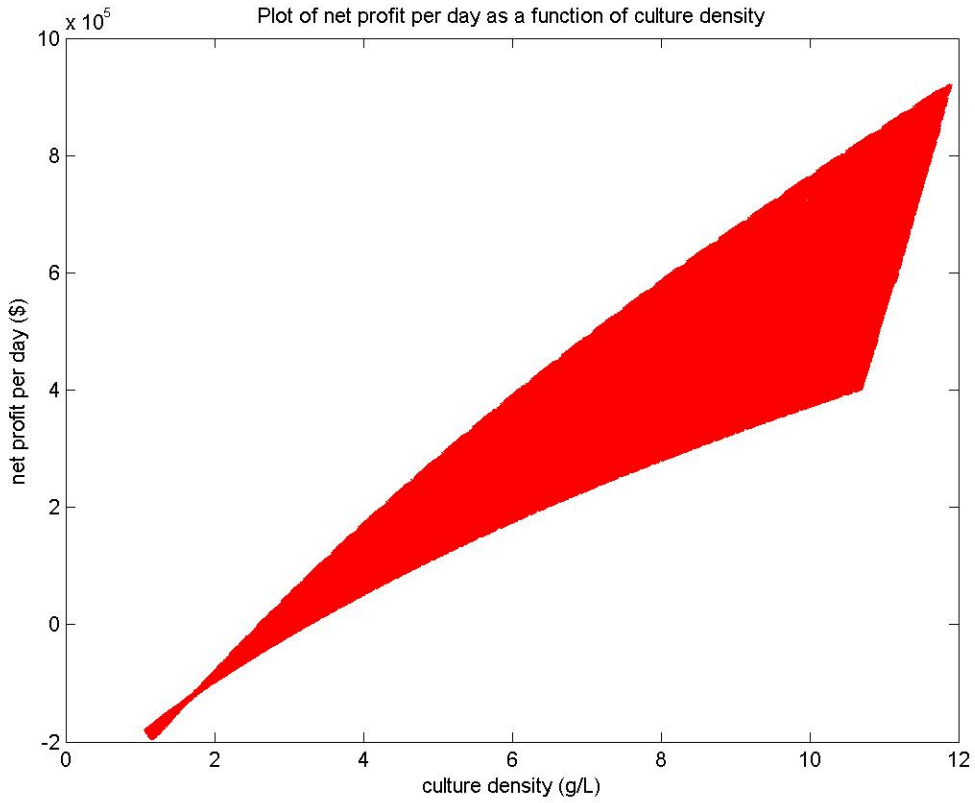

Figure 65: Net profit as a function of culture density for solar illuminated PBR's without wastewater treatment and lipid content of 75% (0-12 g/L).

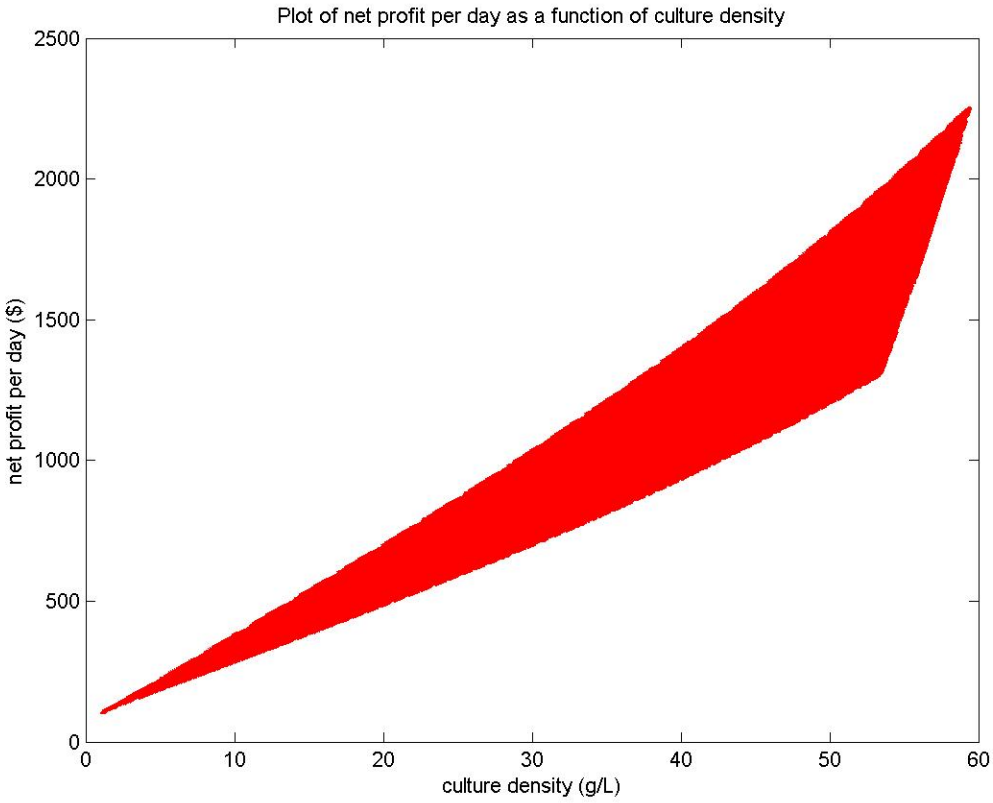

Figure 66: Net profit as a function of culture density for solar illuminated PBR's with wastewater treatment and lipid content of 46% (0-60 g/L).

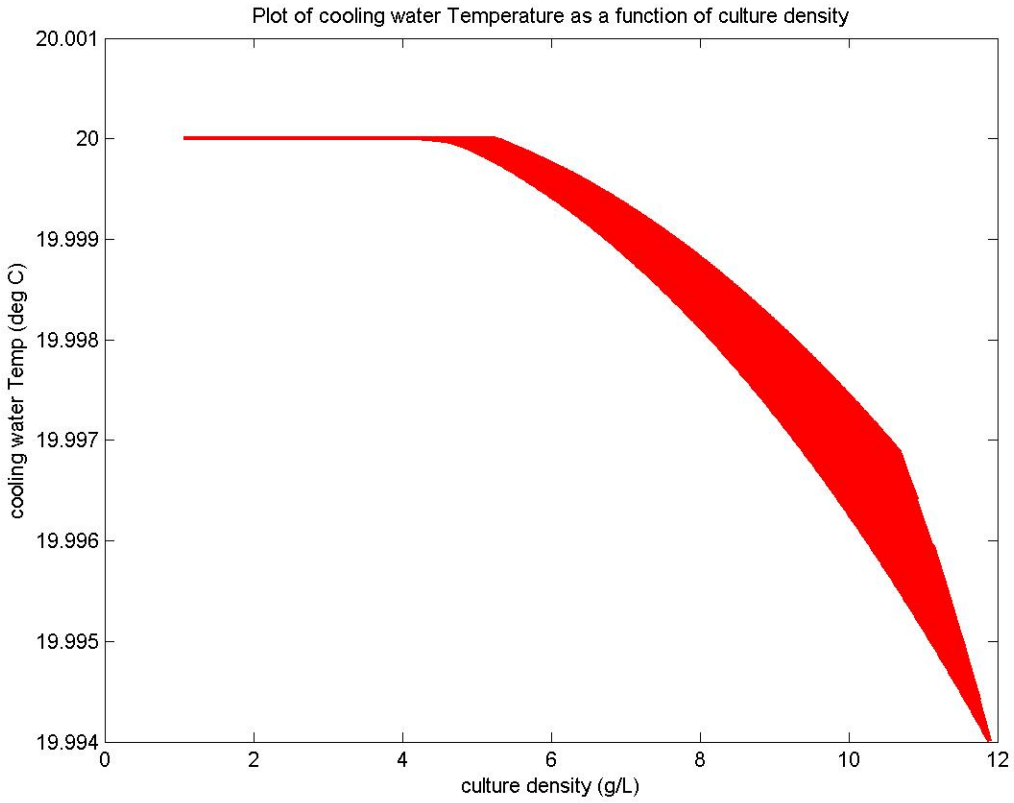

Figure 67: Cooling water temperature as a function of culture density for solar illuminated PBR's (0-12 g/L).

Fluorescent Illuminated ALR

In a fluorescent illuminated ALR without including wastewater treatment, a local minimum in net cost is found to exist at 47 - 48 g/L, which results in an ALR total diameter of 1.57 m and a maximum length of 2.7 m. However, after showing a decrease in average net profit, the net profit again begins to increase beyond the initial optimal to whatever is set as the maximum constraint. Thus, the 49 - 75 g/L culture density is a density to avoid because the likelihood of incurring a loss is higher. Other than this break in slope, the net profit increases along with the culture density. As the light path length

Equation (7) is adjusted, the optimal culture density changes accordingly with the geometry, but the light path length does not significantly impact net profit or cost. At optimal density near 47 g/L the fluorescent ALR growth scenario begins to break even at a facility size of 10,000 L, shows an average net profit of $249.60/day without wastewater and $497.78/day with wastewater at a facility size of 20,000 L. Incorporating wastewater becomes more important as the facility size grows since results with a facility size of 1e8 Liters show an average net profit of $853,329.15 per day when incorporating wastewater treatment, and -$772,090 per day without incorporating wastewater. Figure (68) shows the solution has located the global minimum at the boundary when inoculum density is set at infinity.

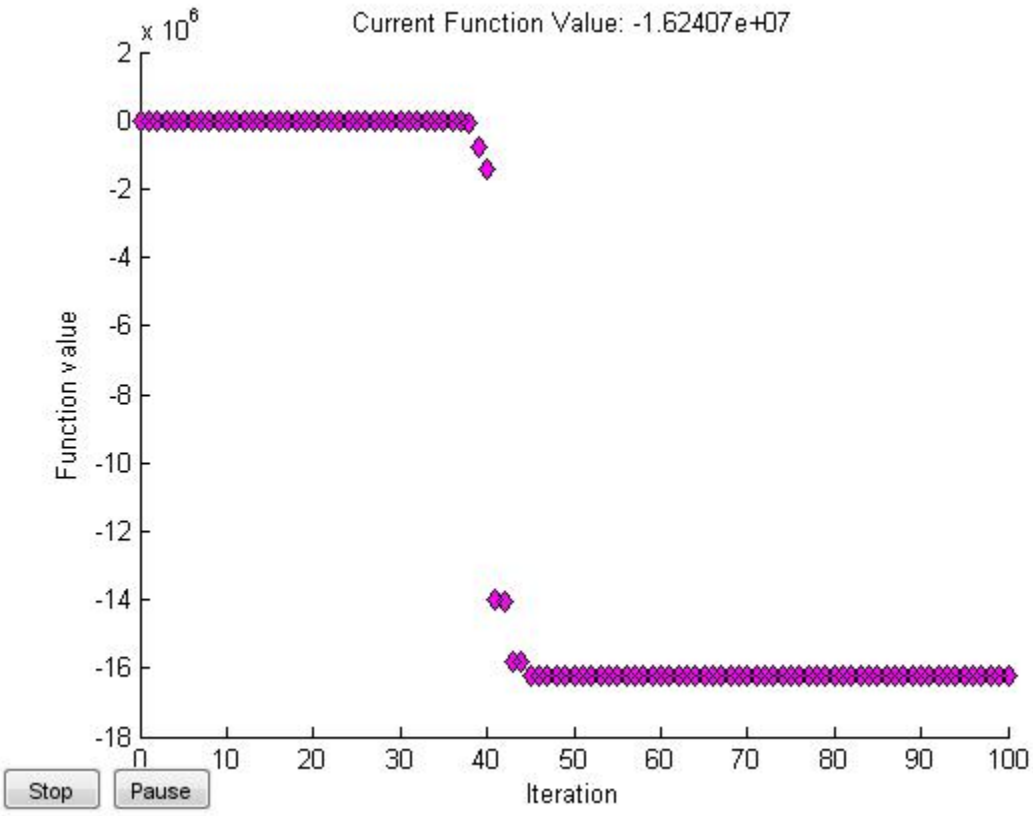

Figure 68: Final Cost as a function of run iterations for fluorescent illuminated ALR optimization with maximum culture density constraint set at infinity.

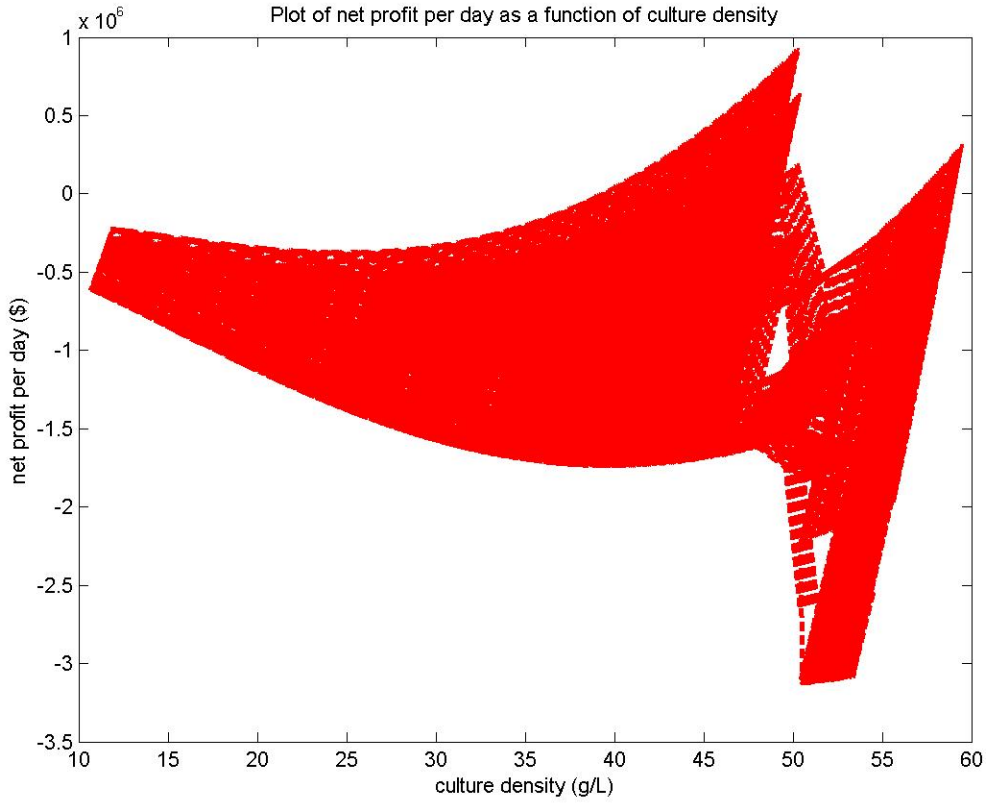

Figure 69: Net profit vs. culture density for an ALR fluorescent illuminated growth scenario without wastewater treatment and lipid content of 75% (20,000 L facility).

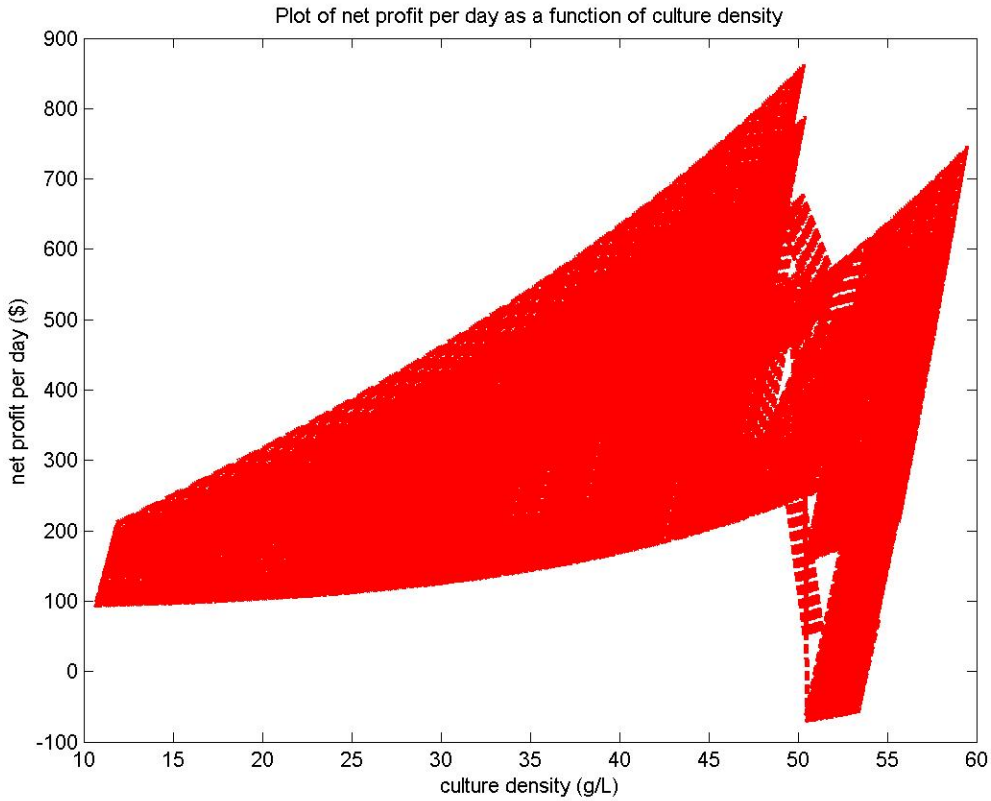

Figure 70: Net profit vs. culture density for an ALR fluorescent lighting growth scenario with wastewater treatment and lipid content of 46% (20,000 L facility).

Comparison between Figures (69) and (70) reveals that including wastewater treatment mitigates the risks of large losses which are more possible without the additional cost benefits of including wastewater treatment.

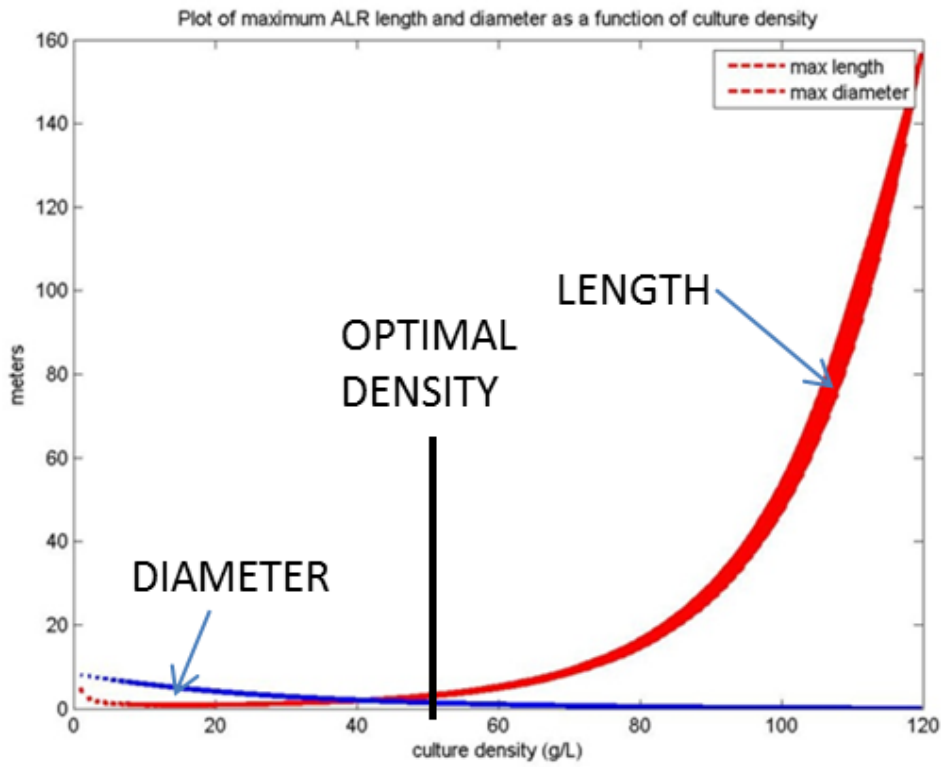

Figure 71: ALR diameter and length as a function of culture density.

Figure (71) reveals where optimal density is found in relation to ALR total diameter based on light path length, and ALR length based on oxygen saturation. The diameter goes to zero as the culture density increases, which causes the length to go to infinity. At optimal density, however, the diameter and length are practical at 1.57 m and 2.7 m, respectively.

LED Illuminated ALR

ALR's with LED lighting do show a net profit, and although not quite as profitable as the fluorescent illuminated ALR, the optimization leads to the maximum size facility. The capital cost of the LED lighting is only $0.13 more than that for fluorescent lighting, so the price need not reduce much in order to yield a more profitable

scenario. Similar to fluorescent illuminated ALR's, this growth scenario has a local net cost minimum at 48.6 g/L with the same geometry as the fluorescent illuminated ALR. The fact that both scenarios have local optimums in the same location confirms the results and verifies the optimal density is a result of the system interdependencies instead of the exact cost/profit ratio.

The corresponding scenario with a 20,000 L facility at the local optimal density of approximately 48 g/L with LED lighting shows an average net loss of $20.65 per day without wastewater, and a net profit of $311.98 per day with wastewater. If capital cost per Watt is adjusted to match fluorescent at $0.35/Watt per year, the scenario starts showing a maximum net profit at a culture density of 22.65 g/L without including wastewater. Similar to a fluorescent illuminated ALR the importance of incorporating wastewater treatment to show a net profit increases as the facility grows in size.

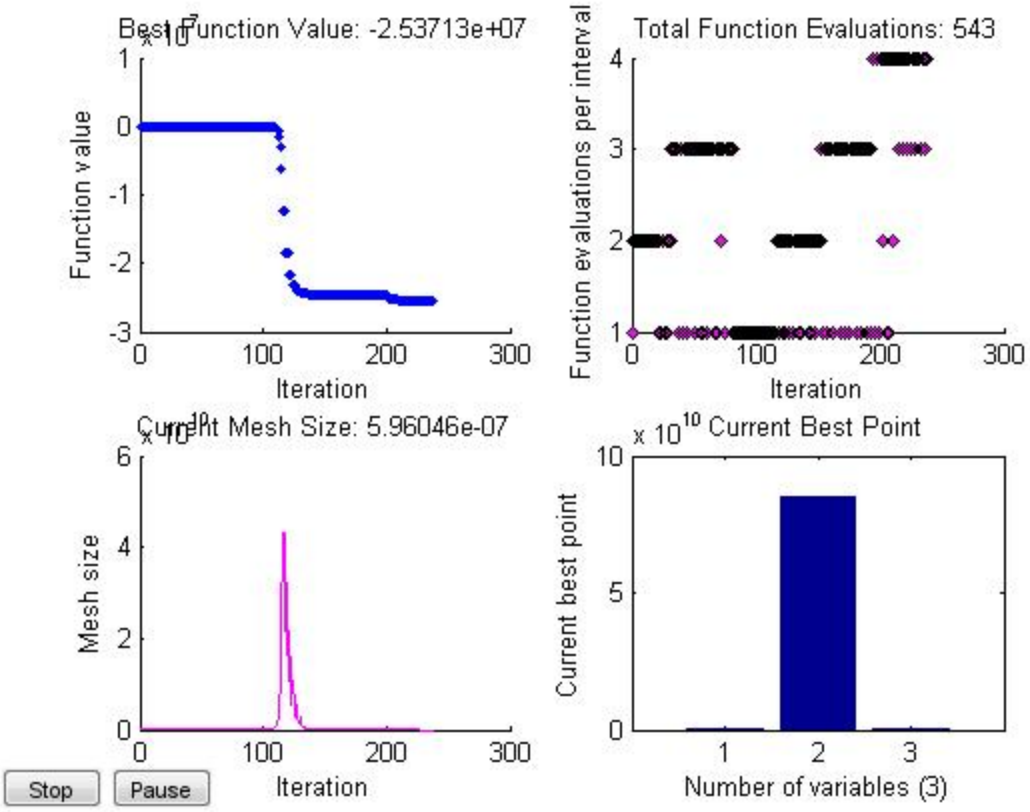

Figure 72: Optimization results for artificially illuminated ALR optimization with maximum culture density constraint set at infinity.

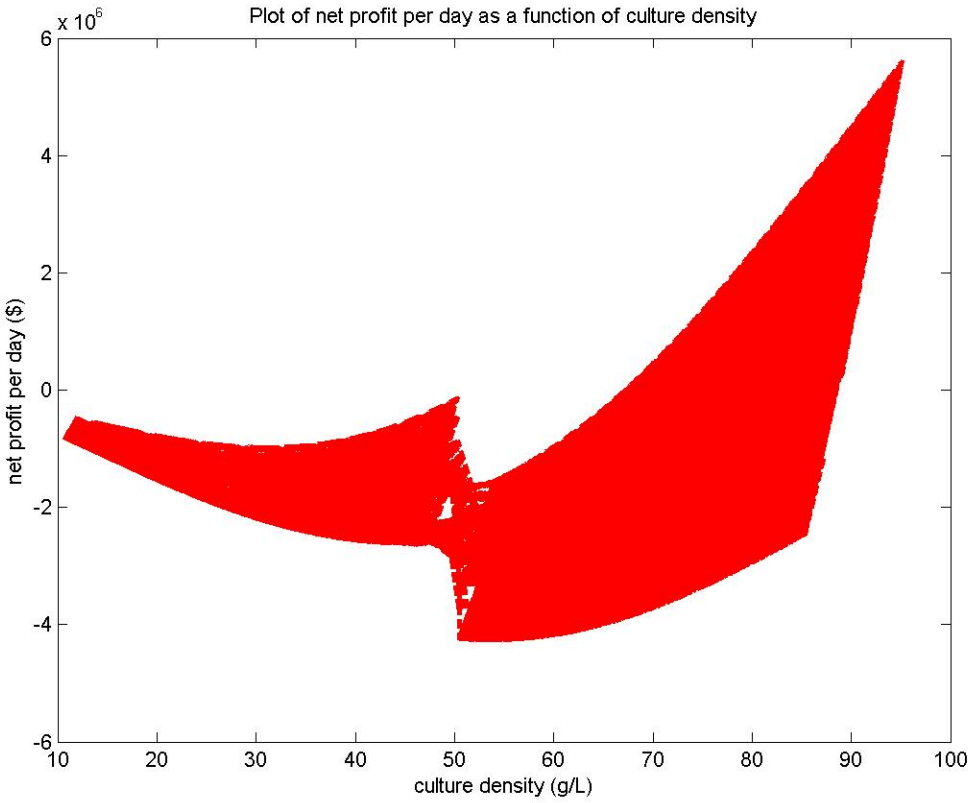

Figure 73: Net profit vs. culture density for an ALR LED lighting growth scenario without wastewater treatment and lipid content of 75% (20,000 L facility).

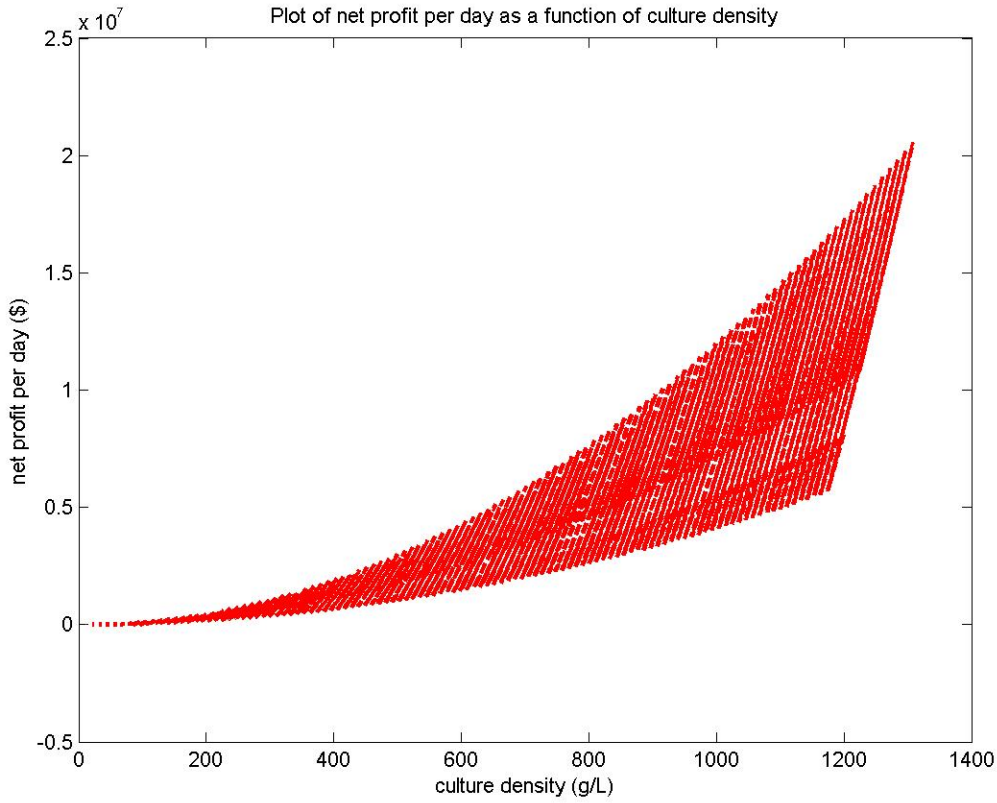

Figure 74: Net profit as a function of culture density showing ultra-high densities in an artificially illuminated ALR growth scenario.

Figure (74) shows the local minimum is not visible in the slope when considering a larger range of culture densities. Simultaneously, the risk increases as the range of potential profits cover a wider range with increasing culture density. Even if the risk of loss could be reduced, the high algal density in Figure (74) is impractical due to temperature increase and reduced light path length, which are evident in model results (see figures below).

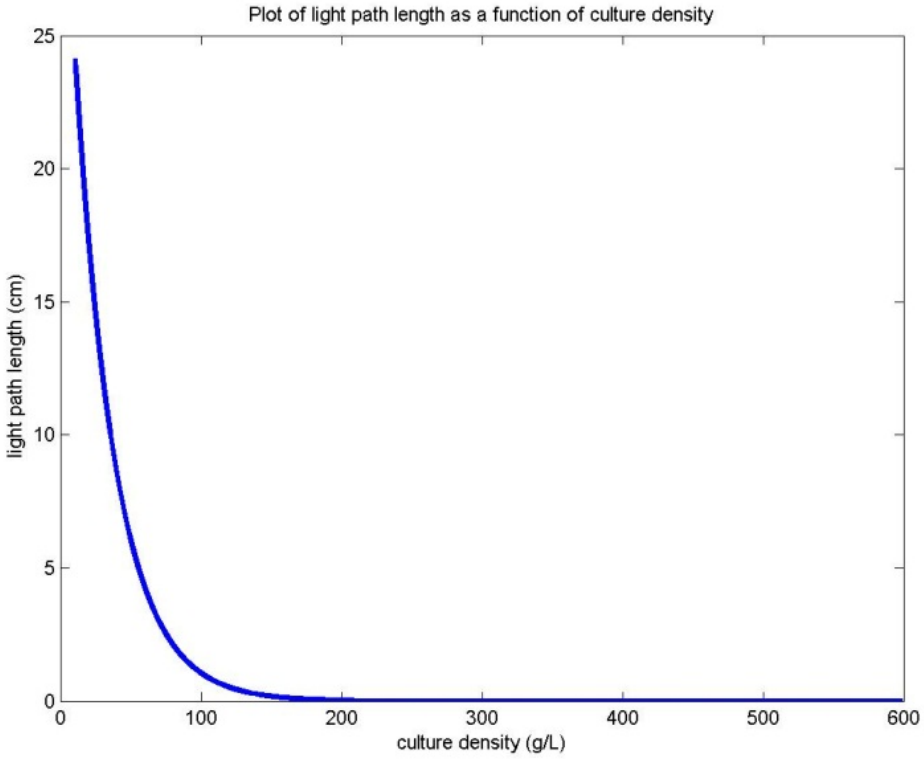

Figure 75: Light path length as a function of culture density at high densities.

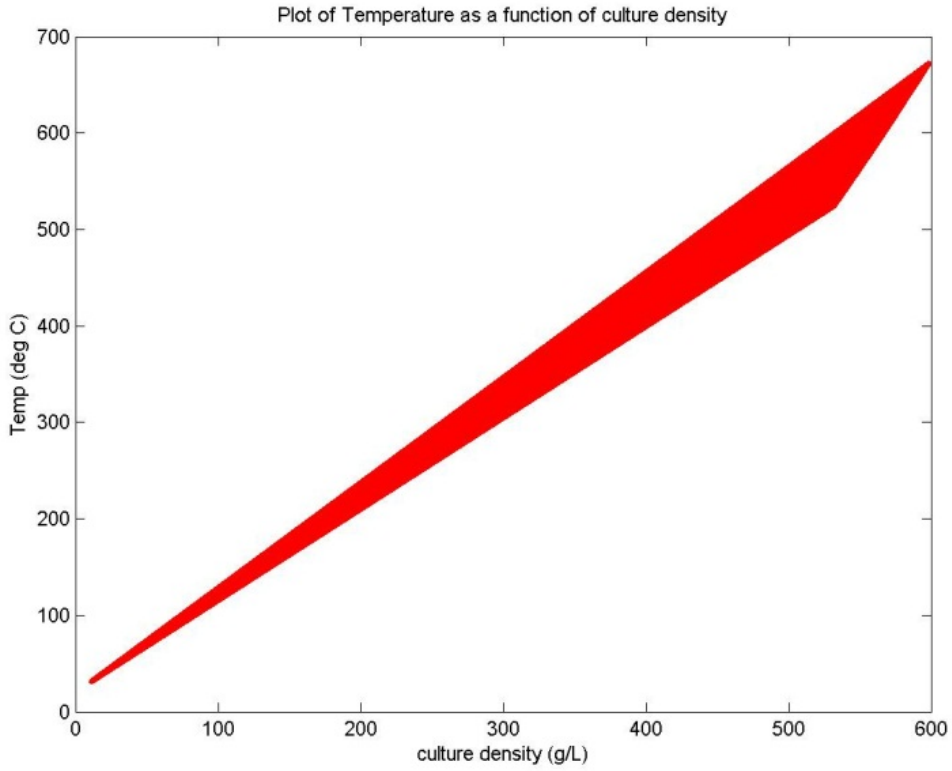

Figure 76: Culture temperature as a function of culture density at high densities.

Funding/Investment

When determining the NPV (net present value) and IRR (internal rate of return) of an algal growth scenario, both the duration of operation and the size of the facility affect results. The size of the facility affects investment viability because of the size of initial investment required. All growth scenarios are examined with a time period of 15 years operation and beginning at a relatively small size of 7,500 L since as the initial investment decreases the NPV improves. While NPV decreases as the facility size, and therefore, the initial investment increases, the IRR becomes a maximum at optimal

density at various sizes depending on the growth scenario. Decreasing the market rate to 0.0008 does decrease the gap between minimum and maximum NPV, but it remains negative and improves only for the worst case scenario.

Since LED illuminated ALR's at the determined capital cost of $0.48 per Watt per year shows negative NPV and IRR, the capital cost is manipulated to compare results and determine if a positive NPV can be achieved. (At $0.35 per Watt per year the LED illuminated ALR is equivalent to fluorescent illuminated ALR in costs.) A positive NPV is not achieved for LED lighting even at $0.10 per Watt per year, but the IRR does improve to a small extent. The only growth scenario to show a positive IRR is the solar illuminated PBR when wastewater treatment is incorporated and lipid content is 75%. NPV is positive in the solar illuminated PBR growth scenario starting at a culture density of around 95 g/L, 75% lipid content, and incorporating wastewater treatment. However, even then the IRR remains below the assumed market rate of 8% at 5.2%. Surprisingly, the open pond growth scenario financial attractiveness does not improve when incorporating wastewater treatment due to the large losses.

Growth Scenario	Max NPV ($)	Size (L)	Culture Density(g/L)	Annual IRR (%)
Solar lit PBR w/ WW	-3.68E+07	3.50E+06	74-83	-4.68%
Solar lit PBR	-3.98E+07	3.50E+06	74-83	-5.72%
Fluorescent lit ALR w/ WW	-2.45E+08	5.50E+05	45-50	-26.00%
Fluorescent lit ALR	-2.46E+08	5.50E+05	45-50	-28.08%
Fluorescent lit ALR	-1.45E+10	5.00E+07	21-25	NaN
LED lit ALR ($0.48/W/year) w/ WW	-2.90E+08	5.50E+05	45-50	-27.56%
LED lit ALR ($0.48/W/year)	-2.97E+08	5.50E+05	45-50	-31.20%
LED lit ALR($0.10/W/year) w/ WW	-6.52E+07	5.50E+05	45-50	-19.24%
LED lit ALR($0.10/W/year)	-6.60E+07	5.50E+05	45-50	-20.28%
Open Pond (w/ and w/o WW)	-1.25E+08	2.00E+04	.32-.36	NaN

Table 20: Optimization results of various growth scenarios incorporating financial analysis (lipid content = 46%).

Growth Scenario	Max NPV ($)	Size (L)	Culture Density(g/L)	Annual IRR (%)
Solar lit PBR w/ WW	5.19E+06	3.50E+06	96-107	5.20%
Solar lit PBR w/ WW	-1.82E+07	3.50E+06	74-83	0.35%
Solar lit PBR	-2.12E+07	3.50E+06	74-83	-0.33%
Fluorescent lit ALR w/ WW	-2.43E+08	5.50E+05	45-50	-22.36%
Fluorescent lit ALR	-2.44E+08	5.50E+05	45-50	-22.88%
Fluorescent lit ALR	-1.44E+10	5.00E+07	21-25	-24.96%
LED lit ALR ($0.48/W/year) w/ WW	-2.95E+08	5.50E+05	45-50	-23.40%
LED lit ALR ($0.48/W/year)	-2.95E+08	5.50E+05	45-50	-23.40%
LED lit ALR($0.10/W/year) w/ WW	-6.34E+07	5.50E+05	45-50	-16.12%
LED lit ALR($0.10/W/year)	-6.39E+07	5.50E+05	45-50	-17.16%
Open Pond w/ WW	-1.25E+08	2.00E+04	.32-.36	-8.14%
Open Pond	-1.25E+08	2.00E+04	.32-.36	NaN
Open Pond	-3.87E+10	2.00E+04	148-165	NaN

Table 21: Optimization results of various growth scenarios incorporating financial analysis (lipid content = 75%).

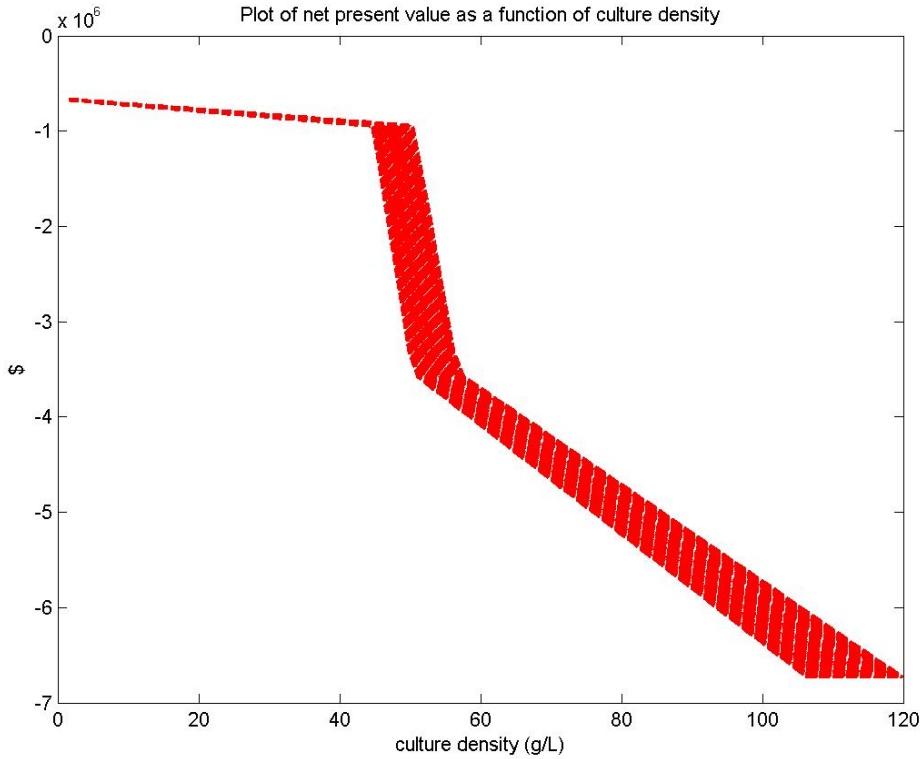

Figure 77: NPV for fluorescent illuminated ALR at interest rate of .08% (7,500 L).

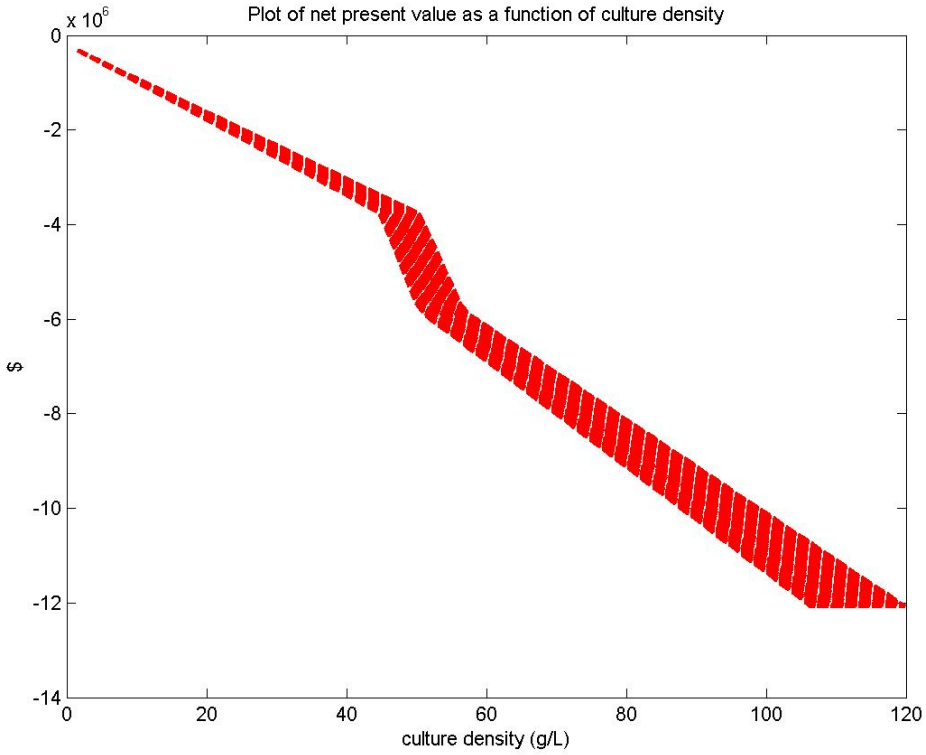

Figure 78: NPV for fluorescent illuminated ALR at interest rate of 50% (7,500 L).

Similarly, when the interest rate is raised to 50%, the worst case scenario NPV decreases, but the best case scenario NPV remains about the same which makes sense since a higher interest rate represents a higher risk.

As a reminder, since this study represents a one point in time analysis and investment decisions are based on many additional factors specific to the situation, the conclusions drawn for investment attractiveness based on NPV and IRR should be subjected to further evaluation by potential investors.

Open Pond

Open pond growth scenario in this model will never be an attractive investment opportunity even when wastewater treatment is included. Even when the gas and water pump energy, paddlewheel energy, employee cost, and land cost are set at zero, there still remains a net loss of some $43,000,000.00 per day for a 100,000 kg biomass/year facility. NPV is -$1.25e8 and IRR is undefined when algal facility is one pond of 20,000 liters at expected maximum algal density of 0.32 - 0.37 g/L regardless of wastewater treatment incorporation or lipid content. Wastewater treatment improves net loss results by approximately $500,000, which is significant on its own, but only makes a small dent in the immense loss so that is not evident in the NPV or IRR. The NPV continues to worsen as pond size or culture density increase and the IRR remains negative until it is undefined. When a net profit per day was found through omitting several costs detailed in the optimization section and the light path length equation was modified, the NPV and IRR remain negative.

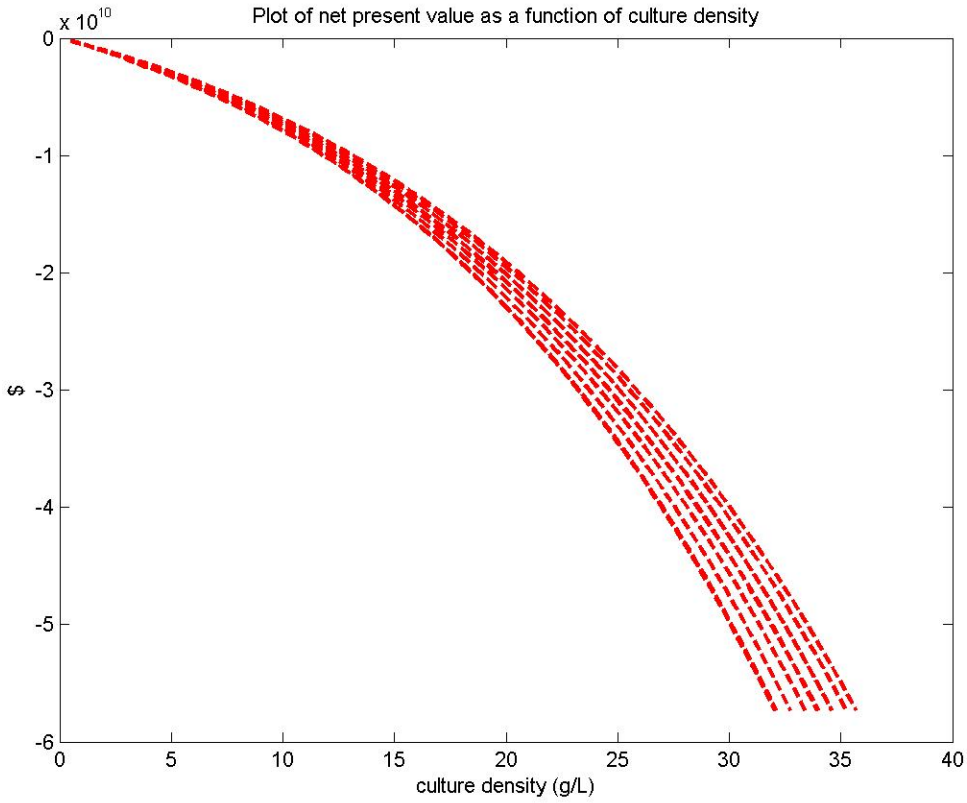

Figure 79: NPV as a function of culture density for Open Pond growth scenario.

Solar Illuminated PBR

At a density of 2.5 g/L (the density at which net profit per day is first seen in the optimization) and a facility size of 7,500 L, the NPV is < 0 and payback period is 1,295 years. Also, the calculations for solar illuminated PBR's don't include an evaporated water replacement cost, but this could be a significant factor depending on the growth scenario and whether other cooling methods are implemented.

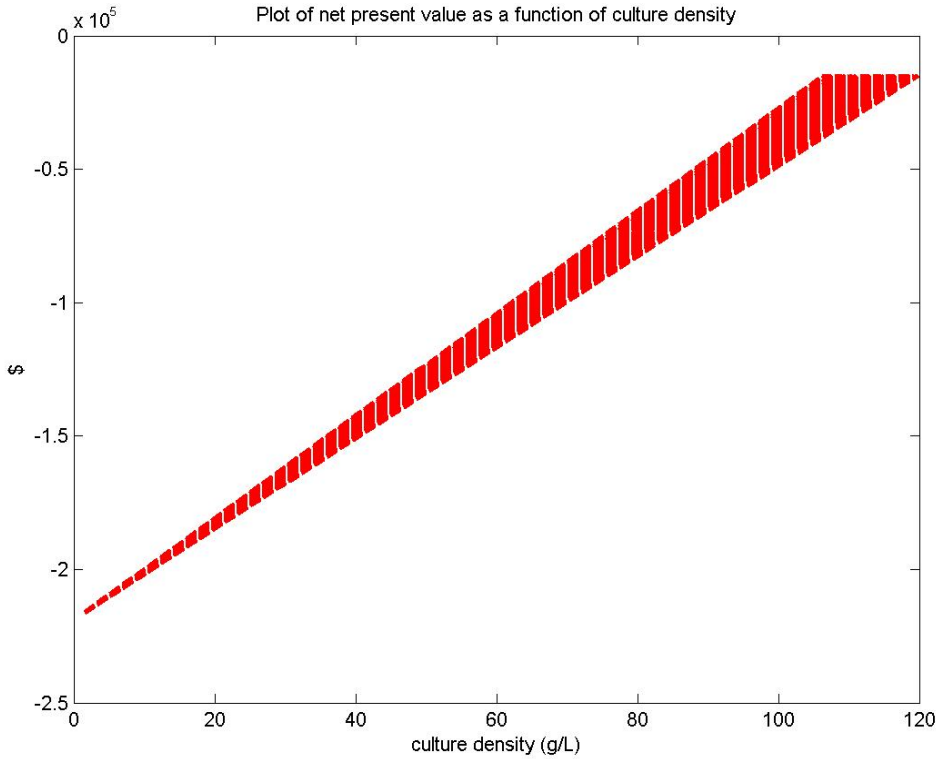

Figure 80: Net present value of solar illuminated PBR as a function of culture density (7,500 L).

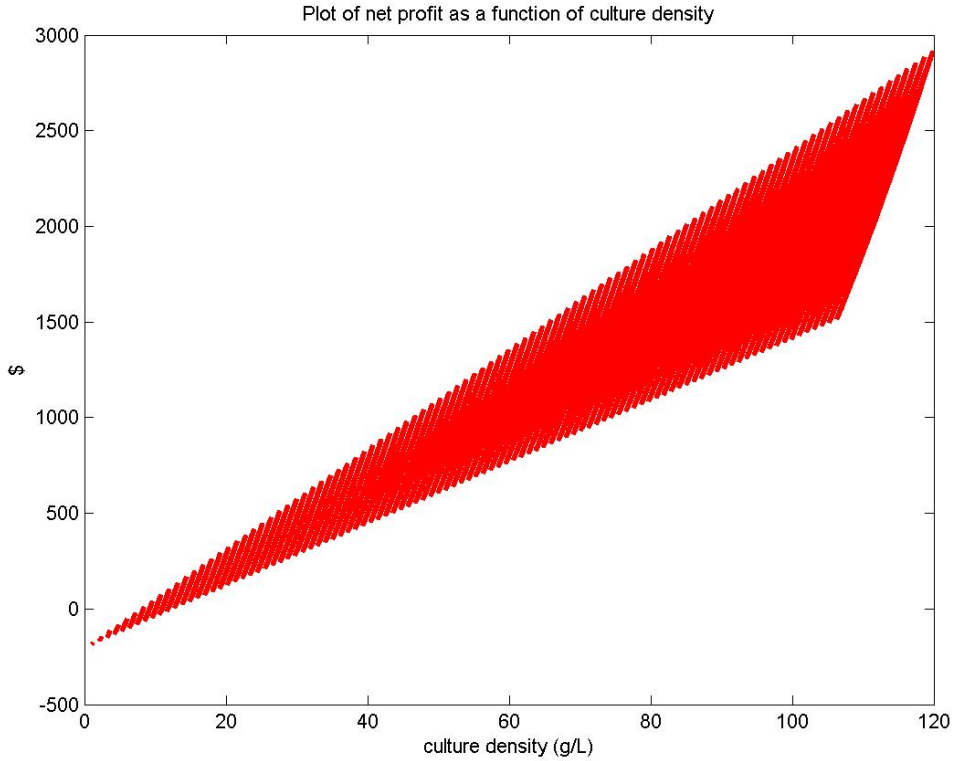

Figure 81: Net profit of solar illuminated PBR as a function of culture density without wastewater treatment (7,500 L).

Annual IRR for a 7,500 L facility is positive starting at around a density of 11 g/L, continues to increase as the density increases beyond practical, and reaches 3.86% at a density of 120 g/L when including wastewater treatment and a lipid content of 46%.

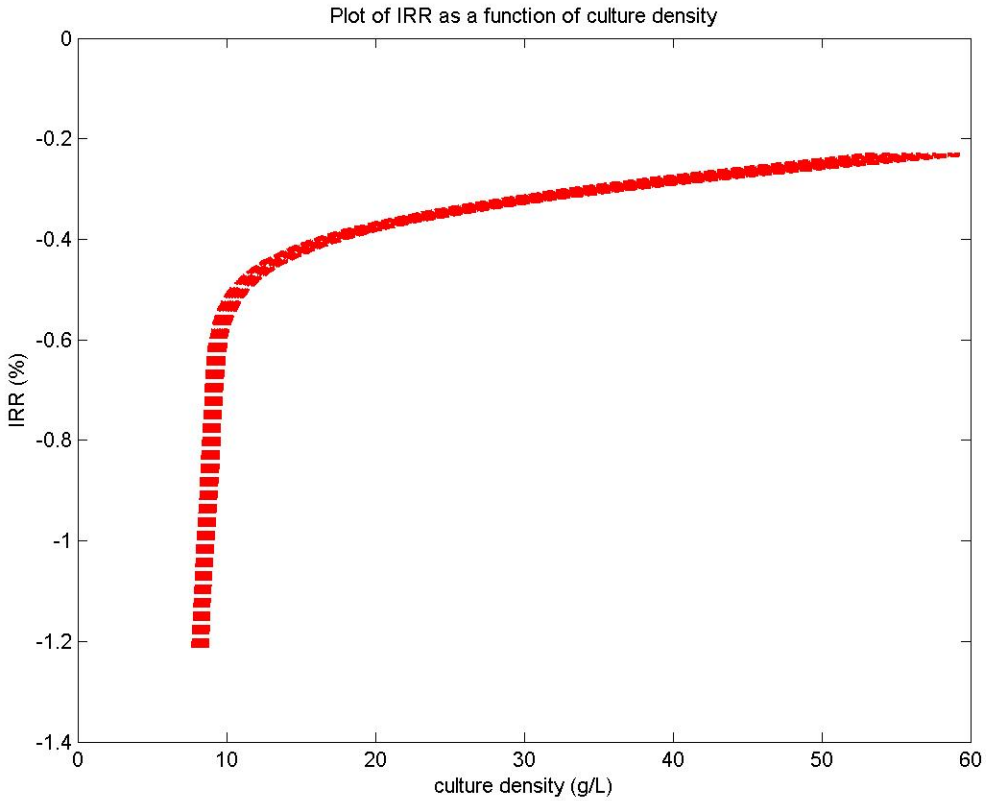

Figure 82: Weekly IRR of solar illuminated PBR as a function of culture density (7,500 L).

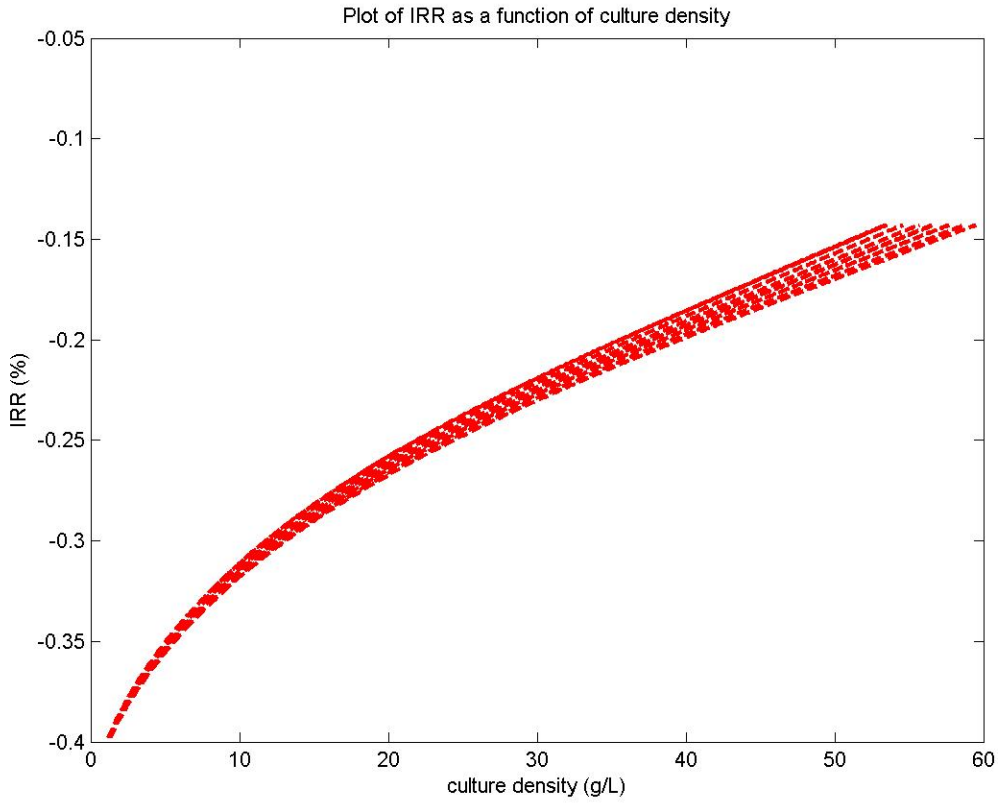

Figure 83: Weekly IRR of solar illuminated PBR as a function of culture density (20,000 L).

A positive NPV and benchmark IRR for solar illuminated PBR's at a proven culture density (~1 g/L) is never attained. Annual IRR reaches 6.87% at a culture density of 107 g/L and facility size of 3.5e6 Liters, and continues to increase along with facility size as culture density increases. NPV is positive starting at around a culture density of 95 g/L and a facility size of 3.5e6, with a respectable annual IRR of 5.2%.

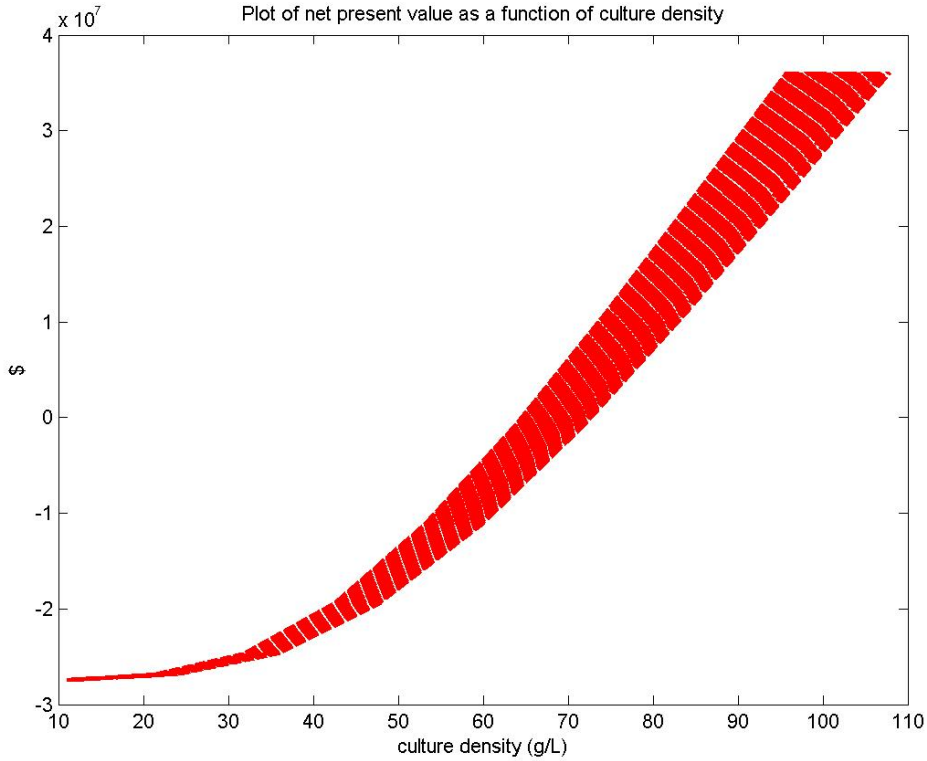

Figure 84: Net present value of solar illuminated PBR as a function of culture density (3,500,000 L).

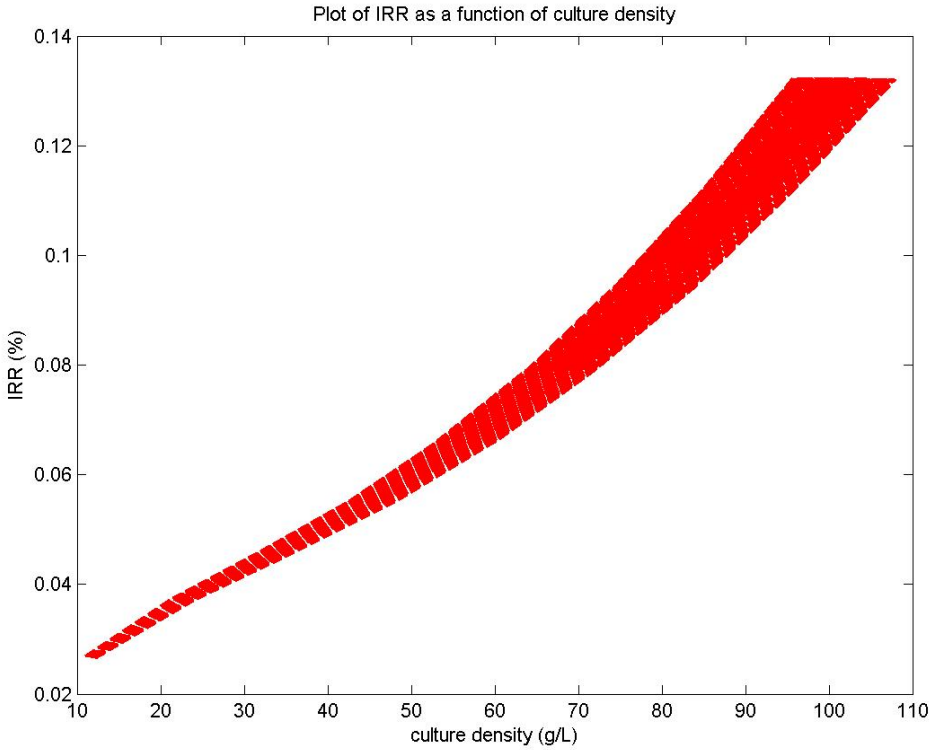

Figure 85: Weekly IRR of solar illuminated PBR as a function of culture density (3,500,000 L).

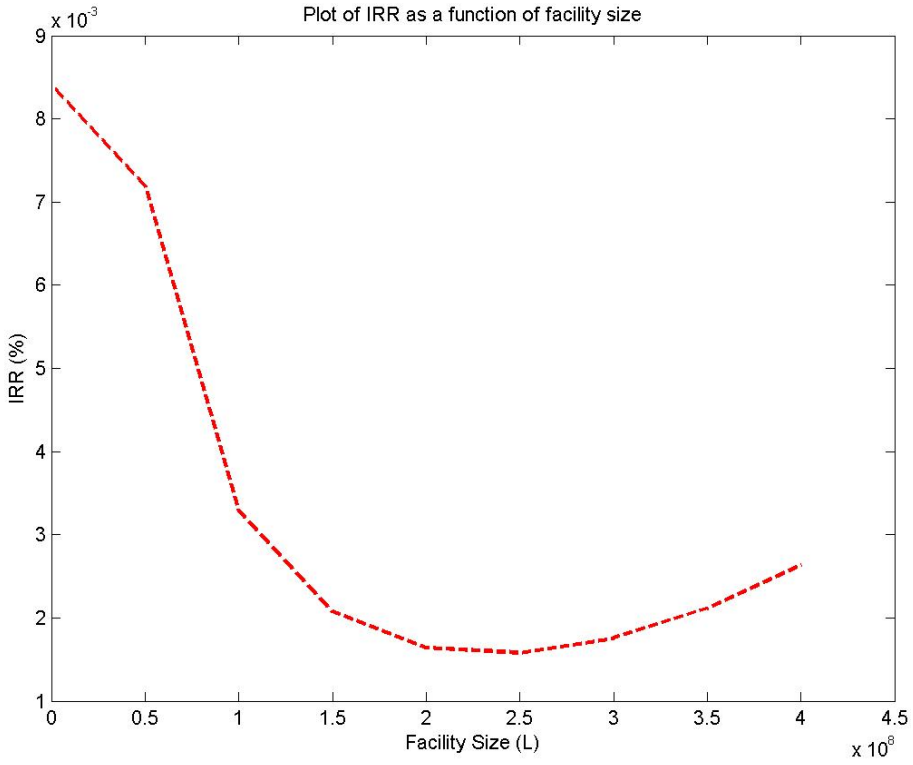

Figure 86: Weekly IRR of solar illuminated PBR as a function of facility size at culture density of ~95 g/L.

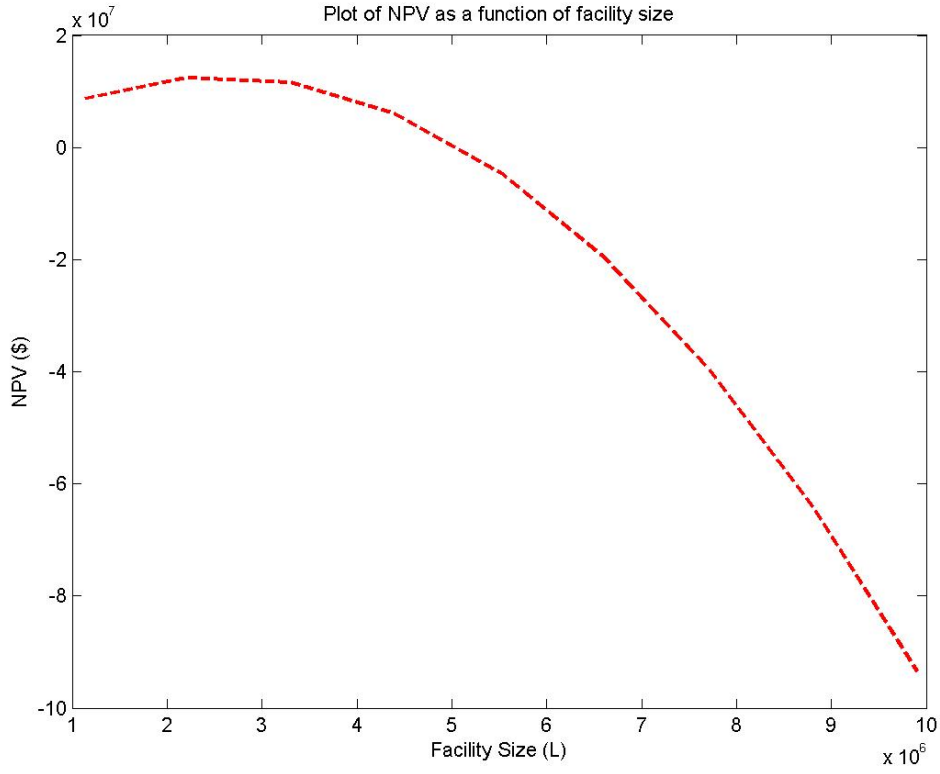

Figure 87: NPV of solar illuminated PBR as a function of facility size at culture density of ~95 g/L.

Fluorescent Illuminated ALR

ALR with fluorescent lighting at local optimal density of approximately 48 g/L shows a payback period of about 121 years. Increasing the density doesn't aid in the prognosis since increasing density also increases lighting requirements, reduces geometry and, thus, increases costs. NPV and IRR are never positive in this growth scenario, even when including wastewater treatment and increasing lipid content to 75%.

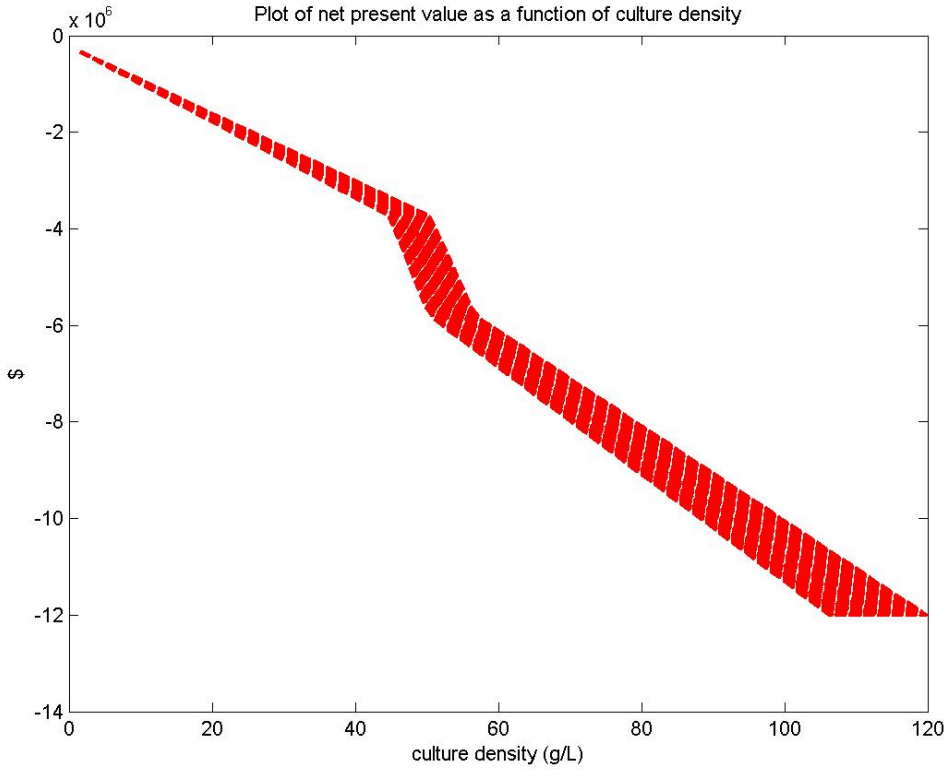

Figure 88: NPV of fluorescent illuminated ALR as a function of culture density without wastewater (7,500 L facility).

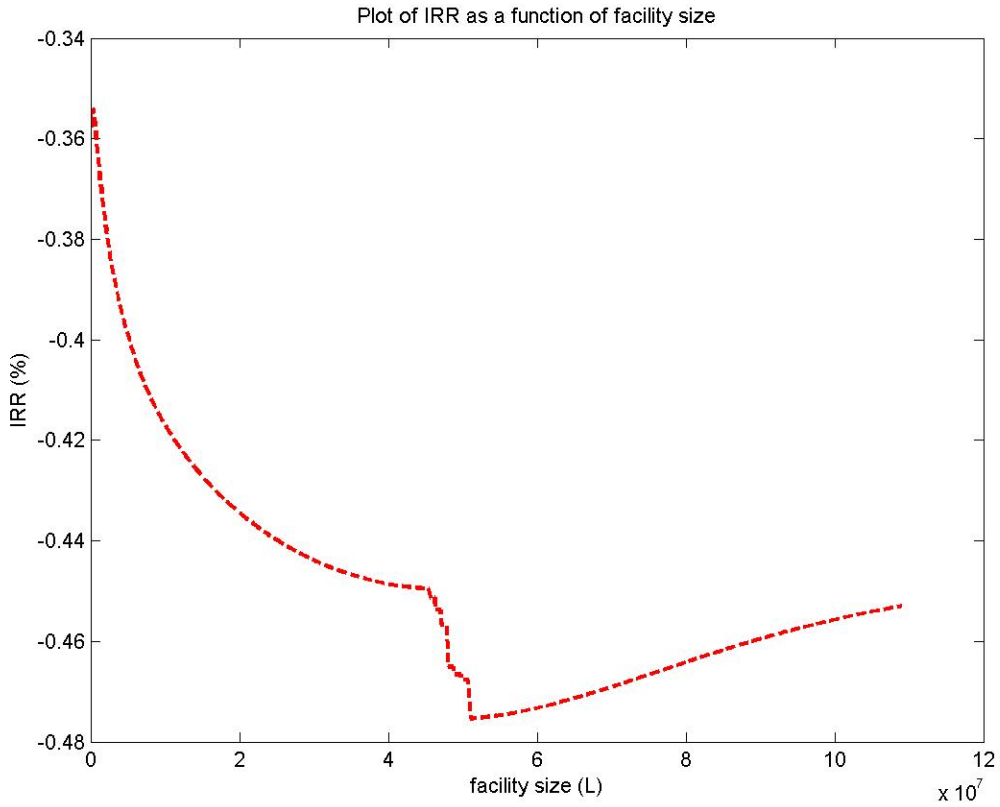

Figure 89: Weekly IRR of fluorescent illuminated ALR as a function of facility size with wastewater (various densities, 75% lipid content).

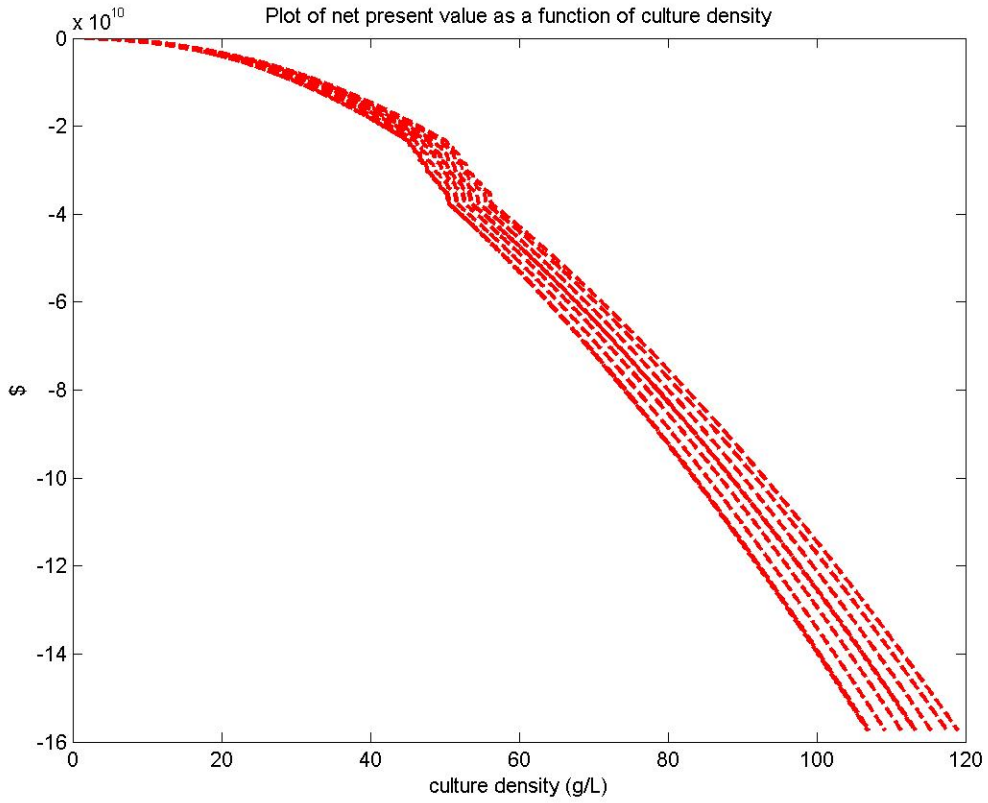

Figure 90: NPV of fluorescent illuminated ALR as a function of culture density with wastewater and 75% lipid content.

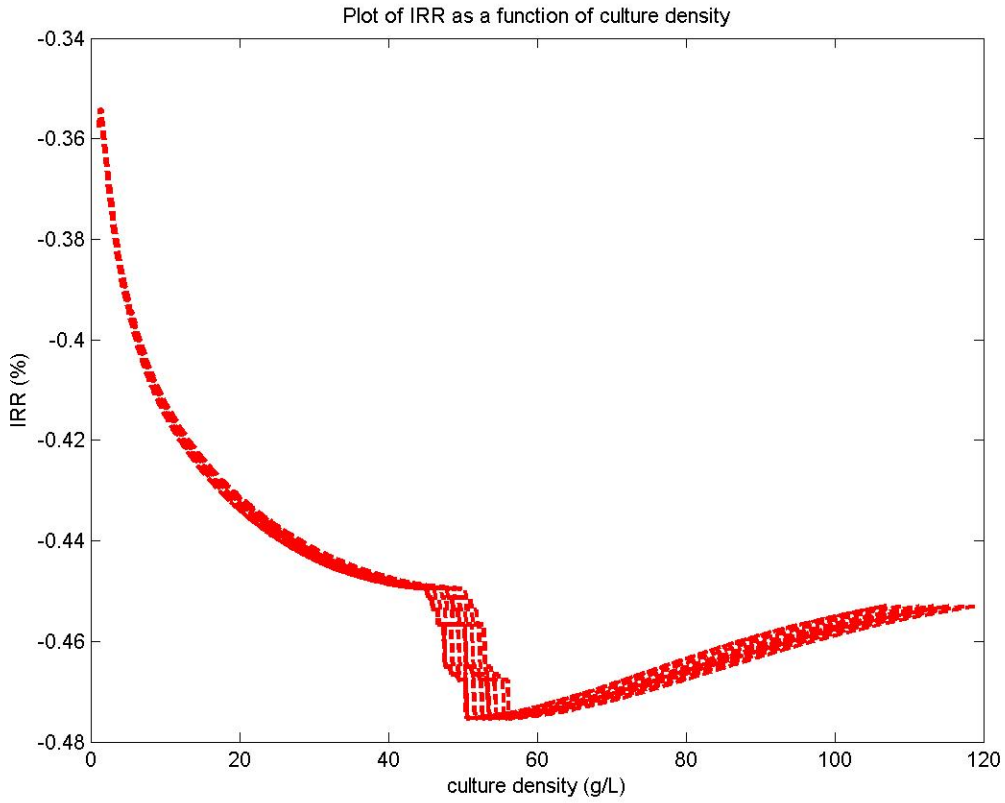

Figure 91: Weekly IRR of fluorescent illuminated ALR as a function of culture density with wastewater, 75% lipid content and facility size from 1.1e5 to 1.0901e8 Liters.

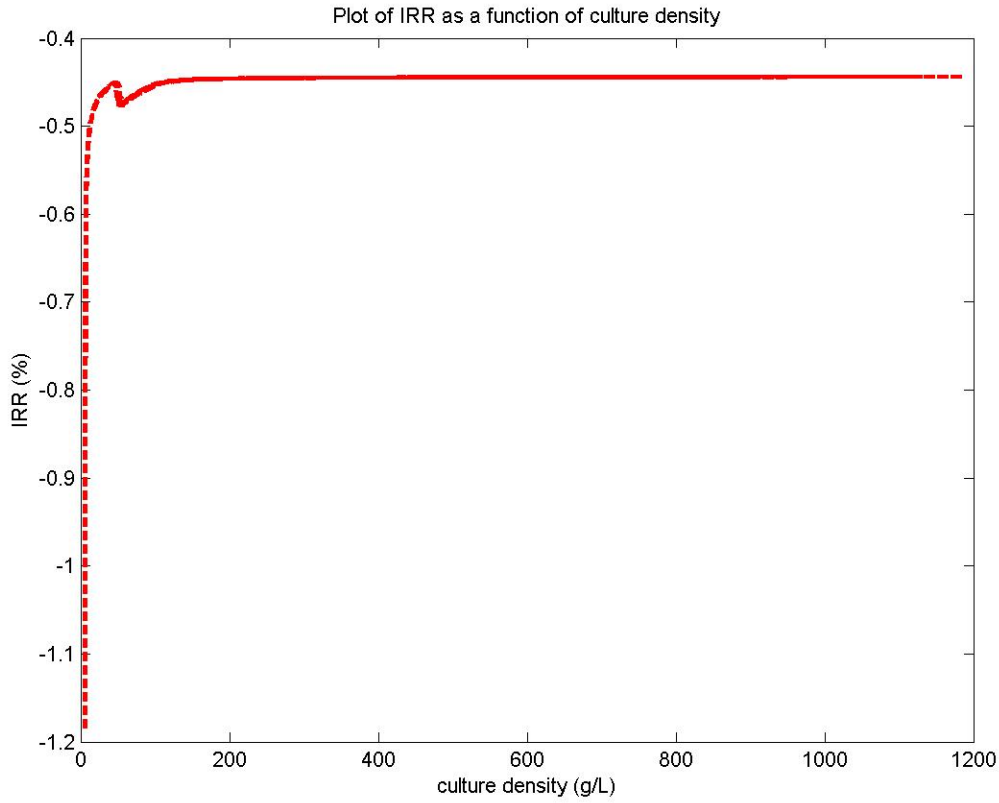

Figure 92: Weekly IRR of fluorescent illuminated ALR as a function of culture density, including ultra-high density (7,500 L facility).

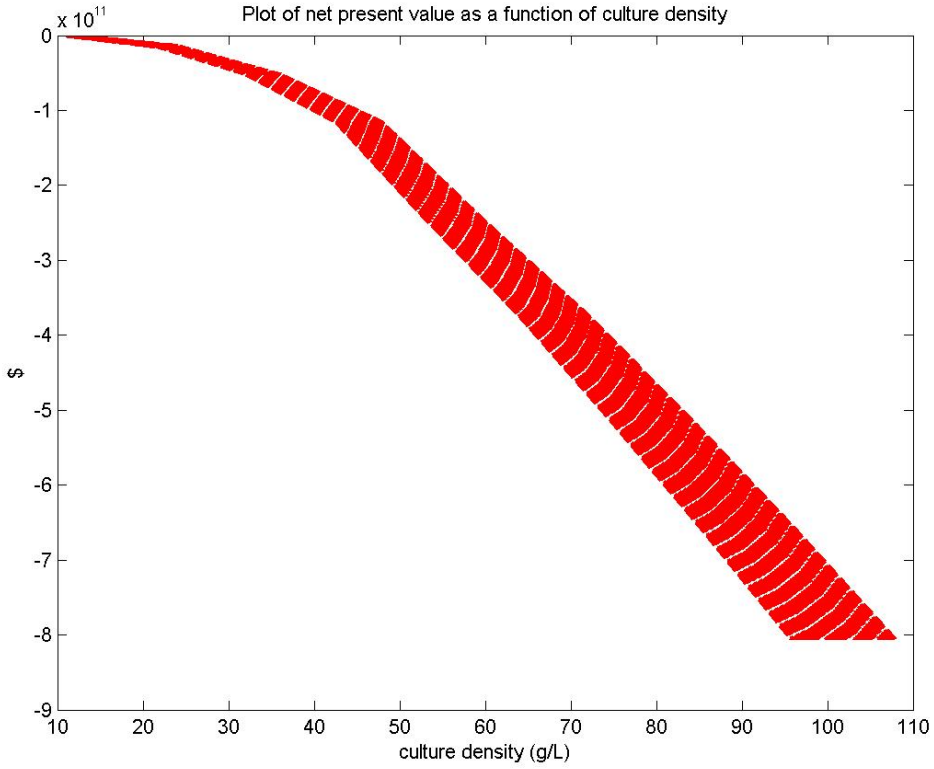

Figure 93: NPV of fluorescent illuminated ALR as a function of culture density, with facility size from 10,000 L to 4e8 L.

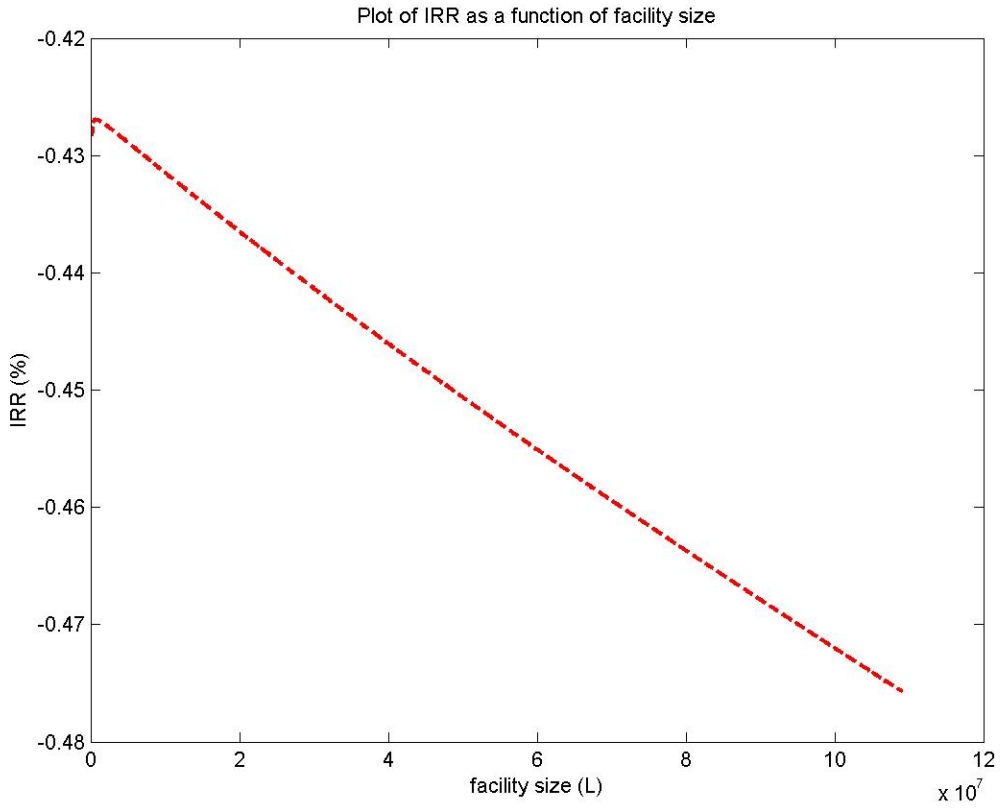

Figure 94: Weekly IRR of fluorescent illuminated ALR as a function of facility size, at culture density of 23-26 g/L and 75% lipid content.

Annual IRR for a fluorescent illuminated ALR growth scenario decreases with increasing facility size as well as increasing culture density up to a density of about 65 g/L where the IRR begins to increase with the culture density but remains negative. The IRR and NPV remain negative even when simulating optimized net profit conditions.

LED Illuminated ALR

An ALR with LED lighting exhibits a similar local optimal density as fluorescent illuminated ALR's at 47 - 48 g/L. This density possesses an NPV of -$3.1432e7, a weekly IRR of -23.4%, and payback period of over 100 years for a 7,500 Liter facility. If

lighting capital is reduced to $0.10 per Watt per year, the initial investment is reduced sufficiently that the NPV is -$6.34e7 and annual IRR remains negative at -16.12% when wastewater is incorporated in a 550,000 Liter facility. An ALR with LED lighting capital cost adjusted to $0.35 per Watt per year has an annual IRR and NPV results identical to the fluorescent illuminated ALR. Similar to the fluorescent illuminated ALR, a positive NPV and IRR are never found for the LED illuminated ALR growth scenario.

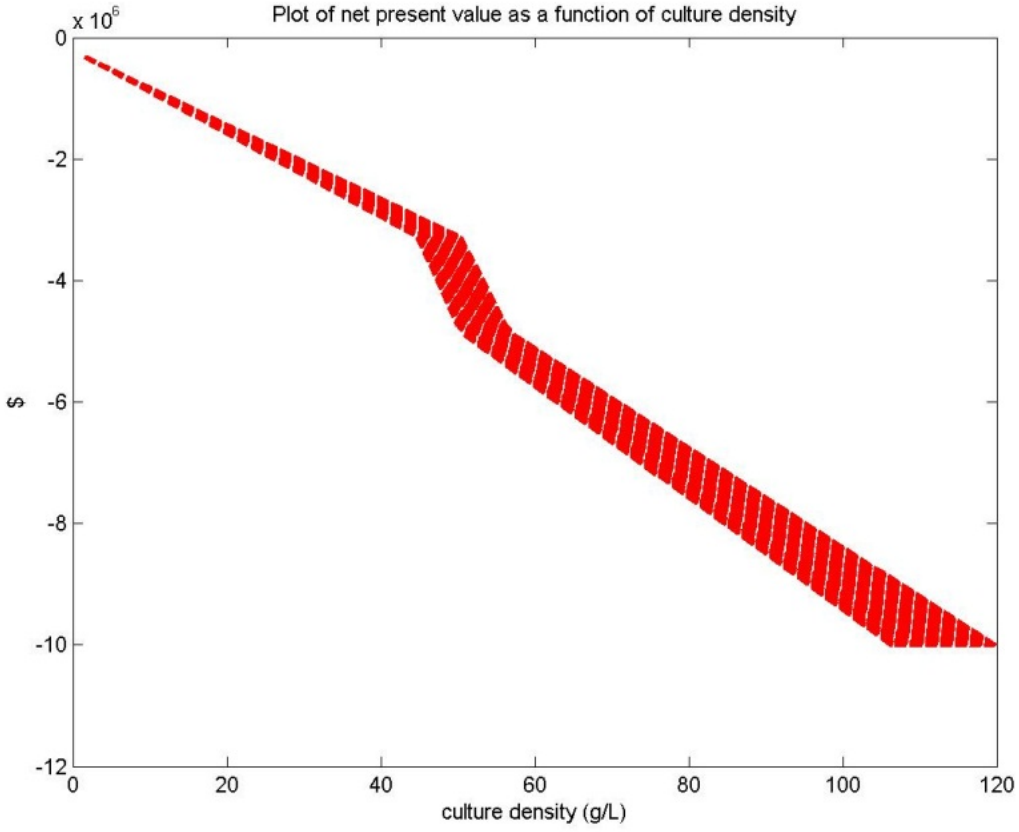

Figure 95: NPV of LED illuminated ALR as a function of culture density (7,500 L).

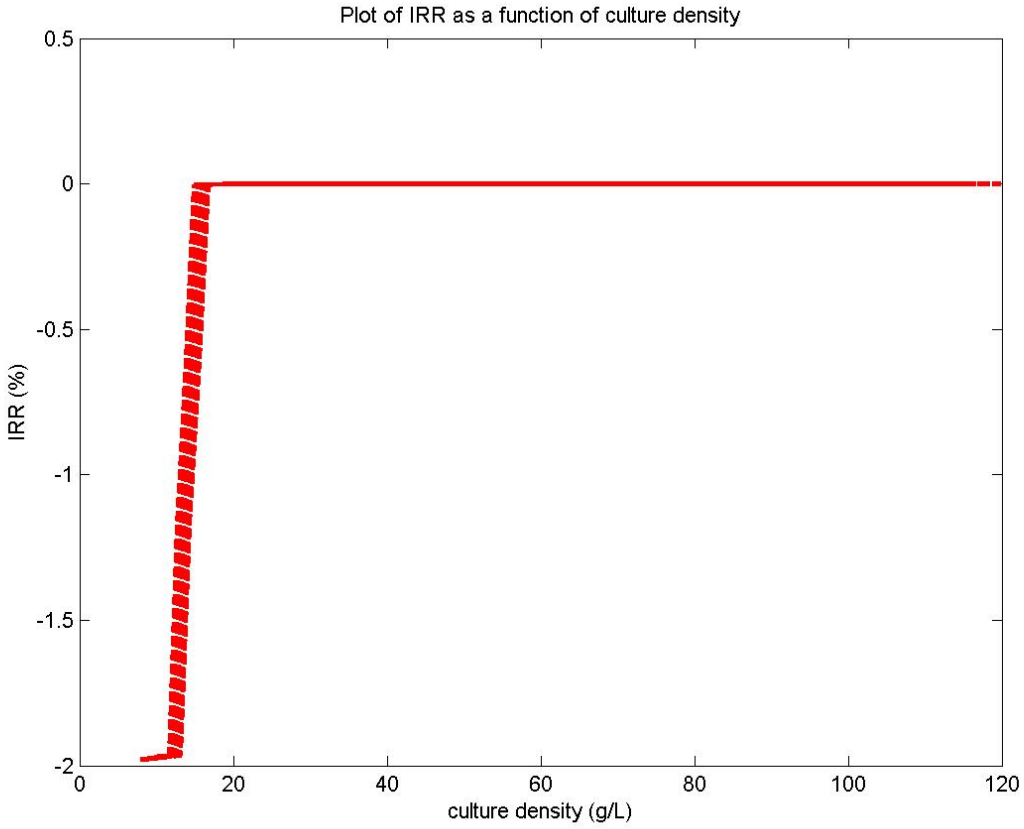

Figure 96: Weekly IRR of LED illuminated ALR as a function of culture density (7,500 L).

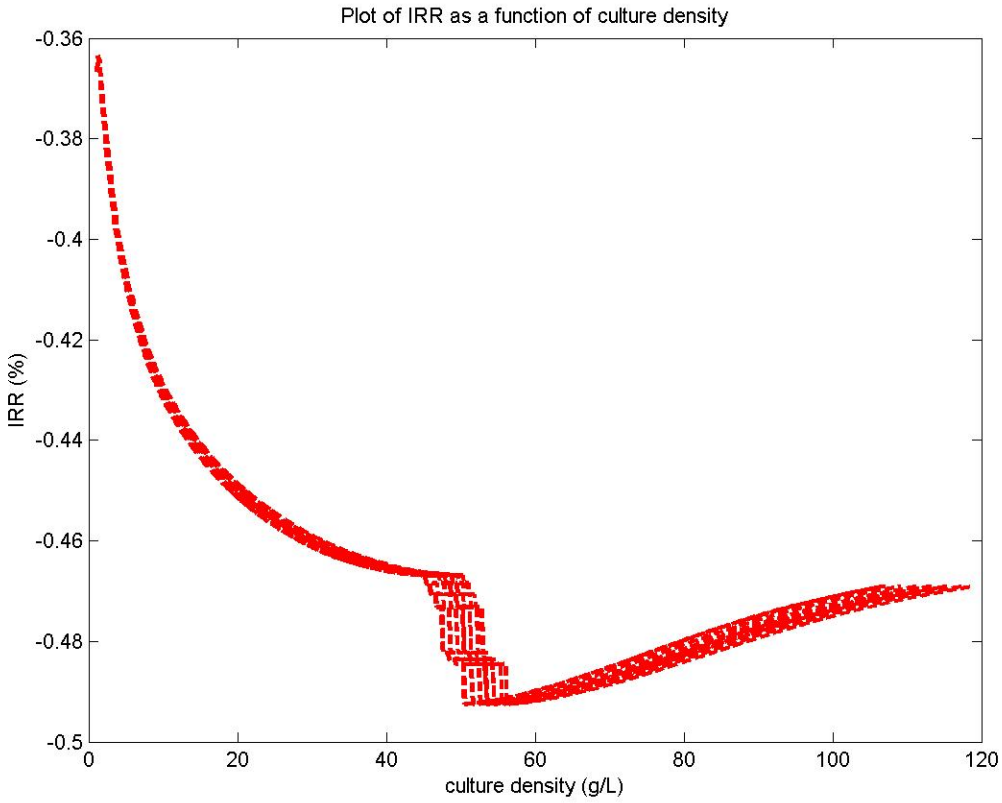

Figure 97: Weekly IRR of LED illuminated ALR as a function of culture density for facility size 1.1e5 to 1.0901e8 L with wastewater treatment and lipid content of 75%.

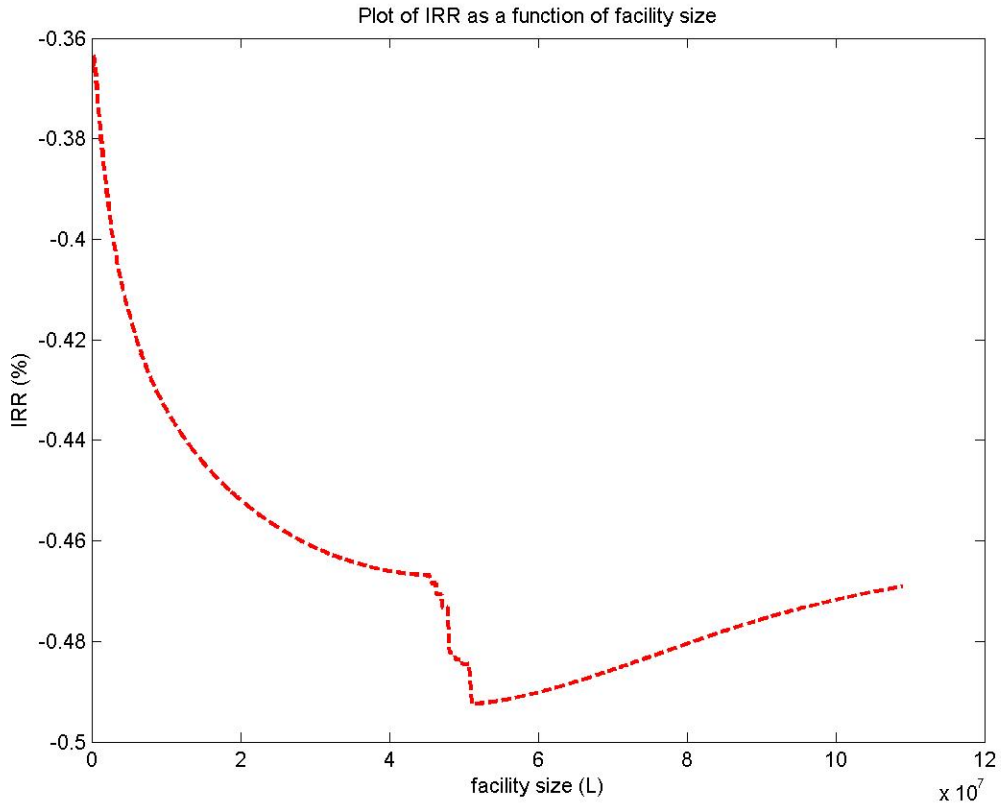

Figure 98: Weekly IRR of LED illuminated ALR as a function of facility size with wastewater treatment and lipid content of 75%.

Incorporating wastewater treatment in the LED and fluorescent illuminated ALR scenarios result in a slightly improved NPV, but it remains negative. NPV and IRR remained negative in all artificially illuminated ALR growth scenarios.

Chapter Four: Discussion

Comparison between this study and past studies reveals why there is so much disparity in the literature and among researchers concerning productivity and yield values. The comparisons with the algal cell size and resulting productivity, between different algal growth scenarios, optimal density, and areal vs. volumetric productivity are illuminating and offer further insight for areas of needed standards for measuring productivity. Also, cost factors which are not included in other techno-economic studies are revealed to greatly influence results, especially operating costs including pumping, creating large scale turbulence, and replacing evaporated water in open pond growth scenarios. When these additional costs are included, the cost of harvesting is revealed to be a much smaller percentage of total costs than previous studies claim for all algal growth scenarios. Future studies do well to define productivity results, species, growth rate and lipid content assumed, growth scenario details including interfaces, cost factors which were included, and how cost factors which were not included might impact results.

While detailed systems analysis was lacking in the literature, results indicate the commercial production of algae for biofuels has not been realized because it is neither economically viable nor sustainable. The systems analysis performed in this study revealed the investment scenario for any algal growth scenario to be at present poor, even when various options are optimized, a daily net profit is evident, and costs are minimized. Despite a favorable business case due to increasing demand with many potential

customers and partners, the technology is lacking for algal produced biodiesel to be competitive with petro-diesel. While financial investment optimizes at a specific facility size, scaling up of current processes and technologies do not solve the fundamental issues outlined below for any growth scenario. Previous studies have proposed that advances in harvesting technologies are needed for economic viability of biofuel produced from algal growth. However, results show the harvesting costs are a small portion of the total costs and the emphasis in technology development should be placed on increasing productivity more efficiently. Inefficiencies with water use and fluid dynamics dominate for open ponds; temperature, low culture density, and lighting distribution are the main concern for solar illuminated photobioreactors; and lighting capital cost is the main concern for artificially illuminated photobioreactors.

The only options which show the potential from a commercial standpoint to show a positive IRR are solar illuminated photobioreactors if the density can be proven achievable at around 76 g/L, wastewater treatment is included, efficient thermal management is achieved, and for artificially illuminated air lift reactors if the capital cost of the lighting is greatly minimized or not included. The capital expenditure and operating expenses of a photobioreactor growth scenario are less than an open pond growth scenario from economical and energy perspectives. Solar illuminated photobioreactors show the most potential of any growth scenario without any improvements in lighting efficiency. Where the proven density for solar illuminated photobioreactors is around 1 g/L, the model shows a net profit beginning at around 2.5 g/L, so growth improvements must be made. Also, the inevitable temperature increase

for solar illuminated photobioreactors from solar heat must be compensated for or managed, and this calculation was not included in the model.

LED illuminated air lift reactors show the most potential for sustainable algal growth if capital cost of LED lighting capital cost is reduced. Fluorescent illuminated air lift reactors come in a close second, but even if the capital cost is reduced for fluorescent lighting, it will remain the less desirable option to LED lighting because of higher operating costs and carbon emissions. Also, there will be some thermal effect of fluorescent lighting which was not included in the model. Additional heat would be of no concern for LED lighting since only PAR wavelengths can be chosen with LED lighting. The light path length does not have significant impact on the artificially illuminated air lift reactors optimal density, but improvements in lighting distribution could reduce the amount of lighting required, thereby reducing the lighting capital cost. The analysis involved in determining the required Watts/Liter is unique to this study as part of a techno-economic analysis which includes an artificially illuminated ALR growth scenario.

While photobioreactors show a small potential for one day being an attractive investment opportunity, especially if partnering with governments or airlines to lower the initial investment, it is difficult to say the same for the open pond growth scenario. The open pond growth scenario shows very little potential to be economically or environmentally sustainable. The model used the same growth rate for all growth scenarios though it will likely be lower in open pond growth scenarios due to sub-optimal fluid dynamics, light and nutrient distribution. A conservative estimate of only 0.1 - 10%

loss from open pond algal density for both nighttime losses and contamination was calculated. Also, even though the application of open ponds will likely be in or close to an urban setting, the rural cost of land ($2300/acre) was used for calculating costs in the model except where noted. Increasing the culture density of open ponds with all costs included does not ever yield a profitable scenario even if the lipid content is assumed at a maximum of 75%. Interestingly, when the model did not include reserving the inoculum density to continue algal growth following harvest, the results did concur with the literature to some extent and showed more potential. It is likely this is a cause for many overestimates in the literature, besides omitting or over-simplifying other key costs such as pumping, employee and paddlewheel operating costs. Costs for producing each kilogram of biomass are comparable to the literature only for the open pond rural scenario at unproven open pond algal density of 16.99 g/L, and not including many key costs such as paddlewheel, inoculum, and pump operating costs.

Land is a limiting factor for open ponds not only for cost reasons, but also for environmental and cultural reasons since the large amount of land required will compete with agriculture. While the required land is clearly objectionable, one also must consider the amount of land which is physically and politically available and that which is affordable. When considered within the scope of locations with climate and water sources, the results are crippling. Additionally, open pond algal farms will face health and safety concerns related to excessive water and land use, and environmental impact will be significant. All the optimizations in this study included rural land cost, and supercritical CO_2, oven, and filter press for harvesting options. This means costs would

be raised substantially for an open pond growth scenario in an urban setting with different harvesting options.

The most important steps to be taken in an open pond growth scenario are to lower water lost to evaporation and reduce the amount of surface area required. Water use is a very large cost factor, and also raises societal and environmental concerns. Additionally, nearly all operating costs need to be reduced, including the pumping, paddlewheel, water, and employee costs. All of these operating costs are related to the large amount of surface area required. Replacing evaporated water and employee costs are the highest operating costs. The energy required from the paddlewheels to maintain a flow velocity of 0.03 m/s for 8 hours per day is a significant open pond operating cost, closely following the pumping of gas to the 20 gas sumps per pond operating 24 hours per day. Results reveal how the roughness factor for a concrete liner versus a clay liner affects costs significantly. The full implications of the large surface area required for an open pond scenario to produce 100,000 kg of dry biomass per year (about 1 barrel of biodiesel per day) where the algal density is 0.32 - 0.37 g/L become evident. The land required is some 825,000 acres or about 1289 square miles.

Some more recent studies have concluded nutrients are a significant cost previously overlooked by most researchers in the past (Christenson & Sims, 2011) (US DOE, 2010) (ANL;NREL;PNNL, 2012). Many studies do not include the cost of nutrients in their techno-economic analysis and very few, if any, include the biggest contributors to cost per the results contained in this study: pH, salt, and antibiotics (see Appendix B). This is especially true for an open pond growth scenario since these

particular nutrients must be administered by the volume of media, not by the algal biomass yield. However, past studies have assumed if wastewater is used, nutrients need not be supplied. Results detailed here indicate the highest cost factors for nutrients would not be supplied by wastewater or flue gas, and may even be more important in a wastewater treatment scenario. For example, the threat of contamination is much higher in a wastewater treatment scenario, which may necessitate more antibiotics. Also, pH buffer will be more vital when using flue gas and/or wastewater. This analysis reveals the costs for nutrients are significant and should be included in any realistic techno-economic analysis.

Some literature has found the key cost and price variables likely to have the biggest impact on the economic performance of the algal cultivation are those for petroleum crude, algal oil, carbon credits from carbon dioxide capture, and commercial fertilizer (Putt, 2007). Brentner, et al. (2011) predicted the most sensitive impact factor to algal culture density is land use. Findings here indicate the biggest impacts on the economic performance of algal cultivation are the culture density and corresponding required surface area which includes the land use, pumping, and employee cost. Commercial fertilizer is not a significant cost factor and is not required if flue gas or wastewater is supplied. While the amount of flue gas from a typical power plant was found to be capable of supporting a very large algal facility, carbon credits and the price of petroleum would have to exceed what is predicted or even imagined in order for algal biofuel production to compete with petroleum.

The majority of profit in an algal growth scenario is from human supplements or wastewater treatment. These two products cannot be produced simultaneously since wastewater treatment will make the algal product unfit for human consumption. Additionally, the human supplement product has a limited customer base and the market will be quickly saturated. For these reasons, the product with the most potential to make algal biofuel production viable is wastewater treatment. This study also revealed the culture density necessary for nitrogen and phosphorus removal from municipal wastewater, which is a higher density than expected in an open pond growth scenario. The culture density of solar illuminated photobioreactors will be the most effective of the growth scenarios for treating wastewater.

The fluid dynamics design and optimization for air lift reactors show it is possible to use known equations to develop a model that allows optimization of productivity based on flow velocity and resulting fluid dynamics, mass flow rate, culture density, cost/profit ratio, CO_2 feed rate, O_2 removal, lighting and geometry. Results reveal that a Newtonian flow can be assumed at expected algal densities and flow velocity. No other studies had performed a viscosity analysis using equations developed to describe non-colloidal dilute suspensions in an external field including effects of culture media (nutrients or wastewater), culture density, saltwater and temperature. Comparison of viscous shear stress to the shear stress per cell at expected culture densities reveal maximum shear stress margin prior to algal cell damage.

Optimal algal growth conditions where the flow is heterogeneous, circulation time is independent of gas velocity, interfacial area reaches a near constant, and level of shear

stress is acceptable can be pinpointed through modeling. Maintenance of heterogeneous flow is vital to avoid suboptimal homogeneous or potentially damaging transitional or slug flow. Model results reveal that many studies have maintained suboptimal flow conditions which may produce non-Newtonian characteristics as gravity exerts a greater influence than the fluid dynamics ($V_G \leq 0.2$ m/s) and is suboptimal homogeneous or slug flow with an eddy Kolgomorov length far exceeding the optimal 10 μm greater than the cell length. Fluid dynamics analysis could improve growth results through determining what conditions maintain heterogeneous, churn turbulent flow. This analysis indicates that in order to maintain heterogeneous flow and constant interfacial area shear rate should be kept between 7,000 and 8,000 s^{-1}.

A local optimal culture density is found for artificially illuminated air lift reactors around 47 - 48 g/L, which results in an air lift reactor total diameter of 1.57 m and a maximum length of 2.7 m based on maximum O_2 levels. The larger diameter enables easier cleaning of the PBR surfaces. Also, results reveal the temperature increase from the photosynthetic process is manageable through replacing the volume of water used in the photosynthetic process at a cooler temperature. The light path length limits pond depth prior to oxygen exceeding levels found to damage microalgal growth in open ponds.

The optimized geometry also revealed the importance of adding a vertical component to an algal growth scenario to reduce all costs which are influenced by the amount of surface area and to improve fluid dynamics. The solar illuminated photobioreactor design presented here may be optimized further through building helical

stacks of tubes. Also, the optimized air lift reactor and solar illuminated culture densities result in a minimum diameter of 0.34 m, which eases concern over maintenance costs since the container may be cleaned through use of a pole mounted squeegee or similar apparatus.

A cheaper, innovative method for light distribution would aid all growth scenarios, although this alone will not enable a profitable scenario for open ponds. Through light distribution the capital cost of lighting could be reduced as well as increase density and depth of the open pond growth scenario, thereby requiring less surface area. Results indicate that if light path length could be optimized through the use of mirrors or some other innovation, costs would at least remain more constant as culture density increases to a certain point (about 50 g/L for artificially illuminated air lift reactors and 0.3398 g/L for open ponds).

Results for harvesting options were interesting for a few reasons. First, the harvesting costs are a much smaller percentage of overall costs (1 - 5%) than predicted by other studies. Second, the cost savings as well as environmental benefits of using supercritical CO_2 as a solvent instead of traditional solvents is significant. Third, use of a centrifuge is not cost prohibitive if the culture density is close to photobioreactor density of 40 - 50 g/L contrary to what is stated in the literature. Cost of inducing lysis using electromagnetism is nearly 25% greater than using a more efficient centrifuge. Inducing lysis through manipulating pH shows significant cost benefits, but this process is yet unproven. Even if harvesting costs are minimized, the costs detailed above for each growth scenario are dominant and prevent an attractive investment profile.

End product results include the fact that biogas and biodiesel profits remain minimal at the most of some $150.00 per day for a 100,000 kg of biomass per year facility. Unless there is a more efficient method of applying methane to algal or power plant energy use, the methane yield does not justify the cost of the microturbines. There is potential of using the methane directly in a power plant if located nearby, but profit is still negligible at less than $100 per day for a ~100,000 kg/year facility. While wastewater treatment is the end product which shows the most potential, it is not sufficient to make an algal growth scenario a worthy investment.

Another key finding from the study is the carbon emissions of all types of algal facilities exceed those of petro-diesel by at least thirteen times even when including carbon consumption of power plant flue gas. The energy in to energy out ratio (MJin/MJout) is at least 10:1 for the PBR growth scenario and about 55:1 for the open pond growth scenario. The carbon emissions from operating the facility only were included, so if one were to include the emissions resulting from producing the materials, the environmental impact would be revealed to be even more detrimental. Even if the investment scenario is improved and an algal growth scenario is found to be financially attractive, it would remain environmentally disastrous. In order to match or produce less carbon emissions than petro-diesel, huge strides in processing technology is necessary.

Chapter Five: Summary

Results show the variables not included in previous studies are important and impact results. Through creating and running the system models, the worst and best case scenarios along with the accompanying technology have been revealed. Productivity optimization based on the same algal growth rate has been accomplished in four different growth scenarios, and financial feasibility has been analyzed for each scenario. Algal growth for biofuel production is not environmentally or economically sustainable with current technology, even when including integration with a power plant and/or wastewater treatment. The only growth scenario to exhibit a positive NPV is solar illuminated photobioreactors at an unproven culture density. While financial feasibility is lacking at proven productivities and lighting costs, the necessary algal densities in each growth scenario along with necessary reductions in costs have been identified.

It took 27 years to achieve a 50% improvement in canola production. Improvement in productivity can be achieved through technical and biological approaches. Improvements in system design for better light utilization and improved mixing as well as increased algal density for solar illuminated photobioreactors are necessary. This study shows it is possible to standardize or optimize algal growth scenarios through modeling, which would result in more consistent quality and quantity of algae produced. This study has also demonstrated that providing optimal fluid dynamics for nutrient distribution, waste removal and lighting distribution are easily solved with a vertical, artificially illuminated photobioreactor. However, results indicate

that a scalable, commercially viable system for producing microalgae is not possible in any growth scenario at this time.

Open pond growth scenarios do not show potential of ever being economically or environmentally sustainable with current technology, and would require reduction in input energy requirements for nearly every process. Even if the potentially detrimental environmental effects of biologically altered algae are avoided, the health and safety concerns of waste disposal and water usage remain in an open pond growth scenario.

While microalgae have the potential to be grown on brackish water and undesirable land, the energy inputs still far outweigh the energy derived. In order to produce just a small percentage of the fossil fuels used annually, a microalgae open pond growth scenario would require an unacceptable amount of land area and fresh water. Photobioreactors, while capable of using much less land and water, require energy inputs which far exceed those required to access petro-diesel.

The carbon footprint of filling a barrel with petro-diesel totals approximately 4,500 grams of CO_2. Consider that every kilowatt-hour of electricity emits 15.9 grams of CO_2, and the average American household uses 29 kilowatt hours (461 grams of CO_2) of electricity every day. This means the carbon footprint of living in an American house for ten days is roughly equivalent to the amount of petro-diesel required to fill a tank twice (assuming a ~15 gallon tank). If the carbon footprint of burning that petro-diesel is added, approximately 67.6 grams of CO_2 per gallon (EPA, 2012), the carbon footprint of burning one tank of petro-diesel is roughly equivalent to the carbon footprint of living in an American house for a week. It is apparent that the main issue with petro-diesel is not

acquiring it (until supply began to dwindle), but the enormous demand and the burning of fossil fuels to satisfy our lifestyle.

Even if a reliable, sustainable, and carbon neutral source of biofuel was secured, past history shows the demand would accelerate along with the supply. Our culture energy demands must decrease along with a continuing search for sustainable and renewable energy supplies in order to successfully prevent or manage future energy shortage and climate change. Presumably, as petro-diesel supply dwindles, a renewable source of transportation fuel will be required and become economically sustainable as the price rises. However, if we hope to lessen our environmental impact or even maintain status quo through using biofuels derived from microalgae, tremendous improvements must be made in algal growth facility design and the technologies implemented.

Further Research

Accuracy of cost estimation would increase for both growth scenarios if the analysis incorporated a detailed schedule. For an open pond scenario there are many time based effects on growth that were not considered or were minimized in this model such as necessary inoculum development in photobioreactors prior to introduction to open ponds, nighttime losses, cloudy days, poor or cold weather, and change in seasons. This would enable more accurate estimates of pumping and storage volume needed. If improved culture density is proven in solar illuminated photobioreactors or capital cost for artificial lighting is greatly reduced, performance of a Class 3, Budget Authorization or Control Estimate is recommended for that particular growth scenario (DOE, 2011). Also, some additional probable costs for photobioreactors which were not included in this

model include pH sensors, thermometers, CO_2 and O_2 sensors, and heat exchangers. A more detailed model to determine temperature changes in an open pond growth scenario including all the environmental factors would be a useful endeavor. Also, a thermal analysis for solar illuminated PBR's and fluorescent illuminated ALR's would improve result accuracy. Further definition of optimal shear stress levels specific to each algae species is recommended.

Solar illuminated photobioreactor modeling would benefit from including more detail, including pH, temperature, and more accurate water evaporation costs. Including pH and temperature requirements for photobioreactor maximum lengths would be beneficial to further optimize geometry. Further analysis into air lift reactor geometry is possible and recommended using the equations detailed in the small scale turbulence methodology section of this study. More detail could also be included in the financial analysis such as transportation costs, shipment timing by farm size and production rate, and insurance.

Additional research may reveal difference in paddlewheel technology or an entirely different method of inducing flow velocity in an open pond growth scenario. Accordingly, solutions to the massive amount of pumping involved must be presented, which could include adding a vertical component to the system while decreasing surface area required and new pumping technology.

A novel method for controlling temperature in solar illuminated photobioreactors that doesn't involve water evaporation could possibly make this growth scenario sustainable. One option is to use excess thermal energy to power the facility. Similarly,

lower cost lighting and/or better method for light distribution could possibly enable a sustainable artificially illuminated photobioreactor growth scenario.

The model reveals is there is much potential in the basic algal growth rate and a need to obtain higher yields than reported in the past. Additional data on beneficial viscous shear stress levels as a function of algae species and culture density will assist in defining design parameters. An improved solution for determining shear rate in photobioreactors is needed. More research into light path length and the optimal shear stress per algal cell will improve result accuracy. Innovative growth scenarios have some potential with microalgae, such as a growth scenario which includes small algal "farms" in each person's home that utilizes energy already present, such as fans, solar, or wastewater leaving the house. Biofilm reactors and immobilized algal growth systems were not included in the analysis due to lack of data, but this may be considered an area of potential study.

Similar system modeling could be applied to other production scenarios, especially technologies considered environmentally sustainable to determine whether that claim is true or not. Similar analysis will benefit any production cycle where improvements are currently made by empiric observations instead of scientific principles or bioassays. Other applications for this type of modeling include optimizing the entire product system in a virtual environment well before physical assembly and testing, optimizing existing production processes, analysis of where costs must be minimized, and methods for improving productivity. While cost/profit ratios can be identified without the use of a model, the results of modifying a process are not detailed sufficiently

for a complicated, interdependent process. A system model can be used to simulate interfaces, which makes it possible to see downstream effects of changing a process.

References

Akhilesh, K.S., Vasumathi, K.K., Premalatha, M. (2011). Simulation of solar light intensity distribution in open pond photobioreactor. *International Journal of Current Science, 1*, 50-57.

Alabi, A. O., Tampier, M., & Bibeau, E. (2009). Microalgae technologies & processes for biofuels/bioenergy in British Columbia: Current technology, suitability & barriers to implementation. British Columbia Innovation Council: Seed Science.

Alcaine, A. A. (2010). Biodiesel from Microalgae. Stockholm: Royal School of Technology.

Al-Dahhan, M. H., & Luo, H.-P. (2006). Culturing Microalgae in Photobioreactors: Advanced Modeling and Experimentation. CREL meeting (p. 22). St Louis: University of Washington School of Engineering & Applied Science.

Al-Masry, W.A., & Chetty M. (1996). On the estimation of effective shear rate in external loop airlift reactors: non-Newtonian fluids. *Resources, Conservation and Recycling, 18*, 11-24.

Ashraf, M., Javaid, M., Rashid, T., Ayub, M., Zafar, A., Ali, S., et al. (2011). Replacement of expensive pure nutritive media with low cost commercial fertilizers for mass culture of freshwater algae, *Chlorella vulgaris*. *International Journal of Agriculture & Biology, 13*, 484-490.

Augusti, S. & Kalff, J. (1989). The influence of growth conditions on the size dependence of maximal algal density and biomass. *Limnol. Oceanogr., 34*(6), 1104-1108.

Barberio, G., Aresta, M., & Dibenedetto, A. (2005). Utilization of macro-algae for enhanced CO2 fixation and biofuels production: Development of a computing software for an LCA study. *Fuel Processing Technology, 86* (14-15), 1679-1693.

Barbosa, M.J.G.V. (2003). *Microalgal photobioreactors: Scale up and optimization.* Ph.D. Thesis, Wageningen University, Wageningen, The Netherlands, ISBN: 90-5808-898-7.

Batan, L., Quinn, J., Willson, B., Bradley, T. (2010). Net energy and greenhouse gas emission evaluation of biodiesel derived from microalgae. *Environmental Science Technology, 44,* 7975-7980.

Bayless, D., Kremer, G., Prudich, M., Stuart, B., Vis-Chiasson, M., & Cooksey, K. *Enhanced Practical Photosynthetic CO2 Mitigation*. Various: U.S. Department of Energy.

BCC Research, Inc. (2008). The global market for carotenoids. Report ID: FOD025C. Retrieved November 21, 2012 from www.bccresearch.com.

Beal, C.M., Stillwell, A.S., King, C.W., Cohen, S.M., Berberoglu, H., Bhattarai, R.P., Connelly, R., Webber, M.E., Hebner, R.E. (2012). *Energy return on investment for algal biofuel production coupled with wastewater treatment.* University of Texas at Austin, Austin, TX 78712, USA.

Beardall, J., & Quigg, A. (2003). Protein turnover in relation to maintenance metabolism at low photon flux in two marine microalgae. *Plant, Cell and Environmen , 26,* 693-803.

Beardall, J., Ihnken, S., & Quigg, A. (2008). Gross and net primary production: closing the gap between concepts and measurements. *Aquatic Microbial Ecology, 56,* 113-122.

Beardall, J., Quigg, A., & Wydrzynski, T. (2003). Photoacclimation involves modulation of the photosynthetic oxygen-evolving reactions in *Dunaliella tertiolecta* and *Phaeodactylum tricornutum*. *Functional Plant Biology, 30,* 301-308.

Behrens, P. W. (2005). Photobioreactors and fermentators: The light and dark sides of growing algae. In: Andersen, R.A. [Ed.] *Algal Culturing Techniques.* Academic Press, San Diego, pp. 578.

Beneman, J., Pedroni, P. M., Davison, J., Beckert, H., & Bergman, P. (2004). Technology Roadmap for Biofixation of CO2 and Greenhouse Gas Abatement with Microalgae. (pp. 1-11). U.S. Department of Energy-National Energy Technology Laboratory.

Benemann, J.R., & Oswald, W.J. (1996). *Systems and economic analysis of microalgae ponds for conversion of CO_2 to biomass.* Final report, U.S. Department of Energy.

Berberoglu, H., Barra, N., Pilon, L., & Jay, J. (2008). Growth, CO2 consumption, and H2 production of Anaebaena variabilis ATCC29413-U under different irradiances and CO2 concentrations. *Journal of Applied Microbiology, 104,* 105-121.

Berman-Frank, I., Quigg, A., Finkel, Z. V., Irwin, A. J., & Haramaty, L. (2007). nitrogen-fixation strategies and Fe requirements in cyanobacteria. *Association of Limnology and Oceanography, 5* (52), 000-000.

Biggs, M.C. (1975). Constrained Minimization Using Recursive Quadratic Programming. In: L.C.W. Dixon and G.P. Szergo [Eds.] *Towards Global Optimization*, North-Holland, pp. 341–349.

Bilanovic, D., Shelef, G., Sukenik, A. (1988). Flocculation of microalgae with cationic polymers - effects of medium salinity. *Biomass, 17,* 65-76.

Bligh, E.G., & Dyer, W.J. (1959). A rapid method of total lipid extraction and purification. *Can. Journal of Bio. and Phys., 37,* 8, 911-917.

Brenner, H. (1969). Rheology of a dilute suspension of dipolar spherical particles in an external field. *Journal of Colloid and Interface Science, 32,* 1, 141-158.

Brentner, L.B., Eckelman, M.J., Zimmerman, J.B. (2011). Combinatorial life cycle assessment to inform process design of industrial production of algal biodiesel. *Environmental Science & Technology, 45,* 7060-7067.

Brune, D., Lundquist, T., & Benemann, J. (2009, N/A N/A). Microalgal biomass for greenhouse gas reductions: Potential for replacement of fossil-fuels and animal feeds. La Jolla, CA, USA.

Bussell, S., Sullivan, L., Kulikowski-Tan, A., & Weaver, D. (2008). Algae based carbon absorption for natural gas-fired power plants. Technical Brief. La Jolla, CA, USA: Carbon Capture Corp.

Byrd, R.H., J. C. Gilbert, & Nocedal, J. (2000). A Trust Region Method Based on Interior Point Techniques for Nonlinear Programming, *Mathematical Programming, 89,* 1, 149–185.

Camacho, F.G., Gomez, A.C., Fernandez, F.G.A., Sevilla, J.F., Grima, E.M. (1999). Use of concentric-tube airlift photobioreactors for microalgal outdoor mass cultures. *Enzyme and Microbial Technology, 24,* 164-172.

Cantrell, K., Ducey, T., Ro, K., & Hunt, P. (2008). Livestock waste-to-bioenergy generation opportunities. *Bioresource Technolog , 99* (17), 7491-7953.

Carrington, D. (2012) Leaked Data: Palm biodiesel as dirty as fuel from tar sands. *The Guardian,* January 27, 2012. Retrieved February 6, 2012 from: http://guardian.co.uk

Carvalho, A. P., & Malcata, F. X. (2001). Transfer of Carbon Dioxide within cultures of microalgae: Plain bubbling versus hollow-fiber modules. *Biotechnol. Prog., 17,* 265-272.

Carvalho, A. P., Meireles, L. A., & Malcata, F. X. (2006). Microalgal reactors: A review of enclosed system designs and performances. *Biotechnol. Prog. , 22,* 1490-1506.

Chaumont, D. (1993). Biotechnology of algal biomass production: a review of systems for outdoor mass culture. *Journal of Applied Phycology, 5,* 593-604.

Chase, R.B., Jacobs, R.F., & Aquilano, N.J. (2006). *Operations management for competitive advantage.* (11th ed.). New York: McGraw-Hill.

Chhabra, R.P. & Richardson, J.F. (2008). Non-Newtonian flow and Applied Rheology: Engineering Applications, Second Edition. Elsevier Science and Technology books, Inc., Elsevier Ltd.

Chinnasamy, S., Bhatnagar, A., Hunt, R.W., Das, K.C. (2010). Microalgae cultivation in a wastewater dominated by carpet mill effluents for biofuel applications. *Bioresource Technology, 101,* 3097-3105.

Chisti, Y. (2007). Biodiesel from microalgae. *Biotechnology Advances, 25,* 294-306.

Chisti, Y. (2008). Biodiesel from microalgae beats bioethanol. *Trends in Biotechnology, 26,* 3, 126-131.

Chrismadha, T., & Borowitzka, M. A. (1994). Effect of cell density and irradiance on growth, proximate composition and eicosapentaeonic acid production of *Phaeodactylum tricornutum* grown in a tubular photobioreactor. *Journal of Applied Phycology, 6,* 67-74.

Christenson, L. & Sims, R. (2011). Production and harvesting of microalgae for wastewater treatment, biofuels, and bioproducts. *Biotechnology Advances, 29,* 686-702.

Clarens, A.F., Resurrenccion, E.P., White, M.A., Colosi, L.M. (2010). Environmental life cycle comparison of algae to other bioenergy feedstocks. *Environ. Sci. Technol., 44,* 1813-1819.

Columbia Boulevard Wastewater Treatment Plant. (September, 2006). *Energy Management using Microturbine Technology.* Portland, Oregon. Retrieved February 1, 2012 from: http://www.naseo.org/committees/energyproduction/documents/Energy_Management_using_Microturbine_Technology.pdf

Contreras, A., Garcia, F., Molina, E., & Merchuk, J. (1998). Interaction between CO2-mass transfer, light availability, and hydrodynamic stress in the growth of Phaeodactylum triconutum in a concentric tube airlift photobioreactor. *Biotechnology and Bioengineering, 60* (3), 317-325.

Cornet, J.F., Dussap, C.G., Dubertret, G. (1992a). A structured model for simulation of cultures of the cyanobacterium, *Spirulina platensis* in photobioreactors: Coupling between light transfer and growth kinetics. *Biotechnol. Bioeng., 40,* 817-825.

Creswell, LeRoy (2010). Phytoplankton for aquaculture feed. SRAC Publication No. 50004. Retrieved January 18, 2012 from https://srac.tamu.edu/index.cfm/event/getFactSheet/whichfactsheet/224/.

Davis, E.A., Dedrick, J., French, C.S., Milner, H.W., Myers, J., Smith, J.H.C., & Spoehr, H.A. (1953). Laboratory experiments on *Chlorella* culture. *Algal Culture from Laboratory to Pilot Plant* (ed. J.S. Burlew), 105-153. Washington D.C.: Carnegies Institute of Washington.

ANL;NREL;PNNL. (June, 2012). *Renewable Diesel from Algal Lipids: An Integrated Baseline for Cost, Emissions, and Resource Potential from a Harmonized Model.* ANL/ESD/12-4; NREAL/TP-5100-55431; PNNL-21437. Argonne, IL: Argonne National Laboratory; Golden, CO: National Renewable Energy Laboratory; Richland, WA: Pacific Northwest National Laboratory.

Degen, J., Uebele, A., Retze, A., Schmid-Staiger, U., Trosch, W. (2001). A novel airlift photobioreactor with baffles for improved light utilization through the flashing light effect. *Journal of Biotechnology, 92,* 89-94.

Demirbas, A., & Demirbas, M. F. (2010). *Algae Energy: Algae as a New Source of Biodiesel.* ISBN:9781849960496: Springer.

Department of Energy (May 9, 2011). Cost Estimating Guide. Retrieved 06/11/2012 from: https://www.directives.doe.gov.

Dimitrov, K. (2007). Greenfuel Technologies: A case study for industrial photosynthetic energy capture. Retrieved February 4, 2012 from: http://www.ecolo.org/documents/documents_in_english/biofuels-Algae-CaseStudy-09.pdf.

Dismukes, G. (2008). Algal Photosynthesis. Princeton University: Princeton University Dept of Chemistry & Princeton Environmental Institute.

Dismukes, G., Carrieri, D., Bennette, N., Ananyev, G., & Posewitz, M. (2008). Aquatic phototrophs: efficient alternatives to land-based crops for biofuels. *Current Opinion in Biotechnology, 19* (3), 235-240.

Doran, P.M. (1993). Design of reactors for plant cells and organisms. *Advanced Biochemical Engineering, 48,* 115-168.

Doshi, V. V. (2006). *Measurement of Algal Growth Rate between Harvests in an Artificially Illuminated Photobioreactor Under Flue Gas Conditions.* Ohio University: Russ College of Engineering and Technology.

Einstein, A., (1906). A new determination of molecular dimensions. *Ann. Physik., 19,* 289.

Einstein, A., (1911). A new determination of molecular dimensions. *Ann. Physik., 34,* 591.

Eishi, T., & Toshihiko M. (2000). *An illustrated guide to freshwater zooplankton in Japan.* Tokyo: Tokai Daigaku Shuppankai.

Environmental Protection Agency (2004). Generating electricity with coal mine methane-fueled micro turbines. *Air and Radiation, 6202J,* March, 2004. Retrieved February 1, 2012 from: http://epa.gov/coalbed/docs/microturbine.pdf.

Environmental Protection Agency (2012). Cap and Trade. Retrieved March 21, 2012 from: http://www.epa.gov/captrade/.

Environmental Protection Agency (2012). Egrid2012, Version 1.0, year 2009 data. Retrieved May 8, 2013 from: http://www.epa.gov/cleanenergy/energy-resources/refs.html.

Evodos (2011). Total Dewatering Algae. Retrieved May 1, 2013 from: http://www.evodos.eu/market-specific-solutions/algae.html.

Falciatore, A., Ribera d'Alcala, M., Croot, P., Bowler, C. (2000). Perception of environment signals by a marine diatom. *Science, 288,* 2363-2366.

Ferreira, B. S., Fernandes, H. L., Reis, A., & Mateus, M. (1998). Microporous hollow fibres for Carbon Dioxide absorption: Mass transfer model fitting and the supplying of Carbon Dioxide to microalgal cultures. *J. Chem. Technol. Biotechnol., 71,* 61-70.

Finkel, Z. V., Beardall, J., Flynn, K. J., Quigg, A., Rees, T. A., & Raven, J. A. (2010). Phytoplankton in a changing world: cell size and elemental stoichiometry. *Journal of Plankton Research, 32* (1), 119-137.

Finkel, Z. V., Quigg, A. S., Chiampi, R. K., Schofield, O. E., & Falkowski, P. G. (2007). Phylogenetic diversity in cadmium: phosphorus ratio regulation by marine phytoplankton. *Association of Limnology and Oceanography, 52* (3), 1131-11389.

Fisher, N., & Cowdell, R. (1982). Growth of marine planktonic diatoms on inorganic and organic nitrogen. *Marine Biology, 72* (2), 147-155.

Flynn, K. J., Raven, J. A., Rees, T. A., Finkel, Z., Quigg, A., & Beardall, J. (2010). Is the growth rate hypothesis applicable to microalgae? *J. Phycol., 46*, 1-12.

Food and Agriculture Organization of the United Nations (1997). *Renewable biological systems for alternative sustainable energy production.* Job No: W7241, Version 128. Retrieved February 1, 2012 from: http://www.fao.org/docrep/w7241e/w7241e0h.htm

Fournadzieva, S., Bohadgieva, K., Fytikas, M., & Popovski, K. (2001). *A conception of geothermal application in common microalgal development in balkan countries.* International Summer School on Direct Application of Geothermal Energy . Greece: Division of Earth Sciences.

Frac, M., Jezierska-Tys, S., & Tys, J. (2010). Microalgae for biofuels production and environmental applications: a review. *Journal of Biotechnology, 9* (54), 9227-9236.

Frank, E.D., Han, J., Palou-Rivera, I., Elgowainy, A., Wang, M.Q. (2012). Methane and nitrous oxide emissions affect the life-cycle analysis of algal biofuels. *Environmental Research Letters, 7,* 1-10.

Frederickson, A.G., Brown, A.H., Millar, R.L., & Tsuchiya, H.M. (1961). Optimum conditions for photosynthesis in optically dense cultures of algae. *Journal of the American Rocket Science, 31,* 1429-1435.

Gardner, J. (2011, June 8). Don't Discount Biofuels. Retrieved September 13, 2011, from Xconomy: http://www.xconomy.com/national/2011/06/08/dont-discount-biofuels/

General Atomics. (2009, January 19). General Atomics to Develop Algae-Derived Jet Fuel under DARPA Contract. Retrieved December 21, 2011, from General Atomics and Affiliated Partners: http://www.ga.com/news.php?read=1&id=177&page=4

Golueke, C.G., Oswald, W.J., Gotaas, H.B. (1956). Anaerobic Digestion of Algae. *Applied Microbiology,* September 4, 1956. Retrieved January 31, 2012 from: http://www.ncbi.nlm.nih.gov/pmc/articles/PMC1057253/pdf/applmicro00309-0054.pdf.

Greene, D.L., & Plotkin, S.E. (2011). Reducing greenhouse gas emissions from US transportation. Prepared for the *Pew Center on Global Climate Change.* January, 2011.

Greenwell, H., Laurens, L., Shields, R., Lovitt, R., & Flynn, K. (2010). Placing microalgae on the biofuels priority list: a review of the technological challenges. *Journal of the Royal Society Interface, 7,* 703-726.

Greenwood, N. & Earnshaw, A. (1997). *Chemistry of the Elements* (2nd ed.). Oxford: Butterworth-Heinemann. ISBN 0080379419.

GREET, The Greenhouse Gases, Regulated Emissions, and Energy Use in Transportation Model, GREET 1.8d.1, developed by Argonne National Laboratory, Argonne, IL, released August 26, 2010.

Griffiths, D. (1973). Factors affecting the photosynthetic capacity of laboratory cultures of the diatom *Phaeodactylum tricornutum*. *Marine Biolog, 21* (2), 91-97.

Grima, E. M., Perez, J. S., Camacho, F. G., & Medina, A. R. (1993). Gas-liquid transfer of atmospheric CO2 in microalgal cultures. *J. Chem. Tech. Biotechnol., 56,* 329-337.

Hall, D. O., Fernandez, F. A., Guerrero, E. C., Rao, K. K., & Grima, M. (2003). Outdoor helical tubular photobioreactors for microalgal production: modeling of fluid-dynamics and mass transfer and assessment of biomass productivity. *Journal of Biotechnology and Bioengineering, 82* (1), 62-73.

Han, S.P., (1977). A Globally Convergent Method for Nonlinear Programming. *J. Optimization Theory and Applications, 22,* 297.

Hartman, P. & Cleland, J. (2007). Wastewater treatment performance and cost data to support an affordability analysis for water quality standards. *ICF International,* Lexington, Massachusetts, May 31, 2007.

Herbing, I.H. & Keating, K. (2003). *Temperature-induced changes in viscosity and its effects on swimming speed in larval haddock.* Institute of Marine Research, Bergen, Norway, ISBN 82-7461-059-8.

Hibberd (1981). Notes on the taxonomy and nomenclature of the algal classes *Eustigmatophyceae* and *Tribophyceae* (Synonym *Xanthophyceae*). *Botanical Journal of the Linnean Society 82*: 93-119,

Ho, T.-Y., Quigg, A., Finkel, Z. V., Milligan, A. J., Wyman, K., Falkowski, P. G., et al. (2003). The elemental composition of some marine phytoplankton. *Journal of Phycology, 39,* 1145-1159.

Holdsworth, E. (1985). Effect of growth factors and light quality on the growth, pigmentation and photosynthesis of two diatoms, *Thalassiosira gravida* and *Phaeodactylum tricornutum*. *Marine Biology, 86,* 253-262.

Hondzo, M. & Lyn, D. (1999). Quantified small-scale turbulence inhibits the growth of green alga. *Freshwater Biology, 41,* 51-61.

Hu, Q., Sommerfeld, M., Jarvis, E., Ghirardi, M., Posewitz, M., Seibert, M., et al. (2008). Microalgal triacylglycerols as feedstocks for biofuel production: perspectives and advances. *Plant Journal, 54* (4), 621-639.

Huber, M.L., Perkins, R.A., Laesecke, A., Friend, D.G., Sengers, J.V., Assael, M.J., Metaxa, I.N., Vogel, E., Mares, R., Miyagawa, K. (2009). New International Formulation for the Viscosity of H2O. *J. Phys. Chem. Ref. Data, 38,* 2, 101-125.

Iancu, P., Velea, S., Plesu, V., Muscalu, C., & David, R. (2010). Modelling and simulation of CO2 absorption in alkaline buffer solutions in gPROMS. *Chemical Engineering Transactions, 21,* 679-684.

Illman, A., Scragg, A., & Shales, S. (2000). Increase in *Chlorella* strains calorific values when grown in low nitrogen medium. *Enzyme and Microbial Technology, 27* (8), 631-635.

James, S.C., & Boriah, V. (2010). Modeling algae growth in an open-channel raceway. *Journal of Computational Biology, 17,* 895-906.

Janssen, M., Tramper, J., Mui, L. R., & Wijffels, R. H. (2002). Enclosed outdoor photobioreactors: Light regime, photosynthetic efficiency, scale-up, and future prospects. *Biotechnology and Bioengineering, 81* (2), 193-210.

Jenkinson, I.R. (1986). Oceanographic implications of non-newtonian properties found in phytoplankton cultures. *Nature, London, 323,* 435-437.

Jibuti, L., Rafai, S., & Peyla, P. (2012). Suspensions with a tunable effective viscosity: a numerical study. *Journal of Fluid Mechanics, 693,* 345-366.

Johnston, L., Hausman, E., Biewald, B., Wilson, R., White, D. (2011). 2011 Carbon Dioxide Price Forecast. Synapse Energy Economics, February, 11, 2011.

Kadam, K. (2002). Environmental implications of power generation via coal-microalgae co-firing. Energy, 27 (10), 905-922.

Kadam, K. (1997). Power plant flue gas as source of CO2 for microalgae cultivation: economic impact of different process options. *Energy Conversion and Management, 38,* 505-510.

Kang, C. D., Han, S. J., Choi, S. P., & Sim, S. J. (2010). Fed-batch culture of astaxanthin-rich *Haematococcus pluvialis* by exponential nutrient feeding and stepwise light supplementation. *Bioprocess and Biosystems Engineering, 33* (1), 133-139.

Karassik, I.J., Messina, J.P., Cooper, P., & Heald, C.C. (2001). *Pump Handbook* (3rd Ed.). New York: McGraw-Hill.

Kaye & Laby (2005). Tables of Physical & Chemical Constants (16th edition 1995). 2.1.4 Hygrometry. Kaye & Laby Online. Version 1.0 (2005), Retrieved January 13, 2013 from: www.kayelaby.npl.co.uk.

Kazuhisa M. (1997). *Renewable biological systems for alternative sustainable energy production* (FAO Agricultural Services Bulletin - 128). Final. FAO - Food and Agriculture Organization of the United Nations.

Kerzner, H. (2006). *Project Management: A Systems Approach to Planning, Scheduling, and Controlling* (9th Ed.). Hoboken, NJ: John Wiley & Sons.

Kong, Q., Li, L., Martinez, B., Chen, P., Ruan, R. (2010). Culture of microalgae *Chlamydomonas reinhardtii* in wastewater for biomass feedstock production. *Appl Biochem Biotechnol, 160,* 9-18.

Krieger, I.M., & Dougherty, T.J. (1959). A mechanism for non-Newtonian flow in suspensions of rigid spheres. *Transactions of the Society of Rheology, III,* 137-152.

Kwangyong, L., & Choul-Gyun, L. (2002). Nitrogen removal from wastewaters by microalgae without consuming organic carbon sources. *Journal of Microbiology Biotechnology, 12* (6), 979-985.

Lane, Jim. (2012, February 8). Aviation and military biofuels: new thinking on finance, fuels. *Biofuels Digest*. Retrieved February 27, 2012 from: http://www.biofuelsdigest.com/bdigest/2012/02/08/aviation-and-military-biofuels-new-thinking-on-finance-fuels/.

Lee, C.-G., & Palsson, B. O. (1994). High-density algal photobioreactors using light-emitting diodes. *Biotechnology & Bioengineering, 44,* 1161-1167.

Lee, Y.-K., & Hing, H.-K. (1989). Supplying CO2 to photosynthetic algal cultures by diffusion through gas-permeable membranes. *Appl. Microbiol Biotechnol, 31,* 398-301.

Lelleveld, J., Lechtenbohmer, S., Assonov, S., Brenninkmeijer, C., Dienst, C., Fishedick, M., et al. (2005). Greenhouse gases: Low methane leakage from gas pipelines. *Nature, 434,* 841, 842.

Liebert, T. (2007). CO2 Sequestration by Algae Reactors. Retrieved September 13, 2011, from Kansas Sierra Club: http://kansas.sierraclub.org/Wind/AlgaeReactors.htm

Lopez-Elias, J.A., Enriquez-Ocana, F., Pablos-Mitre, M.N., Huerta-Aldez, N., Leal, S., Miranda-Baeza, A., Nieves-Soto, M., Vasquez-Salgado, I. (2008). Growth and biomass production of *Chaetoceros muelleri* in mass outdoor cultures: Effect of the hour of the inoculation, size of the inoculum and culture medium. *Rev. Invest. Mar., 29*(2), 171-177.

Lopez-Elias, J.A., Voltolina , D., Mercado, I.S., Nieves, M., Equivel, B.C. (2005). Growth, composition and biomass yields of *Chaetoceros muelleri* mass cultures with different routines and tank depths. *Rev. Invest. Mar., 26*(1), 67-72.

Lu, C., Rao, K., Hall, D., & Vonshak, A. (2001). Production of eicosapentaenoic acid (EPA) in *Monodus subterraneus* grown in a helical tubular photobioreactor as affected by cell density and light intensity. *Journal of Applied Phycology, 13* (6), 517-522.

Lundquist, T.J., Woertz, I.C., Quinn, N.W.T., & Benemann, J.R. (2010). A Realistic Technology and Engineering Assessment of Algae Biofuel Production. Civil and Environmental Engineering Department, California Polytechnic State University, San Luis Obispo, California.

Lux Research (2012). Pruning the Cost of Bio-Based Materials and Chemicals. LRMCI-R12-2.

MacIntyre, H.I., & Cullen, J. J. (2005). Using cultures to investigate the physiological ecology of microalgae. In: Andersen, R.A. [Ed.] *Algal Culturing Techniques.* Academic Press, San Diego, pp. 287-326.

Maldonado, E.M. & Latz M.I. (2007). Shear-stress dependence of dinoflagellate bioluminescence. *Biol. Bull., 212,* 242-249.

Maloney, B., Iliffe, T. M., Gelwick, F., & Quigg, A. (2011). Effect of nutrient enrichment on naturally occurring macroalgal species in six cave pools in Bermuda. *Phycologia, 50* (2), 132-143.

Matlab (2012). High-level language and interactive environment for numerical computation, visualization, and programming. [Computer software and manual]. Natick, MA: Mathworks.

McCall, J. (2011). Apparatus and methods for production of biodiesel. United States Patent 7950181 B2, May 31, 2011.

Merchuk, J.C., & Berzin, I. (1995). Distribution of energy dissipation in airlift reactors. *Chemical Engineering Science, 50,* 14, 2225-2233.

Merchuk, J.C., & Gluz, M. (2002). Bioreactors, Air-Lift Reactors. Encyclopedia of Bioprocess Technology. Retrieved May 16, 2012 from: http://chem.engr.utc.edu/ench435/2004/FromTablet/bioreactors.pdf

Merchuk, J., & Wu, X. (2003). Modeling of photobioreactors: application to bubble column simulation. *Journal of Applied Phycology, 15*, pp. 163-170.

Miao, X., & Wu, Q. (2004). High yield bio-oil production from fast pyrolysis by metabolic controlling of *Chlorella* protothecides. *Journal of Biotechnology, 110* (1), 85-93.

Michels, M.H.A., van der Goot, A.J., Norsker, N., Wijffels, R.H. (2010). Effects of shear stress on the microalgae *Chaetoceros muelleri*. *Bioprocess Biosystem Engineering, 33,* 921-927.

Molina Grima, E., Belarbi, E.H., Acien, F.G., Fernandez, A., Robles Medina, A., Chisti, Y. (2003). Recovery of microalgal biomass and metabolites: process options and economics. *Biotechnology Advances, 20,* 491-515.

Molina Grima, E., Fernandez, J., Acien, F., & Chisti, Y. (2001). Tubuluar photobioreactor design for algal cultures. *Journal of Biotechnology, 92*, 113-131.

Molina Grima, E., Fernandez, A., Camacho, F. G., Camacho Rubio, F., & Chisti, Y. (2000). Scale-up of tubular photobioreactors. *Journal of Applied Phycology, 12,* 355-368.

Morris, I., & Glover, H. (1974). Questions on the mechanism of temperature adaptation in marine phytoplankton. *Marine Biology, 24* (2), 147-154.

Nagase, H., Yoshihara, K.-i., Eguchi, K., Okamoto, Y., Murasaki, S., Yamashita, R., et al. (2001). Uptake pathway and continuous removal of nitric oxide from flue gas using microalgae. *Biochemical Engineering Journal, 7*, 241-246.

Nishikawa, M., Kato, H., Hashimoto, K. (1977). Heat transfer in aerated tower filled with non-Newtonian fluid. *Ind. Eng. Chem., Process Des. Dev., 16* (1), 133-136.

Oilgae (2013). "Algal Biodiesel Characteristics & Properties" Retrieved November 20, 2011 from: http://www.oilgae.com/algae/oil/biod/char/char.html.

Olaizola, M., Bridges, T., Flores, S., Griswold, L., Morency, J., & Nakamura, T. (2003). Microalgal removal of CO2 from flue gases: CO2 capture from a coal combustor. Kailua-Kona: U.S. Department of Energy award No. DE-FC26-00NT40934.

Olenina, I., Hajdu, S., Edler, L., Andersson, A., Wasmund, N., Busch, S., Göbel, J., Gromisz, S., Huseby, S., Huttunen, M., Jaanus, A., Kokkonen, P., Ledaine, I. and Niemkiewicz, E. (2006). Biovolumes and size-classes of phytoplankton in the Baltic Sea. *HELCOM Balt.Sea Environ*. Proc. No. 106, 144pp. Retrieved May 9, 2012 from: http://nordicmicroalgae.org/taxon/Tetraselmis%20cordiformis.

Origin Oil (2012). "Algae Appliance Model 4". Retrieved March 7, 2012 from: http://originoil.com/.

Parrish, C. C., & Wangersky, P. (1987). Particulate and dissolved lipid classes in cultures of *Phaeodactylum tricornutum* grown in culture turbidostats with a range of nitrogen supply rates. *Marine Ecology - Progress Series, 35,* 119-128.

Patil, V., Tran, K.-Q., & Gielrod, H. R. (2008). Towards sustainable production of biofuels from microalgae. *International Journal of Molecular Sciences, 9,* 1188-1198.

Pedroni, P., & Benemann, J. (2003). Microalgae for greenhouse gas abatement: an international R&D opportunity. *EniTecnologie, 1,* 24-28.

Perry, R.H. & Green, D.W. (2008). Perry's Chemical Engineers' Handbook, (Eighth Ed.). New York:McGraw-Hill Engineering.

Peters, F., Arin, L., Marrase, C., Berdalet, E., Sala, M.M. (2006). Effects of small-scale turbulence on the growth of two diatoms of different size in a phosphorus-limited medium. *Journal of Marine Systems, 61,* 134-148.

Pisutpaisal, N., & Boonyawanich, S. (2008). Hydrocarbon yield from *Botryoccoccus braunii* under varied growth conditions and extraction methods. *Research Journal of Biotechnology* (Special Issue: Sp. Iss. SI), 296-300.

Pittman, J.K., Dean, A.P. Osundeko, O. (2011). The potential of sustainable algal biofuel production using wastewater resources. *Bioresource Technology, 102,* 17-25.

Preston, B.L., Snell, T.W., Fields, D.M., Weissburg, M.J. (2001). The effects of fluid motion on toxicant sensitivity of the rotifer *Brachionus calyciflorus. Aquatic Technology, 52,* 117-131.

Prueksakorn, K. & Gheewala, S.H. (2006). Energy and greenhouse gas implications of biodiesel production from *Jatropha curcas L*. The 2nd Joint International Conference on "Sustainable Energy and Environment (SEE 2006)", November, 21-23, 2006, Bangkok, Thailand.

Putt, R. (2007). *Algae as a biodiesel feedstock: A feasibility assessment.* Auburn, AL: Center for Microfibrous Materials Manufacturing (CM3), Department of Chemical Engineering, Auburn University.

Qiang, H., & Richmond, A. (1996). Productivity and photosynthetic efficiency of *Spirulina platensis* as affected by light intensity, algal density and rate of mixing in a flat plate photobioreactor. *Journal of Applied Phycology , 8* (2), 139-145.

Quigg, A., Kevekordes, K., Raven, J. A., & Beardall, J. (2006). Limitations of microalgal growth at very low photon fluence rates: The role of energy slippage. *Photosynth Res, 88*, 299-310.

Radmer, R., Behrens, P., & Arnett, K. (1986). Analsis of the productivity of a continuous algal culture system. Columbia: Martek Corporation.

Rafai, S., Jibuti, L., & Peyla, P. (2010). Effective viscosity of microswimmer suspensions. *Physical Review Letters, 104,* 1098102, March, 5, 2010.

Ramanathan, G., Rajarathinam, K., Boothapandi, M., Abirami, D., Ganesamoorthy, G., & Duraipandi. (2011). Construction of vertical tubular photobioreactor for microalgae cultivation. *Journal of Algal Biomass Utilization, 2* (2), 41-52.

Ranga, R. A., & Ravishankar, G. (2007). Influence of CO2 on growth and hydrocarbon production in *Botryococcus braunii*. *Journal of Microbiology and Biotechnology, 17* (3), 414-419.

Ragni, M., & D'Alcala, M. R. (2007). Circadian variability in the photobiology of *Phaedactylum tricornutum* pigment content. *Journal of Plankton Research, 29* (2), 141-156.

Rawson, K.J., & Tupper, E.C. (1968). Basic ship theory. American Elsevier, New York.

Renaud, S.M., Parry, D.L., Thinh, L.V., Kuo, C., Padovan, A. & Sammy, N. (1991). Effect of light intensity on the proximate biochemical and fatty acid composition of *Isochrysis* sp. and *Nannochloropsis oculata* for use in tropical aquaculture. *Journal of Applied Phycology, 8*, 381, 387.

Richardson, J.W., Outlaw, J.L., Allison M. (2010). The economics of microalgae oil. *AgBioForum, 13*, 2, 119-130.

Richmond, A. (2004). Principles for attaining maximal microalgal productivity in photobioreactors: an overview. *Hydrobiologia, 512*, 33-37.

Rijstenbil, J., Wihnholds, J., & Sinke, J. (1989). Implications of salinity fluctuation for growth and nitrogen metabolism of the marine diatom *Ditylum brightwellii* in comparison with *Skeletonema costatum*. *Marine Biology, 101* (1), 131-141.

Rittman, B. (2008). Opportunities for renewable bioenergy using microorganisms. *Biotechnology and Bioengineering, 100* (2), 203-212.

Sato, T., Yamada, D., & Hirabayashi, S. (2010). Development of virtual photobioreactor for microalgae culture considering turbulent flow and flashing light effect. *Energy Conversion and Management, 51,* 6, 1196-1201.

Schlagermann, P. Gottlicher, G., Dillschneider, R., Rosello-Sastre, R., & Posten, C. (2012). Composition of algal oil and its potential as biofuel. *Journal of Combustion,* 2012, 1-14.

Schumpe, A. & Deckwar, W.D. (1987). Viscous media in tower bioreactors: Hydrodynamic characteristics and mass transfer properties. *Bioprocess Engineering, 2,* 79-94.

Scragg, A., Illman, A., Carden, A., & Shales, S. (2002). Growth of microalgae with increased calorific values in a tubular bioreactor. *Biomass & Bioenergy, 23* (1), 67-73.

Sheehan, J., Dunahay, T., Benemann, J., & Roessler, P. (1998). A Look Back at the U.S. Department of Energy's Aquatic Species Program-Biodiesel from Algae. Golden: National Renewable Energy Laboratory.

Shen, Y., Yuan, W., Pei, Z., & Mao, E. (2008). Culture of microalga *Botryococcus* in livestock wastewater. *Transactions of the ASABE , 51* (4), 1395-1400.

Shen, Y., Yuan, W., Pei, Z.J., Wu, Q., & Mao, E. (2009). Microalgae mass production methods. *Transactions of the ASABE, 52*(4), 1275-1287.

Shi, D., Xu, Y., & Morel, F.M. (2009). Effects of the pH/pCO_2 control method on medium chemistry and phytoplankton growth. *Biogeosciences, 6,* 1199-1207.

Siemens (2011). *Flue Gas Desulfurization.* Water Technologies. Retrieved February 2, 2012 from: http://www.water.siemens.com/en/power/flue_gas_desulfurization/Pages/default.aspx.

Siron, R. Giusti, G., & Berland, B. (1989). Changes in the fatty acid composition of *Phaeodactylum tricornutum* and *Dunaliella tertiolecta* during growth and under phosphorus deficiency. *Marine Ecology Progress Series, 55,* 95-100.

Smayda, T., & Mitchell-Innes, B. (1974). Dark survival of autotrophic, planktonic marine diatoms. *Marine Biology, 25* (3), 195-202.

Soh, L. & Zimmerman, J. (2011). Biodiesel production: the potential of algal lipids extracted with supercritical carbon dioxide. *Green Chemistry, 13,* 1422-1429.

Sokolov, A., & Aranson, I.S. (2009). Reduction of viscosity in suspension of swimming bacteria. *Physical Review Letters, 103,* 148101, October, 2, 2009.

Sonnekus, M. J. (2010). *Effects of salinity on the growth and lipid production of ten species of microalgae from the Swartkops Saltworks: A biodiesel perspective.* Nelson Mandela University.

Sturm, B.S.M., & Lamer, S.L. (2011). An energy evaluation of coupling nutrient removal from wastewater with algal biomass production. *Applied Energy, 88,* 3499-3506.

Suggett, D. J., Stambler, N., Prasil, O., Kolber, Z., Quigg, A., Vazquez-Dominguez, E., et al. (2009). Nitrogen and phosphorus limitation of oceanic microbial growth spring the Gulf of Aqaba. *Aquatic Microbial Ecology, 56,* 227-239.

Sun, A., Davis, R., Starbuck, M., Ben-Amotz, A., Pate, R., Pienkos, P.T. (2010). Comparative cost analysis of algal oil production for biofuels. *Energy, 36* (8), 5169-5179.

Sylvan, J. B., Quigg, A., Tozzi, S., & Ammerman, J. W. (2007). Eutrophication-induced phosphorus limitation in the Mississippi River plum: Evidence from fast repetition rate fluoremetry. *Association for the Sciences of Limnology and Oceanography, 52* (6), 2679-2685.

Talbot, P., Gortares, M., Lencki, R., & de la Noue, J. (1991). Absorption of CO2 in algal mass culture systems: A different characterization approach. *Biotechnology and Bioengineering, 37,* 834-842.

Tchobanoglous, G., Burton, F.L., Stensel, H.D. (2003) *Wastewater Engineering: Treatment and Reuse.* Metcalf & Eddy Inc., McGraw Hill.

Thomas, W.H., & Gibson, C.H. (1990). Effects of small-scale turbulence on microalgae. *Journal of Applied Phycology, 2,* 71-77.

Tiehm, A., Herwig, V., Neis, U. Particle size analysis for improved sedimentation and filtration in wastewater treatment. *Technical University of Hamburg-Harburg, Department of Waste Water Management, Hamburg, Germany.*

Torres, A.P., & Lopez, R.G. (2010). *Measuring daily light integral in a greenhouse.* Purdue University, Department of Horticulture and Landscape Architecture, HO-238-W. Retrieved February 8, 2012 from: http://www.extension.purdue.edu/extmedia/HO/HO-238-W.pdf.

Tredici, M.R., & Zitelli, G.C. (1998). *Efficiency of sunlight utilization: Tubular versus flat photobioreactors.* John Wiley & Sons, 1998.

Trujillo, F.J., Lee, I.A.L., Hsu, C.H., Safinski, T., Adesoji, A.A. (2008). Hydrodynamically enhanced light intensity distribution in a externally-irradiated novel aerated photoreactor: CFD simulation and experimental studies. *International Journal of Chemical Reactor Engineering, 6*, Article A58.

Tsoglin, L., Gabel, B., Falkovich, T., & Semenenko, V. (1996). Closed photobioreactors for microalgal cultivation. *Russian Journal of Plant Physiology, 43* (1), 131-136.

Tsukahara, K., & Sawayama, S. (2005). Liquid fuel production using microalgae. *Journal of the Japan Petroleum Institute, 48* (5), 251-259.

U.S. DOE (2010). *National Algal Biofuels Roadmap*. U.S. Department of Energy, Office of Energy Efficiency and Renewable Energy, Biomass Program.

U.S. Environmental Protection Agency (2006). *Contributions of CAIR/CAMR/CAVR to NAAQS Attainment: Focus on Control Technologies and Emission Reductions in the Electric Power Sector.* Office of Air and Radiation, April 18, 2006. Retrieved March 21, 2012 from: http://www.epa.gov/airmarkets/progsregs/cair/docs/naaqsattainment.pdf

Van Walsem, J., Morgan, F., Jacobson, S.A., Rainer, P., McIntire, J.R., Michonski, S.A., Posner, A. (2011). Solar biofactory, photobioreactors, passive thermal regulation systems and methods for producing products. US Patent US 2011/0151507A1, June 23, 2011.

Vargaftik, N.B., Volkov, B.N. Voljak, L.D. (1983). International tables of the surface-tension of water. *Journal of Physical and Chemical Reference Data, 12*, 817-820.

Vasudevan, V., Stratton, R.W., Pearlson, M.N. Jersey, G.R., Beyene, A.G., Weissman, J.C., Rubino, M., Hileman, J.I. (2012). Environmental performance of algal biofuel technology options. *Environmental Science & Technology, 46*, 2451-2459.

Verma, M.N., Mehrotra, S., Shukla, A., & Mishra, B.N. (2009). Prospective of biodiesel production utilizing microalgae as the cell factories: A comprehensive discussion. *African Journal of Biotechnology, 9*, 10, 1402-1411.

Vega, J.M.P., Roan, M.A.C., Saavedra, M.del P.S., Ramirez, D.T., Davalos, C.R. (2010). Effect of culture medium and nutrient concentration on fatty acid content of *Chaetoceros muelleri. Rev Latinoam Biotecnol Amb. Algal, 1*, 1, 6-15.

Wang, L., Min, M., Li, Y., Chen, P., Chen, Y., Liu, Y., Wang, Y., & Ruan, R. (2010). Cultivation of green algae *Chlorella* sp. In different wastewaters from municipal wastewater treatment plant. *Appl. Bioch. Biotechnol., 162*, 1174-1186.

Watson, D.G., Davis, J.J., Hanson, W.C. (1963) Relationship between wet weight and dry weight of the periphyton. *Association for the Sciences of Limnology and Oceanography, 8* (2), 309-311.

Wolf, Josh (2012). *Lipid vacuole fusion and L.E.V.I.* January 30, 2012. Retrieved April 1, 2012 from: http://www.wolfbiodiesel.com.

Wu, J. & He, C. (2010). Experimental and modeling investigation of sewage solids sedimentation based on particle size distribution and fractal dimension. *International Journal of Environmental Science Technology, 7,* 1, 37-46.

Wyman, C. (1994). Alternative fuels from biomass and their impact on carbon-dioxide accumulation. *Applied Biochemistry and Biotechnology, 45* (6), 897-915.

Xcel Energy (2011). Comanche Station Emissions Summary thru 04Q2011. Retrieved March 19, 2012 from http://www.xcelenergy.com/staticfiles/xe/Corporate/Environment/Comanche%20Station%20Emissions%20Summary%20thru%204Q2011.pdf.

Yongmanitchai, W. & Ward, O.P. (1991). Growth of and Omega-3 fatty acid production by *Phaeodactylum tricornutum* under different culture conditions. *Applied and Environmental Microbiology, 57* (2), 419-425.

Zhu, X., Long, S.P., Ort, D.R. (2008). What is the maximum efficiency with which photosynthesis can convert solar energy into biomass? *Current Opinion in Biotechnology, 19,* 153-159.

Zou, N., Zhang, C., Cohen, Z., Richmond, A. (2000). Production of eicosapentaenoic acid (EPA) in ultrahigh cell density cultures of *Nannochloropsis* sp. (Eustigmatophyceae). *European Journal of Phycology, 35,* 127-133.

Zsuzsa C., Michael H., Karsten S., Clemens, P. (2001). Light distribution in a novel photobioreactor-modeling for optimization. *Journal of Applied Phycology, 13,* 325-333.

Appendix A

Outputs from Model:

Fluid Dynamics Outputs:
Shear stress
Shear stress per cell
Vorticity
Surface Tension
Bubble drift velocity
Superficial gas velocity
Kolgomorov length
Kolgomorov length w/ bubble dissipation
CO2 transfer time needed
CO2 transfer time available
Interfacial area
Dissipation rate (viscous)
Dissipation rate (bubbles)
Effective viscosity (salt)
Effective viscosity (fresh)
Effective viscosity (ww)
Pressure at depth
Number of sparger pores required
Other Physics Outputs:
Power Plant flue gas output
Types/amounts of gas required
All nutrient amounts required
Water required for photosynthesis
Water lost to evaporation in open ponds
Lighting watts required
Increase in culture temp from photosynthesis
Required water temp to replace that used in photosynthesis
Algal density after one day's growth
Light path length
Recommended PBR diameter
Yield dry weight of biomass
Yield lipids
Energy required/carbon footprint
Amount of Oxygen created

Financial Outputs:
Operating costs:
Nutrients
Transesterification
Lighting watts required
Harvesting equipment operating costs
Water
Capital/Financing Costs:
Land
Piping
Pumps
Harvesting equipment
Lighting
Acrylic for PBR's
Pond liner
Spargers
Electrical installation
Profit:
Biodiesel
Biogas
Animal Feed
EPA
CO2 credits
WW treatment

Appendix B

Comparison with other techno-economic studies:

Culture density	x		x			
Algal strain	x	x				
Algal strain lipid content and size	x					
Growth rate	x					x
Lighting source/path length	x					
Biomass yield	x	x		x	x	x
Effective viscosity	x					
Fluid dynamics profile	x					
Adaptable growth scenario	x			x		
Dry weight of biomass	x					x
Operating costs	x	x	x	x	x	x
Carbon footprint of harvesting/lighting options	x		x			
Energy req harvesting/lighting options	x		x		x	x
Cost of harvesting/lighting options	x		x			
Paddlewheel operating cost	x		x			x
Transesterification cost/output	x		x			
Flue gas from coal power plant vs. algae reqts	x					
Nutrients supplied by wastewater	x					
Nutrients needed/cost	x	x				x
co2	x	x	x			x
phosphorus	x	x	x			x
nitrogen	x	x	x		x	x
iron	x	x		x		
antibiotics	x					
salt	x					
pH buffer	x					
energy req for nutrients	x					
Pumping kWh/capex and opex	x		x			
Water cost	x	x	x	x	x	x
Water used for photosynthesis	x					
Water lost to evaporation in open ponds	x		x		x	x
Lighting watts req/day	x					
Lighting capital and opex costs	x					
Increase in culture temp from photosynthesis	x	x				
Employee cost	x	x	x	x	x	x
Organic Solvents	x		x	x	x	x
Well Costs					x	
Employee tax			x			x
Supercritical co2 as a solvent	x					
Capital cost	x	x	x	x		x
Installation costs	x		x	x		x
Water Pumps	x		x	x		x
Tanks (Settling)	x		x	x		x
Harvesting Equipment	x			x		x
Harvesting Equipment sized by algal output	x					
Land	x	x	x	x	x	x
Pipelines	x		x	x		
Digester pit	x			x		
Digester pit cover	x			x		
Scrubber/dryer	x					
Flue gas pump	x		x	x		

Variable	Model	Shen, et al., 2008	ANL;NREL; PNNL, 2012	Putt, 2007	Richardson, et al., 2010	Lux Research, 2012
Generator	x			x		
Exhaust blower	x			x		
Culture pumps	x					x
Spargers/Diffusers	x			x		x
Paddlewheels	x			x	x	x
Pond Site Preparation						x
Liner	x	x	x	x		
Office		x	x			
Financing cost	x				x	x
Profit from Biodiesel	x		x	x		x
Profit from Biogas	x			x		
Profit from Animal Feed	x					x
Profit from EPA	x					
Profit from Beta-Carotene		x				

Appendix C

Values assigned to variables in model:

Variable	Value	Units
rural land	$2,300.00	per acre
urban land	$103,000.00	per acre
electricity	$0.11	per kWh
Photobioreactor material^	$7.50	per Liter
carbon credit*#	$20.00	per ton
LED capital*	$0.48	per W/year
Fluor capital*	$0.35	per W/year
methanol for transesterification**	0.10	kg/kg oil
methanol as solvent***#	14.00	g/g biomass
cost methanol**	$0.0018	per g
cost hexane or chloroform	$0.06	per gram of biomass
EM lysis***	23,040.00	L/day/unit
EM lysis*** capital	$50,000.00	cost/unit
EM lysis*** maint	$0.05	*capital cost/unit
EM lysis*** opex	0.002	kwh/liter
Filter press****opex	$0.0000025	per dry weight g
Filter press****capital	$9,009.00	per ton
conveyor oven operating	0.0028	kwh per gram
conveyor oven capital	$9,009.00	per ton
wastewater particles	0.0004	m3/m3
wastewater treatment capital*****	$0.41	per gallon of design flow
wastewater treatment operating profit	$0.06	per gallon
APR	0.08	.0832 effr/weekly
max O2 per L	0.028	g/L
iron nutrient	$0.02	per pound
co2 nutrient	$0.00153	per gram
phosphorus nutrient	$0.0014	per gram
pH buffer	.000552-.0011	$ per Liter of culture
antibiotics	$0.005	per gram
salt	.005-.008	$ per Liter of culture
nitrogen nutrient	$0.0014	per gram
installation costs	$7,600.00	per acre
cost fab pbr's	$500.00	per pbr
spargers	$197.00	per sparger (10/pond, 1/PBR)
paddlewheel	$3,000.00	per paddlewheel (1/pond)
pond liner	$4.00	per m2
digester pit	$6,600.00	per digester pit
digester pit cover	$12,600.00	per cover

Variable	Value	Units
piping	$12.70	per meter
generator	$25,000.00	per generator
exhaust blower	$1,000.00	per blower
tanks	$1.14	per Liter (to hold .33 total volume)
water pump	$500.00	per pump
culture pump	$5,000.00	per pump
gas pump	$10,000.00	per pump
water cost	$0.375	per m3
microturbines capital cost****#	$2,575.00	per kW generated
microturbine efficiency****#	27.000	%
engineering fee	$7.00	% of total construction cost
biodiesel price per barrel	$120-$150	per barrel
EPA content of lipid	.0257-.0347	X lipid content
EPA price	$2.15	per gram
microturbine capital cost	$900.00	per kW produced
qty of employees	0.08	people per hectare
employee salary	$60,000.00	per year
animal feed	$246.00	per ton
co2 produced from electricity	140.53	kg/kwh per year
hours/day paddlewheel operation	8.00	hours/day
flow velocity in open pond	0.03	m/s
*# Source: Johnston, et al., 2011		
*Source: www.IndustryLED.biz, includes replacements and disposal fees, assumes constant operation		
**Source: Lux Research, 2012		
***Source: Origin Oil.com, 2012		
****Source: Micronics, opex includes energy, water, consumable parts, and labor		
*****Souce: Hartman & Cleland, 2007, range of .41 to 2.41 to remove N to 5 mg/L		
**#Source: Micronicsinc.com, 2013		
***#Source: Bligh & Dyer, 1959		
****#Source: EPA, 2004		
^sourced from various sites, cost applies to glass and acrylic, priced to purchase 2-3x qty over 15 years		

Appendix D

Screen shot of Matlab library:

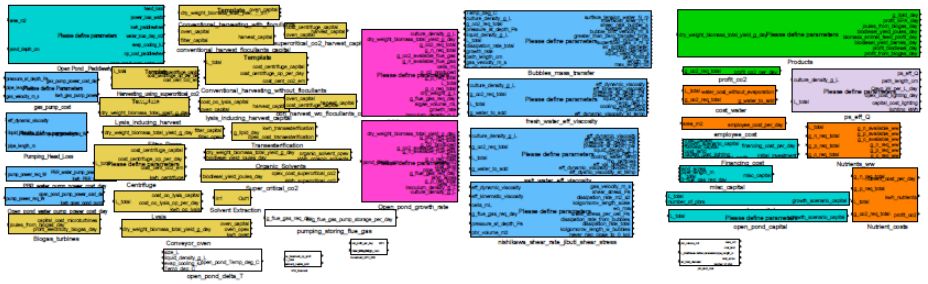

Screen shot of PBR model:

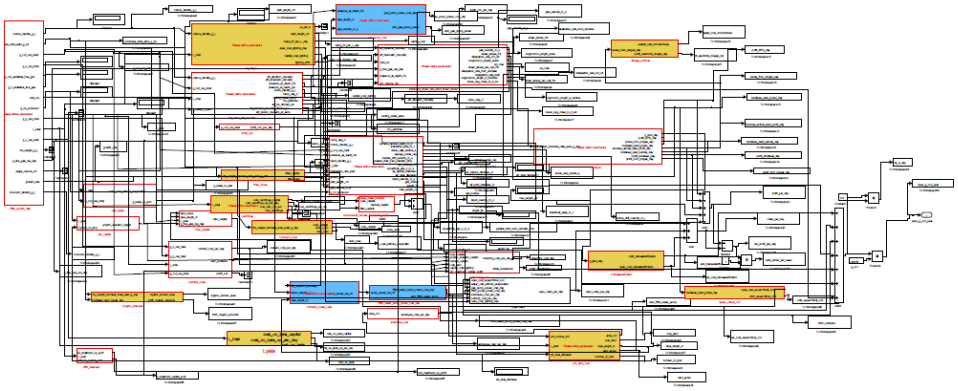

Screen shot of open pond model:

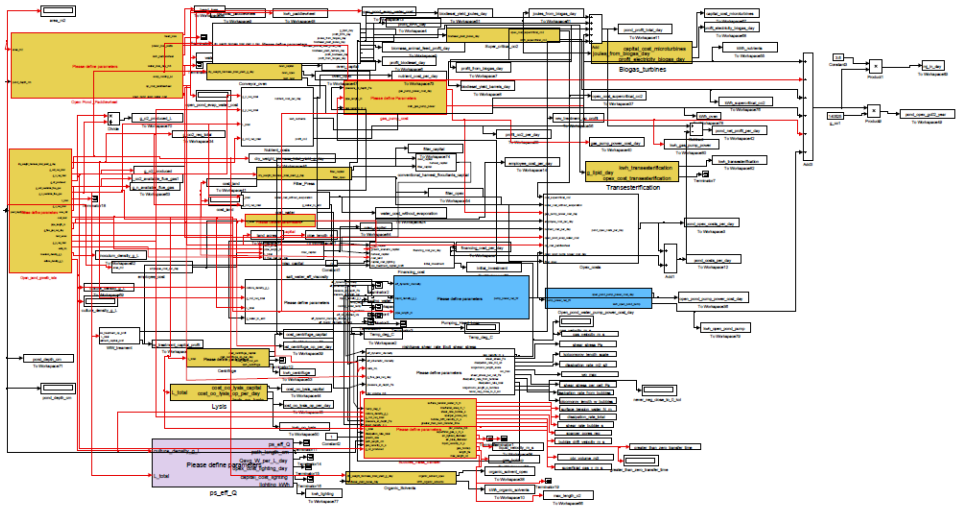

Screen shot of mass transfer module:

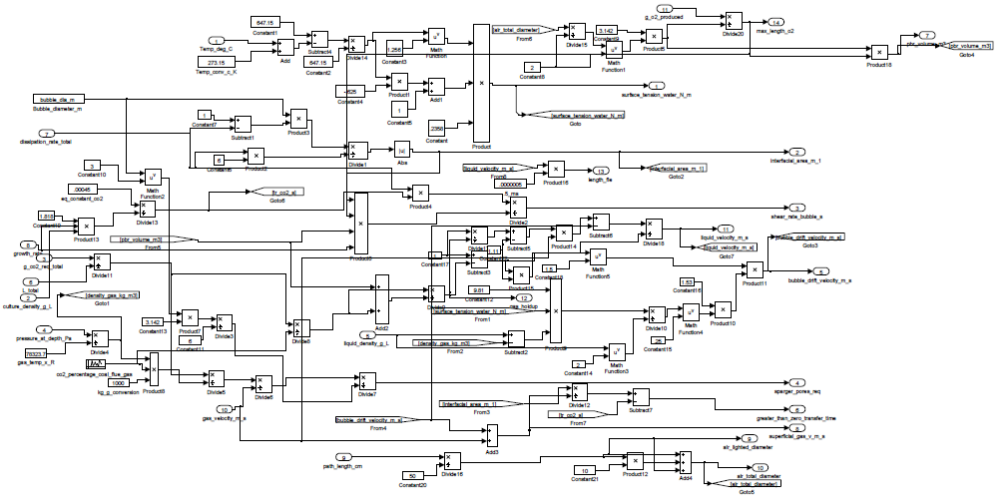

Appendix E

Optimization objective function for PBR/ALR growth scenario:

```
clc;




%% Set Initial Values

L_total                   = 7500; % Initial value
inoculum_density_cells_mL = 2000; % Initial value, 2.36x10^7 fluor
lipid_content             = .75; %Initial value

X0 = [L_total, inoculum_density_cells_mL, lipid_content];

InitialCost = CostFunction_PBR(X0);

%% Display Initial Values

disp('Initial Values');

L_total                       %#ok<NOPTS>
inoculum_density_cells_mL     %#ok<NOPTS>
lipid_content                 %#ok<NOPTS>
InitialCost                   %#ok<NOPTS>

%% Run Search
options = optimset('MaxFunEvals',600,'Algorithm','interior-
point','DiffMinChange',400000,'TolCon',.000000000001,'TolFun',.00000000
000001,'Hessian','bfgs');
% options =
optimset('MaxFunEvals',600,'Algorithm','sqp','TolCon',.00000000001,'Tol
Fun',.0000000000001);
[X,FinalCost,ExitFlag,Output] =
fmincon(@CostFunction_PBR,X0,[],[],[],[],[7500,
2000,.75],[7500,420000000,.75],[],options);


%% Get Final Values

L_total                       = X(1); % Final value
inoculum_density_cells_mL     = X(2); % Final value
lipid_content                 = X(3); % Final value

%% Display Final Values
```

```
disp('Final Values');

L_total                         %#ok<NOPTS>
inoculum_density_cells_mL       %#ok<NOPTS>
lipid_content                   %#ok<NOPTS>
FinalCost                       %#ok<NOPTS>
```

Constraint function for PBR/ALR growth scenario:

```
function Cost1 = CostFunction_PBR(X)

L_total                         = X(1);
inoculum_density_cells_mL       = X(2);
lipid_content                   = X(3);

%% Write Parameters to Base Workspace

assignin('base','L_total',L_total);
assignin('base','inoculum_density_cells_mL',inoculum_density_cells_mL);
assignin('base','lipid_content',lipid_content);


%% Run Simulation
%
% ToWorkspace blocks will dump results within this function scope.
%

sim('pbr_system');

%% Calculate Cost
%
% 'pond_costs_per_day' and 'pond_profit_total_day' are vectors of
length
% 201 so use the average cost.  Minimum or maximum could also be used.
%

Cost = mean(costs_per_day - profit_per_day);
Cost1 = mean(Cost);

end
```

Optimization objective function for Open Pond growth scenario:

```
clc;
```

```
%% Set Initial Values

inoculum_density_cells_mL = 150000000; % Initial value
lipid_content             = .75; %Initial value

X0 = [inoculum_density_cells_mL, lipid_content];

InitialCost = CostFunction(X0);

%% Display Initial Values

disp('Initial Values');


inoculum_density_cells_mL     %#ok<NOPTS>
lipid_content                 %#ok<NOPTS>
InitialCost                   %#ok<NOPTS>

%% Run Search
options = optimset('MaxFunEvals',600,'Algorithm','interior-
point','TolCon',.00000000001,'TolFun',.0000000000001,'Hessian','lbfgs')
;

[X,FinalCost,ExitFlag,Output] =
fmincon(@CostFunction,X0,[],[],[],[],[1500,.46],[Inf,.75],[],options);


%% Get Final Values


inoculum_density_cells_mL     = X(1); % Final value
lipid_content                 = X(2); % Final value

%% Display Final Values

disp('Final Values');


inoculum_density_cells_mL     %#ok<NOPTS>
lipid_content                 %#ok<NOPTS>
FinalCost                     %#ok<NOPTS>
```

Constraint function for Open Pond growth scenario:

```
function Cost1 = CostFunction(X)
```

```
inoculum_density_cells_mL     = X(1);
lipid_content                 = X(2);

%% Write Parameters to Base Workspace

assignin('base','inoculum_density_cells_mL',inoculum_density_cells_mL);
assignin('base','lipid_content',lipid_content);


%% Run Simulation
%
% ToWorkspace blocks will dump results within this function scope.
%

sim('open_pond_system');

%% Calculate Cost
%
% 'pond_costs_per_day' and 'pond_profit_total_day' are vectors of
length
% 201 so use the average cost.  Minimum or maximum could also be used.
%

Cost = mean(pond_costs_per_day - pond_profit_total_day);
Cost1 = mean(Cost);

end
```